UNIVERSITY OF CALIFORNIA,
IRVINE

Boron–Heteroatom Addition Reactions via Borylative Heterocyclizations

DISSERTATION

submitted in partial satisfaction of the requirements
for the degree of

DOCTOR OF PHILOSOPHY

in Chemistry

by

Kim Ngan Thi Tu

Dissertation Committee:
Professor Suzanne A. Blum, Chair
Professor Larry E. Overman
Professor Christopher D. Vanderwal

2018

Table of Contents

Page

List of Figures iv

List of Schemes v

List of Tables vi

Acknowledgements vii

Curriculum Vitae viii

Abstract of the Dissertation x

Chapter 1: Introduction to Boron–Heteroatom Addition Reactions via Borylative Heterocyclizations 1
- Introduction 1
- References 7

Chapter 2: Kinetic Study of Carbophilic Lewis Acid-Catalyzed Oxyboration and the Noninnocent Role of Sodium Chloride 10
- Introduction 10
- Results and Discussions 12
- Conclusions 20
- References 20
- Experimental 22
- References for Experimental Section 27

Chapter 3: Oxyboration With and Without a Catalyst: Borylated Isoxazoles via B–O σ-Bond Addition 28
- Introduction 28
- Results and Discussions 30
- Conclusions 43
- References 43
- Experimental 46
- References for Experimental Section 77

Chapter 4: An Oxyboration Route to a Single Regioisomer of Borylated Dihydrofurans and Isochromenes 82
- Introduction 82
- Results and Discussions 84
- Conclusions 93
- References 93
- Experimental 96
- References for Experimental Section 151

Chapter 5: Copper-Catalyzed Aminoboration from Hydrazones to Generate Borylated Pyrazoles 152
- Introduction 152
- Results and Discussions 154

Conclusions 160
References 161
Experimental 163
References for Experimental Section 184

List of Figures

Page

Figure 1.1. Previous work on developing addition of B–X bonds to alkynes and syntheses of borylated heterocycles 2
Figure 1.2. Initial thought process for the development of borylative heterocyclizations 3
Figure 1.3. Direct Addition: from a preformed B–heteroatom σ bond.....5
Figure 1.4. Formal Addition: from from separate reagents 7
Figure 2.1. a. Plot of formation of **2.2** versus time using 2.5 mol % IPrAuTFA at 50 °C, showing a nonzero-order rate dependence on substrate concentration. b. First-order fit plot with 2.5 mol % catalyst. c. Second-order fit plot with 2.5 mol % catalyst. d. First-order fit plot with 5.0 mol % catalyst. e. Second-order fit plot with 5.0 mol % catalyst. 18
Figure S2.1. Figure S2.1. a. First-order fit plot for average of triplicate runs with 1.25 mol % catalyst. b. Second-order fit plot for average of triplicate runs with 1.25 mol % catalyst.....25
Figure S2.2. a. First-order fit plot for average of triplicate runs with 2.5 mol % catalyst. b. Second-order fit plot for average of triplicate runs with 2.5 mol % catalyst. 26
Figure S2.3. a. First-order fit plot for average of triplicate runs with 7.5 mol % catalyst. b. Second-order fit plot for average of triplicate runs with 7.5 mol % catalyst.....27
Figure 4.1. Undesired dihydrofurans without boron, **4.5**.....86

List of Schemes

Page

Scheme 1.1. Plausible mechanism for the direct oxyboration of alkynyl phenols 4
Scheme 1.2. First report on Au-catalyzed oxyboration 5
Scheme 1.3. First report on Au-catalyzed aminoboration 6
Scheme 2.1. Traditional role of metal catalyst to activate B–X bond vs. new role of metal catalyst to activate C–C π bond, in B–X addition reactions to C–C π bonds 11
Scheme 2.2. Proposed Mechanism for Oxyboration 13
Scheme 2.3. Revised proposed mechanism for oxyboration 19
Scheme 3.1. Comparison of previous methods and new oxyboration method for the synthesis of 4-borylated isoxazoles. 30
Scheme 3.2. Reaction substrate scope. Substrates shown in blue are incompatible with alternative routes. All substrates give exclusively 4-borylated regioisomer 34
Scheme 3.3. Proposed mechanisms for a) catalyzed and b) uncatalyzed oxyboration.....36
Scheme 3.4. Organogold-to-boron transmetalation via ion pair.....38
Scheme 3.5. Oxyboration synthesis of valdecoxib 42
Scheme 4.1. Comparison of previous method and oxyboration method 84
Scheme 4.2. 3-Borylated Dihydrofurans Substrate Scope.....85
Scheme 4.3. 4-Borylated isochromenes.....88
Scheme 4.4. 4-Borylated isochromene substrate scope 90
Scheme 4.5. Synthesis of isochromenes via hydroboration–oxyboration 90
Scheme 4.6. Structure Elucidation.....91
Scheme 4.7. Downstream Functionalization 93
Scheme 5.1. Comparison of previous methods (a-c) and d) this aminoboration method.....154
Scheme 5.2. Reaction substrate scope 158
Scheme 5.3. Proposed mechanism for Cu(II)-catalyzed aminoboration reaction 160

List of Tables

Page

Table 2.1. Oxyboration of NaCl-free generated substrate **2.1** and the effect of NaTFA additive on this reaction 16
Table S2.1. Kinetic Plots for the NaCl-free Conditions. 24
Table 3.1. Selected Data from Optimization Study 31
Table 3.2. Initial reaction development with and without catalyst 32
Table SI-3.1. Uncatalyzed Oxyboration 65
Table 4.1. Isolation methods 89
Table S4.1. Optimization of Oxyboration Reaction towards Borylated Dihydrofurans **4.3** with [B] = Bcat and R_2 = *p*-MeC_6H_4 (**SI-4.1**): Catalyst Screening 103
Table S4.2. Optimization of Oxyboration Reaction towards Borylated Dihydrofurans **4.3** with [B] = Bcat and R_2 = *p*-MeC_6H_4 (**SI-4.1**): Concentration, Temperature, Catalyst Loading Screenings 104
Table S4.3. Optimization of Oxyboration Reaction with Bcat (R^2 = *n*-C_3H_7) 105
Table S4.4. ^{1}HNMR spectroscopy yield of borylated dihydrofurans **4.3** 106
Table S4.5. ^{1}H NMR spectroscopy yield of 4-borylated isochromenes **4.11** 108
Table S4.6. Catalyst screening 132
Table 5.1. Optimization study for the formation of amino boric ester **5.2** 156
Table 5.2. Optimization study for the formation of borylated pyrazole **5.3a** 157
Table S5.1. ^{1}HNMR spectroscopy yield of borylated pyrazole **5.3** 176

Acknowledgements

I would like to first thank the people that are closest to me, my husband Long Nguyen, my father Hau Tu, my mother Kim Tin Dinh, and my little sister Thuy Tien Tu. You have been with me at every step, always supportive and loving. You listened to all my complaining, frustrations, and you have been so understanding with my crazy schedule. All the late nights, all the weekends that I was gone for work, you were patiently waiting for me, never a complaint. I am very grateful for having you on this journey, and I'm proud to be your wife, your daughter, and your sister!

I would like to thank Professor Suzanne A. Blum for her mentorship and continuous support throughout this journey. You are my idol since day one and will always be! You are a great example of strength, resilience, intelligence, and humility.

I am proud to be a member of the Blum family! All of you have made my journey so enjoyable, and I have learnt so much from you guys, inside and outside of the lab. I enjoyed all the happy and not-so-happy time we've shared and I know each and everyone of you will be successful at achieving your dreams.

I would also like to thank the National Institute of Health (NIH), the National Science Foundation (NSF), The Gebel's family, and the UC Regents for their financial supports.

Curriculum Vitae
Kim Ngan Tu

EDUCATION

- **University of California - Irvine, Irvine, California**, Ph.D. in Chemistry, Fall 2018
- **California State University - Long Beach, California**, M.S. in Chemistry, August 2013
- **University of California - Los Angeles, Los Angeles, California**, B.S. in Chemistry, June 2010
- **Pasadena City College, Pasadena, California**, A.A. in Chemistry, June 2008

RESEARCH EXPERIENCE

Ph.D., Advisor: Prof. Suzanne A. Blum, January 2014–December 2018
Graduate Student Researcher
Boron–Heteroatom Addition Reactions via Borylative Heterocyclizations
M.S., Advisor: Prof. Kensaku Nakayama, December 2010–July 2013
Graduate Student Researcher
Bivalent Organophosphates as Inhibitors of Butyrylcholinesterase for Treatment of Alzheimer's Disease
B.S., Advisor: Prof. Alison McCurdy, June 2008–August 2008
Undergraduate Student Researcher

PUBLICATIONS AND PATENTS

5. "An Oxyboration Route to a Single Regioisomer of Borylated Dihydrofurans and Isochromenes." **Tu, K. N.**; Gao, C.; Blum, S. A. *J. Org. Chem.* **2018**, *83*, 11204–11217.
4. "Boron–Heteroatom Addition Reactions via Borylative Heterocyclization: Oxyboration, Aminoboration, and Thioboration." Issaian, A.;[*] **Tu, K. N.**;[*] Blum, S. A. *Acc. Chem. Res.* **2017**, *50*, 2598–2609. [*]co-first authorship
3. "Oxyboration with and without a Catalyst: Borylated Isoxazoles via B–O σ-Bond Addition." **Tu, K. N.**; Hirner, J. J.; Blum, S. A. *Org. Lett.* **2016**, *18*, 480–483.
2. "Kinetic Study of Carbophilic Lewis Acid Catalyzed Oxyboration and the Noninnocent Role of Sodium Chloride." Johnson, J. S.; Chong, E.; **Tu, K. N.**; Blum, S. A. *Organometallics* **2016**, *35*, 655–662.
1. "Organoboron Compounds and Methods of Making Organoboron Compounds." Blum, S. A., **Tu, K. N.**; Faizi, D. J.; Chong, E.; Hirner, J. J. US Provisional Patent 62/198,410.

HONORS AND AWARDS

- University of California–Irvine Regents' Dissertation Fellowship (2017)
- Gebel Graduate Student Award (University of California, Irvine, 2016)
- John and Elizabeth Leonard Scholarship in Chemistry (California State University, Long Beach, 2012)
- Outstanding research award in Physical and Mathematical Sciences, 24th Annual Student Research Competition (California State University, Long Beach, 2012)
- Maria Erlinda Co Sarno Scholarship in Chemistry (California State University, Long Beach, 2011)
- Department Honors (University of California, Los Angeles, 2010)
- Scholarship Award (University of California, Los Angeles, 2008)
- Margaret Farrer Scholarship (Pasadena City College, 2008)
- Lorraine Wyler Division Award in Chemistry (Pasadena City College, 2008)

PRESENTATIONS

16th Boron Chemistry Meeting in the Americas – Boston, MA

- Poster Presentation: "A Regioselective Oxyboration Route to Borylated Dihydrofurans and Isochromenes." June 2018.

Division of Organic Chemistry Graduate Research Symposium – Portland, OR

- Poster Presentation: "Oxyboration: Addition of B-O sigma bonds to C-C pi bonds." July 2017.

251st ACS National Meeting – San Diego, CA

- Oral Presentation in Metal-Mediated Reactions & Syntheses: "Oxyboration: Addition of B-O sigma bonds to C-C pi bonds." March 2016.

PROFESSIONAL MEMBERSHIPS/LEADERSHIP

- UCI Chemistry Department Graduate Student and Postdoc Organic Symposium Coorganizer, 2015–2017
- American Chemical Society, 2010–2018
- Academic Advancement Program, University of California, Los Angeles, Member, 2008–2010

Abstract of the Dissertation

Boron–Heteroatom Addition Reactions via Borylative Heterocyclizations

By

Kim Ngan Tu

Doctor of Philosophy in Chemistry

University of California, Irvine, 2018

Professor Suzanne A. Blum, Chair

Organoboron compounds and heterocycles are powerful building blocks and precursors for organic synthesis, including for drug discovery, and for agrochemical and material synthesis. The common strategy for the synthesis of borylated heterocycles involves two separate synthetic steps: first, synthesis of the heterocyclic core, and second, borylation of the core through established methods such as transition metal-catalyzed C–H or C–X activation/borylation or lithiation/borylation. The alternative syntheses of *O*- and *N*-heterocycles via borylative cyclization are developed and reported herein. These reactions provide access to heterocyclic core and install boron in one synthetic step, with complementary bond disconnections, regiochemistry, and functional-group compatibility to current methods. Mechanistic and kinetic studies for direct oxyboration (Chapter 2) were investigated to understand the role of gold catalyst and byproduct NaCl. The syntheses of borylated isoxazoles and dihydrofurans via gold-catalyzed direct oxyboration reactions or uncatalyzed conditions (Chapter 3 and 4, respectively) followed. The mechanism of the gold-catalyzed reaction is proposed to proceed via addition of B–O σ bonds to Au(I)-activated C–C π bonds to afford cyclization, followed by transmetalation of the organogold intermediate to achieve the desired borylated heterocycles. Finally, a copper-catalyzed direct aminoboration reaction was discovered, which affords borylated pyrazoles (Chapter 5). These

methods provide low-cost, alternative routes to borylated heterocycles that can be further functionalized via metal-catalyzed cross-coupling reactions.

Chapter 1

Introduction to Boron–Heteroatom Addition Reactions via Borylative Heterocyclizations

Abstract: This chapter provides a brief introduction to the field of borylative heterocyclization reactions that give access to borylated heterocycles. The context of the Blum Group's previous studies and the experiments in this thesis in relation to the field are also discussed. This chapter is reprinted with permission in part from a previously published Account[1] where I served as co-first author.

Introduction

Organoboron reagents are building blocks of choice for organic synthesis and drug discovery.[2] Heterocycles containing oxygen, nitrogen, and sulfur are found in many diverse classes of natural products,[3] and ethers and amines are in nearly 25% and 85% respectively of the top-grossing pharmaceuticals in the United States for 2012. Thus, the development of methods to construct borylated heterocycles would aid in the development of pharmaceuticals. In 2014, the Blum Group became interested in developing methods to generate borylated heterocycles through the activation of B–X bonds. The typical strategies in the field to generate borylated heterocycles include activation of B–X bonds through oxidative addition or σ-bond metathesis to prime them for addition to C–C π bonds (Figure 1.1a), or a two-step sequence to construct *O*-, *N*-, and *S*-heterocyclic cores, then to borylate the core through established methods such as transition metal-catalyzed C–H/C–X activation/borylation[4–7] and lithiation/borylation[8,9] (Figure 1.1b), or cycloaddition[10–12] (Figure 1.1c). Yet a number of desirable heterocyclic building blocks are unavailable in borylated form and existing routes to others are incompatible with key functional groups or lack access to complementary regioisomers. There are multiple reports on the direct addition of B–element bonds across C–C multiple bonds for element = H,[13,14] C,[15] Si,[14,16] Sn,[14,17] S,[18] B,[14,19] Cl,[20] Br,[21] and I[21] which proceed through oxidative addition into the B–element σ bond

using transition metal catalysts such as Ni(0), Pd(0), or Pt(0). However, presumably due to the extremely high strength of the B–O bond,[22] there was no report on the corresponding activation of B–O σ bonds and direct addition to C–C multiple bonds, until the Blum group's discovery of the first direct oxyboration reaction in 2014.[23]

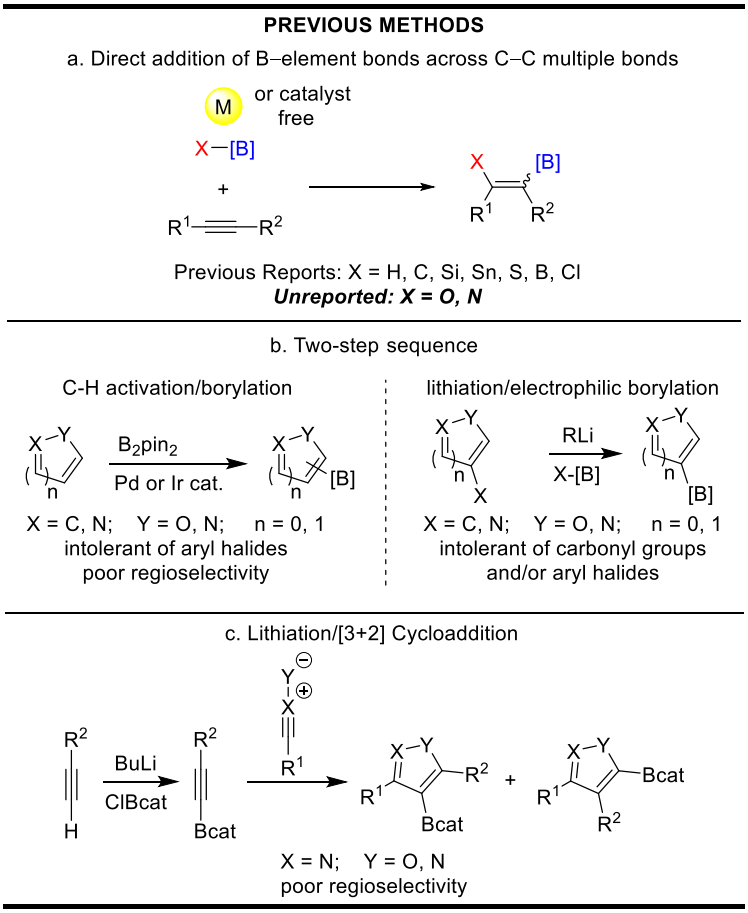

Figure 1.1. Previous work on developing addition of B–X bonds to alkynes and syntheses of borylated heterocycles.

Prior to our group's development of boron–heteroatom addition reactions, we had been developing dual catalytic systems with gold and palladium.[24] These studies addressed a shortfall in gold catalysis, namely that organogold intermediates[25,26] had limited subsequent reactivity: turnover in these systems was almost always achieved by quenching with proton,[27] carbocation,[28] silyl,[29] or sulfonyl.[30] We considered if these intermediates could instead be trapped by palladium under dual catalytic gold/palladium conditions, leading to increased carbon–carbon bond forming

opportunities. While this concept was successful, it remained limited by the oxidative addition that produced the organopalladium partner[31,32] (a limitation overcome later by Nevado with aryl iodides[33]). We therefore wondered if we might be able to trap these intermediates with stoichiometric boron rather than catalytic palladium, because boron would provide cheap and stable products that could be stored indefinitely. Through a future synthetic step, the resulting organoboron products could be cross-coupled to diverse oxidative addition partners using known chemistry. This initial thought process guided our first discovery of gold-catalyzed direct boron–element addition reactions (Figure 1.2).[23]

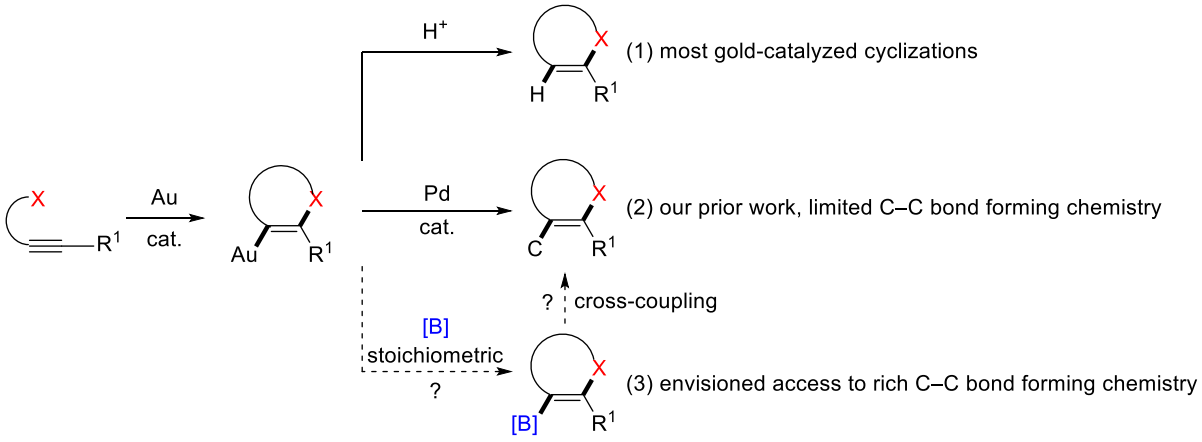

Figure 1.2. Initial thought process for the development of borylative heterocyclizations.

Led by previous graduate student Joshua Hirner, our laboratory initially focused on the addition of the B–O σ bond in **1.2**, derived from phenol **1.1**. Initial studies identified IPrAuTFA as the optimal catalyst. We hypothesized that the carbophilic Lewis acid IPrAu cation might activate the C–C π bond toward attack by the B–O σ bond (intermediate **1.5** or **1.6**). Cyclization would afford organogold **1.7** and boric ester **1.8**, which then would undergo a previously unreported organogold-to-boron transmetalation to generate the desired borylated benzofuran **1.9** (Scheme 1.1).

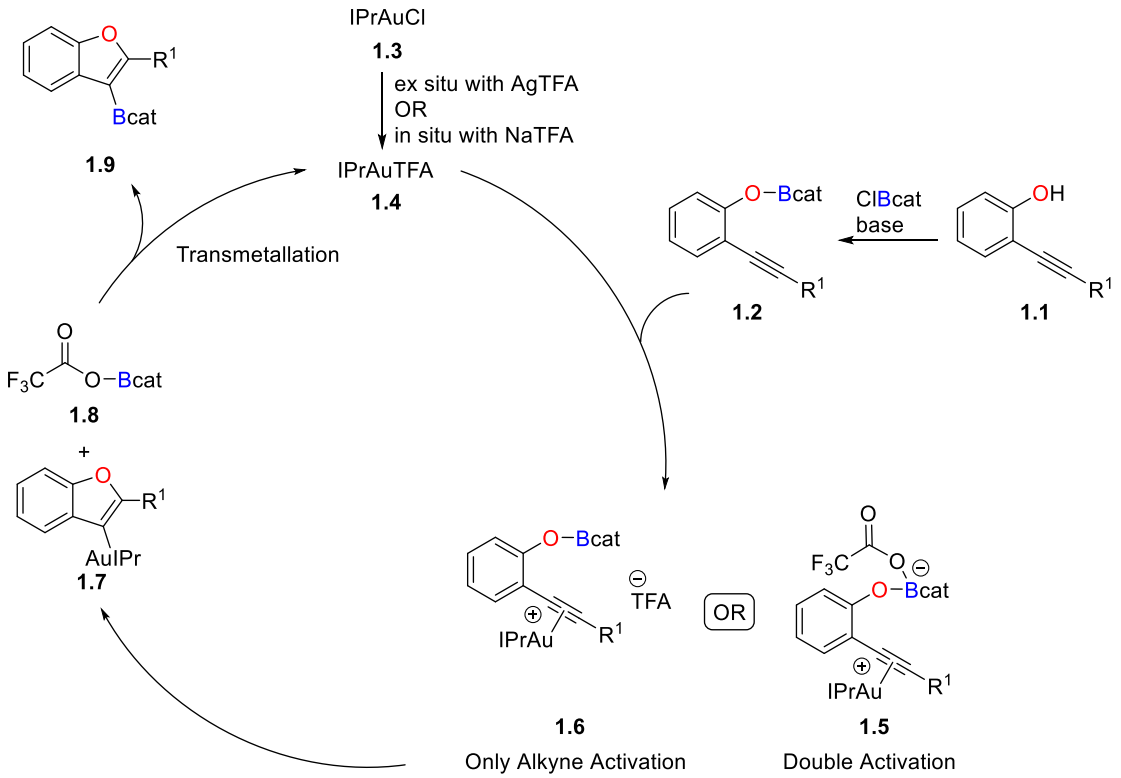

Scheme 1.1. Plausible mechanism for the direct oxyboration of alkynyl phenols

The oxyboration reaction successfully transformed alkynyl phenols **1.1** into borylated benzofurans **1.9** through a one-pot procedure (Scheme 1.2). The reaction was tolerant of a variety of functional groups, some of which are incompatible with current competing borylation methods.[3,5,7] The catechol boronic esters are labile to hydrolysis and not stable toward silica column chromatography. They were converted to the organotrifluoroborate, *N*-methyliminodiacetic acid (MIDA) boronate, or pinacolboronate esters as bench-stable derivatives, which were readily available for downstream functionalization.

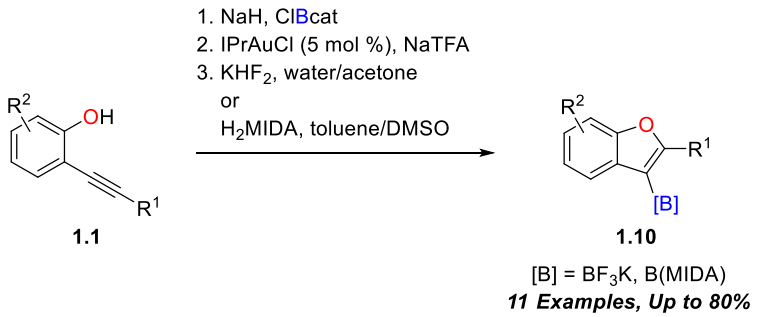

Scheme 1.2. First report on Au-catalyzed oxyboration

Motivated by this initial report,[23] the Blum Group initiated a research program to develop borylative heterocyclization methods with and without catalysts through direct addition reactions of B–O and B–N σ bonds onto carbon–carbon π bonds. This direct borylation method enables the preparation of synthetically useful building blocks[3] via new bond disconnections, with complementary regiochemistry and with tolerance of functional groups that are incompatible with existing methods (e.g., aryl halides, competing heterocycles, and/or electrophilic groups).[4–12] In this approach, heterocyclization and borylation occur in the same synthetic step. We use the term **direct** when referring to addition reactions starting from a preformed B–element σ bond that is part of the productive reaction mechanism (Figure 1.3).

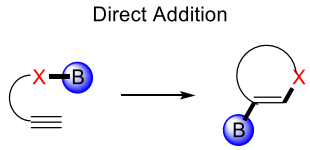

Figure 1.3. Direct Addition: from a preformed B–heteroatom σ bond.

Postdoctoral scholar Dr. Eugene Chong next examined a direct aminoboration strategy.[34] The B–N σ bond is weaker than B–O σ bond (105 kcal/mol for B–N versus 130 kcal/mol for B–O), which could be easier to manipulate.[22] Our laboratory's target structures were borylated indoles, which are privileged scaffolds for biological active compounds,[35,36] and offered an opportunity to study the compatibility of the working mechanistic hypothesis of gold-catalyzed π-

bond activation with B–N bonds. The optimized aminoboration reaction tolerated a variety of functional groups that are incompatible with one or more of the traditional strategies toward borylated heterocycle synthesis (Scheme 1.3).[4,6,8] As one example, because of the challenges in functional group compatibility with major synthetic routes, borylated bromoindoles were synthesized previously with mercury acetate.[37] However, our aminoboration method provided a mercury-free route to borylated bromoindole.

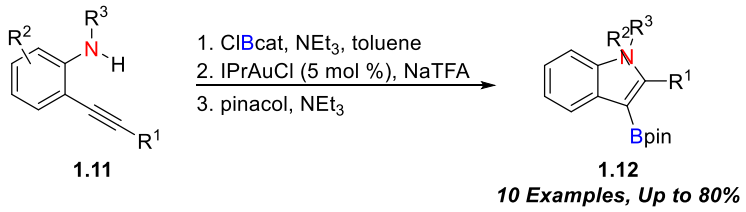

1.11 **1.12**

10 Examples, Up to 80%

Scheme 1.3. First report on Au-catalyzed aminoboration

Concurrently, the Blum group developed formal addition reactions of B–O, B–N, and B–S bonds or their net equivalents onto carbon–carbon π bonds. The term **formal** is used when referring to addition reactions without formation of the B–element bond at any point in the productive reaction. Existing formal borylative heterocyclization reports use $B(C_6F_5)_3$, in the cyclization of alkynyl amides,[38] esters[39,40] and anilines[41] to make zwitterionic products. These products, though obtained in one synthetic step, lack the neutral heterocycle and the diverse potential to be functionalized at the $B(C_6F_5)_3$ group, because cross-coupling conditions and other derivatization reactions for this group are not yet widely established.[42] Here, our group has developed commercially available ClBcat as an alternative reagent for formal boron–heteroatom addition reactions through borylative heterocyclization.[43,44] Reactions with ClBcat proceed through spontaneous cyclization/dealkylation sequences. The resulting neutral borylated products are primed to take advantage of the rich cross-coupling and derivatization chemistry available to organoboron compounds. We also describe the fundamental mechanistic studies of both direct and

formal addition reactions and provide further insight into developing future reactions in these areas.[45]

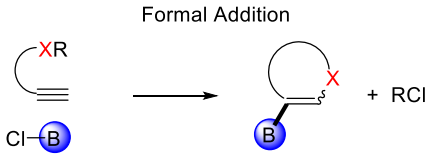

Figure 1.4. Formal Addition: from separate reagents.

My thesis research focused on developing direct borylation methodology and occurred currently with the development of the direct aminoboration chemistry and the formal borylation methods from other group members. The specific area of my research was direct oxyboration and aminoboration reactions towards syntheses of borylated isoxazoles, dihydrofurans, and pyrazoles. The significance of my contribution was the discovery of the first uncatalyzed direct oxyboration reaction and the first copper-catalyzed direct aminoboration that provide more economical routes to access these borylated heterocycles, especially in large-scale or industrial scale syntheses. The detailed mechanistic and kinetic studies for the direct borylation method will be discussed in Chapter 2 and the knowledge gained from this study then aided in the subsequent development of additional direct borylation reactions involving boron–nitrogen and boron–oxygen σ bonds to form borylated isoxazoles (Chapter 3), dihydrofurans (Chapter 4), and pyrazoles (Chapter 5), respectively.

References

(1) Issaian, A.; Tu, K. N.; Blum, S. A. *Acc. Chem. Res.* **2017**, *50*, 2598–2609.
(2) Miyaura, N. *Top. Curr. Chem.* **2002**, *219*, 11–59.
(3) Majumdar, K. C.; Chattopadhyay, S. K. Wiley-VCH, 2011.
(4) Murata, M.; Oyama, T.; Watanabe, S.; Masuda, Y. *J. Org. Chem.* **2000**, *65*, 164–168.
(5) Larsen, M. A.; Hartwig, J. F. *J. Am. Chem. Soc.* **2014**, *136*, 4287–4299.
(6) Hartwig, J. F. *Acc. Chem. Res.* **2012**, *45*, 864–873.
(7) Sharp, M. J.; Cheng, W.; Snieckus, V. *Tetrahedron Lett.* **1987**, *28*, 5093–5096.
(8) Lauer, M.; Wulff, G. *J. Organomet. Chem.* **1983**, *256*, 1–9.

(9) Mullens, P. R. *Tetrahedron Lett.* **2009**, *50*, 6783–6786.
(10) Denmark, S. E.; Kallemeyn, J. M. *J. Org. Chem.* **2005**, *1*, 2839–2842.
(11) Moore, J. E.; Davies, M. W.; Goodenough, K. M.; Wybrow, R. A. J.; York, M.; Johnson, C. N.; Harrity, J. P. A. *Tetrahedron* **2005**, *61*, 6707–6714.
(12) Browne, D. L.; Helm, M. D.; Plant, A.; Harrity, J. P. A. *Angew. Chem. Int. Ed.* **2007**, *46*, 8656–8658.
(13) Hall, D. G. Wiley-VCH, 2011.
(14) Miyaura, N. In *Catalytic Heterofunctionalization*; Wiley-VCH Verlag GmbH: Weinheim, FRG; pp 1–45.
(15) Suginome, M. *Chem. Rec.* **2010**, *10*, 348–358.
(16) Suginome, M.; Nakamura, H.; Ito, Y. *Chem. Commun.* **1996**, No. 24, 2777.
(17) Onozawa, S.; Hatanaka, Y.; Sakakura, T.; Shimada, S.; Tanaka, M. *Organometallics* **1996**, *15*, 5450–5452.
(18) Ishiyama, T.; Nishijima, K.; Miyaura, N.; Suzuki, A. *J. Am. Chem. Soc.* **1993**, *115*, 7219–7225.
(19) Marder, T. B.; Norman, N. C. *Top. Catal.* **1998**, *5*, 63–73.
(20) Lappert, M. F.; Prokai, B. *J. Organomet. Chem.* **1964**, *1*, 384–400.
(21) Hara, S.; Dojo, H.; Takinami, S.; Suzuki, A. *Tetrahedron Lett.* **1983**, *24*, 731–734.
(22) Sanderson, R. Elsevier Science, 1983.
(23) Hirner, J. J.; Faizi, D. J.; Blum, S. A. *J. Am. Chem. Soc.* **2014**, *136*, 4740–4745.
(24) Hirner, J. J.; Shi, Y.; Blum, S. A. *Acc. Chem. Res.* **2011**, *44*, 603–613.
(25) Li, Z.; Brouwer, C.; He, C. *Chem. Rev.* **2008**, *108*, 3239–3265.
(26) Gorin, D. J.; Sherry, B. D.; Toste, F. D. *Chem. Rev.* **2008**, *108*, 3351–3378.
(27) Antoniotti, S.; Genin, E.; Michelet, V.; Genêt, J.-P. *J. Am. Chem. Soc.* **2005**, *127*, 9976–9977.
(28) Zhang, L. *J. Am. Chem. Soc.* **2005**, *127*, 16804–16805.
(29) Nakamura, I.; Sato, T.; Terada, M.; Yamamoto, Y. *Org. Lett.* **2007**, *9*, 4081–4083.
(30) Nakamura, I.; Yamagishi, U.; Song, D.; Konta, S.; Yamamoto, Y. *Angew. Chem. Int. Ed.* **2007**, *46*, 2284–2287.
(31) Shi, Y.; Roth, K. E.; Ramgren, S. D.; Blum, S. A. *J. Am. Chem. Soc.* **2009**, *131*, 18022–18023.
(32) Al-Amin, M.; Roth, K. E.; Blum, S. A. *ACS Catal.* **2014**, *4*, 622–629.
(33) García-Domínguez, P.; Nevado, C. *J. Am. Chem. Soc.* **2016**, *138*, 3266–3269.
(34) Chong, E.; Blum, S. A. *J. Am. Chem. Soc.* **2015**, *137*, 10144–10147.
(35) Bandini, M.; Eichholzer, A. *Angew. Chem. Int. Ed.* **2009**, *48*, 9608–9644.
(36) Horton, D. A.; Bourne, G. T.; Smythe, M. L. *Chem. Rev.* **2003**, *103*, 893–930.
(37) Garg, N. K.; Sarpong, R.; Stoltz, B. M. *J. Am. Chem. Soc.* **2002**, *124*, 13179–13184.
(38) Melen, R. L.; Hansmann, M. M.; Lough, A. J.; Hashmi, A. S. K.; Stephan, D. W. *Chem. - A Eur. J.* **2013**, *19*, 11928–11938.
(39) Hansmann, M. M.; Melen, R. L.; Rominger, F.; Hashmi, A. S. K.; Stephan, D. W. *J. Am. Chem. Soc.* **2014**, *136*, 777–782.
(40) Wilkins, L. C.; Hamilton, H. B.; Kariuki, B. M.; Hashmi, A. S. K.; Hansmann, M. M.; Melen, R. L. *Dalt. Trans.* **2016**, *45*, 5929–5932.
(41) Voss, T.; Chen, C.; Kehr, G.; Nauha, E.; Erker, G.; Stephan, D. W. *Chem. - A Eur. J.* **2010**, *16*, 3005–3008.
(42) Soltani, Y.; Wilkins, L. C.; Melen, R. L. *Angew. Chem. Int. Ed.* **2017**, *56*, 11995–11999.

(43) Faizi, D. J.; Issaian, A.; Davis, A. J.; Blum, S. A. *J. Am. Chem. Soc.* **2016**, *138*, 2126–2129.
(44) Faizi, D. J.; Davis, A. J.; Meany, F. B.; Blum, S. A. *Angew. Chem. Int. Ed.* **2016**, *55*, 14286–14290.
(45) Issaian, A.; Faizi, D. J.; Bailey, J. O.; Mayer, P.; Berionni, G.; Singleton, D. A.; Blum, S. A. *J. Org. Chem.* **2017**, *82*, 8165–8178.

Chapter 2

Kinetic Study of Carbophilic Lewis Acid-Catalyzed Oxyboration and the Noninnocent Role of Sodium Chloride

Abstract: In the present study, the oxyboration reaction catalyzed by IPrAuTFA in the presence and absence of NaTFA has been examined with kinetic studies, mass spectrometry, and ^{1}H NMR and ^{11}B NMR spectroscopy. Data from monitoring the reactions over the temperature range from 30–70 °C, the catalyst range from 1.3–7.5 mol %, and the NaTFA additive range from 2.5–30 mol % suggests a mechanism that involves rate-determining catalyst generation. Data from additive studies that replaced NaTFA with NaBARF (BARF = tetrakis[3,5-bis(trifluoromethyl)phenyl]borate) or Bu_4NTFA as alternative additives suggest catalyst quenching from residual NaCl remaining from a one-pot substrate synthesis/reaction method is the cause of this effect, despite the low solubility of this NaCl byproduct in toluene. Material produced through an alternative, sodium-chloride free substrate synthesis exhibited faster reaction rates, consistent with a change in rate-determining step that depended on the substrate synthesis route. This chapter is reprinted in part, with permission, from a previous published report where I served as third author.[1] The text has been modified to focus on my contribution.

Introduction

Despite major progress in developing B–X element addition reactions to carbon–carbon π systems,[2–4] the corresponding B–O addition—oxyboration—remained unknown until it yielded to gold catalysis in 2014.[5] The role of the gold catalyst was proposed to be activation of the π system, a strategy orthogonal to other metal catalyzed B–X σ-bond addition reactions which typically proceed through oxidative addition or σ-bond metathesis of the B–X bond (Scheme 1). This gold-catalysis working mechanistic strategy has since been successfully applied to B–N[6] and B–O[5,7] bond addition reactions to make organoboron heterocyclic building blocks; yet the rationale for the proposed pathway has been largely limited to analogy to existing carbophilic Lewis acid catalysis[8–13] rather than experimental observations (Scheme 2.1).[5] Additionally, the working

mechanistic postulate for the oxyboration of alkynes included possible participation of trifluoroacetate (TFA) additive.

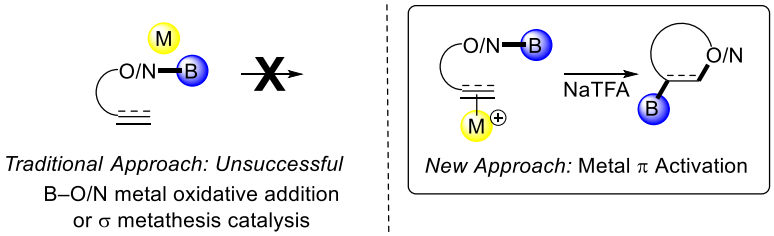

Scheme 2.1. Traditional role of metal catalyst to activate B–X bond vs. new role of metal catalyst to activate C–C π bond, in B–X addition reactions to C–C π bonds

We herein investigate the kinetics of the gold-catalyzed oxyboration reaction in the synthesis of borylated benzofurans (eq 2.1) that serve as building blocks for the synthesis of functionalized heterocycles. A practical feature of the originally reported method was the ability to generate the requisite B–O bond of the starting material from phenols and *B*-chlorocatecholborane (ClBcat) in one pot, without the need to isolate this moisture sensitive intermediate. The kinetic data shows consistency with the proposed carbophilic activation pathway but identifies an unanticipated kinetic dependence on the reagents used and route of synthesis in the prior one-pot substrate-construction step. More specifically, the presence of NaCl generated during the one-pot substrate synthesis can be noninnocent to the reaction,[14] analogous to the reported silver salt effects on gold catalysis.[15–17] Similar to silver halides, sodium chloride has a low solubility in organic solvents, yet we show that sufficient quantities remain in solution to influence reactivity. A possible explanation for the role of NaTFA additive as a chloride scavenger and transmetalation partner with gold chloride is thus provided herein. It is envisioned that these studies will assist in the development of methods for addition reactions of these previously recalcitrant B–X bonds to C–C π systems and thus enable rapid access to heterocyclic borylated building blocks for drug discovery and materials synthesis. Further, these studies may

inform on the development of dual-metal/metalloid catalytic chemistry for gold that currently requires halide-free conditions.[18]

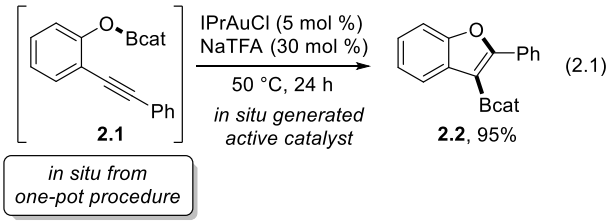

Results and Discussions

Carbophilic Lewis Acid Activation Mechanistic Proposal with Bifunctional Activation. The proposed mechanism for the oxyboration reaction in the synthesis of borylated benzofurans is shown in Scheme 2.2. The original mechanistic hypothesis for oxyboration featured IPrAuTFA **2.4** as a bifunctional Lewis acidic/basic catalyst, in which the $IPrAu^+$ moiety participates in carbophilic Lewis acid activation of the alkyne in **2.1**, and the TFA counterion coordinates to boron, to assemble intermediate **2.5**. Nucleophilic attack on the Au-activated C–C π bond with the TFA-activated B–O bond in **2.5**, through transition state **2.6**, generates organogold intermediate **2.8** and catB(TFA) **2.9**.[5] Subsequent Au-to-B transmetalation[18,19] between **2.8** and **2.9** affords the borylated benzofuran **2.2** and regenerates the IPrAuTFA catalyst. To our knowledge, our initial report of oxyboration was the first example of organogold to boron transmetalation,[5–7,18–20] the reverse reaction had been reported.[21–25] Given that the forward and reverse transmetalation reactions are both reported, it seems plausible that small differences in the structure of the reagents affect which side of the transmetalation reaction is thermodynamically favored. Prior studies in our laboratory identified that some transmetalation systems with gold and boron are in equilibrium.[19]

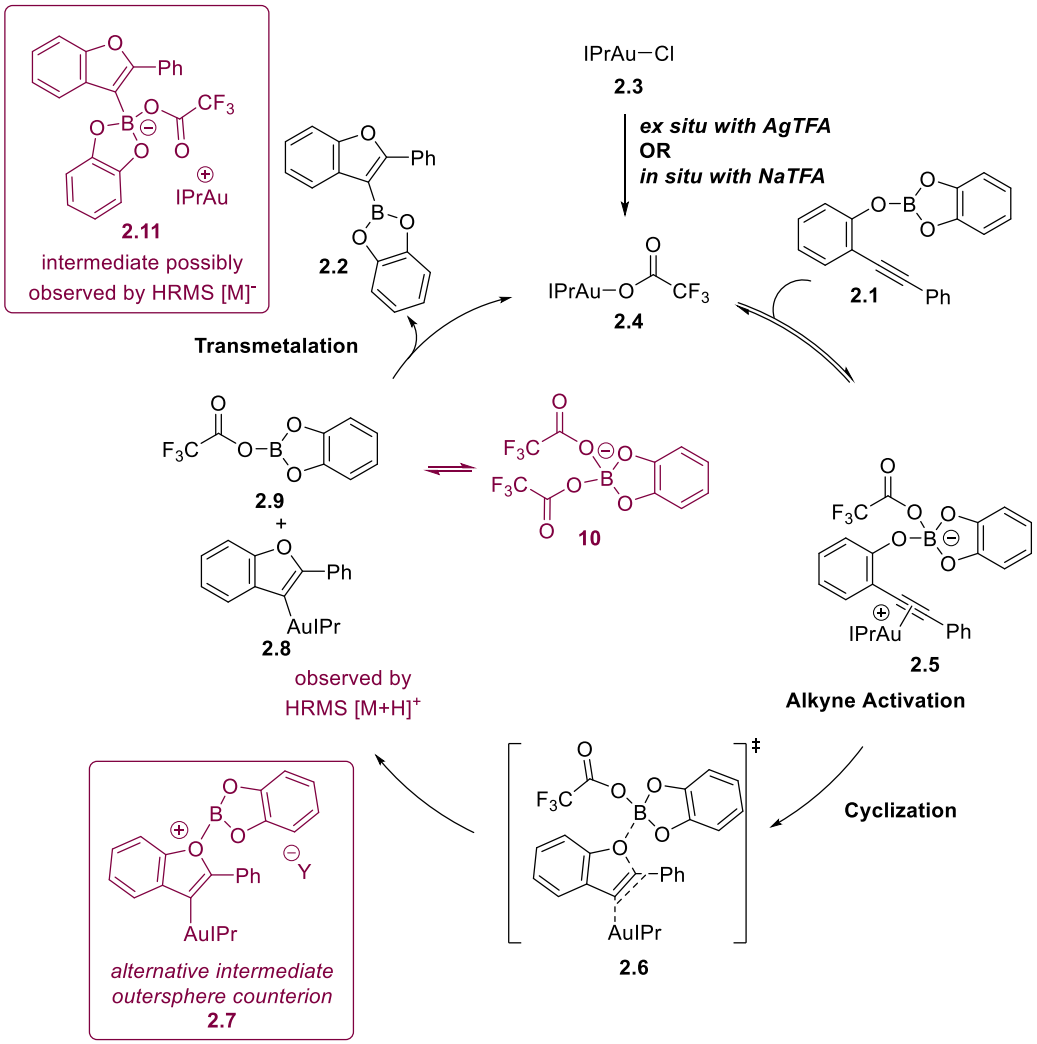

[a] Originally proposed structures in the catalytic cycle from ref. 4 shown in black; additional data/possible intermediates from this work shown in purple (Y = BF_4, SbF_6 or TFA)

Scheme 2.2. Proposed Mechanism for Oxyboration[a]

Carbophilic Lewis Acid Activation Mechanistic Proposal without Bifunctional Activation. Alternatively, substrate **2.1** could be undergoing a carbophilic Lewis acid gold-mediated cyclization, wherein trifluoroacetate serves as an outer sphere ion (eq 2.2). A nucleophilic attack of the oxygen lone pair to the IPrAu-activated C–C π bond could generate key alternative intermediate organogold benzofuran/catechol borenium adduct **2.7** that serves as a precursor to the borylated benzofuran product **2.2**. This pathway would be increasingly plausible

with the less coordinating counterion on gold.[26–28] The counterion TFA is intermediate in coordinating ability, raising both possibilities.

Initial analysis of the reaction mixture of the oxyboration reaction in eq 2.1 prior to reaction completion by ESI-HRMS was done by graduate student Joel Johnson, revealed the presence of molecular ion peaks consistent with the TFA-coordinated tetraborate component [M^-, *m/z* = 425.0820] of intermediate **2.5**, or possibly in the cyclized intermediate **2.11**, and organogold intermediate **2.8** [$(M+H)^+$, *m/z* = 779.3294]. These initial findings suggested the viability of gold and trifluoroacetate intermediates in the oxyboration reaction, as proposed in Scheme 2.2. The simple detection of compounds, however, does not imply kinetic relevance. To further probe the role of gold and counterion, the reaction order with respect to substrate **2.1** and trifluoroacetate via kinetic studies of the transformation of **2.1** to **2.2** under standard condition in the presence of NaCl (eq 2.2), and investigation into whether the oxyboration reaction can also be catalyzed by carbophilic Lewis acid catalysis in the absence of assistance by TFA were done by previous graduate student Joel S. Johnson and previous postdoctoral scholar Dr. Eugene Chong. My contribution to this study through investigating the reaction order with respect to the catalyst IPrAuTFA and the detrimental role of NaCl is described below.

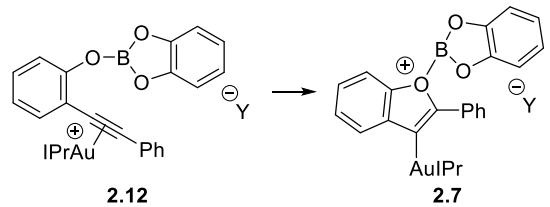

2.12 **2.7** (2.2)

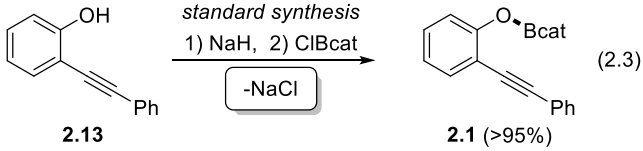

2.13 **2.1** (>95%) (2.3)

We considered the possibility that the presence of NaCl byproduct, generated during the preparation of **2.1** (eq 2.3), might have detrimental effect to the reaction. As the IPrAuCl complex was previously shown to be an incompetent catalyst for this reaction,[5] we hypothesized that NaCl, although only limitedly soluble in toluene, might not be benign. It might cause catalyst inhibition from counterion exchange with the IPrAuTFA catalyst into the inactive IPrAuCl complex (eq 2.4), such that the rate-determining step under the reaction conditions was regeneration of the active catalyst.[34,35] We further hypothesized that the additional NaTFA[5,6] might be preventing this catalyst quenching by chloride through the common ion effect to push the equilibrium of eq 2.4 to the left to increase the concentration of the active IPrAuTFA catalyst. Hence, a chloride-free synthetic route to starting material **2.1** was examined next.

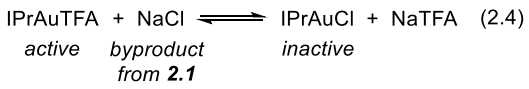

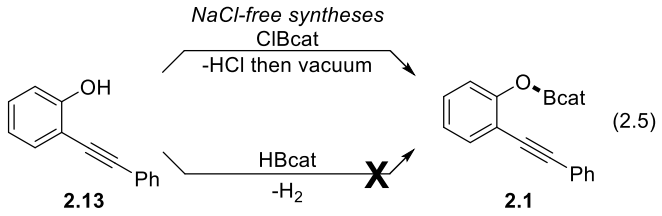

*Change in route of synthesis of substrate **2.1**: sodium chloride-free generation was performed by graduate student Joel Johnson and described here for context.* The treatment of **2.13** with one equiv of ClBcat (eq 2.5, top arrow), followed by removal of the HCl byproduct under vacuum, afforded **2.1** in quantitative yield via a route suitable for small-scale mechanistic experiments; This approach is less practical from a synthetic standpoint than the previous substrate synthesis due to the formation of corrosive HCl gas and the requirement to trap this gas under vacuum. Unfortunately, the exploration of an alternative synthesis of **2.1** from the reaction of **2.13**

and HBcat (eq 2.5, bottom arrow) that could generate less corrosive hydrogen gas as the byproduct was unsuccessful.

With this project's status, I investigated the reaction order with respect to gold, and found that the kinetic dependence on gold varied depending on the method of substrate synthesis. With substrate **2.1** in hand using eq 2.5, the kinetics of NaCl-free oxyboration reaction was examined (Table 2.1). With 5 mol % IPrAuTFA catalyst alone in the absence of any additive, a significantly faster reaction rate for the formation of **2.2** was observed with $k_{obs} = 54 \pm 6$ μM s^{-1} (Table 2.1, entry 2), than the rate observed with the previously reported NaCl-present conditions using 5 mol % IPrAuTFA and the largest amount of additive 30 mol % NaTFA ($k_{obs} = 9.2 \pm 1.1$ μM s^{-1}). These drastically different k_{obs} values observed between NaCl-free and NaCl-present conditions support the hypothesis that NaCl is indeed inhibiting gold catalysis, presumably due to the chloride quenching of the catalytically active $IPrAu^{+}$ species into inactive IPrAuCl.

Table 2.1. Oxyboration of NaCl-free generated substrate **2.1** and the effect of NaTFA additive on this reaction

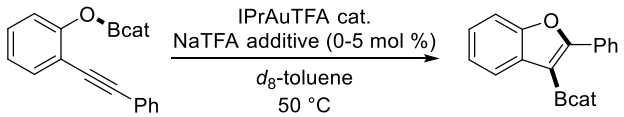

2.1 (from eq 2.5)
from NaCl-free synthesis

2.2

entry	IPrAuTFA (mol %)	NaTFA (mol %)	k_{obs} (μM s^{-1})
1	0	0	no formation of **2.2**
2	5.0	0	54 ± 6
3	5.0	5.0	19 ± 1

Under the conditions of Table 2.1, the reaction no longer displayed zero-order substrate kinetics. This result was consistent with a change in rate-determining step such that the rate was no longer limited by catalyst generation.

In order to examine the kinetic dependence on substrate and catalyst concentration more clearly under NaCl-free conditions, I varied the catalyst loading from 0, 1.25, 2.5, 5, and 7.5 mol % and the fit of the reaction kinetics was examined. Neither zero, first, nor second order kinetics fit the full reaction course (example, 2.5 mol % catalyst, average of triplicate runs, Figure 2.1a). Specifically, the first-order assessment plot displayed a slight data curvature that deviated from the linear fit for both 2.5 and 5 mol % catalyst Figure 2.1b,d). The second-order assessment plot deviated slightly at early reaction times with 2.5 mol % catalyst but fit well for the full measured reaction course for 5.0 mol % (Figure 2.1c,e). Because the rate of product formation was slower than required for a good fit at early times, these fits may imply a catalyst induction period. In the case of 7.5 mol %, wherein the reaction was sufficiently fast that initial rates were not measured, the kinetics best fit first order (see experimental section for data and fits from 1.25 and 7.5 mol % catalyst.) This deviation at early conversions precluded using initial rates to determine the order in the gold catalyst. In the absence of catalyst no product formation occurred (Table 2.1, entry 1).

Interestingly, the addition of 5 mol % NaTFA additive under NaCl-free reaction conditions lead to a decreased reaction rate (k_{obs} = 19 ± 1 μM s^{-1}; Table 2.1, entry 3); under these conditions, the previously accelerating additive had a decelerating effect. The increased availability TFA in solution may shift the equilibrium between proposed species (TFA)Bcat **2.9** and $[(TFA)_2Bcat]^-$ **2.10**, towards **2.10** (Scheme 2.2). The plausibility of such an equilibrium and proposal was supported by the detection of **2.10** by MS in a related model reaction between commercially available ClBcat, as a surrogate boron electrophile to (TFA)Bcat, and NaTFA. Therefore, NaTFA additive is necessary to overcome catalyst inhibition by NaCl, but an additional equivalent of NaTFA respective to gold can impede catalysis.

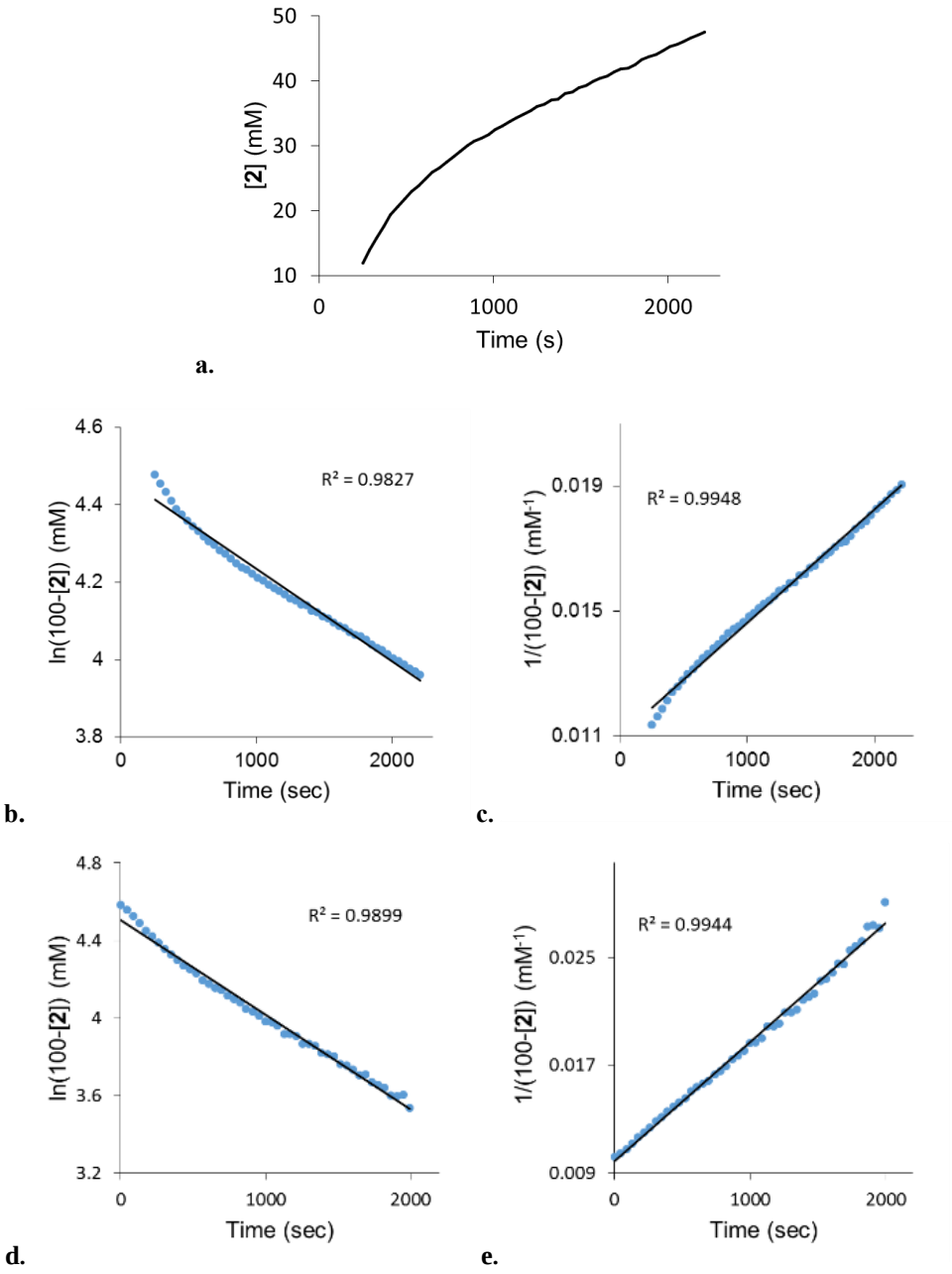

Figure 2.1. a. Plot of formation of **2.2** versus time using 2.5 mol % IPrAuTFA at 50 °C, showing a nonzero-order rate dependence on substrate concentration. b. First-order fit plot with 2.5 mol % catalyst. c. Second-order fit plot with 2.5 mol % catalyst. d. First-order fit plot with 5.0 mol % catalyst. e. Second-order fit plot with 5.0 mol % catalyst.

Given these results with chloride-free conditions, the catalysts with and without the possibility of Lewis-base assistance display reactivity sufficiently similar for the conclusion that Lewis-base assistance is not a requirement for oxyboration; nevertheless, the operation of such an assisted mechanism with the TFA counter ion when it is present cannot be ruled out.

In the scenario that oxyboration mechanism is indeed operated independently by carbophilic Lewis acid catalysis by $IPrAu^+$ species without the innersphere assistance with counterion (Y^-), we propose that the reaction follows the revised pathway shown in Scheme 2.3. One possible transmetalation mechanism is that after intermediate **2.12** undergoes IPrAu-catalyzed cyclization, the resulting two cyclized intermediates **2.7** could undergo intermolecular transmetalation to afford product **2.2** and regenerate the catalyst. While the concentration of two activated complexes might be low, analogous gold-activated cyclization intermediates have been observed to build up by NMR in other systems.[20] An alternative consistent mechanism that avoids the need to bring two activated molecules together involves intermediate **2.7** reacting with starting material **2.1** in a metal/metalloid transfer step. This alternative mechanism is also plausible.

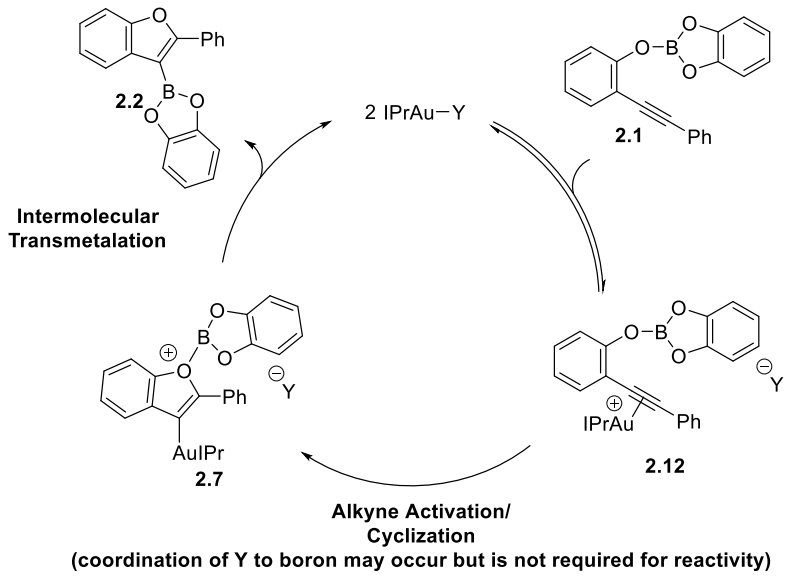

Scheme 2.3. Revised proposed mechanism for oxyboration

Conclusions

The revised proposed mechanism arose from my kinetic measurements identified a dependence on the route of substrate synthesis. When residual sodium chloride was present, the catalyst was quenched, despite the low solubility of this ionic compound in toluene. However,

chloride-induced catalyst inhibition of cationic gold can be circumvented by using the NaTFA additive, and its substoichiometric addition was beneficial to reviving the catalytic activity of gold. Determination of the noninnocent role of sodium chloride is expected to facilitate catalytic reaction development because sodium salts are increasingly attractive for late-metal catalyst generation, given that the alternative silver salts have already been established to be noninnocent. The understanding of reaction mechanism for Lewis-acid catalyzed oxyboration is similarly anticipated to assist in the development of new B–X addition reactions to alkynes and alkenes.

References

(1) Johnson, J. S.; Chong, E.; Tu, K. N.; Blum, S. A. *Organometallics* **2016**, *35*, 655–662.
(2) Miyaura, N. In *Catalytic Heterofunctionalization*; Wiley-VCH Verlag GmbH: Weinheim, FRG; pp 1–45.
(3) Suginome, M. *Chem. Rec.* **2010**, *10*, 348–358.
(4) Barbeyron, R.; Benedetti, E.; Cossy, J.; Vasseur, J.-J.; Arseniyadis, S.; Smietana, M. *Tetrahedron* **2014**, *70*, 8431–8452.
(5) Hirner, J. J.; Faizi, D. J.; Blum, S. A. *J. Am. Chem. Soc.* **2014**, *136*, 4740–4745.
(6) Chong, E.; Blum, S. A. *J. Am. Chem. Soc.* **2015**, *137*, 10144–10147.
(7) Tu, K. N.; Hirner, J. J.; Blum, S. A. *Org. Lett.* **2016**, *18*, 480–483.
(8) Dorel, R.; Echavarren, A. M. *Chem. Rev.* **2015**, *115*, 9028–9072.
(9) Hashmi, A. S. K.; Frost, T. M.; Bats, J. W. *Org. Lett.* **2001**, *3*, 3769–3771.
(10) Hashmi, A.; Enns, E.; Frost, T.; Schäfer, S.; Frey, W.; Rominger, F. *Synthesis (Stuttg).* **2008**, *2008*, 2707–2718.
(11) Zhang, Y.; Xin, Z.-J.; Xue, J.-J.; Li, Y. *Chinese J. Chem.* **2008**, *26*, 1461–1464.
(12) Hashmi, A. S. K.; Ramamurthi, T. D.; Rominger, F. *Adv. Synth. Catal.* **2010**, *352*, 971–975.
(13) Abbiati, G.; Marinelli, F.; Rossi, E.; Arcadi, A. *Isr. J. Chem.* **2013**, *53*, 856–868.
(14) Hirner, J. J.; Roth, K. E.; Shi, Y.; Blum, S. A. *Organometallics* **2012**, *31*, 6843–6850.
(15) Shi, Y.; Peterson, S. M.; Haberaecker, W. W.; Blum, S. A. *J. Am. Chem. Soc.* **2008**, *130*, 2168–2169.
(16) Lu, Z.; Han, J.; Hammond, G. B.; Xu, B. *Org. Lett.* **2015**, *17*, 4534–4537.
(17) Wang, D.; Cai, R.; Sharma, S.; Jirak, J.; Thummanapelli, S. K.; Akhmedov, N. G.; Zhang, H.; Liu, X.; Petersen, J. L.; Shi, X. *J. Am. Chem. Soc.* **2012**, *134*, 9012–9019.
(18) Hirner, J. J.; Shi, Y.; Blum, S. A. *Acc. Chem. Res.* **2011**, *44*, 603–613.
(19) Hirner, J. J.; Blum, S. A. *Tetrahedron* **2015**, *71*, 4445–4449.
(20) Shi, Y.; Roth, K. E.; Ramgren, S. D.; Blum, S. A. *J. Am. Chem. Soc.* **2009**, *131*, 18022–18023.
(21) Forward, J. M.; Fackler, J. P.; Staples, R. J. *Organometallics* **1995**, *14*, 4194–4198.
(22) Partyka, D. V.; Zeller, M.; Hunter, A. D.; Gray, T. G. *Inorg. Chem.* **2012**, *51*, 8394–8401.
(23) Partyka, D. V.; Zeller, M.; Hunter, A. D.; Gray, T. G. *Angew. Chem. Int. Ed.* **2006**, *45*,

8188–8191.
(24) Hofer, M.; Gomez-Bengoa, E.; Nevado, C. *Organometallics* **2014**, *33*, 1328–1332.
(25) Smith, D. A.; Roşca, D.-A.; Bochmann, M. *Organometallics* **2012**, *31*, 5998–6000.
(26) Strauss, S. H. *Chem. Rev.* **1993**, *93*, 927–942.
(27) Beck, W.; Suenkel, K. *Chem. Rev.* **1988**, *88*, 1405–1421.
(28) Krossing, I.; Raabe, I. *Angew. Chem. Int. Ed* **2004**, *43*, 2066–2090.
(29) Akoka, S.; Barantin, L.; Trierweiler, M. *Anal. Chem.* **1999**, *71*, 2554–2557.
(30) Hansmann, M. M.; Melen, R. L.; Rudolph, M.; Rominger, F.; Wadepohl, H.; Stephan, D. W.; Hashmi, A. S. K. *J. Am. Chem. Soc.* **2015**, *137*, 15469–15477.
(31) Warner, A. J.; Lawson, J. R.; Fasano, V.; Ingleson, D. M. J. *Angew. Chem. Int. Ed. Engl.* **2015**, *54*, 11245.
(32) Chen, C.; Kehr, G.; Fröhlich, R.; Erker, G. *J. Am. Chem. Soc.* **2010**, *132*, 13594–13595.
(33) Anslyn, E. V.; Dougherty, D. A. University Science: Sausalito, 2006; p 396.
(34) Sanford, M. S.; Ulman, M.; Grubbs, R. H. *J. Am. Chem. Soc.* **2001**, *123*, 749–750.
(35) Rosner, T.; Pfaltz, A.; Blackmond, D. G. *J. Am. Chem. Soc.* **2001**, *123*, 4621–4622.
(36) Wang, F.-P.; Chen, D.-L.; Deng, H.-Y.; Chen, Q.-H.; Liu, X.-Y.; Jian, X.-X. *Tetrahedron* **2014**, *70*, 2582–2590.
(37) de Frémont, P.; Marion, N.; Nolan, S. P. *J. Organomet. Chem.* **2009**, *694*, 551–560.

Experimental

General Methods

All manipulations were conducted under nitrogen atmosphere using a glovebox or standard Schlenk techniques unless stated otherwise. All chemicals were used as received from commercial sources unless otherwise noted. Sodium trifluoroacetate (NaTFA) was dried at 130 °C under vacuum (10 mTorr) for 24 h before use. Toluene, CH_2Cl_2, and Et_2O were purified by passage through an alumina column under argon pressure on a push-still solvent system. d_8-Toluene was dried over CaH_2, degassed using three freeze-pump-thaw cycles, and vacuum transferred prior to use. ^1H, ^{11}B and ^{19}F NMR spectra were recorded on a Bruker AVANCE-600 or Bruker DRX-400 spectrometer. All chemical shifts (δ) are reported in parts per million (ppm) and referenced to the residual proton solvent peak (δ = 7.26 ppm for $CDCl_3$, δ = 2.08 ppm for d_8-toluene in ^1H NMR spectra). ^{11}B and ^{19}F NMR spectroscopy experiments are referenced to the absolute frequency of 0 ppm in the ^1H dimension according to the Xi scale. Low- and high-resolution mass spectrometry data were obtained at the University of California, Irvine.

Synthesis of 2-(phenylethynyl)phenol (2.13). A flame dried 1 L round-bottom flask equipped with a stir bar was charged with 2-iodophenol (14.0 g, 63.6 mmol), CuI (1.09 g, 5.71 mmol), and $Pd(PPh_3)_2Cl_2$ (1.33 g, 1.89 mmol). To this flask, toluene (320 mL), diisopropylamine (8.90 mL, 63.6 mmol), and phenylacetylene (10.5 mL, 95.4 mmol) were added sequentially. The reaction mixture was stirred for 8.5 h at 25 °C. Ethyl acetate (100 mL) was added and the organic layer was washed with saturated ammonium chloride solution (50 mL), then brine (50 mL), and dried over sodium sulfate. The organic layer was filtered, concentrated, and the resulting dark brown oil was purified by flash chromatography (12% EtOAc in hexanes). The resultant oil was further recrystallized from hexanes to afford a brown crystalline solid (6.82 g, 55%). ^1H NMR (600 MHz,

$CDCl_3$): δ 7.58-7.56 (m, 2H), 7.45 (dd, *J* = 7.6, 1.6 Hz, 1H), 7.40-7.39 (m, 3H), 7.31-7.28 (m, 1H), 7.02 (dd, *J* = 8.3, 0.8 Hz, 1H), 6.94 (td, *J* = 7.5, 1.0 Hz, 1H), 5.89 (s, 1H). This spectrum is in agreement with previously reported spectral data.[1]

Synthesis of IPrAuTFA (2.4). IPrAuCl (124 mg, 0.200 mmol) and AgTFA (44.2 mg, 0.200 mmol) were weighed in separate vials. IPrAuCl was dissolved in CH_2Cl_2 (1 mL), and this solution was transferred to the vial containing AgTFA. Additional CH_2Cl_2 (1 mL) was used to rinse the vial during the transfer. The vial was capped with a Teflon-coated cap and covered in aluminum foil, and the reaction mixture was stirred for 30 h in the glovebox. The resulting reaction mixture was then filtered through glass fiber filter paper. The filtrate was concentrated in vacuo to afford a colorless solid (110 mg, 79%). This complex was used without further purification, and its ^{1}H spectrum is in agreement with previously reported spectral data.[2] ^{1}H NMR (400 MHz, d_8-toluene): *δ* 7.13 (t, *J* = 7.8 Hz, 2H), 6.97 (d, *J* = 7.8 Hz, 4H), 6.30 (s, 2H), 2.47 (septet, *J* = 6.8 Hz, 4H), 1.36 (d, *J* = 6.8 Hz, 12H), 1.03 (d, *J* = 6.8 Hz, 12H).

General Procedure for the Preparation of Kinetic Experiment Samples. *Example given for NaCl-free synthesis of **2.1** (eq 2.5, top arrow) and subsequent oxyboration reaction using 5 mol % IPrAuTFA:* **2.13** (34.0 mg, 0.175 mmol) was dissolved in d_8-toluene (250 μL) and added to the vial containing *B*-chlorocatecholborane (27.0 mg, 0.175 mmol). Additional d_8-toluene (250 μL) was used to rinse and transfer. The solution was allowed to sit for 20 min, and the HCl byproduct and solvent removed under vacuum for 40 min. The resulting compound **2.2** was dissolved in d_8-toluene (1400 μL). From this boric ester stock solution, 400 μL was transferred to a J. Young NMR tube and capped with a rubber septum. This was repeated a total of three times to create three identical samples. To prepare the 5 mol % IPrAuTFA stock solution, the IPrAuTFA catalyst (6.1 mg, 0.0088 mmol) was dissolved in d_8-toluene (350 μL).

General Procedure for Kinetic Experiments. The J. Young NMR tube containing **2.2** (from above procedure) and one gas tight syringe with 100 μL of the IPrAuTFA solution, capped with a rubber stopper, were removed from the glovebox. The rubber septum on the J. Young NMR tube was wrapped in Parafilm. The sample in the J. Young NMR tube was immediately transported to the NMR spectrometer, which underwent temperature calibration before sample injection. The IPrAuTFA solution was injected using the gas tight syringe into the J. Young NMR tube. This tube was shaken and inserted into the NMR spectrometer. Acquisition of spectra immediately followed. The acquisition time was set to 6 s. A 90° pulse was used. The line broadening was set to 1 Hz. The number of scans per experiment = 1. The number of dummy scans = 0. Fifty experiments were conducted sequentially with 34 s delays between experiments.

Table S2.1. Triplicate kinetic Plots for the NaCl-free Conditions.

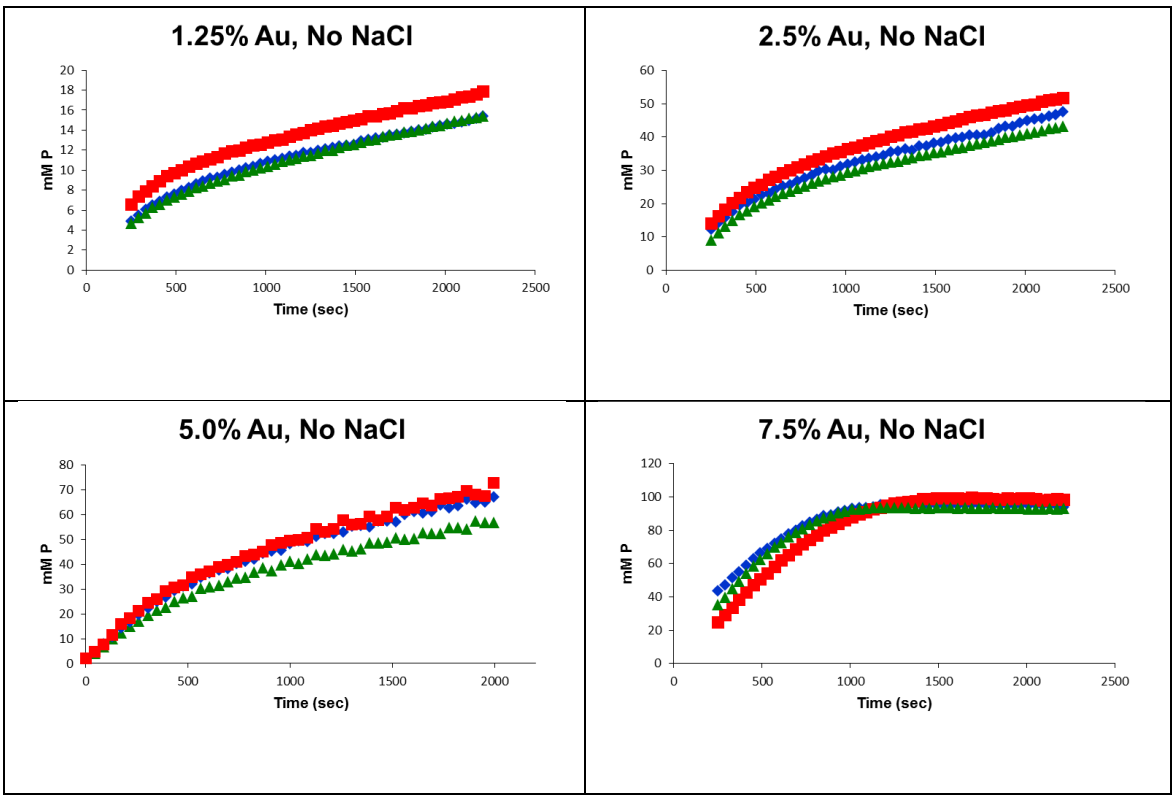

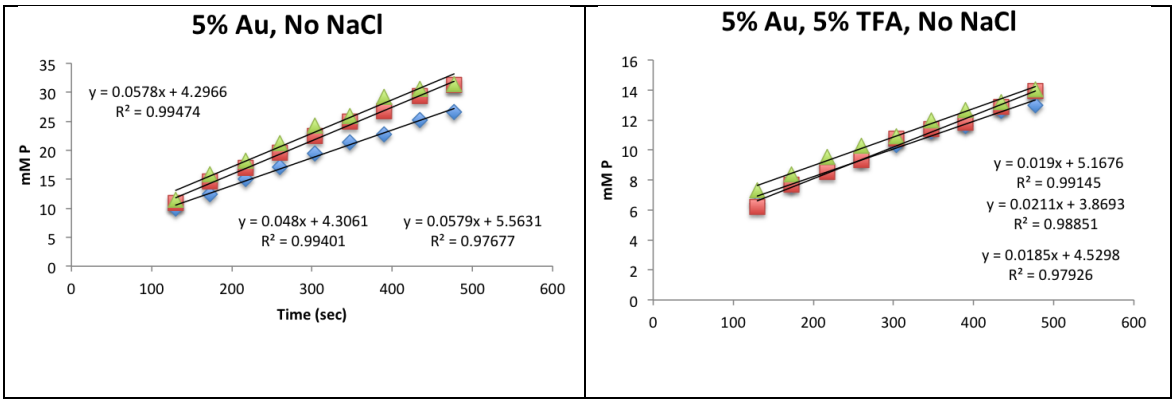

Comparison of 1st Order and 2nd Order Substrate Fittings Under Chloride-Free Conditions.

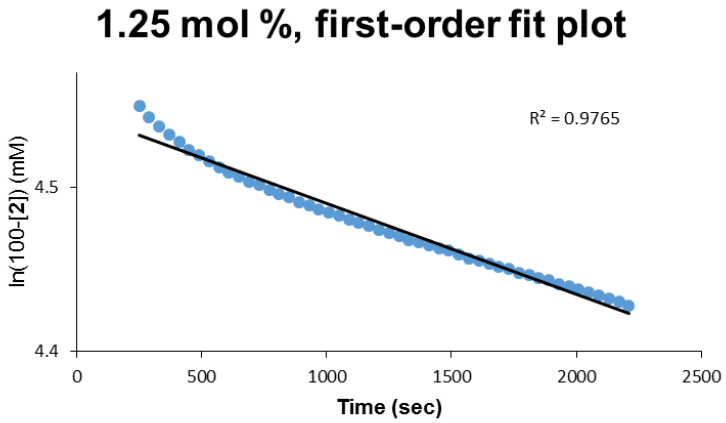

a.

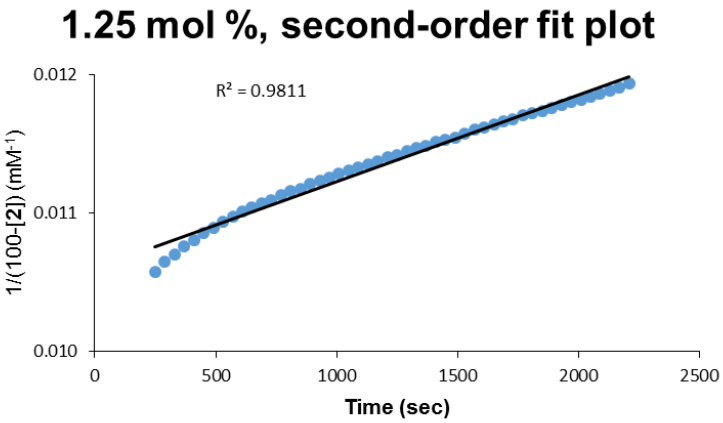

b.

Figure S2.1. a. First-order fit plot for average of triplicate runs with 1.25 mol % catalyst. **b.** Second-order fit plot for average of triplicate runs with 1.25 mol % catalyst.

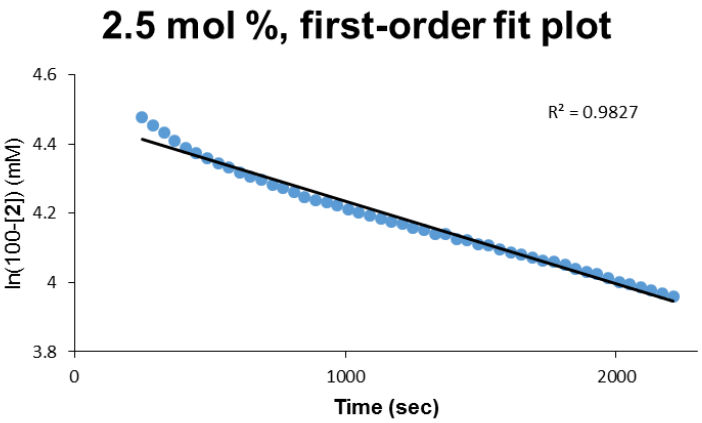

a.

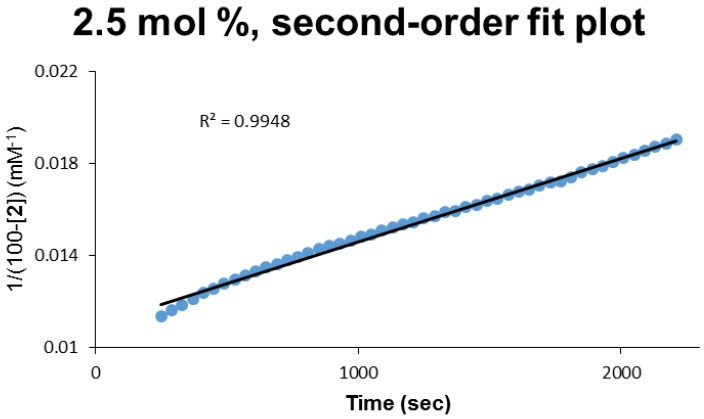

b.

Figure S2.2. a. First-order fit plot for average of triplicate runs with 2.5 mol % catalyst. **b.** Second-order fit plot for average of triplicate runs with 2.5 mol % catalyst.

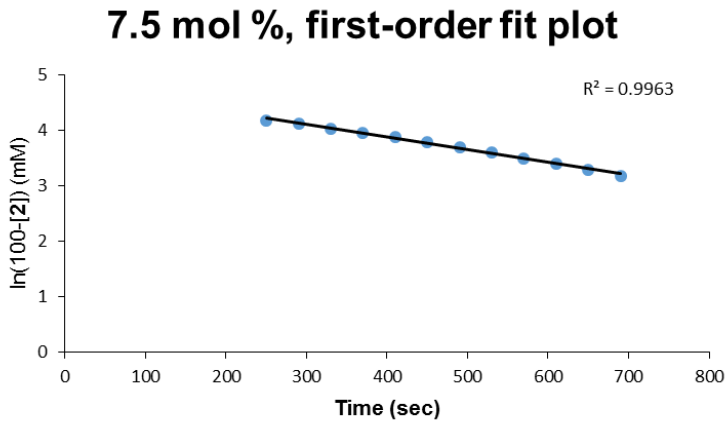

a.

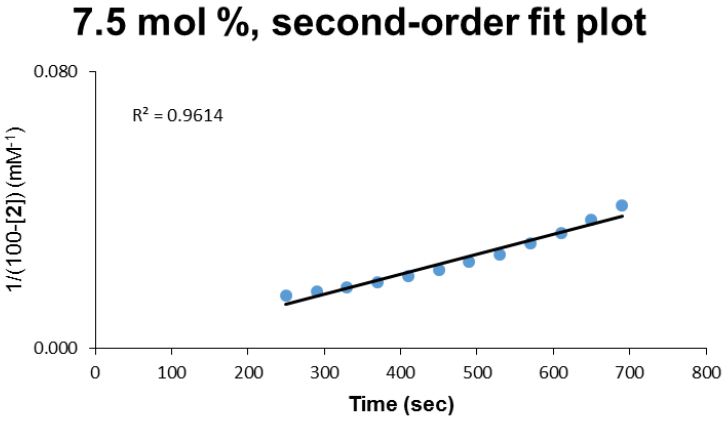

b.

Figure S2.3. a. First-order fit plot for average of triplicate runs with 7.5 mol % catalyst. **b.** Second-order fit plot for average of triplicate runs with 7.5 mol % catalyst.

References for Experimental Section

(1) Hirner, J. J.; Faizi, D. J.; Blum, S. A. *J. Am. Chem. Soc.* **2014**, *136*, 4740–4745.
(2) Chong, E.; Blum, S. A. *J. Am. Chem. Soc.* **2015**, *137*, 10144–10147.
(3) Jeon, J. Y.; Varghese, J. K.; Park, J. H.; Lee, S.-H.; Lee, B. Y. *Eur. J. Org. Chem.* **2012**, *2012*, 3566–3569.
(4) de Frémont, P.; Marion, N.; Nolan, S. P. *J. Organomet. Chem.* **2009**, *694*, 551–560.

Chapter 3

Oxyboration With and Without a Catalyst: Borylated Isoxazoles via B–O σ-Bond Addition

Abstract Herein we report an oxyboration reaction with activated substrates that employs B–O σ bond additions to C–C π bonds to form borylated isoxazoles, which are potential building blocks for drug discovery. While this reaction can be effectively catalyzed by gold, it is the first example of uncatalyzed oxyboration of C–C π bonds by B–O σ bonds—and only the second example that is catalyzed. This oxyboration reaction is tolerant of groups incompatible with alternative lithiation/borylation and palladium-catalyzed C–H activation/borylation technologies for the synthesis of borylated isoxazoles. Mechanistic experiments, including a stoichiometric organogold-to-boron transmetalation reaction, identify a two-step transmetalation process with breakdown of a tetracoordinate borate/cationic gold ion pair as the rate-determining step in this transmetalation reaction and plausibly in the overall catalytic oxyboration reaction. The complimentary bond disconnections and functional-group tolerance enabled by this method are highlighted in the synthesis of valdecoxib, a COX-2 inhibitor, and its ester-containing analog. The scalability of the reaction is demonstrated by a gram-scale uncatalyzed oxyboration reaction. This chapter is reprinted in part, with permission from a previously published report where I served as first author.[1]

Introduction

Isoxazoles[2] exhibit a wide variety of biological activities, including analgesic,[3] antibiotic,[4] antidepressant,[5] and anticancer[6] activities. Consequently, borylated isoxazoles are valuable bench-stable building blocks for drug discovery.[7–11] Oxyboration reactions that proceed through the addition of B–O σ bonds to C–C π bonds would be an attractive route to these and other building blocks by transforming easily formed B–O σ bonds into more difficult to form B–C σ bonds. Yet the addition of B–O σ bonds to C–C multiple bonds had remained elusive for 65 years[12,13] until our first report in 2014.[14] We herein report catalyzed and uncatalyzed oxyboration routes to borylated isoxazoles. This is the first report of uncatalyzed oxyboration of C–C π bonds with B–O σ bonds. This oxyboration method is tolerant of a wide variety of functional groups and produces

exclusively the 4-borylated regioisomer, which establishes the generality of oxyboration strategies[14–16] to generate borylated heterocycles for drug discovery. Specifically, compounds of this type may currently be accessed through the [3+2] cycloaddition reaction of nitrile oxides and alkynylboronates as shown in Scheme 3.1. However, this method can produce two regioisomers and the alkynylboronate synthesis involves a lithiation step, which is incompatible with other halide or electrophilic substituents.[17] Alternatively, the Pd(0)-catalyzed Miyaura borylation[18,19] and lithiation/electrophilic borylation[20] have been used for the synthesis of borylated heterocycles, but, as with lithiation/cycloaddition, aryl bromides and electrophilic functional groups are reactive under these conditions.

Inspired by previous reports from Perumal[21] and Ueda,[22] who demonstrated analogous Au-catalyzed rearrangements of oximes to form 4-substituted isoxazoles without boron, we considered that analogous routes to borylated isoxazoles may be assessable through oxyboration. We hypothesized that this gold-catalyzed oxyboration reaction could proceed through carbophilic Lewis acid activation of the C–C π bond, a mechanistically distinct route to B–Element addition reactions.[14–16] The oxyboration reaction developed here is an operationally simple one-pot procedure from oximes and requires no isolation of reaction intermediates (Scheme 3.1).

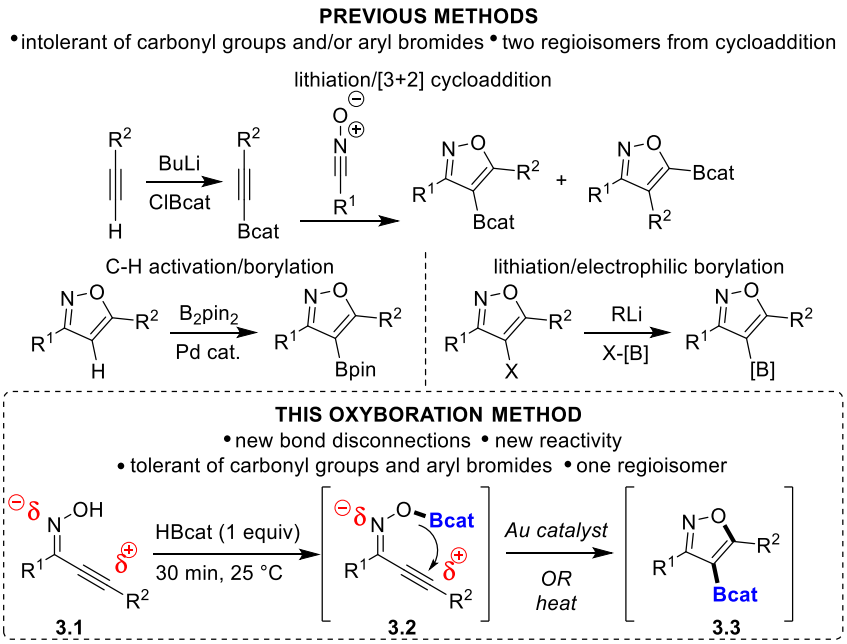

Scheme 3.1. Comparison of previous methods and new oxyboration method for the synthesis of 4-borylated isoxazoles

Results and Discussion

Building on an initial hit by graduate student Joshua John Hirner with a gold catalyst, I developed the reaction through optimization studies with model substrate **3.1a**. We first investigated a series of Au catalysts through varying oxidation state and counterion (Table 3.1, entries 1–5). The catalyst IPrAuTFA proved an optimal balance of counterion coordinating ability.[23] The catalyst IPrAuOAc, with the more strongly coordinating acetate ion[24] did not lead to any detectable product formation. A control reaction with catalytic NaTFA (Table 3.1, entry 6) in place of IPrAuTFA showed no product, confirming a key role for the gold. Control experiments with IPrAuCl (no product formation) and separately with AgTFA (30% ^{1}H NMR yield of product vs. 90% under identical conditions but with IPrAuTFA) confirmed the catalytic activity was optimal with IPrAuTFA and not its synthetic precursors (Table 3.1, entries 7–9). A survey of catalyst loading and reaction temperature (Table 3.1, entries 10–13) determined the optimal loading to be 2.5 mol %, resulting in full conversion (90% ^{1}H NMR yield) after 6 h at 50 °C.

Table 3.1. Selected Data from Optimization Study[a]

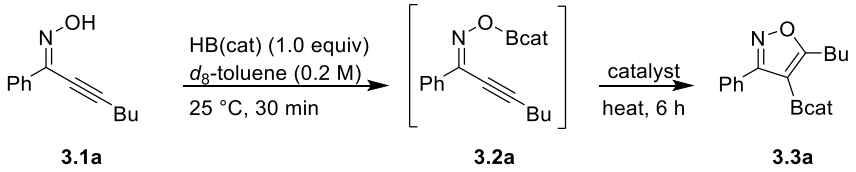

3.1a **3.2a** **3.3a**

entry	catalyst	temperature (°C)	cat. loading (% mol)	yield[b]
1	AuCl	50	2.5	0
2	$AuCl_3$	50	2.5	0
3	IPrAuOAc	50	2.5	0
4	IPrAuOTs	50	2.5	34
5	IPrAuTFA	50	2.5	90
6	NaTFA	50	2.5	0
7	None	50	0	0
8	IPrAuCl	50	2.5	0
9	AgTFA	50	2.5	48
10	IPrAuTFA	50	1.0	85[c]
11	IPrAuTFA	50	5.0	90
12	IPrAuTFA	50	10	92
13	IPrAuTFA	25	10	89[d]

[a]Reactions were carried out on a 0.10 mmol scale. [b]Yields were determined by the ERECTIC method using mesitylene as ^{1}H NMR external standard. [c]23 h. [d]22 h.

Interestingly, oxyboration of **3.1a** could be carried out under catalyst-free conditions, albeit with higher temperatures and longer reaction times. Specifically, heating **3.1a** to 110 °C for 17 h afforded **3.3a** in 58% ^{1}H NMR yield (Table 3.2). Similarly, cyclization of **3.1c** under catalyst-free conditions of 110 °C for 17 h produced **3.3c** in 89% ^{1}H NMR yield. We hypothesize that the Michael-acceptor/polar character of the starting materials enables this catalyst-free oxyboration through lowering the barrier of cyclization (Scheme 3.1); alternatively, the nucleophilic nitrogen lone pair[25] of the hydroxylimine may coordinate and activate the boron. Identification of this class of activated substrates thus provides access to catalyst-free reactivity that was not possible within our earlier reported oxyboration substrates.[14–16] In contrast to the reactivity exhibited by **3.1a** and **3.1c**, when silylated **3.1f** was used as the substrate for catalyst-free oxyboration, only B–O σ-bond

formation was observed (boric ester **3.2f**), and no cyclized products were formed even after an extended time of heating at 110 °C. This lack of reactivity possibly derives from the steric hindrance and the electron-donating ability of the trimethylsilyl group[26] adjacent to the alkyne carbon, which may alter the polarization of the alkyne, rendering it less susceptible of nucleophilic attack. Because of its reduced temperatures, shorter reaction times, and no action with the silylated substrate, the metal-catalyzed route was selected for further isolation.

Table 3.2. Initial reaction development with and without catalyst

	R^1/R^2	IPrAuTFA 6 h, 50 °C	Uncatalyzed 6 h, 50 °C	Uncatalyzed 17 h, 110 °C
2.1a	Ph/Bu	90%	<1%	58%
2.1c	4-BrPh/Bu	93%	4%	89%
2.1f	Ph/TMS	87%	<1%	<1%

This oxyboration method provided a new set of bond disconnections to access previously unreported isoxazole pinacol boronic esters **3.4a**–**3.4k** (except **3.4f**[17]), which are isolable by silica gel chromatography and are bench-stable building blocks for a variety of downstream reactions[7,8] as shown in Scheme 3.2. The numbers in parentheses denote the ^{1}H NMR spectroscopy yield of catechol boronic ester **3.3** relative to an external standard. The numbers outside the parentheses in the first row denote the isolated yield of bench-stable pinacol boronic ester **3.4**.[27] The numbers outside the parentheses in the second row correspond to the reaction time of the uncatalyzed oxyboration when run at 110 °C. After completion of the catalytic reaction, PPh_3 was employed to quench the active catalyst IPrAuTFA by trapping it as the catalytically inactive $[IPrAuPPh_3]^+$.[28]

We herein compare the catalyzed reaction yields with those obtained through the uncatalyzed method for each substrate. To permit direct comparison, both reactions were performed at 0.2 M in substrate. The lengthy reaction times for the uncatalyzed reaction were reduced at higher concentration in substrate upon scale-up (vide infra, eq 3.3). With the exception

of silylated **3.1f**, all substrates showed uncatalyzed reactivity at longer reaction times. Bulky substituents such as tert-butyl and trimethylsilyl, however, only produced very low ^{1}H NMR yield (24% for **3.3d** and <1% for **3.3f**), with the starting materials remaining. Thus they required catalysis for synthetically useful product formation. The electron poor *p*-CF_3 substrate and 3-furyl substrate, required a rather lengthy 18–21 d to reach full conversion at 110 °C. In many cases, the cost benefit of obtaining the product under catalyst-free conditions may be desired in exchange for elevated temperatures and marginally longer reaction times, most notably with **3.4c**, **3.4e**, **3.4h**, **3.4i**, **3.4k**, reactions which achieved similar ^{1}H NMR yields to the catalyzed reactions in 20–65 h.

Interestingly, substrates that exhibited slow conversions under the catalyzed conditions for apparent electronic reasons (rather than steric reasons) such as **3.1i** and **3.1k** were the faster converting substrates under the uncatalyzed conditions; it may be that the electronics that favor π Lewis acid catalysis though gold–alkyne binding disfavor cyclization in the absence of a catalyst. This orthogonality in electronic and steric substrate reactivity highlights the complementarity provided by the catalyzed and uncatalyzed methods. Both the metal-catalyzed and the uncatalyzed oxyboration reactions are tolerant of functional groups that would otherwise be sensitive to alternative borylation methods. For example, aryl bromide **3.1c** smoothly undergoes oxyboration to produce borylated isoxazole **3.3c** (93% ^{1}H NMR yield, 65% isolated yield of **3.4c** with a catalyst; 91% ^{1}H NMR yield without a catalyst). This substrate would be sensitive to a lithiation/borylation sequence[20,29] because of competitive lithium/halogen exchange,[30] and to an alternative palladium-catalyzed borylation[18,19] because of competitive oxidative addition of the aryl–bromide bond. The nitro group in **3.1e** and the ester group in **3.1k** are similarly tolerated, producing oxyboration product **3.3e** in 90% ^{1}H NMR yield (60% isolated yield of **3.4e**) and **3.3k** in 94% ^{1}H NMR yield (64% isolated yield of **3.4k**) under catalysis whereas these groups are

intolerant of alternative lithiation techniques.[20] Furan-substituted **3.4b** demonstrates the complementary bond disconnections enabled by oxyboration to avoid competitive ortho-borylation of the furan ring[31] which would compete under alternative lithiation/borylation strategies (85% ^{1}H NMR yield of **3.3b**; 71% isolated yield of **3.4b**).

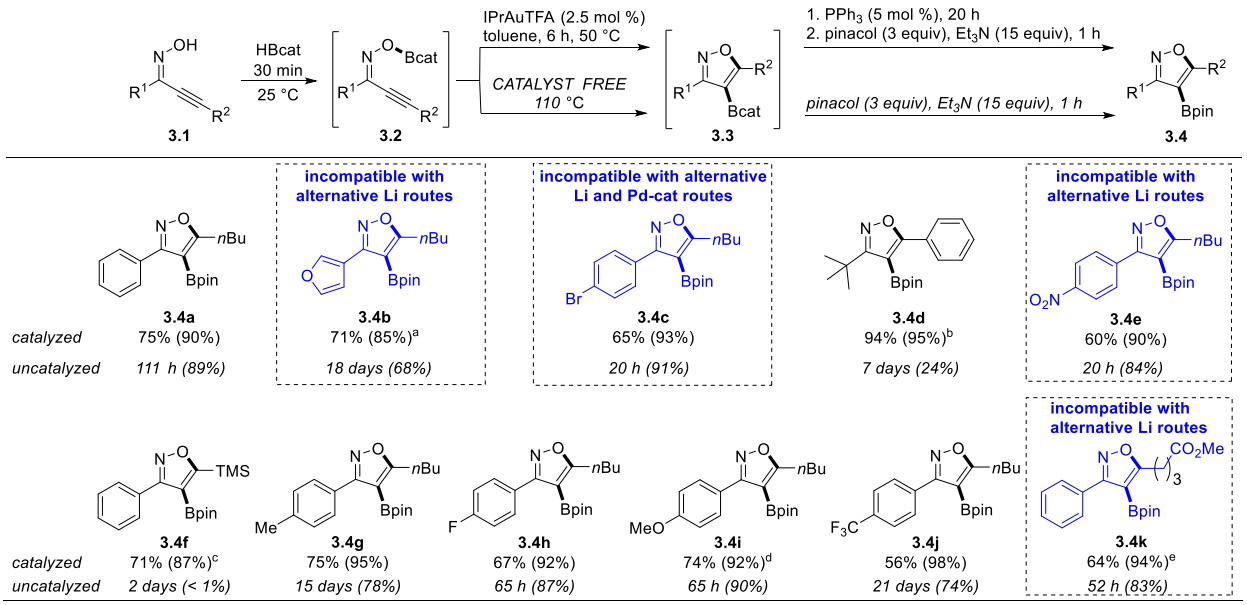

Scheme 3.2. Reaction substrate scope. Substrates shown in blue are incompatible with alternative routes. All substrates give exclusively 4-borylated regioisomer

In addition, heteroaryl (**3.4b**), aliphatic (**3.4d**), electron-poor aryl (**3.4e**, **3.4j** and **3.4k**), silyl (**3.4f**), and electron-rich aryl (**3.4g** and **3.4i**) are all compatible with the reaction conditions. Some substrates required higher reaction temperature and/or longer reaction time to achieve full conversion under catalytic conditions, while no reaction was observed when the same conditions were applied in the absence of an Au catalyst. Oxyboration products **3.3d** and **3.3f** required 110 °C for 4 h and 90 °C for 24 h, respectively, which may be caused by the steric hindrance of the tert-butyl and the silyl groups. Electron-rich aryl **3.3i** and heteroaryl **3.3b** required heating at 60 °C for 24 h and 50 °C for 24 h, respectively, which may be attributed to the electron-donating ability of these substituents to reduce the electrophilicity of boron.

A plausible catalytic cycle for the π Lewis acid catalyzed oxyboration reaction is shown in Scheme 3.3a that highlights the proposed activation of the C–C π bond by the carbophilic Lewis acid catalyst[32,33] that provides a mechanistically distinct route for B–X σ bond addition, and possible concurrent activation of the B–O σ bond by coordination of trifluoroacetate ion in intermediate **3.6**. Subsequent addition of the nucleophilic B–O σ bond to the resulting Au-alkyne π complex of intermediate **3.6** in a concerted manner forms the carbon–oxygen bond of the isoxazole core and generates a new carbon–gold σ-bond as shown in intermediate **3.7**.

Alternatively, the π Lewis acid catalyzed cyclization steps can occur in a different order, in which the nucleophilic oxygen of the boric ester **3.8** attacks the activated alkyne to generate an oxonium ion **3.9** in the first step, and then the outersphere trifluoroacetate ion removes the Bcat group in the second step to produce **3.7** and **3.10** (eq 3.1). This pathway is supported by similar mechanisms in gold-catalyzed and -mediated cyclizations, such as has been detected by ^{1}H NMR spectroscopy in stoichiometric studies,[16] proposed as intermediates in the fluorination of oxime ethers to generate 4-fluoroisoxazoles,[34] and detected as likely catalytic intermediates in gold and palladium cooperatively catalyzed cyclization/cross-coupling reactions.[28,35]

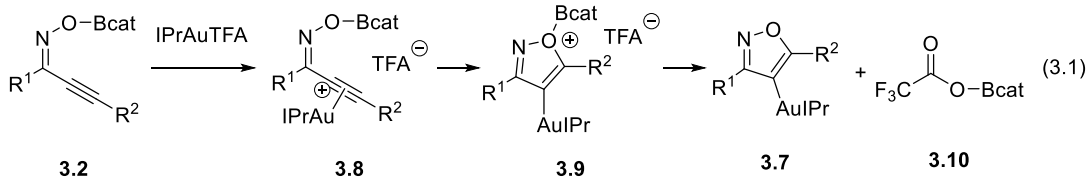

In the next step of the proposed mechanism, the carbon–gold bond in **3.7** is nucleophilic at carbon[16,36,37] and is primed for transmetalation with electrophilic boron intermediate **3.10**. The mechanism of the reaction between **3.7** and **3.10** to form ion pair **3.11** may involve an electrophilic aromatic substitution, with rearomatization and loss of the AuIPr cation. The accessibility of this transmetalation step is not well established; to our knowledge, our previous report is the first of

transmetalation from organogold to boron.[14,15] The reverse reaction from organoboron to gold is better studied,[38–41] as is the general ability of organogold compounds to transmetalate with other metals and metalloids.[35,42–44]

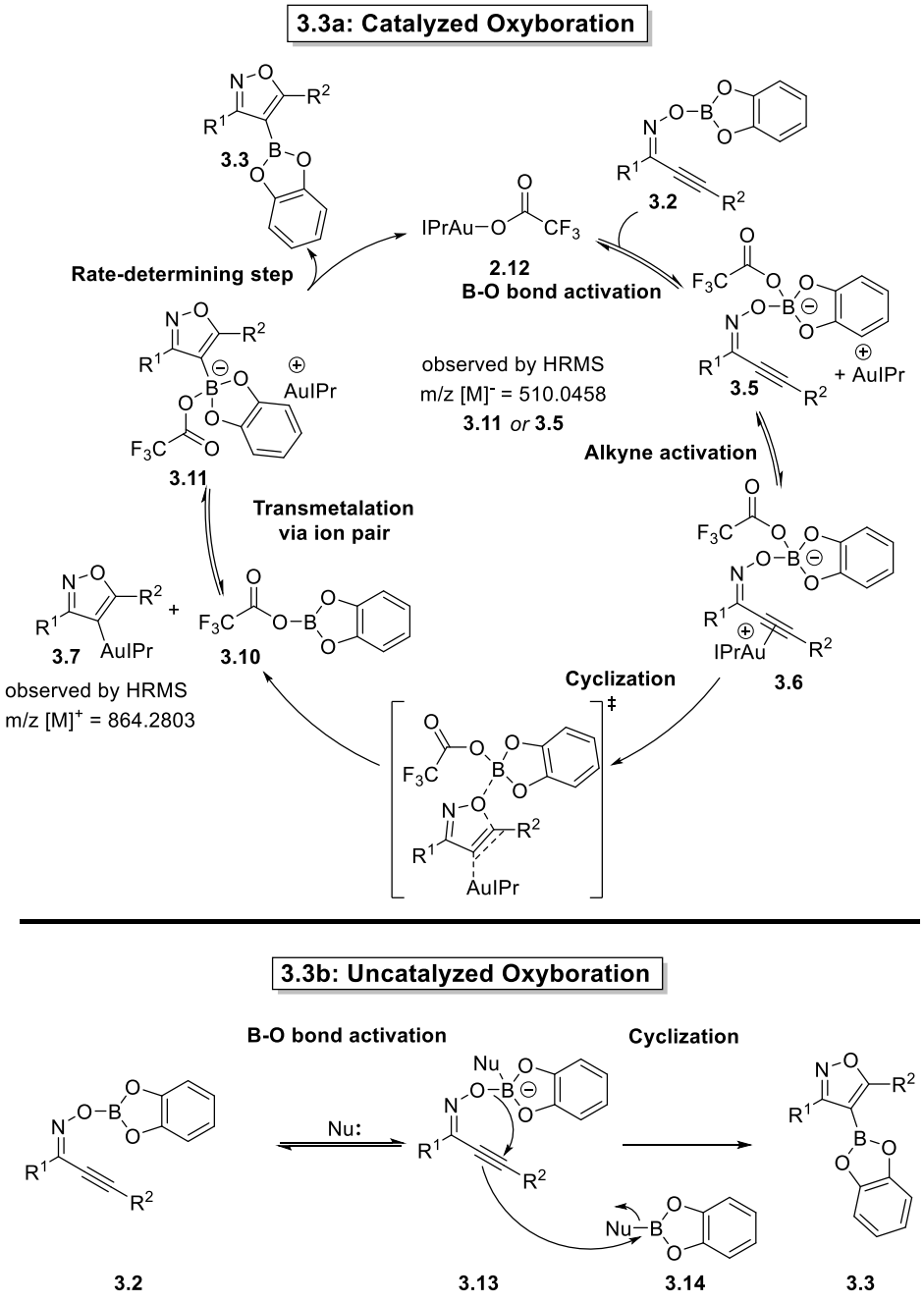

Scheme 3.3. Proposed mechanisms for a) catalyzed and b) uncatalyzed oxyboration

The proposed mechanism for the uncatalyzed oxyboration reaction is shown in Scheme 3.3b. A nucleophile (Nu) could coordinate to boron in **3.2**, activating the B–O σ bond as shown in **3.13**. This tetracoordinate boron species **3.13** then undergo cyclization with **3.14** to form boronate **3.3** and regenerate the nucleophile. The nature of the nucleophile is currently unknown but it may be another molecule of **3.2**, potentially coordinating to boron through the nucleophilic lone pair on the nitrogen.[25]

Mechanistic Studies. Optimization of the counterion in the catalyst IPrAuX produced yield data consistent with the assignment of an active role for the X^- rather than simply a spectator required for charge balance. Specifically, the catalyst IPrAuOTs, with the less coordinating tosylate counterion is often employed in other reported Au(I) catalyzed reactions,[23,24] a result attributed to its weakly coordinated tosylate and thus highly Lewis acidic Au^+ cation equivalent. Yet in oxyboration, this tosylate catalyst produced product **3.3a** in lower yield than did IPrAuTFA, despite the fact that trifluoroacetate anion is more strongly coordinating and should therefore produce a weaker and less active gold catalyst[23,24] (^{1}H NMR spectroscopy yield at t = 6 h for IPrAuOTs (34%; IPrAuTFA 90%). This result is somewhat surprising in light of the other reported applications of weakly coordinating anions in homogeneous Au(I) catalysis;[23,24] and is consistent with the hypothesis that the anion could be assisting the reaction by coordinating to boron to activate the B–O σ bond in borate **3.5** and/or by assisting transmetalation in **3.10** or **3.11**.[14,15] The catalyst IPrAuTFA proved an optimal balance of counterion coordinating ability. The complex IPrAuOAc, with the more strongly coordinating acetate ion[24] did not lead to any detectable product formation.

In order to probe the viability of the proposed intermolecular organogold-to-boron transmetalation reaction in our system, the proposed neutral organogold intermediate **3.7a** was

generated by independent synthesis[34] (Scheme 3.4). In our hands, an attempted in situ synthesis of TFA–Bcat (proposed intermediate **3.10**), adapted from the previously reported synthesis of TfO–Bcat,[27] yielded multiple products. We therefore examined the stoichiometric transmetalation reaction between organogold **3.7a** and readily available *B*-chlorocatecholborane **3.15** as a substitute (Scheme 3.4). This reaction produced the anticipated transmetalation product, catechol boronic ester **3.3a**, in 96% ^{1}H NMR yield, supporting the plausibility of this intermolecular organogold-to-boron transmetalation step in our proposed mechanism. A white precipitate formed gradually during this reaction, which was presumably coproduct IPrAuCl **3.17**, and which is assigned as accounting for the initially detected substoichiometric integration (at t = 10 min) and eventual disappearance (at t = 2 h) of the ^{1}H NMR spectroscopy signals corresponding to **3.17** in solution.

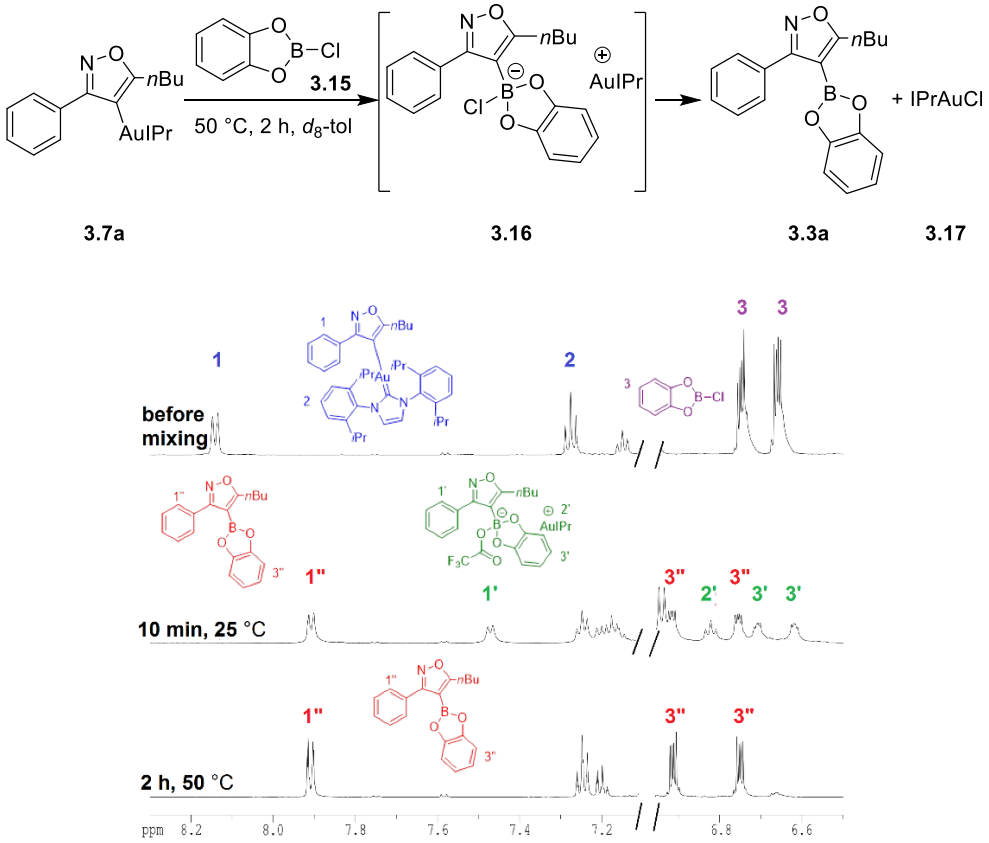

Scheme 3.4. Organogold-to-boron transmetalation via ion pair

Interestingly, ^{1}H NMR spectroscopic analysis of the reaction at t = 10 min, prior to completion, characterized the mechanism of this transmetalation reaction as a two-step process wherein an initial fast transfer of the organic group from gold to boron to make an ion pair is followed by rate-determining breakdown of the ion pair to generate the final neutral products. In Scheme 3.4, 1, 1', 1" are the same proton in the starting material, intermediate, and final product respectively. Specifically, ^{1}H and ^{11}B NMR spectroscopy analysis indicated that the consumption of both starting materials was complete at the first data point, t = 10 min, to generate ion pair **3.16**. The ratio of **3.17** to final neutral organoboron product **3.3a** at this time point was 1:1.5 (^{11}B NMR signal at 17.6 ppm for **3.16** and 31.0 ppm for **3.3a**). This ion pair then decomposed to yield **3.3a** in 96% final ^{1}H NMR spectroscopy yield relative to external standard.

This two-step transmetalation reaction from organogold-to-boron establishes catalytic relevance to the previous observation of tetracoordinate boronate species in mixtures of organogold and boron compounds in model systems with simple substrates.[16]

Analysis of the HRMS of the catalytic oxyboration reaction mixture prior to completion of the reaction at t = 30 min identified two complexes consistent with the mechanistic proposal in Scheme 2.3: neutral organogold complex **3.7c** (*m/z* $[M]^+$ = 864.2803) and a second mass *m/z* $[M]^-$ = 510.0458. Due to the identical *m/z* of anionic complexes **3.11c** and **3.5c**, the mass could correspond to either species or both. The detection of neutral organogold complex **3.7c**, however, suggests the possibility of a catalyst resting state involving the equilibrium between ion pair **3.11** with **3.7** and **3.10** (favoring **3.11**, as seen in the stoichiometric NMR studies, with small concentrations of **3.7** and **3.10**) followed by breakdown of **3.11** to yield **3.3** and regenerate catalyst **3.12**; although its detection alone is not sufficient to establish the catalytic relevance of **3.7c**. These studies suggest that the rate of the overall catalytic cycle may be similarly dictated by the

breakdown of the tetracoordinate boronate intermediate in the transmetalation reaction, which may serve as the rate-determining step.

The detection of TFA-coordinated boron complexes by HRMS is further consistent with an active role for the counterion in the oxyboration reaction rather than simply serving as a spectator to balance the charge on gold(I), as previously suggested by the catalyst optimization studies.

In order to further probe the intermolecularity of the proposed reaction through the intermediacy of **3.7** and **3.10**, a double-label crossover experiment was conducted. Specifically, 2.5 mol % IPrAuTFA was added to 0.5 equiv of **3.2a** and 0.5 equiv of **3.18** in a single reaction vessel (eq 2.2). Non-crossover products **3.3a** plus **3.20** and crossover products **3.21** plus **3.3c** were observed by ^{1}H and ^{11}B NMR spectroscopy. However, a control experiment revealed that the starting boric esters **3.2a** and **3.18** underwent rapid ligand redistribution at ambient temperature even in the absence of catalyst, forming all four possible boric ester starting materials (**3.2a**, **3.2c**, **3.18**, **3.19**). Exchange of the catechol groups in the starting materials was observed as line broadening in the ^{1}H NMR spectra of the mixture generated by combination of **3.2a** and **3.18**. This exchange on the ^{1}H NMR spectroscopy timescale at ambient temperature therefore was significantly more rapid than both the catalyzed and uncatalyzed oxyboration reactions and therefore precluded the employment of a double-label crossover experiment in the evaluation of the intermolecularity of the oxyboration mechanism.

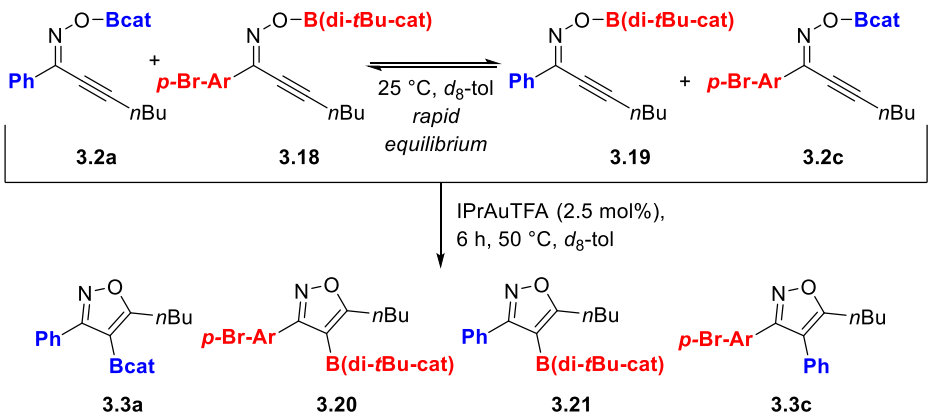

(3.2)

Synthetic Utility. The utility of the oxyboration reaction to generate building blocks for pharmaceutical targets was showcased through the synthesis of valdecoxib, a non-steroidal anti-inflammatory drug (NSAID)[45] and its analog. Our synthetic route is shown in Scheme 3.5. Under standard catalytic conditions, bench-stable pinacol boronate building blocks **3.23** and **3.4k** were generated from oximes **3.22** and **3.1k** in 71% and 64% isolated yields, respectively. Suzuki cross coupling of these borylated isoxazoles with *p*-bromobenzene sulfonamide **3.24** afforded valdecoxib **3.25** and valdecoxib ester analog **3.26** in 62% and 74% isolated yields, respectively. This synthesis provides the key substituted organoboron building block **3.23** in higher isolated yield, compared to the competing route with [3+2] cycloaddition of nitrile oxides and alkylboronates, which formed the same organoboron **3.23** in only 54% isolated yield in a route employed in a previously reported synthesis of valdecoxib.[17]

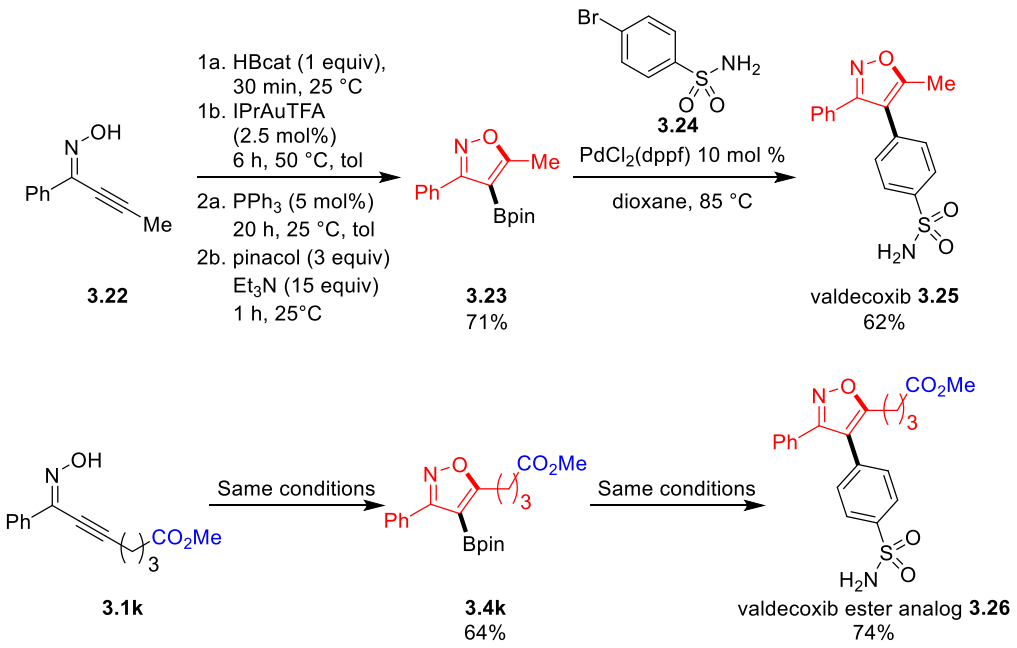

Scheme 3.5. Oxyboration synthesis of valdecoxib

Additionally, the application of oxyboration to the synthesis of ester-containing valdecoxib analog **3.26** showcases the utility of the functional group tolerance of this oxyboration method. Previously reported syntheses of valdecoxib from academic[17,20] and industrial[45] laboratories involve lithiation steps that are not compatible with ester functional groups. These applications demonstrate the versatility and efficiency of the oxyboration reaction for the construction of pharmaceutical targets.

Access to a cost-effective uncatalyzed version of the reaction is particularly desirable on scale, wherein the cost of the catalyst may become a significant consideration that outweighs time considerations. The uncatalyzed oxyboration reaction scales well. Compound **3.1a** was successfully converted to 1.7 g of pinacol boronate **3.4a** on a 7.3 mmol scale under catalyst free conditions in 24 h with 1.0 M in **3.1a** (eq 3.3). The reaction time was reduced significantly when the starting material concentration was increased to the widely employed concentration in the chemical industry. This convenient scalability demonstrates that quantities of these heterocyclic

boronic acid building blocks that are sufficient for multistep downstream synthesis may be prepared by this oxyboration method.

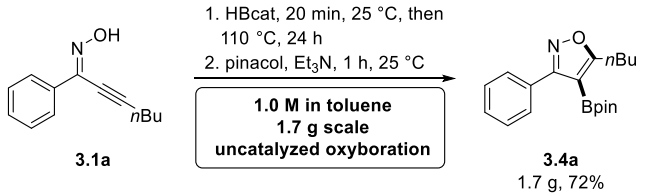

(3.3)

Conclusions

We have developed a method for preparing 4-borylated isoxazoles via oxyboration. This reaction proceeds with catalytic gold(I), or for many substrates without an added catalyst in the first reported uncatalyzed oxyboration reaction of C–C multiple bonds with B–O σ bonds. The reaction conditions are sufficiently mild to form functionalized borylated isoxazoles in good yields and in exclusively one regioisomer. The utility and functional group compatibility of this methodology was highlighted in the synthesis of valdecoxib and a valdecoxib ester analog. Probable reaction intermediates detected by mass spectrometry and by a stoichiometric transmetalation experiment between the organogold intermediate and the boron electrophile, are consistent with a catalyzed mechanism in which the carbophilic Lewis acid catalyst activates the C–C π bond towards B–O σ bond, a new strategy in B–Element addition reactions.[14,15]

References

(1) Tu, K. N.; Hirner, J. J.; Blum, S. A. *Org. Lett.* **2016**, *18*, 480–483.
(2) Pinho e Melo, T. *Curr. Org. Chem.* **2005**, *9*, 925–958.
(3) Burnham, B. S. *Curr. Med. Chem.* **2005**, *12*, 1995–2010.
(4) Calí, P.; Nærum, L.; Mukhija, S.; Hjelmencrantz, A. *Bioorganic Med. Chem. Lett.* **2004**, *14*, 5997–6000.
(5) Liu, J.; Yu, L. F.; Eaton, J. B.; Caldarone, B.; Cavino, K.; Ruiz, C.; Terry, M.; Fedolak, A.; Wang, D.; Ghavami, A.; Lowe, D. A.; Brunner, D.; Lukas, R. J.; Kozikowski, A. P. *J. Med. Chem.* **2011**, *54*, 7280–7288.
(6) Kumbhare, R. M.; Kosurkar, U. B.; Janaki Ramaiah, M.; Dadmal, T. L.; Pushpavalli, S. N. C. V. L.; Pal-Bhadra, M. *Bioorganic Med. Chem. Lett.* **2012**, *22*, 5424–5427.
(7) Mlynarski, S. N.; Karns, A. S.; Morken, J. P. *J. Am. Chem. Soc.* **2012**, *134*, 16449–16451.
(8) Burke, M. D.; Berger, E. M.; Schreiber, S. L. *J. Am. Chem. Soc.* **2004**, *126*, 14095–14104.

(9) Gutiérrez, M.; Matus, M. F.; Poblete, T.; Amigo, J.; Vallejos, G.; Astudillo, L. *J. Pharm. Pharmacol.* **2013**, *65*, 1796–1804.
(10) Vitale, P.; Tacconelli, S.; Perrone, M. G.; Malerba, P.; Simone, L.; Scilimati, A.; Lavecchia, A.; Dovizio, M.; Marcantoni, E.; Bruno, A.; Patrignani, P. *J. Med. Chem.* **2013**, *56*, 4277–4299.
(11) Tzanetou, E.; Liekens, S.; Kasiotis, K. M.; Melagraki, G.; Afantitis, A.; Fokialakis, N.; Haroutounian, S. A. *Eur. J. Med. Chem.* **2014**, *81*, 139–149.
(12) Cragg, R. H.; Lappert, M. F.; Tilley, B. P. *J. Chem. Soc.* **1964**, *0*, 2108–2115.
(13) Matsumi, N.; Chujo, Y. *Macromolecules* **1998**, *31*, 3802–3806.
(14) Hirner, J. J.; Faizi, D. J.; Blum, S. A. *J. Am. Chem. Soc.* **2014**, *136*, 4740–4745.
(15) Chong, E.; Blum, S. A. *J. Am. Chem. Soc.* **2015**, *137*, 10144–10147.
(16) Hirner, J. J.; Blum, S. A. *Tetrahedron* **2015**, *71*, 4445–4449.
(17) Moore, J. E.; Davies, M. W.; Goodenough, K. M.; Wybrow, R. A. J.; York, M.; Johnson, C. N.; Harrity, J. P. A. *Tetrahedron* **2005**, *61*, 6707–6714.
(18) Tang, W.; Keshipeddy, S.; Zhang, Y.; Wei, X.; Savoie, J.; Patel, N. D.; Yee, N. K.; Senanayake, C. H. *Org. Lett.* **2011**, *13*, 1366–1369.
(19) Ishiyama, T.; Murata, M.; Miyaura, N. *J. Org. Chem.* **1995**, *60*, 7508–7510.
(20) Velcicky, J.; Soicke, A.; Steiner, R.; Schmalz, H.-G. *J. Am. Chem. Soc.* **2011**, *133*, 6948–6951.
(21) Praveen, C.; Kalyanasundaram, A.; Perumal, P. *Synlett* **2010**, *2010*, 777–781.
(22) Ueda, M.; Sato, A.; Ikeda, Y.; Miyoshi, T.; Naito, T.; Miyata, O. *Org. Lett.* **2010**, *12*, 2594–2597.
(23) Ciancaleoni, G.; Belpassi, L.; Zuccaccia, D.; Tarantelli, F.; Belanzoni, P. *ACS Catal.* **2015**, *5*, 803–814.
(24) Jia, M.; Bandini, M. *ACS Catal.* **2015**, *5*, 1638–1652.
(25) Fina, N. J.; Edwards, J. O. *Int. J. Chem. Kinet.* **1973**, *5*, 1–26.
(26) Gassman, P. G.; Deck, P. A.; Winter, C. H.; Dobbs, D. A.; Cao, D. H. *Organometallics* **1992**, *11*, 959–960.
(27) Del Grosso, A.; Singleton, P. J.; Muryn, C. A.; Ingleson, M. J. *Angew. Chem. Int. Ed.* **2011**, *50*, 2102–2106.
(28) Shi, Y.; Roth, K. E.; Ramgren, S. D.; Blum, S. A. *J. Am. Chem. Soc.* **2009**, *131*, 18022–18023.
(29) Scott, H. K.; Aggarwal, V. K. *Chem. - A Eur. J.* **2011**, *17*, 13124–13132.
(30) Bailey, W. F.; Patricia, J. J. *J. Organomet. Chem.* **1988**, *352*, 1–46.
(31) Yeung, K.-S. *Top. Heterocycl. Chem.* **2012**, *29*, 47–76.
(32) Gimeno, A.; Cuenca, A. B.; Suárez-Pantiga, S.; De Arellano, C. R.; Medio-Simõn, M.; Asensio, G. *Chem. - A Eur. J.* **2014**, *20*, 683–688.
(33) Tang, Y.; Li, J.; Zhu, Y.; Li, Y.; Yu, B. *J. Am. Chem. Soc.* **2013**, *135*, 18396–18405.
(34) Jeong, Y.; Kim, B.-I.; Lee, J. K.; Ryu, J.-S. *J. Org. Chem.* **2014**, *79*, 6444–6455.
(35) Hirner, J. J.; Shi, Y.; Blum, S. A. *Acc. Chem. Res.* **2011**, *44*, 603–613.
(36) Roth, K. E.; Blum, S. A. *Organometallics* **2010**, *29*, 1712–1716.
(37) Hashmi, A. S.; Toste, F. D.; Wiley InterScience (Online service). Wiley-VCH, 2012.
(38) Sladek, A.; Hofreiter, S.; Paul, M.; Schmidbaur, H. *J. Organomet. Chem.* **1995**, *501*, 47–51.
(39) Forward, J. M.; Fackler, J. P.; Staples, R. J. *Organometallics* **1995**, *14*, 4194–4198.
(40) Partyka, D. V.; Zeller, M.; Hunter, A. D.; Gray, T. G. *Angew. Chem. Int. Ed.* **2006**, *45*,

8188–8191.
(41) Partyka, D. V.; Zeller, M.; Hunter, A. D.; Gray, T. G. *Inorg. Chem.* **2012**, *51*, 8394–8401.
(42) Al-Amin, M.; Johnson, J. S.; Blum, S. A. *Organometallics* **2014**, *33*, 5448–5456.
(43) Hirner, J. J.; Roth, K. E.; Shi, Y.; Blum, S. A. *Organometallics* **2012**, *31*, 6843–6850.
(44) Al-Amin, M.; Roth, K. E.; Blum, S. A. *ACS Catal.* **2014**, *4*, 622–629.
(45) Talley, J. J.; Brown, D. L.; Carter, J. S.; Graneto, M. J.; Koboldt, C. M.; Masferrer, J. L.; Perkins, W. E.; Rogers, R. S.; Shaffer, A. F.; Zhang, Y. Y.; Zweifel, B. S.; Seibert, K. *J. Me* **2000**, *43*, 775–777.

Experimental

General Methods

All reagents were used as received from commercial sources unless otherwise noted. Tetrahydrofuran, acetonitrile and triethylamine were dried by passing through an alumina column under argon pressure on a push still solvent system. Toluene-d_8 was dried over CaH_2, degassed using three freeze-pump-thaw cycles, and vacuum transferred before use. Dioxane was degassed by sparging with nitrogen gas for 1 h. Manipulations were performed in a glovebox under nitrogen atmosphere unless otherwise noted. Analytical thin layer chromatography (TLC) was performed using Merck F_{250} plates and visualized under UV irradiation at 254 nm, or using a basic aqueous solution of potassium permanganate. Flash chromatography was conducted using a Teledyne Isco Combiflash® Rf 200 Automatic Flash Chromatography System, and Teledyne Isco Redisep® 35–70 μm silica gel. All proton and carbon nuclear magnetic resonance (^{1}H and ^{13}C NMR) spectra were recorded on a Bruker DRX-400 spectrometer, Bruker DRX-500 spectrometer outfitted with a cryoprobe, or a Bruker AVANCE-600 spectrometer. Boron nuclear magnetic resonance (^{11}B NMR) spectra were recorded on a Bruker AVANCE-600 spectrometer. Fluorine nuclear magnetic resonance (^{19}F NMR) spectra were recorded on a Bruker DRX-400 spectrometer. All coupling constants were measured in Hertz (Hz). Chemical shifts were reported in ppm and referenced to residual protonated solvent peak (δ_H = 7.26 ppm for $CDCl_3$, δ_H = 2.08 ppm for d_8-toluene, δ_H = 2.05 ppm for d_6-acetone in ^{1}H NMR spectroscopy experiments; δ_C = 77.16 ppm for $CDCl_3$, δ_C = 20.43 ppm for d_8-toluene, δ_C = 29.84 ppm for d_6-acetone in ^{13}C NMR spectroscopy experiments). ^{11}B and ^{19}F NMR spectroscopy experiments were referenced to the absolute frequency of 0 ppm in the ^{1}H dimension according to the Xi scale. High-resolution mass spectrometry data were obtained at the University of California, Irvine.

Synthetic Procedures

Preparation of alkynyl ketone SI-3.2(a–k). General procedure.

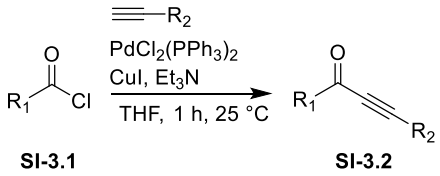

SI-3.1 **SI-3.2**

Ketones were prepared according to a literature procedure.[1] Using standard Schlenk line, to a flame-dried round bottom flask equipped with stir bar under N_2 atmosphere was added acid chloride **SI-5.1** (5.00 mmol, 1.00 equiv), $PdCl_2(PPh_3)_2$ (70.0 mg, 0.10 mmol, 2.0 mol%), CuI (38.0 mg, 0.20 mmol, 4.0 mol%), Et_3N (1.39 mL, 10.0 mmol, 1.00 equiv), and alkyne (1.0 equiv) in dry THF (50 mL) at 25 °C. The resulting reaction mixture was stirred at room temperature for 1 h. The reaction was quenched with DI water (30 mL). The aqueous layer was extracted with EtOAc (3 × 30 mL). The combined organic layers were washed with brine (30 mL), dried over $MgSO_4$, filtered, and concentrated in vacuo. The resulting crude solid was purified by silica gel flash column chromatography using an elution gradient from 100% hexanes to 10% EtOAc in hexanes. Product-containing fractions were combined and concentrated in vacuo to afford **SI-5.2**.

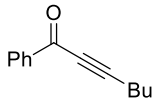

SI-3.2a

1-phenylhept-2-yn-1-one (SI-3.2a) was obtained as yellow oil (1.60 g, 86% isolated yield). TLC (20% EtOAc/hexanes): R_f = 0.50, visualized by UV absorbance. ^{1}H NMR ($CDCl_3$, 500 MHz): δ 8.15–8.13 (m, 2H), 7.61–7.58 (m, 1H), 7.49–7.46 (m, 2H), 2.51 (t, *J* = 7.0 Hz, 2H), 1.67 (quintet, *J* = 7.5 Hz, 2H), 1.52 (sextet, *J* = 7.5 Hz, 2H), 0.97 (t, *J* = 7.5 Hz, 3H). This spectrum is in agreement with previously reported spectral data.[2]

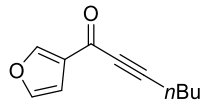

SI-3.2b

1-(3-furyl)hept-2-yn-1-one (SI-3.2b) was obtained as brown oil (1.53 g, 87% isolated yield). TLC (20% EtOAc/hexanes): R_f = 0.47, visualized by UV absorbance. ^{1}H NMR ($CDCl_3$, 500 MHz): δ 8.11 (s, 1H), 7.42 (s, 1H), 6.81 (s, 1H), 2.44 (t, *J* = 7.0 Hz, 2H), 1.63 (quintet, *J* = 7.0 Hz, 2H), 1.49 (sextet, *J* = 7.5 Hz, 2H), 0.95 (t, *J* = 7.5 Hz, 3H). This spectrum is in agreement with previously reported spectral data.[3]

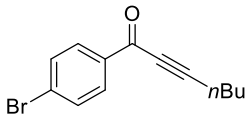

SI-3.2c

1-(4-Bromophenyl)hept-2-yn-1-one (SI-3.2c) was obtained as dark brown oil (2.31 g, 87% isolated yield). TLC (20% EtOAc/hexanes): R_f = 0.55, visualized by UV absorbance. ^{1}H NMR ($CDCl_3$, 500 MHz): δ 7.98 (d, *J* = 8.5 Hz, 2H), 7.62 (d, *J* = 8.0 Hz, 2H), 2.50 (t, *J* = 7.0 Hz, 2H), 1.66 (quintet, *J* = 7.5 Hz, 2H), 1.50 (sextet, *J* = 7.5 Hz, 2H), 0.96 (t, *J* = 7.5 Hz, 3H). This spectrum is in agreement with previously reported spectral data.[4]

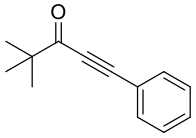

SI-3.2d

1-Phenyl-4,4-dimethyl-pent-1-yn-3-one (SI-3.2d) was obtained as yellow oil (1.35 g, 74% isolated yield). TLC (20% EtOAc/hexanes): R_f = 0.61, visualized by UV absorbance. ^{1}H NMR

($CDCl_3$, 500 MHz): δ 7.59–7.37 (m, 5H), 1.28 (s, 9H). This spectrum is in agreement with previously reported spectral data.[5]

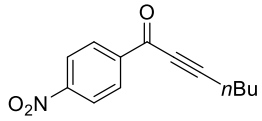

SI-3.2e

1-(4-Nitrophenyl)hept-2-yn-1-one (SI-3.2e) was obtained as reddish orange oil (1.76 g, 76% isolated yield). TLC (20% EtOAc/hexanes): R_f = 0.47, visualized by UV absorbance. ^{1}H NMR ($CDCl_3$, 600 MHz): δ 8.33–8.28 (m, 4H), 2.55 (t, *J* = 7.2 Hz, 2H), 1.69 (quintet, *J* = 7.2 Hz, 2H), 1.51 (sextet, *J* = 7.2 Hz, 2H), 0.98 (t, *J* = 7.2 Hz, 3H). This spectrum is in agreement with previously reported spectral data.[6]

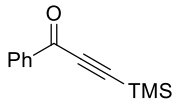

SI-3.2f

1-phenyl-3-trimethylsilyl-prop-2-yn-1-one (SI-3.2f) was obtained as pale yellow oil (1.62 g, 80% isolated yield). TLC (20% EtOAc/hexanes): R_f = 0.67, visualized by UV absorbance. ^{1}H NMR ($CDCl_3$, 500 MHz): δ 8.15 (d, *J* = 7.0 Hz, 2H), 7.62 (t, *J* = 7.0 Hz, 1H), 7.49 (t, *J* = 7.0 Hz, 2H), 0.32 (s, 9H). This spectrum is in agreement with previously reported spectral data.[7]

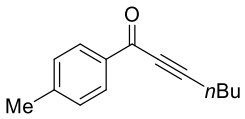

SI-3.2g

1-(4-Methylphenyl)hept-2-yn-1-one (SI-3.2g) was obtained as yellow oil (1.70 g, 85% isolated yield). TLC (20% EtOAc/hexanes): R_f = 0.52, visualized by UV absorbance. ^{1}H NMR ($CDCl_3$,

500 MHz): δ 8.03 (d, *J* = 8.5 Hz, 2H), 7.27 (d, *J* = 9.0 Hz, 2H), 2.50 (t, *J* = 7.0 Hz, 2H), 2.43 (s, 3H), 1.66 (quintet, *J* = 7.5 Hz, 2H), 1.50 (sextet, *J* = 7.5 Hz, 2H), 0.96 (t, *J* = 7.5 Hz, 3H). This spectrum is in agreement with previously reported spectral data.[6]

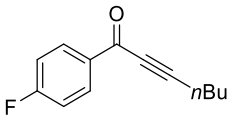

SI-3.2h

1-(4-Fluorophenyl)hept-2-yn-1-one (SI-3.2h) was obtained as yellow oil (1.51 g, 74% isolated yield). TLC (20% EtOAc/hexanes): R_f = 0.57, visualized by UV absorbance. ^{1}H NMR ($CDCl_3$, 500 MHz): δ 8.17–8.14 (m, 2H), 7.15 (t, *J* = 8.5 Hz, 2H), 2.51 (t, *J* = 7.0 Hz, 2H), 1.67 (quintet, *J* = 7.5 Hz, 2H), 1.52 (sextet, *J* = 7.5 Hz, 2H), 0.97 (t, *J* = 7.5 Hz, 3H). This spectrum is in agreement with previously reported spectral data.[8]

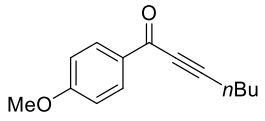

SI-3.2i

1-(4-Methoxyphenyl)hept-2-yn-1-one (SI-3.2i) was obtained as yellow oil (1.74 g, 81% isolated yield). TLC (20% EtOAc/hexanes): R_f = 0.38, visualized by UV absorbance. ^{1}H NMR ($CDCl_3$, 600 MHz): δ 8.10 (d, *J* = 9.0 Hz, 2H), 6.94 (d, *J* = 8.4 Hz, 2H), 3.88 (s, 3H), 2.49 (t, *J* = 7.2 Hz, 2H), 1.66 (quintet, *J* = 7.2 Hz, 2H), 1.50 (sext, *J* = 7.8 Hz, 2H), 0.96 (t, *J* = 7.2 Hz, 3H). This spectrum is in agreement with previously reported spectral data.[6]

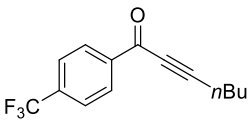

SI-3.2j

1-(4-Trifluoromethylphenyl)hept-2-yn-1-one (SI-3.2j) was obtained as dark yellow oil (2.19 g, 87% isolated yield). TLC (20% EtOAc/hexanes): R_f = 0.48, visualized by UV absorbance. ^{1}H NMR ($CDCl_3$, 500 MHz): δ 8.24 (d, *J* = 8.0 Hz, 2H), 7.75 (d, *J* = 8.0 Hz, 2H), 2.53 (t, *J* = 7.0 Hz, 2H), 1.68 (quintet, *J* = 7.0 Hz, 2H), 1.51 (sext, *J* = 7.5 Hz, 2H), 0.97 (t, *J* = 7.5 Hz, 3H). This spectrum is in agreement with previously reported spectral data.[4]

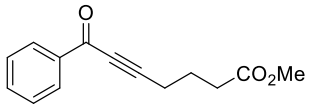

SI-3.2k

Methyl 7-oxo-7-phenyl-hept-5-yn-1-oate (SI-3.2k) was obtained as dark yellow solid (1.95 g, 85% isolated yield). TLC (20% EtOAc/hexanes): R_f = 0.22, visualized by UV absorbance. ^{1}H NMR ($CDCl_3$, 500 MHz): δ 8.12 (d, *J* = 8.0 Hz, 2H), 7.61 (t, *J* = 7.5 Hz, 1H), 7.48 (t, *J* = 7.5 Hz, 2H), 3.70 (s, 3H), 2.60 (t, *J* = 7.0 Hz, 2H), 2.53 (t, *J* = 7.0 Hz, 2H), 2.01 (quintet, *J* = 7.0 Hz, 2H). ^{13}C NMR ($CDCl_3$, 125 MHz): δ 178.2, 173.3, 136.9, 134.1, 129.7, 128.7, 95.1, 80.3, 51.9, 32.8, 23.2, 18.8. HRMS (ESI+) *m / z* calcd for $C_{14}H_{14}O_3$ ($[M+Na]^+$) 253.0841, found 253.0832.

Preparation of alkynyl oxime 3.1a–k. General procedure.

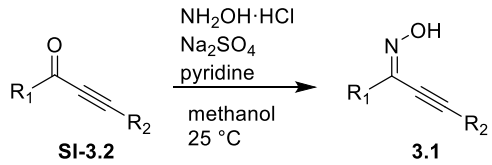

SI-3.2 **3.1**

Oximes were prepared according to a literature procedure.[9] Open to air, a 50 mL round bottom flask was charged with $H_2NOH{\cdot}HCl$ (2.2 equiv), Na_2SO_4 (3.0 equiv), and a stir bar. The solids were suspended in MeOH (20 mL). Pyridine (4.0 equiv) and then ketone **SI-3.2** (1.0 equiv) were added. The reaction was allowed to stir at room temperature until the starting material was consumed completely, as shown by TLC after 5 h. The reaction was quenched with DI water

(25 mL) and extracted with EtOAc (3 × 25 mL). The combined organic layers were washed with brine (25 mL), dried over $MgSO_4$, filtered, and concentrated in vacuo. The crude was purified by silica gel flash column chromatography using a stepwise gradient from 5% to 10% EtOAc in hexanes. Product-containing fractions were combined and concentrated in vacuo to afford **3.1**.

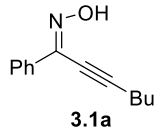

3.1a

(Z)-1-phenylhept-2-yn-1-one oxime (3.1a) was obtained as light yellow solid (38 mg, 22% isolated yield). TLC (20% EtOAc/hexanes): R_f = 0.30, visualized by UV absorbance. ^{1}H NMR (d_8-toluene, 500 MHz): δ 9.12 (s, 1H), 7.98 (d, *J* = 7.5 Hz, 2H), 7.12–7.05 (m, 3H), 2.16 (t, *J* = 7.0 Hz, 2H), 1.37–1.23 (m, 4H), 0.75 (t, *J* = 7.5 Hz, 3H). This spectrum is in agreement with previously reported spectral data.[3]

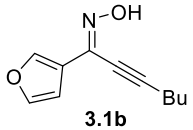

3.1b

(Z)-1-(3-furyl)hept-2-yn-1-one oxime (3.1b) was obtained as yellow solid (115 mg, 6.9% isolated yield).). TLC (20% EtOAc/hexanes): R_f = 0.27, visualized by UV absorbance. ^{1}H NMR ($CDCl_3$, 500 MHz): δ 7.85 (s, 1H), 7.74 (s, 1H), 7.39 (s, 1H), 6.69 (s, 1H), 2.52 (t, *J* = 7.0 Hz, 2H), 1.65 (quintet, *J* = 7.0 Hz, 2H), 1.50 (sextet, *J* = 7.5 Hz, 2H), 0.96 (t, *J* = 7.0 Hz, 3H). ^{13}C NMR ($CDCl_3$, 125 MHz): δ 143.9, 143.3, 136.0, 122.4, 107.5, 102.9, 70.2, 30.4, 22.2, 19.4, 13.7. HRMS (ESI+) *m / z* calcd for $C_{11}H_{13}NO_2$ ($[M+Na]^+$) 214.0844, found 214.0849.

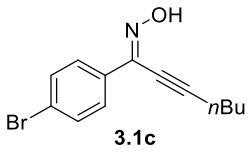

3.1c

(Z)-1-(4-Bromophenyl)hept-2-yn-1-one oxime (3.1c) was obtained as brown solid (0.234 g, 9.6% isolated yield). TLC (20% EtOAc/hexanes): R_f = 0.26, visualized by UV absorbance. ^{1}H NMR ($CDCl_3$, 500 MHz): δ 8.34 (s, 1H), 7.69 (d, *J* = 8.6 Hz, 2H), 7.51 (d, *J* = 8.6 Hz, 2H), 2.58 (t, *J* = 7.1 Hz, 2H), 1.67 (quintet, *J* = 7.1 Hz, 2H), 1.51 (sextet, *J* = 7.5 Hz, 2H), 0.96 (t, *J* = 7.4 Hz, 3H). ^{13}C NMR ($CDCl_3$, 125 MHz): δ 141.6, 132.7, 131.7, 128.2, 124.3, 106.2, 70.2, 30.4, 22.2, 19.6, 13.7. HRMS (ESI+) *m / z* calcd for $C_{13}H_{14}BrNO$ ($[M+Na]^+$) 302.0157, found 302.0148.

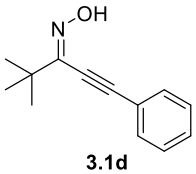

3.1d

(Z)-1-Phenyl-4,4-dimethylpent-1-yn-3-one oxime (3.1d) was obtained as white solid (0.863 g, 58% isolated yield). TLC (20% EtOAc/hexanes): R_f = 0.38, visualized by UV absorbance. ^{1}H NMR (d_8-toluene, 600 MHz): δ 9.58 (s, 1H), 7.37–7.36 (m, 2H), 6.97–6.90 (m, 3H), 1.23 (s, 9H). This spectrum is in agreement with previously reported spectral data.[3]

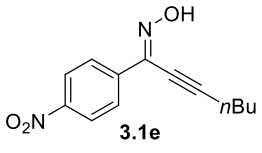

3.1e

(Z)-1-(4-Nitrophenyl)hept-2-yn-1-one oxime (3.1e) was obtained as dark yellow solid (0.112 g, 6.0% isolated yield). TLC (20% EtOAc/hexanes): R_f = 0.26, visualized by UV absorbance. ^{1}H NMR ($CDCl_3$, 600 MHz): δ 8.20 (s, 1H), 8.14–8.13 (m, 2H), 7.91–7.89 (m, 2H), 2.50 (t, *J* = 7.2 Hz, 2H), 1.59 (quintet, *J* = 7.3 Hz, 2H), 1.42 (sextet, *J* = 7.5 Hz 2H), 0.88 (t, *J* = 7.4 Hz, 3H). ^{13}C NMR

($CDCl_3$, 150 MHz): δ 148.6, 140.8, 139.7, 127.4, 123.8, 107.2, 69.9, 30.3, 22.2, 19.6, 13.7. HRMS (ESI-) *m / z* calcd for $C_{13}H_{14}N_2O_3$ ($[M–H]^-$) 245.0926, found 245.0929.

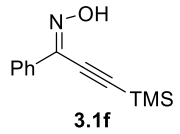

3.1f

(Z)-1-phenyl-3-trimethylsilyl-prop-2-yn-1-one oxime (3.1f) was obtained as white solid (0.885 g, 51% isolated yield). TLC (20% EtOAc/hexanes): R_f = 0.41, visualized by UV absorbance. ^{1}H NMR ($CDCl_3$, 500 MHz): δ 8.11 (s, 1H), 7.83–7.81 (m, 2H), 7.40–7.39 (m, 3H), 0.33 (s, 9H). ^{13}C NMR ($CDCl_3$, 125 MHz): δ 142.1, 133.1, 130.1, 128.6, 126.6, 110.4, 92.7, -0.19. HRMS (ESI+) *m / z* calcd for $C_{12}H_{15}NOSi$ ($[M+Na]^+$) 240.0821, found 240.0815.

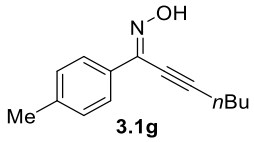

3.1g

(Z)-1-(4-Methylphenyl)hept-2-yn-1-one oxime (3.1g) was obtained as light yellow solid (0.347 g, 19% isolated yield). TLC (20% EtOAc/hexanes): R_f = 0.34, visualized by UV absorbance. ^{1}H NMR ($CDCl_3$, 500 MHz): δ 8.49 (s, 1H), 7.71 (d, *J* = 8.2 Hz, 2H), 7.19 (d, *J* = 8.2 Hz, 2H), 2.58 (t, *J* = 7.1 Hz, 2H), 2.37 (s, 3H), 1.68 (quintet, *J* = 7.3 Hz, 2H), 1.52 (sextet, *J* = 7.5 Hz, 2H), 0.97 (t, *J* = 7.3 Hz, 3H). ^{13}C NMR ($CDCl_3$, 125 MHz): δ 142.4, 140.1, 131.0, 129.5, 126.6, 105.5, 70.7, 30.5, 22.2, 21.5, 19.6, 13.7. HRMS (ESI+) *m / z* calcd for $C_{14}H_{17}NO$ ($[M+Na]^+$) 238.1208, found 238.1200.

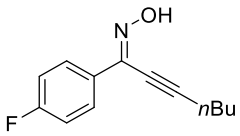

3.1h

(Z)-1-(4-Fluorophenyl)hept-2-yn-1-one oxime (3.1h) was obtained as yellow oil (0.178 g, 11% isolated yield). TLC (20% EtOAc/hexanes): R_f = 0.29, visualized by UV absorbance. ^{1}H NMR ($CDCl_3$, 400 MHz): δ 8.02 (s, 1H), 7.83–7.80 (m, 2H), 7.07 (t, *J* = 8.4 Hz, 2H), 2.58 (t, *J* = 7.2 Hz, 2H), 1.68 (quintet, *J* = 7.2 Hz, 2H), 1.53 (sextet, *J* = 7.6 Hz, 2H), 0.97 (t, *J* = 7.6 Hz, 3H). ^{13}C NMR ($CDCl_3$, 125 MHz): δ 164.9, 162.9, 141.5, 129.85, 129.82, 128.57, 128.50, 115.65, 115.48, 106.0, 70.3, 30.4, 22.2, 19.6, 13.7. ^{19}F NMR ($CDCl_3$, 376 MHz): δ –111.2. HRMS (ESI+) *m / z* calcd for $C_{13}H_{14}FNO$ ($[M+Na]^+$) 242.0957, found 242.0957.

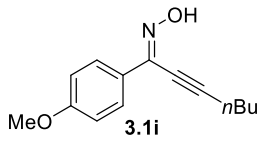

3.1i

(Z)-1-(4-Methoxyphenyl)hept-2-yn-1-one oxime (3.1i) was obtained as yellow solid (0.318 g, 17% isolated yield). TLC (20% EtOAc/hexanes): R_f = 0.19, visualized by UV absorbance. ^{1}H NMR ($CDCl_3$, 600 MHz): δ 8.15 (s, 1H), 7.77–7.76 (m, 2H), 6.91–6.89 (m, 2H), 3.84 (s, 3H), 2.57 (t, *J* = 7.1 Hz, 2H), 1.67 (quintet, *J* = 7.2 Hz, 2H), 1.51 (sextet, *J* = 7.6 Hz, 2H), 0.97 (t, *J* = 7.4 Hz, 3H). ^{13}C NMR ($CDCl_3$, 125 MHz): δ 161.1, 142.1, 128.1, 126.4, 113.9, 105.4, 70.6, 55.5, 30.5, 22.2, 19.6, 13.7. HRMS (ESI+) *m / z* calcd for $C_{14}H_{17}NO_2$ ($[M+Na]^+$) 254.1157, found 254.1158.

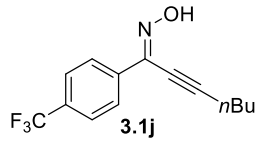

3.1j

(Z)-1-(4-Trifluoromethylphenyl)hept-2-yn-1-one oxime (3.1j) was obtained as light brown solid (0.262 g, 11% isolated yield). TLC (20% EtOAc/hexanes): R_f = 0.32, visualized by UV absorbance. ^{1}H NMR ($CDCl_3$, 500 MHz): δ 8.26 (s, 1H), 7.94 (d, *J* = 8.0 Hz, 2H), 7.64 (d, *J* = 8.0 Hz, 2H), 2.59 (t, *J* = 7.5 Hz, 2H), 1.68 (quintet, *J* = 7.0 Hz, 2H), 1.52 (sextet, *J* = 7.5 Hz, 2H),

0.97 (t, J = 7.5 Hz, 3H). ^{13}C NMR ($CDCl_3$, 125 MHz): δ 141.1, 137.0, 131.7, 131.5, 126.9, 125.5 (q, J = 15 Hz), 123.0, 106.6, 70.0, 30, 4, 22.2, 19.6, 13.7. ^{19}F NMR ($CDCl_3$, 376 MHz): δ –62.8. HRMS (ESI+) m/z calcd for $C_{14}H_{14}F_3NO$ ([M+Na]$^+$) 292.0925, found 292.0920.

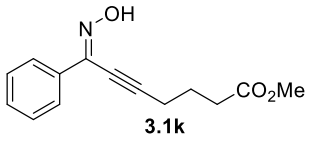

3.1k

Methyl 7-hydroxyimino-7-phenylhept-5-yn-1-oate (3.1k) was obtained as light yellow solid (0.175 g, 8.4% isolated yield). TLC (20% EtOAc/hexanes): R_f = 0.21, visualized by UV absorbance. ^{1}H NMR ($CDCl_3$, 500 MHz): δ 8.51 (s, 1H), 7.82–7.80 (m, 2H), 7.39–7.38 (m, 3H), 3.69 (s, 3H), 2.66 (t, J = 7.0 Hz, 2H), 2.56 (t, J = 7.5 Hz, 2H), 2.02 (quintet, J = 7.0 Hz, 2H). ^{13}C NMR ($CDCl_3$, 125 MHz): δ 173.5, 133.5, 130.0, 129.0 128.6, 126.6, 103.9, 85.6, 51.9, 32.9, 23.6, 19.3. HRMS (ESI+) m/z calcd for $C_{14}H_{15}NO_3$ ([M+Na]$^+$) 268.0950, found 268.0951.

Preparation of IPrAuTFA Catalyst.

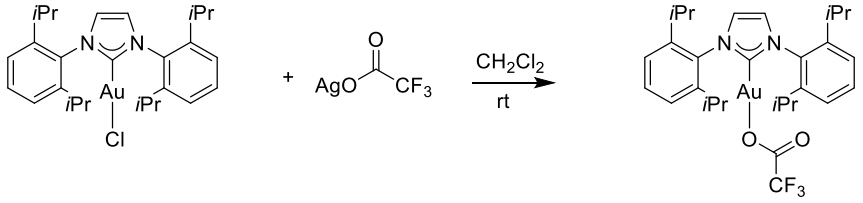

3.17 **SI-3.3** **3.12**

No precautions were taken to exclude air or water. The reaction was conducted in a fume hood with the light turned off. A solution of IPrAuCl **3.17** (124 mg, 200. μmol, 1.00 equiv) in DCM (2.0 mL) was added to a dram vial containing AgTFA **SI-3.3** (48.6 mg, 220. μmol, 1.10 equiv) and a stirbar. A white precipitation was observed. The vial was capped and wrapped with aluminum foil to protect the reaction mixture from light. The reaction was stirred vigorously at 25 °C for 7 h. The resulting suspension was then filtered through a Celite plug (ca. 0.5 mL). The Celite was rinsed with additional DCM (3 × 0.5 mL), and the resulting solution was concentrated

in vacuo to a a white solid. The solid was crushed to a fine powder, from which volatiles were removed at 25 °C and ca. 10 mTorr for 18 h to afford IPrAuTFA **3.12** as a white powder (135 mg, 97% isolated yield). ^{1}H NMR ($CDCl_3$, 500 MHz): δ 7.53 (t, *J* = 7.8 Hz, 2H), 7.31 (d, *J* = 7.8 Hz, 4H), 7.21 (s, 2H), 2.53 (sept, *J* = 7.0 Hz, 4H), 1.35 (d, *J* = 7.0 Hz, 12H), 1.23 (d, *J* = 7.0 Hz, 12H). ^{19}F NMR ($CDCl_3$, 376 MHz): δ -74.1 (s). This spectrum is in agreement with previously reported spectral data.[10]

Optimization of oxyboration reaction conditions.

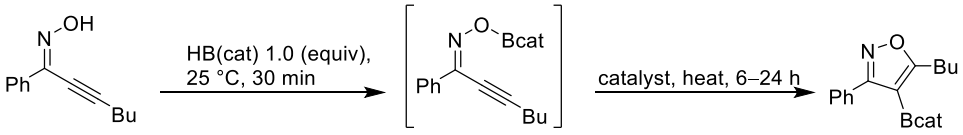

3.1a **3.2a** **3.3a**

Boric ester 3.2a. The reaction was performed inside N_2-filled glovebox. A 1-dram vial was charged with a solution of **3.1a** (20.1 mg, 0.100 mmol, 1.00 equiv) in d_8-toluene (0.30 mL). To this solution was added catecholborane (10.7 µL, 0.100 mmol, 1.00 equiv) at 25 °C. The reaction mixture was stirred for 30 min during which the evolution of H_2 gas was observed, to afford **3.2a**, which was used directly in the screen of reaction conditions without further purification.

^{1}H NMR (d_8-toluene, 600 MHz): δ 8.10–8.09 (m, 2H), 7.12–7.10 (m, 3H), 6.91–6.90 (m, 2H), 6.72 (dd, *J* = 5.3, 3.4 Hz, 2H), 2.12 (t, *J* = 6.8 Hz, 2H), 1.35–1.28 (m, 4H), 0.79 (t, *J* = 7.1 Hz, 3H).

^{11}B NMR (d_8-toluene, 600 MHz): δ 25.4 (s).

Boronic ester 3.3a. Catalyst was dissolved in d_8-toluene (0.2 mL) and added to the dram vial containing **3.2a**. After mixing thoroughly, the reaction mixture was transferred to a J. Young NMR tube, which was capped and removed from the glovebox. The tube was heated in a preheated oil bath at the temperature listed in Table SI-3.1. After heating for the indicated time, the progress of the reaction was monitored by ^{1}H and ^{11}B NMR spectroscopy.

^{1}H NMR (d_8-toluene, 600 MHz): δ 7.92–7.90 (m, 2H), 7.26–7.19 (m, 3H), 6.92–6.90 (m, 2H), 3.26 (s, 3H), 6.76–6.74 (m, 2H), 2.97 (t, *J* = 7.6 Hz, 2H), 1.64 (quintet, *J* = 7.5 Hz, 2H), 1.28 (sextet, *J* = 7.4 Hz, 2H), 0.84 (t, *J* = 7.2 Hz, 3H).

^{11}B NMR (d_8-toluene, 600 MHz): δ 31.2 (s).

General procedure NMR conversions using ERECTIC.

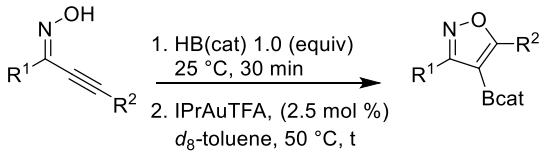

3.1 **3.3**

In a N_2-filled glovebox, an alkynyloxime (0.10 mmol, 1.0 equiv) was dissolved in 0.3 mL d_8-toluene in a 1-dram vial equipped with stir bar. Catecholborane (10.7 µL, 0.100 mmol, 1.00 equiv) was added via gastight syringe to the solution above. The resulting solution was allowed to stir at room temperature for 0.5 h. The catalyst IPrAuTFA (1.8 mg, 0.0025 mmol, 2.5 mol%) was dissolved in 0.2 mL d_8-toluene and transferred via syringe to the solution above. This mixture was then transferred into a J. Young NMR tube, which was sealed and removed from the glove box. Reaction progress was monitored by ^{1}H NMR spectroscopy (600 MHz, d_8-toluene) of **3.3** using the ERECTIC method relative to external mesitylene standard (252 mmol/L in d_8-toluene). This general procedure was used for R_1 = Ph, R_2 = *n*Bu (**3.3a**, 90%, 6 h, 50°C); R_1 = 3-furyl, R_2 = *n*Bu (**3.3b**, 85%, 24 h, 50°C); R_1 = 4-BrPh, R_2 = *n*Bu (**3.3c**, 93%, 6 h, 50°C); R_1 = *t*-Bu, R_2 = Ph (**3.3d**, 95%, 4 h, 110°C); R_1 = 4-NO_2Ph, R_2 = *n*Bu (**3.3e**, 90%, 6 h, 50°C); R_1 = Ph, R_2 = TMS (**3.3f**, 87%, 24 h, 90°C); R_1 = 4-MePh, R_2 = *n*Bu (**3.3g**, 95%, 6 h, 50°C); R_1 = 4-FPh, R_2 = *n*Bu (**3.3h**, 92%, 6 h, 50°C); R_1 = 4-MeOPh, R_2 = *n*Bu (**3.3i**, 92%, 24 h, 60°C); R_1 = 4-CF_3Ph, R_2 = *n*Bu (**3.3j**, 98%, 6 h, 50°C); R_1 = Ph, R_2 = $(CH_2)_3CO_2Me$ (**3.3k**, 94%, 8 h, 50°C).

Synthesis of pinacol boronates 3.4: General procedure.

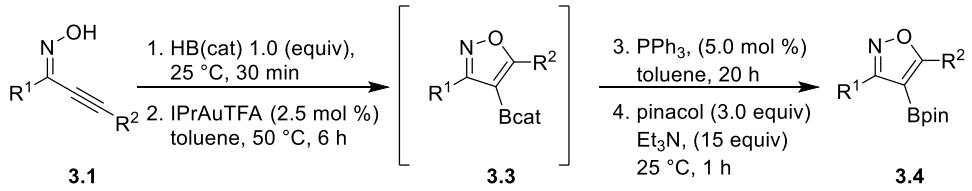

3.1 **3.3** **3.4**

In a N_2-filled glovebox, oxime **3.1** (0.50 mmol, 1.0 equiv) was dissolved in 1.5 mL toluene in a 20-dram vial equipped with stir bar. Catecholborane (53.5 µL, 0.500 mmol, 1.00 equiv) was added via gastight syringe to the solution above. The resulting solution was allowed to stir at room temperature for 0.5 h. The catalyst IPrAuTFA (8.8 mg, 0.012 mmol, 2.5 mol%) was dissolved in 1.0 mL toluene and transferred via syringe to the solution above in a capped vial and the resulting suspension was stirred in a pre-heated copper shot heating bath at appropriate temperature and time. The reaction mixture was then cooled to room temperature and a solution of PPh_3 (6.6 mg, 0.025 mmol, 5.0 mol%) in toluene (3.0 mL) was added. The resulting suspension was stirred for 20 h at room temperature in order to quench IPrAuTFA before proceeding.

Pinacol (177 mg, 1.50 mmol, 3.00 equiv) was dissolved in anhydrous Et_3N (1.04 mL, 7.50 mmol, 15.0 equiv). The resulting solution was added to the quenched reaction mixture, and the resulting suspension was stirred at 25 °C for 1 h. The reaction mixture was then removed from the glovebox. Volatiles were removed in vacuo. The resulting light brown oil was purified by silica gel chromatography using an elution gradient from 100% hexanes to 100% CH_2Cl_2. Solvents were removed in vacuo to afford the desired pinacol boronate **3.4**. All of the pinacol boronates **3.4a-3.4k** are missing one carbon signal in the ^{13}C NMR spectroscopy data. This carbon atom is assigned to the carbon in the newly formed C–B σ bond. This is expected due to the quadrupolar relaxation of B.[11]

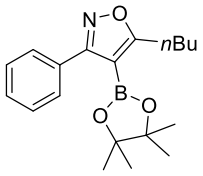

3.4a

Pinacol boronate (3.4a) was obtained as clear oil at 50 °C after 6 h (0.123 g, 75% isolated yield). TLC (40% CH_2Cl_2/hexanes): R_f = 0.10, visualized by UV absorbance. ^{1}H NMR ($CDCl_3$, 600 MHz): δ 7.82–7.80 (m, 2H), 7.41–7.40 (m, 3H), 3.00 (t, *J* = 7.8 Hz, 2H), 1.73 (quintet, *J* = 7.8 Hz, 2H), 1.40 (sextet, *J* = 7.8 Hz, 2H), 1.30 (s, 12H), 0.95 (t, *J* = 7.2 Hz, 3H). ^{13}C NMR ($CDCl_3$, 125 MHz): δ 182.8, 166.1, 130.3, 129.4, 129.1, 128.1, 83.7, 30.7, 27.0, 24.9, 22.4, 13.8. ^{11}B NMR ($CDCl_3$, 192 MHz): δ 29.9 (s). HRMS (ESI+) *m / z* calcd for $C_{19}H_{26}BNO_3$ ($[M+Na]^+$) 350.1907, found 350.1903.

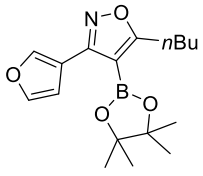

3.4b

Pinacol boronate (3.4b) was obtained as clear oil at 50 °C after 24 h (0.113 g, 71% isolated yield). TLC (40% CH_2Cl_2/hexanes): R_f = 0.09, visualized by UV absorbance. ^{1}H NMR ($CDCl_3$, 500 MHz): δ 8.43 (s, 1H), 7.45–7.44 (m, 1H), 6.96 (s, 1H), 3.00 (t, *J* = 7.5 Hz, 2H), 1.69 (quintet, *J* = 7.5 Hz, 2H), 1.37 (sextet, *J* = 7.5 Hz, 2H), 1.34 (s, 12H), 0.93 (t, *J* = 7.5 Hz, 3H). ^{13}C NMR ($CDCl_3$, 125 MHz): δ 183.6, 158.5, 144.3, 142.9, 116.3, 109.7, 83.8, 30.6, 26.8, 25.0, 22.3, 13.8. ^{11}B NMR ($CDCl_3$, 192 MHz): δ 29.6 (s). HRMS (ESI+) *m / z* calcd for $C_{17}H_{24}BNO_4$ ($[M+Na]^+$) 340.1699, found 340.1691.

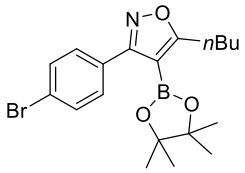

3.4c

Pinacol boronate (3.4c) was obtained as yellow solid at 50 °C after 6 h (0.131 g, 65% isolated yield). TLC (40% CH_2Cl_2/hexanes): R_f = 0.09, visualized by UV absorbance. ^{1}H NMR ($CDCl_3$, 500 MHz): δ 7.71 (d, *J* = 8.5 Hz, 2H), 7.53 (d, *J* = 8.5 Hz, 2H), 3.00 (t, *J* = 7.5 Hz, 2H), 1.71 (quintet, *J* = 7.5 Hz, 2H), 1.41 (sextet, *J* = 7.0 Hz, 2H), 1.30 (s, 12H), 0.95 (t, *J* = 7.0 Hz, 3H). ^{13}C NMR ($CDCl_3$, 125 MHz): δ 183.3, 165.2, 131.3, 130.7, 129.3, 123.8, 83.8, 30.6, 27.0, 24.9, 22.3, 13.8. ^{11}B NMR ($CDCl_3$, 192 MHz): δ 29.7 (s). HRMS (ESI+) *m / z* calcd for $C_{19}H_{25}BBrNO_3$ ($[M+H]^+$) 408.1175, found 408.1163.

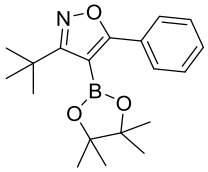

3.4d

Pinacol boronate (3.4d) was obtained as white solid at 110 °C after 4 h (0.154 g, 94% isolated yield). TLC (40% CH_2Cl_2/hexanes): R_f = 0.11, visualized by UV absorbance. ^{1}H NMR ($CDCl_3$, 600 MHz): δ 7.78–7.76 (m, 2H), 7.42–7.41 (m, 3H), 1.44 (s, 9H), 1.34 (s, 12H). ^{13}C NMR ($CDCl_3$, 125 MHz): δ 175.4, 174.7, 130.1, 129.1, 128.3, 125.8, 84.3, 33.4, 29.5, 25.1. ^{11}B NMR ($CDCl_3$, 192 MHz): δ 30.5 (s). HRMS (ESI+) *m / z* calcd for $C_{19}H_{26}BNO_3$ ($[M+H]^+$) 328.2088, found 328.2091.

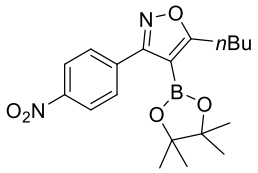

3.4e

Pinacol boronate (3.4e) was obtained as light yellow solid at 50 °C after 6 h (0.112 g, 60% isolated yield). TLC (40% CH_2Cl_2/hexanes): R_f = 0.10, visualized by UV absorbance. ^{1}H NMR ($CDCl_3$, 500 MHz): δ 8.27 (d, *J* = 9.0 Hz, 2H), 8.03 (d, *J* = 8.5 Hz, 2H), 3.04 (t, *J* = 7.5 Hz, 2H), 1.73 (quintet, *J* = 7.0 Hz, 2H), 1.40 (sextet, *J* = 7.0 Hz, 2H), 1.31 (s, 12H), 0.96 (t, *J* = 7.5 Hz, 3H). ^{13}C NMR ($CDCl_3$, 125 MHz): δ 184.0, 164.4, 148.5, 136.8, 130.1, 123.3, 84.0, 30.6, 27.0, 24.9, 22.3, 13.8. ^{11}B NMR ($CDCl_3$, 192 MHz): δ 29.5 (s). HRMS (ESI+) *m / z* calcd for $C_{19}H_{25}BN_2O_5$ ($[M+Na]^+$) 395.1758, found 395.1760.

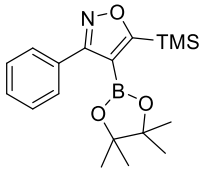

3.4f

Pinacol boronate (3.4f) was obtained as white solid at 90 °C after 24 h (0.122 g, 71% isolated yield). TLC (40% CH_2Cl_2/hexanes): R_f = 0.15, visualized by UV absorbance.^{1}H NMR ($CDCl_3$, 500 MHz): δ 7.78–7.76 (m, 2H), 7.41–7.40 (m, 3H), 1.30 (s, 12H), 0.43 (s, 9H). This spectrum is in agreement with previously reported spectral data.[12]

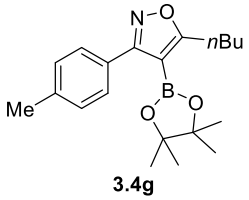

3.4g

Pinacol boronate (3.4g) was obtained as light yellow solid at 50 °C after 6 h (0.128 g, 75% isolated yield). TLC (40% CH_2Cl_2/hexanes): R_f = 0.14, visualized by UV absorbance. ^{1}H NMR ($CDCl_3$, 500 MHz): δ 7.71 (d, *J* = 8.0 Hz, 2H), 7.21 (d, *J* = 8.0 Hz, 2H), 2.99 (t, *J* = 7.5 Hz, 2H), 2.39 (s, 3H), 1.72 (quintet, *J* = 7.5 Hz, 2H), 1.39 (sextet, *J* = 7.5 Hz, 2H), 1.30 (s, 12H), 0.95 (t, *J* = 7.5 Hz, 3H). ^{13}C NMR ($CDCl_3$, 125 MHz): δ 182.7, 166.0, 139.3, 128.92, 128.87, 127.4, 83.7, 30.7, 27.0, 24.9, 22.4, 21.5, 13.8. ^{11}B NMR ($CDCl_3$, 192 MHz): δ 29.9 (s). HRMS (ESI+) *m / z* calcd for $C_{20}H_{28}BNO_3$ ($[M+H]^+$) 342.2244, found 342.2241.

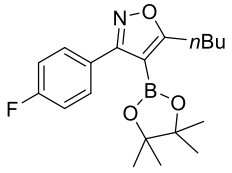

3.4h

Pinacol boronate (3.4h) was obtained as clear oil at 50 °C after 6 h (0.115 g, 67% isolated yield). TLC (40% CH_2Cl_2/hexanes): R_f = 0.11, visualized by UV absorbance. ^{1}H NMR ($CDCl_3$, 500 MHz): δ 7.83–7.80 (m, 2H), 7.09 (t, *J* = 8.7 Hz, 2H), 3.00 (t, *J* = 7.5 Hz, 2H), 1.72 (quintet, *J* = 7.4 Hz, 2H), 1.40 (sextet, *J* = 7.5 Hz, 2H), 1.30 (s, 12H), 0.95 (t, *J* = 7.3 Hz, 3H). ^{13}C NMR ($CDCl_3$, 125 MHz): δ 183.2, 165.3, 164.7, 162.7, 131.0, 126.4, 115.1, 83.8, 30.6, 27.0, 24.9, 22.4, 13.8. ^{11}B NMR ($CDCl_3$, 192 MHz): δ 29.8 (s). ^{19}F NMR ($CDCl_3$, 376 MHz): δ –112.3. HRMS (ESI+) *m / z* calcd for $C_{19}H_{25}BFNO_3$ ($[M+Na]^+$) 368.1813, found 368.1802.

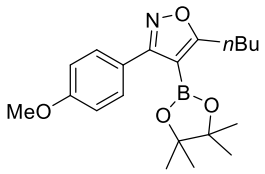

3.4i

Pinacol boronate (3.4i) was obtained as off white solid at 60 °C after 24 h (0.132 g, 74% isolated yield). TLC (40% CH_2Cl_2/hexanes): R_f = 0.23, visualized by UV absorbance. ^{1}H NMR ($CDCl_3$, 600 MHz): δ 7.79 (d, *J* = 8.8 Hz, 2H), 6.92 (d, *J* = 8.8 Hz, 2H), 3.83 (s, 3H), 2.99 (t, *J* = 7.5 Hz, 2H), 1.72 (quintet, *J* = 7.6 Hz, 2H), 1.39 (sextet, *J* = 7.4 Hz, 2H), 1.30 (s, 12H), 0.95 (t, *J* = 7.3 Hz, 3H). ^{13}C NMR ($CDCl_3$, 125 MHz): δ 182.8, 165.7, 160.6, 130.4, 122.8, 113.5, 83.7, 55.4, 30.7, 27.0, 24.9, 22.4, 13.8. ^{11}B NMR ($CDCl_3$, 192 MHz): δ 29.8 (s). HRMS (ESI+) *m / z* calcd for $C_{20}H_{28}BNO_4$ ($[M+Na]^+$) 380.2013, found 380.2002.

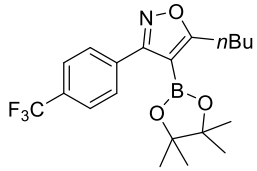

3.4j

Pinacol boronate (3.4j) was obtained as off white solid at 50 °C after 6 h (0.110 g, 56% isolated yield). TLC (40% CH_2Cl_2/hexanes): R_f = 0.15, visualized by UV absorbance. ^{1}H NMR ($CDCl_3$, 600 MHz): δ 7.96 (d, *J* = 8.4 Hz, 2H), 7.66 (d, *J* = 8.4 Hz, 2H), 3.03 (t, *J* = 7.8 Hz, 2H), 1.73 (quintet, *J* = 7.2 Hz, 2H), 1.41 (sextet, *J* = 7.8 Hz, 2H), 1.30 (s, 12H), 0.96 (t, *J* = 7.8 Hz, 3H). ^{13}C NMR ($CDCl_3$, 125 MHz): δ 183.6, 165.1, 133.9, 131.4, 131.2, 129.5, 125.1 (q, *J* = 15.5 Hz), 123.2, 83.9, 30.6, 27.0, 24.9, 22.4, 13.8. ^{11}B NMR ($CDCl_3$, 192 MHz): δ 29.7 (s). ^{19}F NMR ($CDCl_3$, 376 MHz): δ –62.7. HRMS (ESI+) *m / z* calcd for $C_{20}H_{25}BF_3NO_3$ ($[M+H]^+$) 396.1962, found 396.1970.

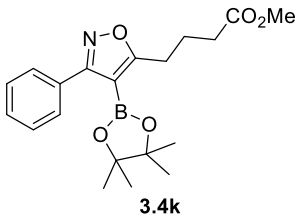

3.4k

Pinacol boronate (3.4k) was obtained as clear oil at 50 °C after 8 h (0.119 g, 64% isolated yield). TLC (100% CH_2Cl_2): R_f = 0.28, visualized by UV absorbance. ^{1}H NMR ($CDCl_3$, 600 MHz): δ 7.81–7.80 (m, 2H), 7.42–7.38 (m, 3H), 3.67 (s, 3H), 3.07 (t, *J* = 7.8 Hz, 2H), 2.40 (t, *J* = 7.8 Hz, 2H), 2.09 (quintet, *J* = 7.2 Hz, 2H), 1.30 (s, 12H). ^{13}C NMR ($CDCl_3$, 125 MHz): δ 181.4, 173.5, 16.2, 130.0, 129.5, 129.1, 128.1, 83.9, 51.7, 33.3, 26.6, 24.9, 23.6. ^{11}B NMR ($CDCl_3$, 192 MHz): δ 29.7 (s). HRMS (ESI+) *m / z* calcd for $C_{20}H_{26}BNO_5$ ($[M+H]^+$) 372.1986, found 372.1983.

Uncatalyzed Oxyboration.

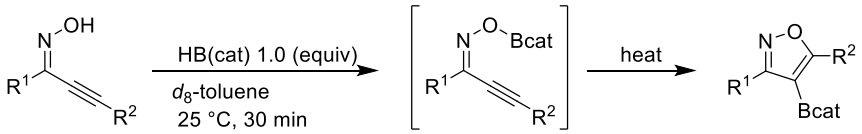

3.1 **3.2** **3.3**

In a N_2-filled glovebox, oxime **3.1** (0.10 mmol, 1.0 equiv) was dissolved in 0.5 mL d_8-toluene in a 1-dram vial equipped with stir bar. Catecholborane (10.7 µL, 0.100 mmol, 1.00 equiv) was added via gastight syringe to the solution above. The resulting solution was allowed to stir at room temperature for 0.5 h. The reaction mixture was transferred via syringe to a J. Young NMR tube, removed from the glovebox, and heated in a preheated oil bath at 110 °C until full consumption of starting materials was achieved, after which the ^{1}H NMR yields were recorded. The ^{1}H NMR yields were determined by the ERECTIC method using mesitylene as the external standard.

Table SI-3.1. Uncatalyzed Oxyboration

	R^1/R^2	Uncatalyzed ^{1}H NMR yield	Time
3.3a	Ph/Bu	89%	111 h
3.3b	3-Furyl/Bu	68%	18 days
3.3c	4-BrPh/Bu	91%	20 h
3.3d	*t*-Bu/Ph	24%	7 days

3.3e	4-NO_2Ph/Bu	84%	20 h
3.3f	Ph/TMS	0%	48 h
3.3g	4-MePh/Bu	78%	15 days
3.3h	4-FPh/Bu	87%	65 h
3.3i	4-MeO/Bu	90%	65 h
3.3j	4-CF_3Ph/Bu	74%	21 days
3.3k	Ph/$(CH_2)_3CO_2Me$	83%	52 h

General procedure for HRMS detection of reaction intermediates.

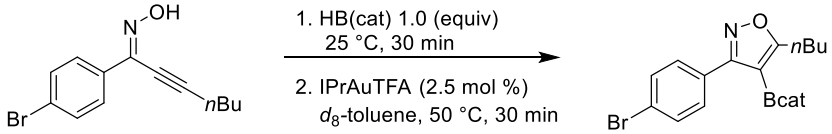

3.1c **3.3c**

In a N_2-filled glovebox, alkynyloxime **3.1c** (28.0 mg, 0.100 mmol, 1.00 equiv) was dissolved in 0.3 mL d_8-toluene in a 1-dram vial equipped with stir bar. Catecholborane (10.7 µL, 0.100 mmol, 1.00 equiv) was added via gastight syringe to the solution above. The resulting solution was allowed to stir at room temperature for 0.5 h. The catalyst IPrAuTFA (1.8 mg, 0.0025 mmol, 2.5 mol%) was dissolved in 0.2 mL toluene and transferred via syringe to the solution above. The vial was capped and the resulting suspension was stirred in a pre-heated 50 °C copper shot heating bath for 30 min. An aliquot of the reaction mixture was withdrawn into a Hamilton 1700 Series Gastight Syringes N Termination (250 µL, N, Gauge: 22s, 2 in., Point style: 3), the tip was placed in a septum as a cap before removing from the glovebox. The sample-containing syringe was quickly carried to the HRMS instrument and injected using ESI technique in positive and negative modes. Due to the extremely high air and moisture sensitivity of the reaction components, no mass calibration was done.

Synthesis of organogold intermediate 3.7a.

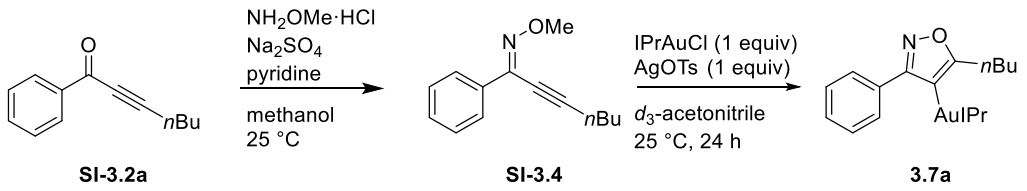

(Z)-1-phenylhept-2-yn-1-one oxime ether (SI-3.4) was prepared according to a literature procedure.[13] In N_2-filled glovebox, a 50 mL round bottom flask was charged with $H_2NOH{\cdot}HCl$ (418 mg, 10.0 mmol, 2.00 equiv), Na_2SO_4 (1.42 g, 10.0 mmol, 2.00 equiv), and a stir bar. The solids were suspended in MeOH (15 mL). Pyridine (1.50 mL, 18.5 mmol, 3.70 equiv) and then ketone **SI-3.2a** (0.93 g, 5.0 mmol, 1.0 equiv) were added. The reaction was allowed to stir at 25 °C for 19 h. The reaction was quenched with 30 mL DI water and extracted with EtOAc (3 × 30 mL). The combined organic layers were washed with brine (30 mL), dried over $MgSO_4$, filtered, and concentrated in vacuo. The crude was purified by silica gel flash column chromatography using a stepwise gradient from 5% to 10% EtOAc in hexanes. Product-containing fractions were combined and concentrated in vacuo to afford **SI-3.4** as light yellow oil (0.53 g, 49% isolated yield). TLC (40% CH_2Cl_2/hexanes): R_f = 0.43, visualized by UV absorbance. ^{1}H NMR ($CDCl_3$, 500 MHz) δ: 7.84–7.82 (m, 2H), 7.37–7.36 (m, 3H), 4.08 (s, 3H), 2.55 (t, *J* = 7.5 Hz, 2H), 1.66 (quintet, *J* = 7.5 Hz, 2H), 1.50 (sextet, *J* = 7.5 Hz, 2H), 0.96 (t, *J* = 7.5 Hz, 3H). This spectrum is in agreement with previously reported spectral data.[13]

Organogold intermediate (3.7a) was prepared according to a lit procedure.[14] In a N_2-filled glovebox, alkynyloxime ether **SI-3.4** (43.0 mg, 0.20 mmol, 1.00 equiv) was dissolved in 1.0 mL anhydrous CH_3CN in a 1-dram vial equipped with stir bar. The resulting solution was transferred into a vial containing IPrAuCl (124 mg, 0.200 mmol, 1.00 equiv) and AgOTs (55.8 mg,

0.200 mmol, 1.00 equiv), allowed to stir at 25 °C for 24 h. The resulting suspension was filtered, washed with anhydrous CH_3CN (3 × 1 ml). The precipitate was dissolved in anhydrous CH_2Cl_2, filtered, and the filtrates were combined. The solvents were removed in vacuo to afford the crude product as a white solid. The crude product was recrystallized with CH_3CN at -35 °C for two days. The purified product was filtered to afford a white solid (89.8 mg, 57% isolated yield). ^{1}H NMR (d_8–toluene, 600 MHz): δ 8.14 (d, *J* = 7.9 Hz, 2H), 7.28 (t, *J* = 7.8 Hz, 2H), 7.15 (t, *J* = 7.4 Hz, 1H), 7.06 (d, *J* = 7.8 Hz, 4H), 7.00 (t, *J* = 7.7 Hz, 2H), 6.44 (s, 2H), 2.60 (quintet, *J* = 6.9 Hz, 4H), 2.40 (t, *J* = 7.4 Hz, 2H), 1.43 (quintet, *J* = 7.6 Hz, 2H), 1.29 (d, *J* = 6.9 Hz, 12H), 1.19 (sextet, *J* = 7.6 Hz, 2H), 1.06 (d, *J* = 6.9 Hz, 12H), 0.86 (t, *J* = 7.3 Hz, 3H). ^{13}C NMR (d_8–toluene, 150 MHz): δ 197.1, 178.0, 169.4, 146.0, 135.4, 135.1, 130.7, 129.6, 128.1, 127.1, 124.3, 122.9, 32.2, 29.5, 29.1, 24.6, 23.9, 22.8.

Organogold-to-boron transmetalation stoichiometric study.

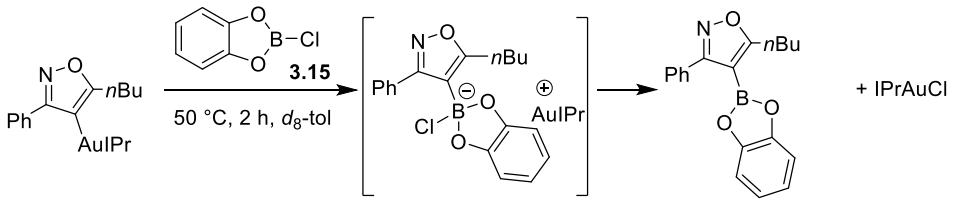

3.7a **3.16** **3.3a** **3.17**

In a N_2-filled glovebox, *B*-chlorocatecholborane **3.15** (3.1 mg, 0.020 mmol, 1.0 equiv) was dissolved in d_8-toluene (0.4 mL). The resulting solution was transferred via pipette to a 1-dram vial containing organogold complex **3.7a** (15.7 mg, 0.0200 mmol, 1.00 equiv). The resulting mixture was transferred via pipette to a J. Young NMR tube, which was capped and removed from the glovebox. An off-white precipitate started to form very early in the reaction mixture. ^{1}H and ^{11}B NMR spectra were acquired at *t* = 10 min. Then the sample was heated in a preheated oil bath at 50 °C. The progress of the reaction was monitored by ^{1}H and ^{11}B NMR spectroscopy. After 2 h,

the reaction was complete and boronic ester **3.3a** was afforded in 96% NMR yield, determined by ERECTIC method with mesitylene as the external standard. For comparison and to facilitate analysis, the ^{1}H NMR stacked plot image in Scheme 3.4 was made by combining the independent ^{1}H NMR spectra of the organogold complex **3.7a** and *B*-chlorocatecholborane in two separate NMR spectroscopy samples (before mixing) into the top most line in the image. The spectrum to the left of the break is from complex **3.7a** and to the right of the break is from *B*-chlorocatecholborane. The ppm scale for the *x*-axis was identical for all four spectra included in this stack plot.

Crossover Experiment.

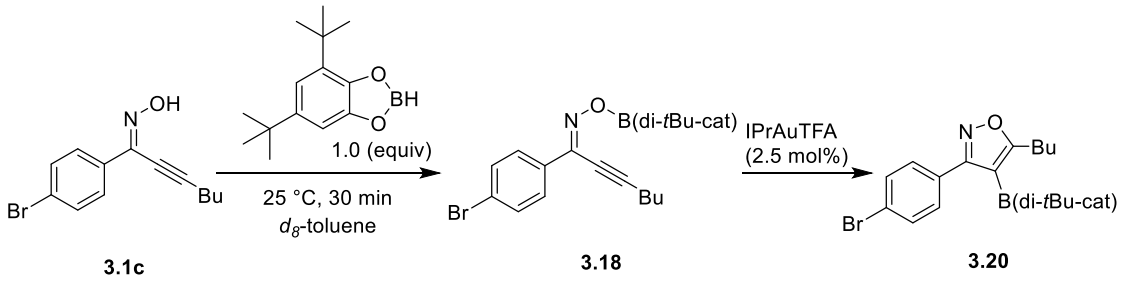

3,5-di-*t*-butylcatechol boric ester 3.18. In a N_2-filled glovebox, alkynyloxime **3.1c** (28.0 mg, 0.100 mmol, 1.00 equiv) was dissolved in 0.3 mL d_8-toluene in a 1-dram vial equipped with stir bar. 3,5-Di-*t*-butylcatecholborane (23.2 mg, 0.100 mmol, 1.00 equiv) was added via gastight syringe to the solution above. The resulting solution was allowed to stir at room temperature for 0.5 h.

^{1}H NMR (d_8-toluene, 600 MHz): δ 7.78 (bs, 2H), 7.15 (d, J = 8.4 Hz, 2H), 7.08–7.07 (m, 2H), 2.10 (t, J = 6.6 Hz, 2H), 1.44 (s, 9H), 1.33–1.28 (m, 4H), 1.23 (s, 9H), 0.80 (t, J = 7.0 Hz, 3H).

^{11}B NMR (d_8-toluene, 600 MHz): δ 25.5 (s).

3,5-di-*t*-butylcatechol boronic ester 3.20. In order to acquire an authentic ^{1}H NMR spectrum of one of the expected products in the crossover experiment, IPrAuTFA (1.8 mg, 0.0025 mmol, 2.5 mol%) was dissolved in 0.2 mL d_8-toluene and transferred via syringe to the dram vial containing **3.18**. After mixing thoroughly, the reaction mixture was transferred to a J. Young NMR tube, which was capped and removed from the glovebox, and heated in a preheated oil bath at 50 °C. The progress of the reaction was monitored by ^{1}H and ^{11}B NMR spectroscopy. After 6 h, 55.6% conversion was observed.

^{1}H NMR (d_8-toluene, 600 MHz): δ 7.64 (d, J = 6.6 Hz, 2H), 7.36 (d, J = 6.6 Hz, 2H), 7.13–7.12 (m, 2H), 3.02 (t, J = 7.7 Hz, 2H), 1.68 (quintet, J = 7.7 Hz, 2H), 1.46 (s, 9H), 1.32–1.30 (m, 2H), 1.25 (s, 9H), 0.86 (t, J = 7.4 Hz, 3H).

^{11}B NMR (d_8-toluene, 600 MHz): δ 30.2 (s).

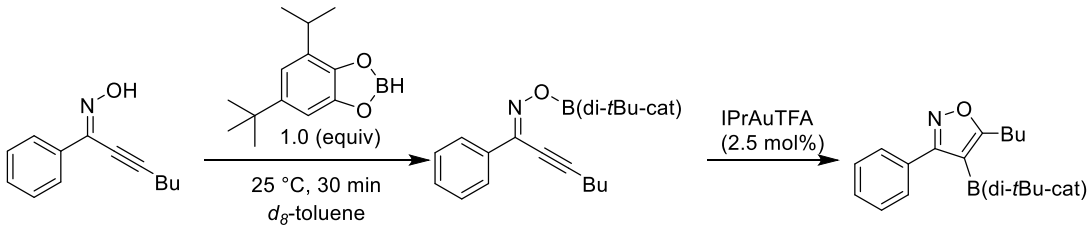

3.1a **3.19** **3.21**

3,5-di-*t*-butylcatechol boric ester 3.19. In a N_2-filled glovebox, alkynyloxime **3.1a** (20.1 mg, 0.100 mmol, 1.00 equiv) was dissolved in 0.3 mL d_8-toluene in a 1-dram vial equipped with stir bar. 3,5-Di-*t*-butylcatecholborane (23.2 mg, 0.100 mmol, 1.00 equiv) was added via gastight syringe to the solution above. The resulting solution was allowed to stir at room temperature for 0.5 h.

^{1}H NMR (d_8-toluene, 600 MHz): δ 8.10 (bs, 1H), 7.13–7.10 (m, 3H), 7.08–7.06 (m, 2H), 2.12 (t, J = 6.7 Hz, 2H), 1.44 (s, 9H), 1.35–1.29 (m, 4H), 1.23 (s, 9H), 0.79 (t, J = 7.1 Hz, 3H).

^{11}B NMR (d_8-toluene, 600 MHz): δ 25.5 (s).

3,5-di-*t*-butylcatechol boronic ester 3.21. In order to acquire an authentic ^{1}H NMR spectrum of one of the expected products in the crossover experiment, IPrAuTFA (1.8 mg, 0.0025 mmol, 2.5 mol%) was dissolved in 0.2 mL d_8-toluene and transferred via syringe to the dram vial containing **3.19**. After mixing thoroughly, the reaction mixture was transferred to a J. Young NMR tube, which was capped and removed from the glovebox, and heated in a preheated oil bath at 50 °C. The progress of the reaction was monitored by ^{1}H and ^{11}B NMR spectroscopy. After 6 h, 37.8% conversion was observed.

^{1}H NMR (d_8-toluene, 600 MHz): δ 7.94 (d, J = 7.6 Hz, 2H), 7.26–7.25 (m, 2H), 7.13–7.12 (m, 2H), 3.03 (t, J = 7.8 Hz, 2H), 1.69 (quintet, J = 7.6 Hz, 2H), 1.38 (s, 9H), 1.37–1.35 (m, 2H), 1.23 (s, 9H), 0.85 (t, J = 7.4 Hz, 3H).

^{11}B NMR (d_8-toluene, 600 MHz): δ 30.3 (s).

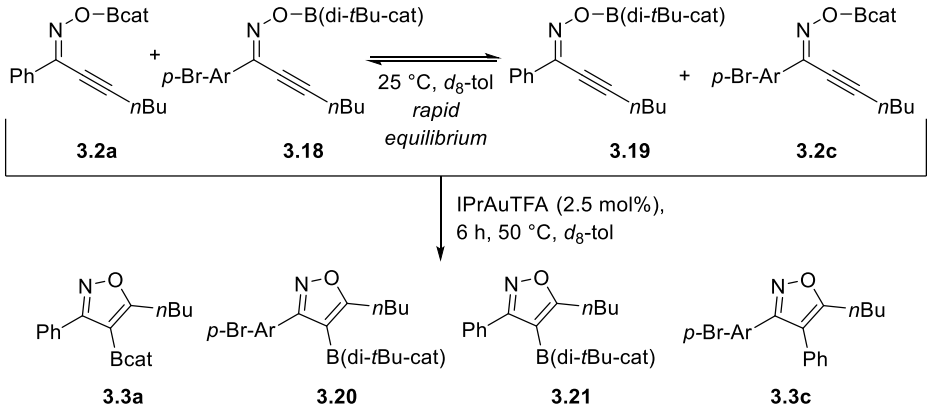

Crossover Experiment. In a N_2-filled glovebox, boric ester **3.2a** (0.050 mmol, 1.0 equiv) and **3.18** (0.050 mmol, 1.0 equiv) were synthesized in two separate 1-dram vials according to the procedures described above in d_8-toluene (0.2 mL each). The catalyst IPrAuTFA (1.8 mg, 0.0025 mmol, 2.5 mol%) was dissolved in 0.1 mL d_8-toluene in a separate 1-dram vial. All three

solutions were mixed thoroughly and transferred to a J. Young NMR tube, removed from the glovebox, and heated in a preheated oil bath at 50 °C. The progress of the reaction was monitored by ^{1}H and ^{11}B NMR spectroscopy. The NMR spectroscopy data indicated the presence of all four products (non-crossover products **3.3a** and **3.20**, and crossover products **3.21** and **3.3c**).

Establishing That the Crossover Products Formed through Pre-equilibrium. In a N_2-filled glovebox, boric ester **3.2a** (0.050 mmol, 1.0 equiv) and **3.11** (0.050 mmol, 1.0 equiv) were synthesized in two separate 1-dram vials according to the procedures described above in d_8-toluene (0.2 mL each). All two solutions were mixed thoroughly and transferred to a J. Young NMR tube, removed from the glovebox. The progress of the reaction was monitored by ^{1}H and ^{11}B NMR spectroscopy. ^{1}H NMR spectroscopy indicated a rapid interconversion between **3.2a** and **3.18** to form a mixture of four boric esters **3.2a**, **3.18**, **3.19**, and **3.2c** in a 1:1:1:1 ratio, approximately.

Synthesis of Valdecoxib and Valdecoxib Ester Analog.

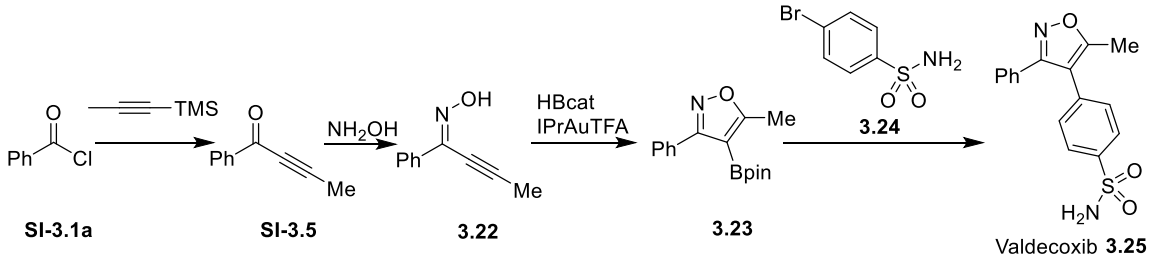

1-phenylbut-2-yn-1-one (SI-3.5) was prepared according to a literature procedure.[15] To a flame-dried 100 mL round bottom flask equipped with stir bar under N_2 atmosphere was added $FeCl_3$ (162 mg, 1.00 mmol, 0.10 equiv). The flask was evacuated and purged with N_2 in three cycles. The reaction flask was cooled to 0 °C in an ice-water bath. Acid chloride **SI-3.1a** (1.16 mL, 10.0 mmol, 1.00 equiv), trimethylsilylpropyne (2.22 mL, 15.0 mmol, 1.50 equiv), and CH_3NO_2 (20.0 mL) were added to the reaction flask at 0 °C under N_2 atmosphere. The reaction mixture was

stirred at 0 °C for 6 h. The reaction mixture was then allowed to warm to 25 °C. The suspension was filtered through a Celite plug (ca. 0.5 mL), and rinsed with dichloromethane (3 × 5 mL). The crude reaction mixture was concentrated in vacuo, purified by silica gel flash column chromatography (5% EtOAc in hexanes) to afford **SI-3.5** as a yellow oil (0.867 g, 60% isolated yield). TLC (20% EtOAc/hexanes): R_f = 0.42, visualized by UV absorbance. ^{1}H NMR ($CDCl_3$, 500 MHz) δ: 8.14 (d, *J* = 7.5 Hz, 2H), 7.60 (t, *J* = 7.5 Hz, 1H), 7.48 (t, *J* = 8.0 Hz, 2H), 2.16 (s, 3H). This spectrum is in agreement with previously reported spectral data.[15]

(Z)-1-phenylbut-2-yn-1-one oxime (3.22) was prepared according to a literature procedure.[9] A 50 mL round bottom flask was charged with $H_2NOH{\cdot}HCl$ (2.2 equiv), Na_2SO_4 (3.0 equiv), and a stir bar. The solids were suspended in MeOH (10 mL). Pyridine (4.0 equiv) and then ketone **SI-3.5** (1.0 equiv) were added. The reaction was stirred at room temperature until the starting material was consumed completely, as shown by TLC. The reaction was quenched with 15 mL DI water and extracted with EtOAc (3 × 15 mL). The combined organic layers were washed with brine (15 mL), dried over $MgSO_4$, filtered, and concentrated in vacuo. The crude was purified by silica gel flash column chromatography using a stepwise gradient from 5% to 10% EtOAc in hexanes. Product-containing fractions were combined and concentrated in vacuo to afford **3.22** as a yellow solid (111 mg, 12% isolated yield). TLC (20% EtOAc/hexanes): R_f = 0.19, visualized by UV absorbance. ^{1}H NMR (d_8–toluene, 500 MHz): δ 9.03 (s, 1H), 7.95–7.93 (m, 2H), 7.11–7.06 (m, 3H), 1.61 (s, 3H). ^{13}C NMR (d_8–toluene, 125 MHz): δ 142.1, 134.4, 129.7, 128.6, 126.9, 100.5, 71.0, 4.1. HRMS (ESI+) *m / z* calcd for $C_{10}H_9NO$ ($[M+Na]^+$) 182.0582, found 182.0579.

Pinacol boronate (3.23). In a N_2-filled glovebox, alkynyloxime **3.22** (31.8 mg, 0.200 mmol, 1.00 equiv) was dissolved in 0.6 mL toluene in a 1-dram vial equipped with stir bar. Catecholborane (21.4 µL, 0.200 mmol, 1.00 equiv) was added via gastight syringe to the solution

above. The resulting solution was allowed to stir at room temperature for 0.5 h. The catalyst IPrAuTFA (3.5 mg, 0.0050 mmol, 2.5 mol%) was dissolved in 0.4 mL toluene and transferred via syringe to the solution above in a capped vial and the resulting suspension was stirred in a pre-heated 50 °C copper shot heating bath for 6 h. The reaction mixture was then cooled to room temperature and a solution of PPh_3 (2.6 mg, 0.010 mmol, 5.0 mol%) in toluene (1.2 mL) was added. The resulting suspension was stirred for 20 h at room temperature in order to quench IPrAuTFA before proceeding.

Pinacol (70.8 mg, 0.600 mmol, 3.00 equiv) was dissolved in anhydrous Et_3N (0.42 mL, 3.0 mmol, 15.0 equiv). The resulting solution was added to the quenched reaction mixture, and the resulting suspension was stirred at 25 °C for 1 h. The reaction mixture was then removed from the glovebox. Volatiles were removed in vacuo. The resulting light brown oil was purified by silica gel chromatography using an elution gradient from 100% hexanes to 100% CH_2Cl_2. Solvents were removed in vacuo to afford the desired pinacol boronate **3.23** as white solid (40.5 mg, 71% isolated yield). TLC (40% CH_2Cl_2/hexanes): R_f = 0.08, visualized by UV absorbance. ^1H NMR ($CDCl_3$, 600 MHz): δ 7.83–7.81 (m, 2H), 7.43–7.39 (m, 3H), 2.61 (s, 3H), 1.30(s, 12H). This spectrum is in agreement with previously reported spectral data.[12]

Valdecoxib (3.25) was prepared according to a literature procedure, but with using building block **3.14** from our method.[12] To a flame-dried 10 mL round bottom flask equipped with stir bar under N_2 atmosphere was added pinacol boronate **3.23** (54.4 mg, 0.191 mmol, 1.00 equiv), $PdCl_2$(dppf)·DCM (15.5 mg, 0.0190 mmol, 0.100 equiv), K_3PO_4 (122 mg, 0.574 mmol, 3.00 equiv), sulfonamide **3.24** (90.2 mg, 0.382 mmol, 2.00 equiv), and degassed dioxane (1.2 mL). The reaction mixture was stirred at 85 °C for 21 h. The reaction mixture was allowed to cool to 25 °C, quenched by DI water (10 mL). The aqueous layer was extracted with dichloromethane (3

× 20 mL). The combined organic layer was washed with brine (20 mL), dried over $MgSO_4$, filtered, and concentrated in vacuo. The crude was purified by silica gel flash column chromatography using an elution gradient from 30% to 40% EtOAc in hexanes to afford **3.25** as a light yellow solid (37.4 mg, 62% isolated yield). TLC (40% EtOAc/hexanes): R_f = 0.14, visualized by UV absorbance. ^{1}H NMR (CD_3OD, 600 MHz) δ: 7.91 (d, *J* = 8.4 Hz, 2H), 7.44–7.35 (m, 7H), 4.84 (s, 2H), 2.49 (s, 3H). This spectrum is in agreement with previously reported spectral data.[12]

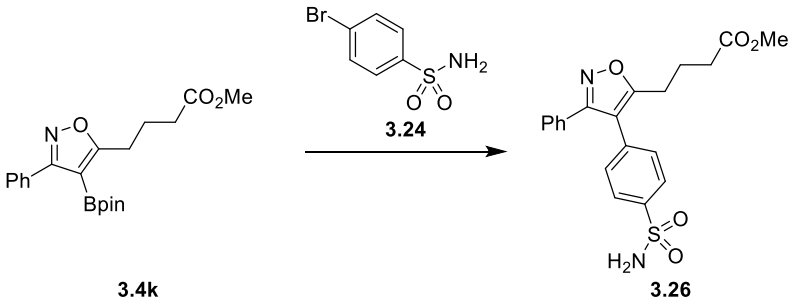

Valdecoxib ester analog (3.26) was prepared according to a literature procedure,[12] using building block **3.4k** from our method. To a flame-dried 10 mL round bottom flask equipped with stir bar under N_2 atmosphere was added pinacol boronate **3.4k** (59.0 mg, 0.159 mmol, 1.00 equiv), $PdCl_2$(dppf)·DCM (13.0 mg, 0.0159 mmol, 0.100 equiv), K_3PO_4 (101 mg, 0.477 mmol, 3.00 equiv), sulfonamide **3.24** (75.0 mg, 0.318 mmol, 2.00 equiv), and degassed dioxane (1.20 mL). The reaction mixture was stirred at 90 °C for 46 h. The reaction mixture was allowed to cool to 25 °C, quenched by DI water (10 mL). The aqueous layer was extracted with dichloromethane (3 × 20 mL). The combined organic layer was washed with brine (20 mL), dried over $MgSO_4$, filtered, and concentrated in vacuo. The crude was purified by silica gel flash column chromatography using an elution gradient from 30% to 40% EtOAc in hexanes to afford **3.26** as a white solid (47.1 mg, 74% isolated yield). TLC (40% EtOAc/hexanes): R_f = 0.14, visualized by UV absorbance. ^{1}H NMR (d_6-acetone, 500 MHz) δ: 7.93–7.91 (m, 2H), 7.45–7.36 (m, 7H), 6.70

(bs, 1H), 3.81 (bs, 1H), 3.57 (s, 3H), 2.94–2.91 (m, 4H), 2.40 (t, J = 7.0 Hz, 2H). ^{13}C NMR (d_6-acetone, 125 MHz): δ 173.3, 170.8, 161.6, 144.3, 134.8, 131.2, 130.3, 129.8, 129.4, 129.1, 127.2, 115.5, 51.6, 33.2, 25.4, 23.5. HRMS (ESI+) m / z calcd for $C_{20}H_{20}N_2O_5S$ ([M+Na]$^+$) 423.0991, found 423.0987.

Gram-scale preparation of 3.4a

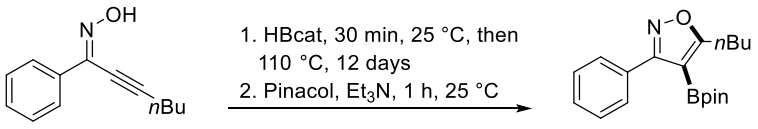

3.1a **3.4a**

The gram-scale uncatalyzed oxyboration reaction was conducted in a N_2-filled glovebox. A flame-dried 100-mL round bottom flask with a stirbar was charged with oxime **3.1a** (1.63 g, 8.10 mmol, 1.00 equiv). Anhydrous toluene (15.0 mL) was added. To the resulting rapidly stirring suspension was added catecholborane (0.867 mL, 8.10 mmol, 1.00 equiv) via gastight syringe, and allowed to stir at room temperature for 30 min. The round bottom flask was heated in a preheated copper shot heating bath at 110 °C until full consumption of starting materials was achieved (12 days).

Pinacol (2.87 g, 24.3 mmol, 3.00 equiv) was dissolved in anhydrous Et_3N (3.37 mL, 24.3 mmol, 3.00 equiv). The resulting solution was added to the quenched reaction mixture, and the resulting suspension was stirred at 25 °C for 2 h. The reaction mixture was then removed from the glovebox. Volatiles were removed in vacuo. The resulting light brown oil was purified by silica gel chromatography using an elution gradient from 100% hexanes to 100% CH_2Cl_2. Solvents were removed in vacuo to afford the desired pinacol boronate **3.4a** as a light yellow oil (1.70 g, 64% isolated yield). Spectral data were identical to those previously obtained for this compound (see page 77).

Reference for Experimental Section

(1) Karpov, A. S.; Müller, T. J. J. *Org. Lett.* **2003**, *5*, 3451–3454.
(2) Trost, B. M.; Schmidt, T. *J. Am. Chem. Soc.* **1988**, *110*, 2301–2303.
(3) Eagon, S.; DeLieto, C.; McDonald, W. J.; Haddenham, D.; Saavedra, J.; Kim, J.; Singaram, B. *J. Org. Chem.* **2010**, *75*, 7717–7725.
(4) Natte, K.; Chen, J.; Neumann, H.; Beller, M.; Wu, X.-F. *Org. Biomol. Chem.* **2014**, *12*, 5590–5593.
(5) Alonso, D. A.; Nájera, C.; Pacheco, M. C. *J. Org. Chem.* **2004**, *69*, 1615–1619.
(6) Huang, B.; Yin, L.; Cai, M. *New J. Chem.* **2013**, *37*, 3137–3144.
(7) Arnold, D. M.; LaPorte, M. G.; Anderson, S. M.; Wipf, P. *Tetrahedron* **2013**, *69*, 7719–7731.
(8) Roy, S.; Davydova, M. P.; Pal, R.; Gilmore, K.; Tolstikov, G. A.; Vasilevsky, S. F.; Alabugin, I. V. *J. Org. Chem.* **2011**, *76*, 7482–7490.
(9) Kung, K. K. Y.; Lo, V. K. Y.; Ko, H. M.; Li, G. L.; Chan, P. Y.; Leung, K. C.; Zhou, Z.; Wang, M. Z.; Che, C. M.; Wong, M. K. *Adv. Synth. Catal.* **2013**, *355*, 2055–2070.
(10) Biasiolo, L.; Trinchillo, M.; Belanzoni, P.; Belpassi, L.; Busico, V.; Ciancaleoni, G.; D'Amora, A.; Macchioni, A.; Tarantelli, F.; Zuccaccia, D. *Chemistry* **2014**, *20*, 14594–14598.
(11) Akitt, J. W. *J. Magn. Reson.* **1970**, *3*, 411–414.
(12) Moore, J. E.; Davies, M. W.; Goodenough, K. M.; Wybrow, R. A. J.; York, M.; Johnson, C. N.; Harrity, J. P. A. *Tetrahedron* **2005**, *61*, 6707–6714.
(13) Waldo, J. P.; Larock, R. C. *J. Org. Chem.* **2007**, *72*, 9643–9647.
(14) Jeong, Y.; Kim, B.-I.; Lee, J. K.; Ryu, J.-S. *J. Org. Chem.* **2014**, *79*, 6444–6455.
(15) Gandeepan, P.; Parthasarathy, K.; Su, T.-H.; Cheng, C.-H. *Adv. Synth. Catal.* **2012**, *354*, 457–468.

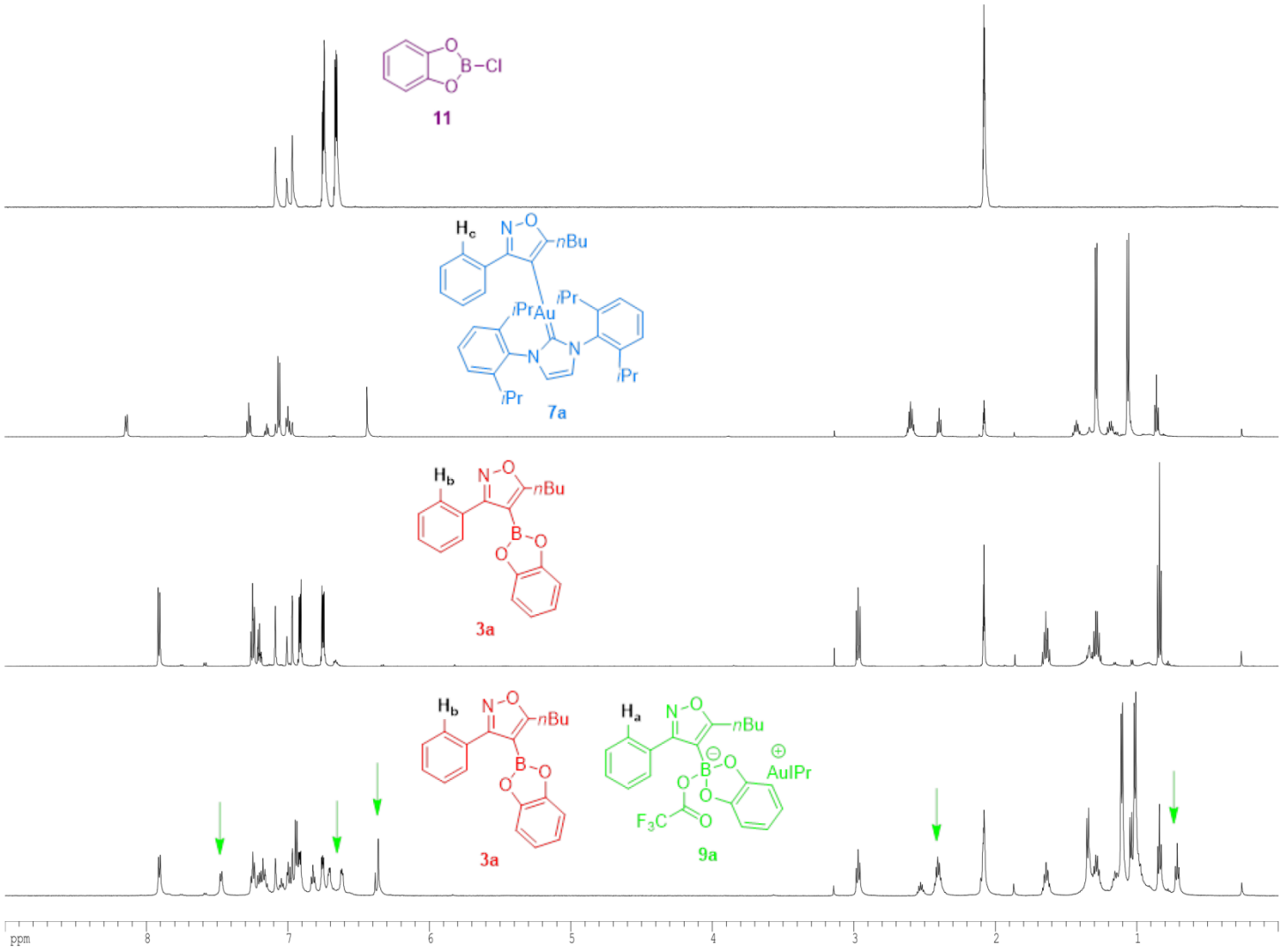
11
7a
3a
3a
9a
ppm
8
7
6
5
4
3
2
1

KT-III-050a
11B spectrum with 1H decoupling

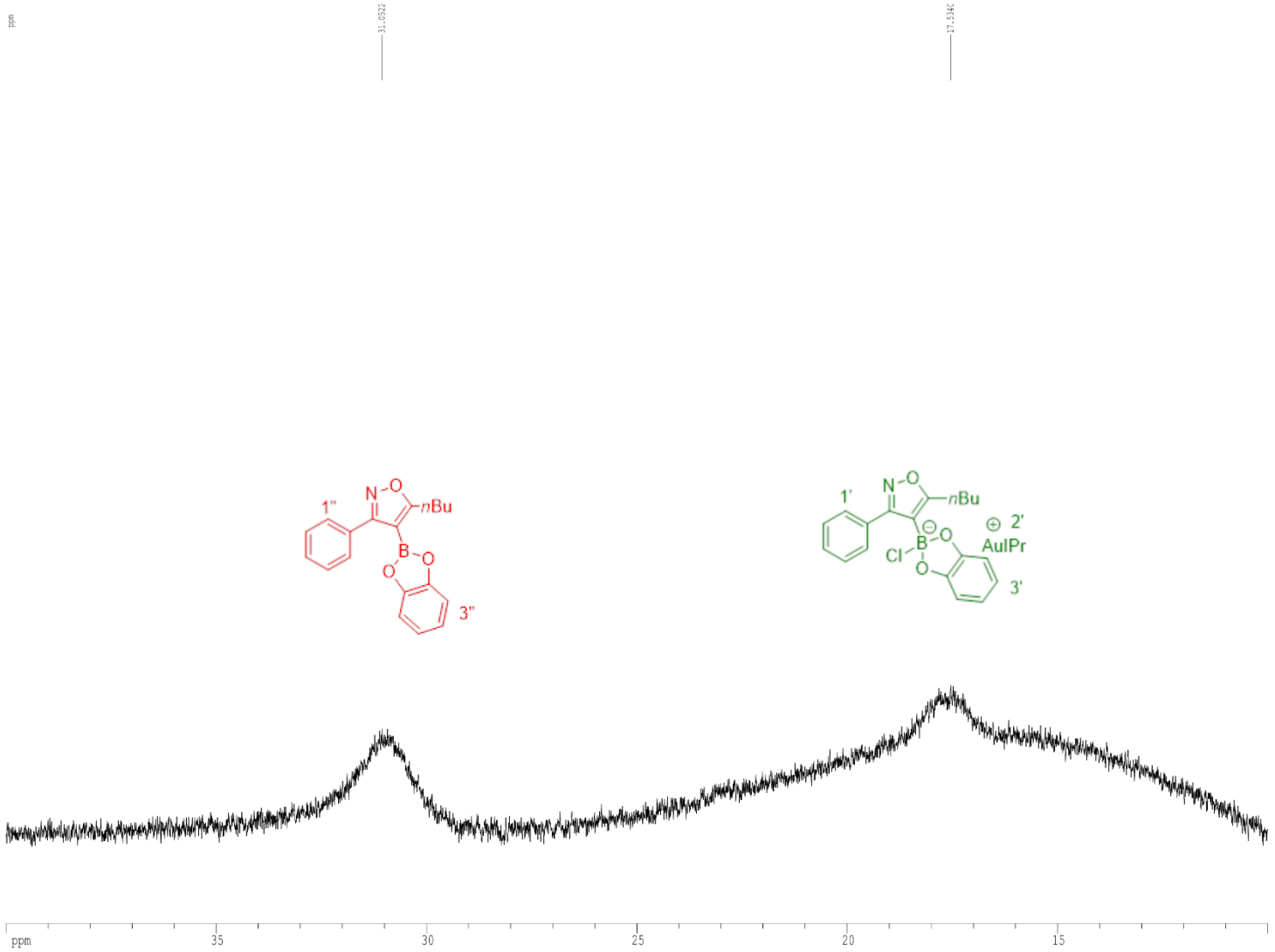

1H spectrum

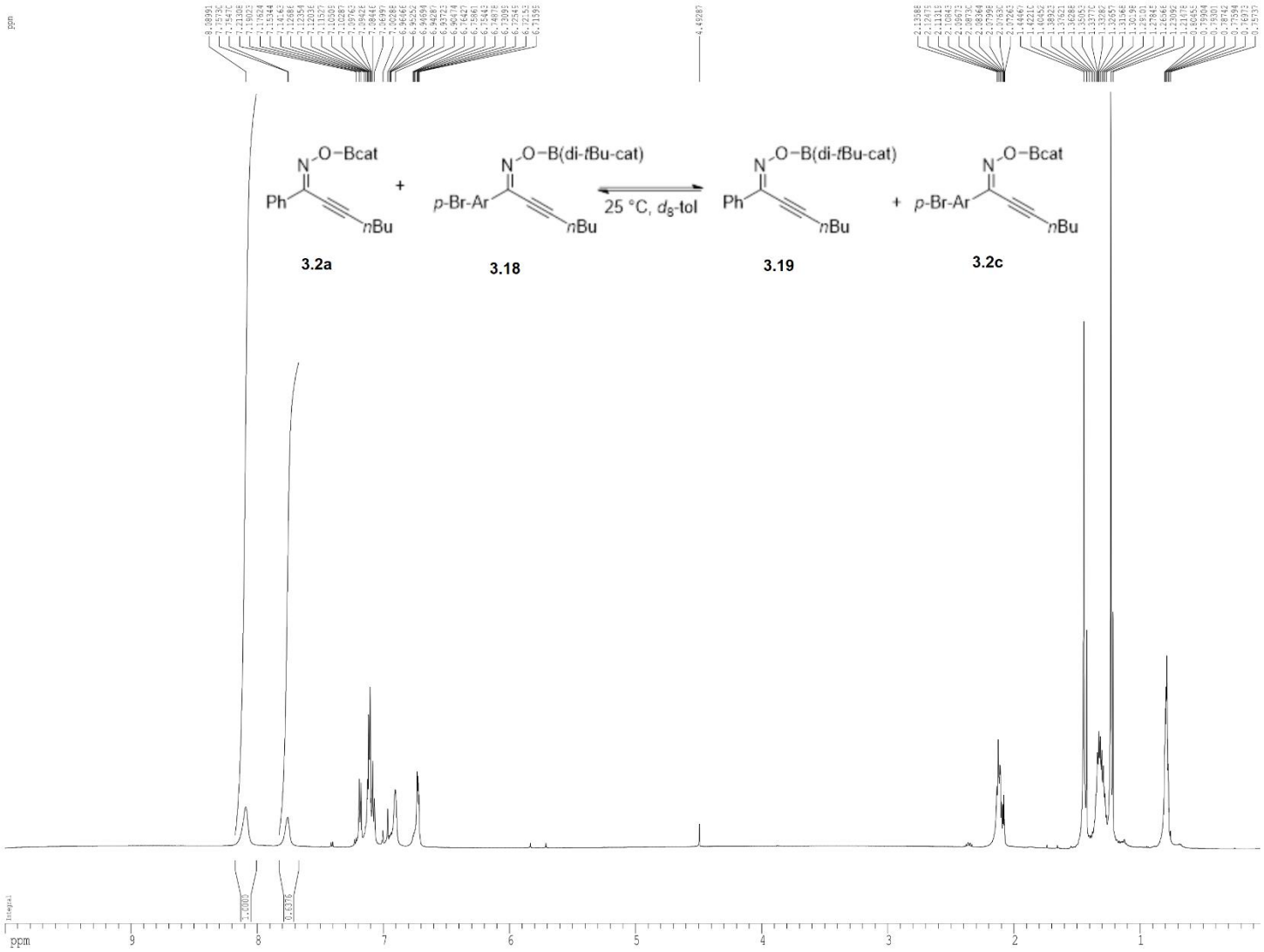
O–Bcat
N
Ph
nBu
3.2a
+
O–B(di-tBu-cat)
p-Br-Ar
3.18
25 °C, d8-tol
3.19
3.2c
ppm
9
8
7
6
5
4
3
2
1

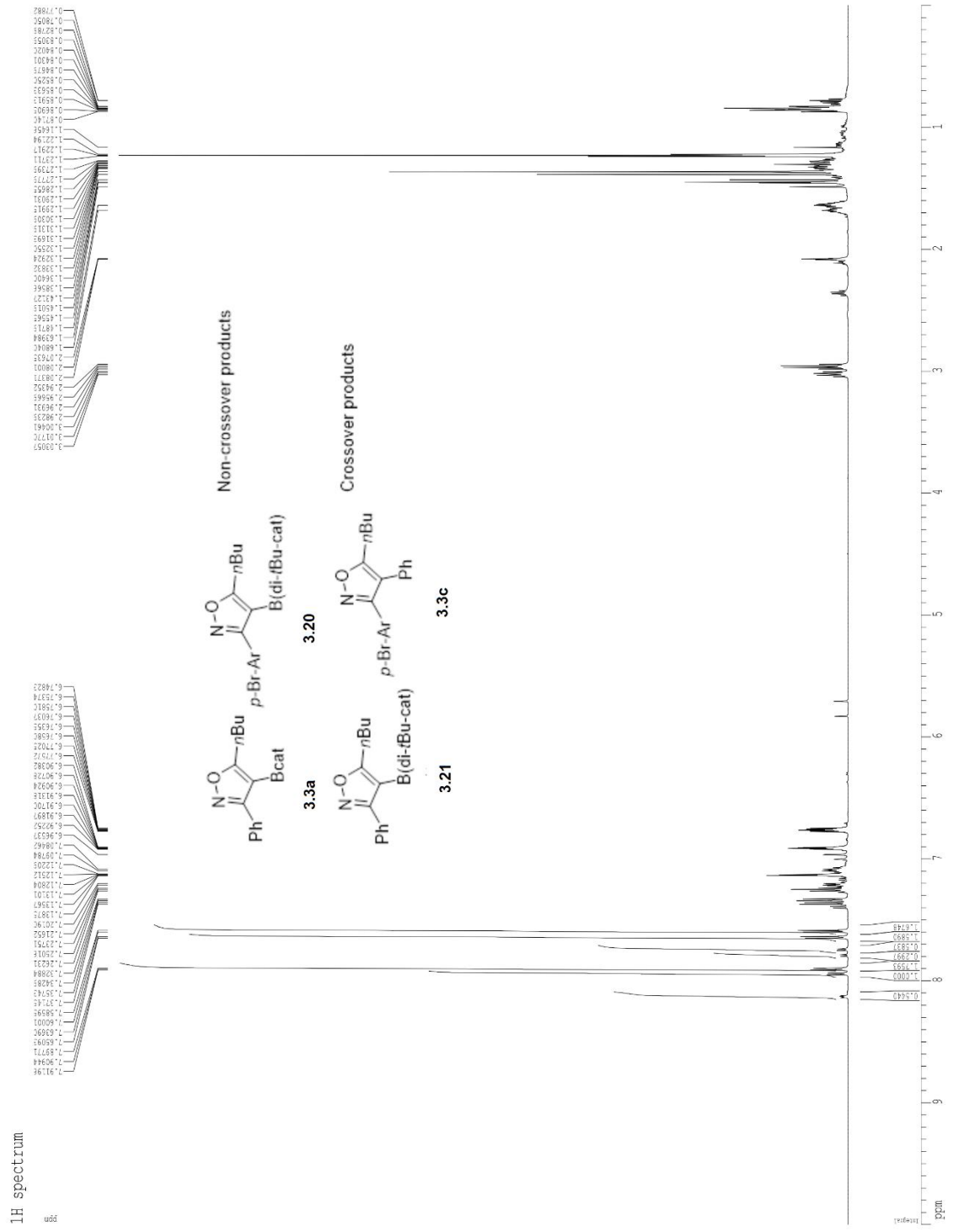
1H spectrum
Non-crossover products
Crossover products
3.3a
3.20
3.21
3.3c
ppm

Chapter 4

An Oxyboration Route to a Single Regioisomer of Borylated Dihydrofurans and Isochromenes

Abstract: An oxyboration reaction that employs B–O σ bonds as addition partners to C–C π bonds to form borylated dihydrofurans and isochromenes has been developed. By nature of the mechanism, the reaction produces exclusively one borylated regioisomer, in contrast to and/or complementary to alternative routes that produce these borylated heterocycles via C–H activation. Access to the borylative heterocyclization route is demonstrated from alcohols directly or from a hydroboration–oxyboration sequence starting from the corresponding ketone, forming the heterocyclic core and installing the boron in one synthetic step. Catechol boronates were directly used as coupling partners in the in situ Suzuki cross coupling reactions without transesterification to pinacol boronates. This chapter is reprinted in part, with permission, from a previously published report where I served as first author, working together with another graduate student Chao Gao[1] whose contribution is noted in the experimental section and in the text.

Introduction

Borylated heterocycles are versatile synthetic intermediates, such as building blocks for drug discovery and for the synthesis of materials.[2,3] The common approach to constructing borylated heterocycles is through construction of the heterocycle followed by borylation in a separate synthetic step.[4] A method for constructing the heterocyclic core and installing the boron in one synthetic step through a borylative heterocyclization reaction would be synthetically appealing due to its complementary bond disconnections, regiochemistry, and functional group tolerance.[5–12] Herein we develop one-step cyclative oxyboration routes to two *O*-heterocycle classes, dihydrofurans and isochromenes, for which existing iridium-catalyzed C–H activation–borylation methods provide unsatisfactory or complementary regioselectivity.[13,14]

We describe the motivation for developing an approach to each of these two *O*-heterocyclic cores separately in more detail: Substituted 2,3-dihydrofurans are found in a range of natural and

synthetic products such as Aflatoxin B_1,[15] with many exhibiting interesting biological activity.[16–22] Yet currently, there is only one report on the synthesis of borylated dihydrofurans, by Miyaura.[13] That reported iridium-catalyzed C–H activation–borylation method proceeded with low regioselectivity, however (Scheme 4.1). Given that the regioselectivity of oxyboration is dictated by the cyclization step, in contrast, we envisioned that an alternative borylative heterocyclization strategy may overcome the challenge of poor regioselectivity in the synthesis of this compound class.[5–7,10]

Similarly, isochromenes are common cores in biologically active compounds, including natural products and pharmaceuticals.[23,24,33,25–32] Due to their ubiquity,[23–28] developing synthetic methods from simple and readily available starting materials has been the focus of ongoing research.[23–25] The extension to isochromenes was completed by graduate student Chao Gao, and his contributions are noted in this chapter.

Synthetic methods to borylated isochromenes, specifically, are synthetically appealing because such compounds could be further functionalized through established cross-coupling reactions.[34,35] There are, however, limited examples for the generation of borylated isochromenes, by Miyaura,[13,14] again via iridium-catalyzed C–H activation/borylation. In that case, exclusive access to the 3-borylated isochromene was reported, whereas we envisioned that the borylative heterocyclization described here would access the complementary 4-borylated isochromene. The development of an oxyboration route to dihydrofurans and isochromenes will now be described in sequence, providing the chronology of the investigations and allowing for comparison and contrast between the two ring systems.

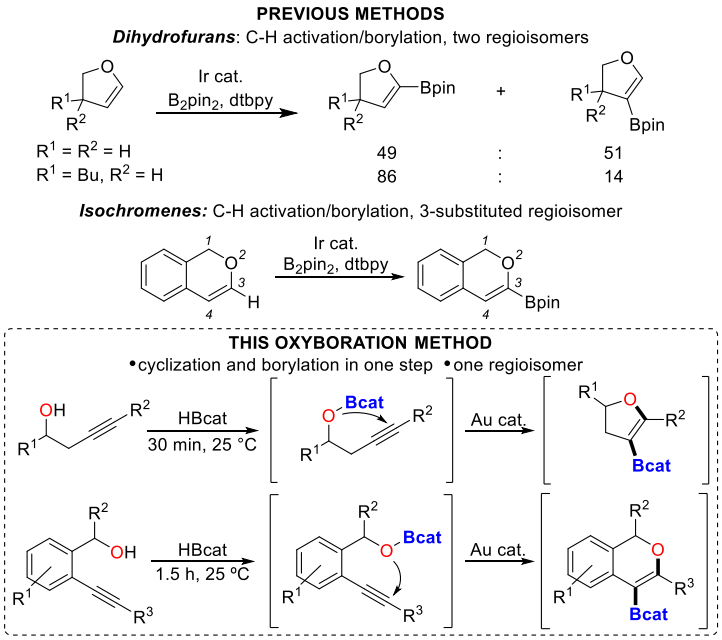

Scheme 4.1. Comparison of previous method and oxyboration method

Results and Discussions

As part of prior oxyboration studies, we had previously identified an initial condition that resulted in gold-catalyzed formation of a borylated dihydrofuran, albeit in low yield.[5] This reaction was an extension of our work accessing other ring systems through oxyboration reactions, wherein we identified that quenching the gold catalyst at the end of the reaction resulted in higher product yields,[5] including on scale.[36] Yet optimization studies herein in the dihydrofuran system (Scheme 4.2) found the opposite result. Quenching the active gold catalyst using triphenylphosphine at the end of the reaction was detrimental to the integrity of the desired product, causing decomposition of the product after 15 h; thus we herein optimized conditions that were absent of triphenyphosphine. Furthermore, the cyclization reaction (**4.2a** to **4.3a**) was particularly sensitive to temperature. Reactions at 40 °C or 50 °C produced similar ^{1}H NMR spectroscopy yields, but reactions at 60–100 °C resulted decreased yields of desired product by promoting product decomposition. Transesterification of the moisture-sensitive catechol boronic ester to the bench-

stable pinacol boronic ester (Bpin) at ambient temperature was performed for final product isolation.[6–10]

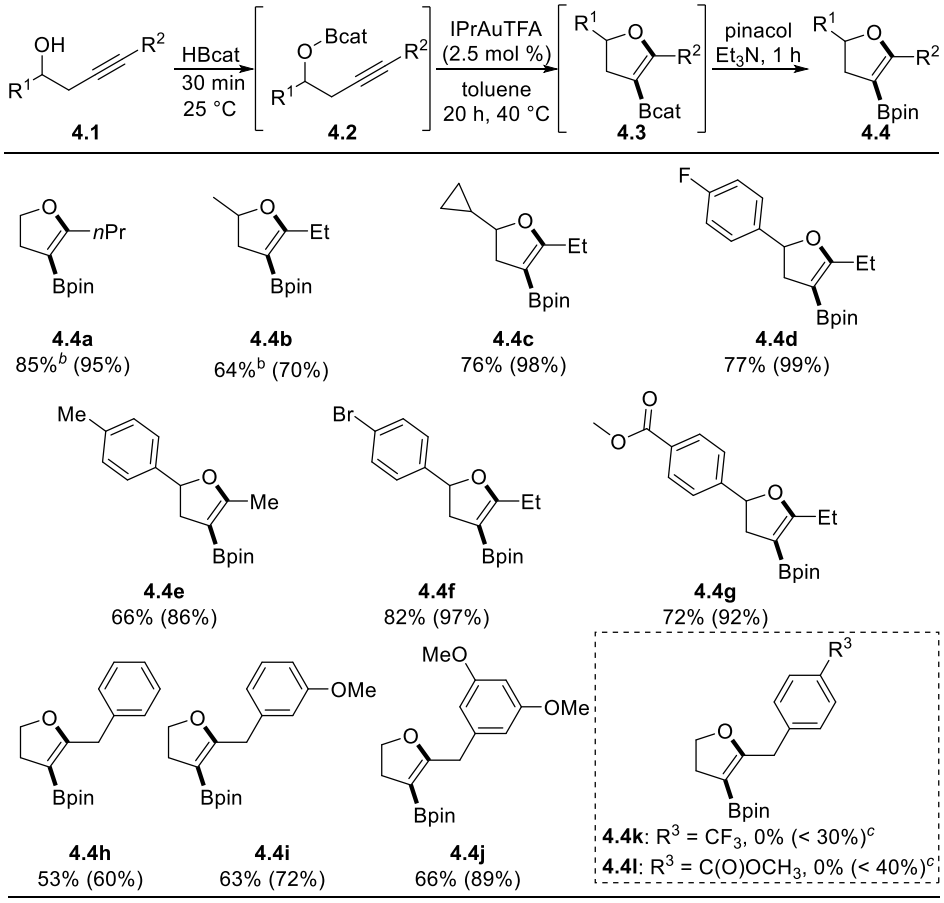

[a]Yield of **4.4** ([1]H NMR spectroscopy yield of **4.3**), [b]benzene as solvent instead of toluene, [c]spectroscopic overlap of impurities resulted in approximate [1]H NMR yield.

Scheme 4.2. 3-Borylated Dihydrofurans Substrate Scope[a]

Under the optimized reaction conditions, the substrate scope was examined (Scheme 4.2). The oxyboration method tolerated functional groups including fluoride (**4.4d**), electron-rich (**4.4e**, **4.4i**, **4.4j**) and electron-poor aryl groups (**4.4g**), and aliphatic substitution (**4.4a**–**4.4c**). The reaction tolerated cyclopropyl (**4.4c**), a fragment of interest in pharmaceutical discovery.[37–42] In contrast to palladium-catalyzed routes to borylated heterocycles,[43] the optimized oxyboration route tolerated bromoarenes (**4.4f**), granting the opportunity for a subsequent cross-coupling reaction at that orthogonal functional group. The borylative cyclization step for these substrates provided

intermediate **4.3** in moderate-to-quantitative ^{1}H NMR spectroscopy yields of a single regioisomer, which was then transesterified to bench-stable **4.4**. The reaction is not compatible with electron-rich R^1 as no conversion to **4.3** was observed when R^1 = *p*-anisyl (see experimental section for more information). Due to the synthetic difficulty of accessing the requisite starting material, no substitution at the 4-position was attempted.

Aryl substitution at R^2, however, resulted in a reaction that did not fully consume **4.2**, stopping at less than 50% consumption. We hypothesized that the phenyl ring in direct conjugation with the alkyne might slow the desired cyclization relative to the rate of catalyst decomposition. This hypothesis was tested by changing to benzyl substituents (i.e., removing the direct conjugation); the reaction then indeed proceeded in good yields for electron-rich or neutral benzyl groups (**4.4h**, **4.4i** and **4.4j**). However, substitution with electron-poor benzyl groups (substrate leading to attempted formation of **4.4k** and **4.4l**, CF_3 and $COOCH_3$, respectively), led to the corresponding dihydrofurans **4.5** with a hydrogen in the place of the desired boron (Figure 4.1; plausibly arising from protodeborylation) as the major reaction products as determined by ^{1}H NMR spectroscopic analysis of the crude reaction mixtures of corresponding **4.3k** and **4.3l**. These relatively low ^{1}H NMR spectroscopy yields of **4.3k** and **4.3l** could not be determined accurately due to overlap between the resonances corresponding to the desired oxyboration product and undesired protiated product. The minor desired catechol boronates in these cases nevertheless did not undergo successful transesterification to isolable pinacol boronates, possibly due to the presence of reactive byproducts under these conditions.

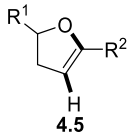

4.5

Figure 4.1. Undesired dihydrofurans without boron, **4.5**.

For the conjugated substrates (R^2 = aryl), which displayed conversions <50%, we considered an alternative formal borylation method. In this method, an electrophilic boron reagent (ClBcat[5–10] identified by our laboratory, or BCl_3 identified by Ingleson[11,12]) activates the C–C π bond and promotes a cyclization–demethylation sequence, without requiring formation of a B–O σ bond in the starting material. We decided to test this alternative route with alkynyl ether **4.6** as a substrate and ClBcat and BCl_3 as activating agents. Desired product **4.8** did not form, but rather partial conversion occurred to a species giving rise to a ^{11}B NMR spectroscopy signal at 11–12 ppm, consistent with tetracoordinated boron, which still maintained the methyl group as depicted in compounds **4.7a** and **4.7b**[44] (eq 4.1). This lack of completed formal borylative heterocyclization reactivity is consistent with our proposed model, in which substrate classes with pK_a of the corresponding heteroatom–H bonds (in this case RO–H) that are greater than 10 have higher potential for successful direct borylation (through B–O σ bonds) than for formal borylation (through intermolecular activation by external boron electrophiles followed by dealkylation).[10]

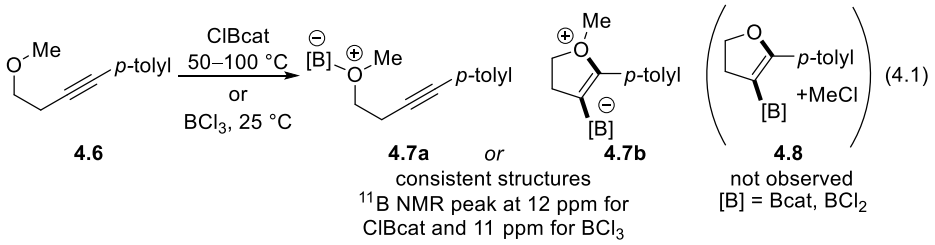

Concurrently, the oxyboration route to borylated isochromenes was investigated by graduate student Chao Gao. These results are included here to provide a full story. The same catalyst was found to be optimal in this case (Scheme 4.3; see experimental section for full catalyst optimization details). The primary challenge in the extension of the method to the synthesis of borylated isochromenes occurred upon attempted product isolation (Table 4.1). These products

showed sensitivity at both the benzylic carbon and the carbon–boron bond, indicated by positions *1* and *4* in structure **4.11**.

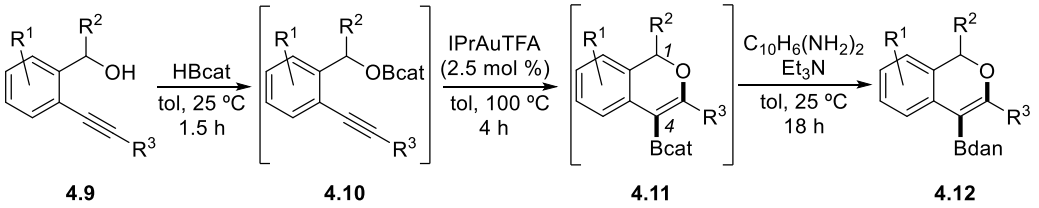

Scheme 4.3. 4-Borylated isochromenes

First, **4.11a** was chosen as the model compound for product isolation optimization. Examination of the crude reaction mixture by ^{1}H NMR spectroscopy showed that cyclization was successful (>95% conversion). In contrast to the dihydrofuran systems, attempted formation of the analogous isochromene Bpin product **4.14a** from **4.11a** through transesterification proved unsuccessful as the product decomposed upon exposure to air (Table 4.1, entry 2).

The model substrate was switched to **4.11b**, which had the benzylic position hindered. With the new substrate, the resulting Bpin product **4.14b** could be isolated. However, the C–Bpin bond was not as robust as in the dihydrofuran systems, resulting in a formation of the protodeborylated product (**4.15**) upon exposure of the product to air for 5 d (Table 4.1, entry 3; see experimental section for full details). Consistent with the reports from Suginome[45] and Wang[46], it was found that transformation with 1,8-diaminonaphthalene (as Bdan) provided a viable isolation method, imparting the desired air stability (Table 4.1, entry 4 and 5, **4.12a** and **4.12b**).

Table 4.1. Isolation methods explored by graduate student Chao Gao

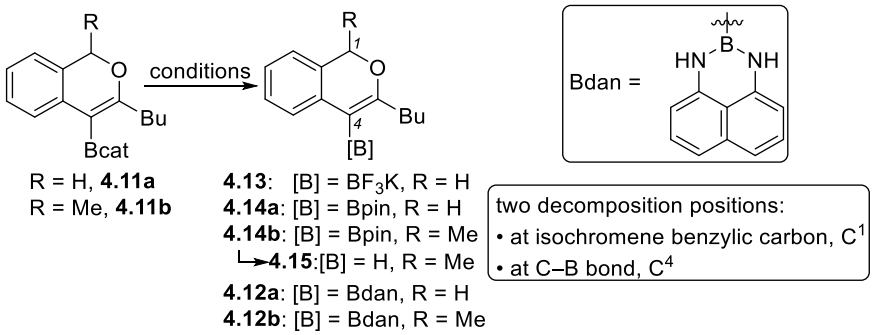

entry	substrate	boron ligand exchange (%)[a]	[B]	benzylic stability	B –C stability
1	**4.11a**	0	BF_3K	N/A	N/A
2	**4.11a**	>99	Bpin	18 h	N/A
3	**4.11b**	>99	Bpin	stable	5 d
4	**4.11a**	>99	Bdan	stable	stable
5	**4.11b**	>99	Bdan	stable	stable

[a] Calculated through ratio of products to starting material in ^{1}H NMR spectra

Under standard reaction conditions of 4 h at 100 ˚C, with isolation as Bdan, the substrate scope was investigated (Scheme 4.4). Products **4.12c**, **4.12e**, **4.12f**, and **4.12g** demonstrated the reaction's tolerance of alkyl and aryl chlorides and fluorides. Products **4.12d** and **4.12e** contained a cyclopropyl and a trifluoromethyl group, respectively, which are desirable for the synthesis of pharmaceuticals and biologically active molecules.[37–41,47] Formation of compound **4.12e** required harsher conditions (120 ˚C, 18 h), plausibly due to the strong electron-withdrawing ability of the trifluoromethyl group adjacent to the oxygen, hindering nucleophilic cyclization. A similar result was observed with **4.12g**, wherein an electron-withdrawing group that was para to the nucleophile resulted a slower cyclization reaction (100 ˚C, 19 h). The successful synthesis of isopropyl **4.12h**, however, showed that a more sterically hindered nucleophile could be tolerated in this intramolecular reaction.

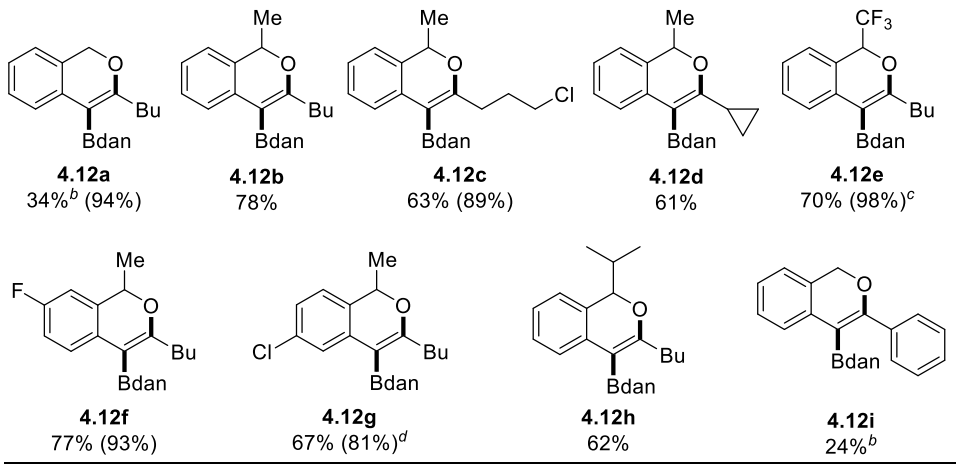

[a]Yield of **4.12** ([1]H NMR yield of **4.11**); [1]H NMR yield of **4.11** was only taken for reactions in which desired and protodeborylated product peaks in [1]H NMR spectra were well separated; [b]challenging isolation; [c]T = 120 ºC, *t* = 18 h; [d]T = 100 ºC, *t* = 19 h

Scheme 4.4. 4-Borylated isochromene substrate scope[a] determined by graduate student Chao Gao

The [1]H NMR yield of **4.12a** (94%) was high, however, significant material was lost upon attempted isolation (34%), presumably due to the instability of the (non-methyl-substituted) benzylic carbon during flash column chromatography. The similarly low yield of **4.12i** (24%) further suggested the instability of this unsubstituted product class.

We were inspired by the work of Nöth[48] to examine if intermediate **4.10b** could be generated directly from **4.16** via reductive hydroboration (Scheme 4.5). This reaction proceeded at 50 ˚C for 5 h in the presence of 2 equiv HBcat. Removing excess HBcat under reduced pressure, followed by oxyboration, produced the desired isochromene product (**4.12b**) in 68% yield. Thus, ketones can serve as complementary starting materials via a hydroboration–oxyboration sequence.

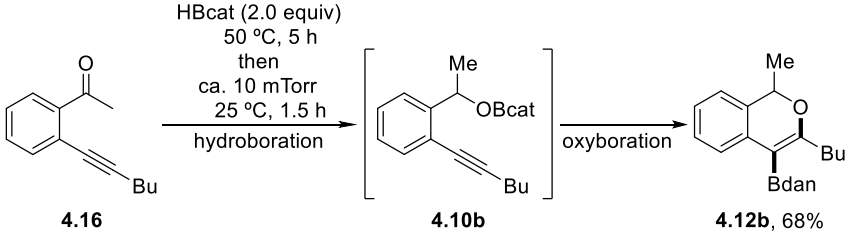

Scheme 4.5. Synthesis of isochromenes via hydroboration–oxyboration

We next turned attention to closer examination of the regioisomeric characterization of product class **4.12**. Compound **4.11** (Bcat cyclization product) was regioisomerically pure on the basis of ^{1}H NMR spectroscopic analysis of the crude reaction mixture. Similar cyclization reactions that generate the alternative 5-membered products (e.g., **4.17** type) have been reported, however, and the ^{1}H NMR spectroscopy differentiation between the 5- and 6-membered ring products may not be straightfoward.[25,49] To establish which regioisomer was generated under the oxyboration route, a structure elucidation study was done (Scheme 4.6). Substrate **4.9b** was subjected to standard oxyboration conditions, and the product was deliberately protodeborylated via an acidic workup to make one of the two possible regioisomers, **4.15** or **4.17**, which was then purified. The ^{1}H NMR spectrum of this sample was consistent with that reported for **4.15**.[25] This material was then subjected to ozonolysis. ^{1}H NMR spectroscopic analysis of the ozonolysis products established the presence of only **4.18** in both the crude and purified samples, and thus that the 6-membered product (**4.15**) was the only cyclization product (corresponding to the 6-membered ring structures shown in Scheme 4.4).

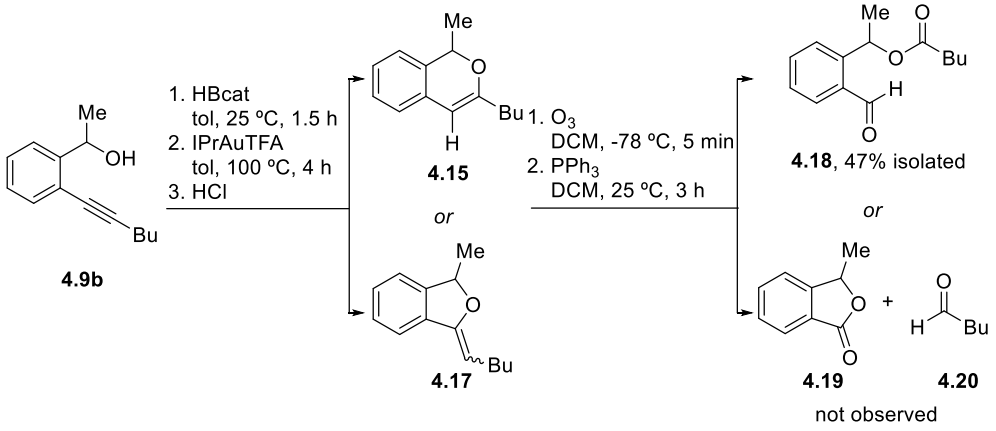

Scheme 4.6. Structure Elucidation performed by graduate student Chao Gao

Synthetic utility. A 6 mmol scale oxyboration reaction smoothly afforded 1.43 g of **4.4a** from **4.1a** in 20 h at 40 °C (75%). On this scale, a catalyst loading reduction to 1.8 mol % was possible, as was a higher substrate concentration (eq 4.2).

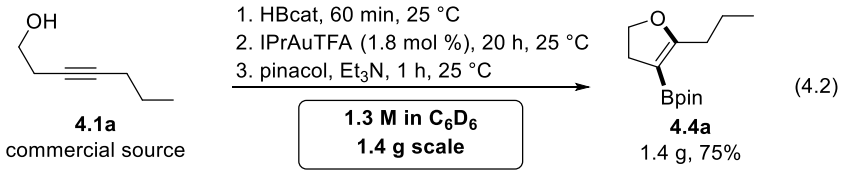

(4.2)

To demonstrate the utility of oxyboration to produce borylated building blocks that are suitable for downstream C–C bond-forming reactions, in situ Suzuki cross-coupling reactions were demonstrated on the Bcat intermediates of both substrate classes. These reactions established that the transesterification/boron group manipulation was not necessary in cases where immediate downstream functionalization was desired.

As mentioned previously, borylated dihydrofurans were found to be sensitive to high temperature during oxyboration optimization. Yet procedures for Suzuki cross-coupling reactions often require elevated temperatures of 70–100 °C.[34,50] The conditions for mild-temperature Suzuki cross-coupling reactions and mechanistic studies by Denmark[51] motivated our examination of cesium hydroxide monohydrate as a reagent for promoting palladium-catalyzed cross-coupling reactions of Bcat intermediate **4.3a**. Employment of this reagent combination at ambient temperature resulted in the successful synthesis of **4.22** and **4.24** directly from catechol boronate **4.3a** (77% and 56% yield, respectively) (Scheme 4.7).

In the case of borylated isochromenes, yields in cross-coupling reactions were found to be highly dependent on quantity of water employed in the reaction (Scheme 4.7). Addition of some water accelerated the cross-coupling reaction, but excesses lead to decomposition of **4.11b** through competing protodeborylation. Optimized addition of 1.1 equiv of water, with $Pd(PPh_3)_4$ and Cs_2CO_3, effectively catalyzed the cross-coupling reaction of **4.11b** with aryl iodide **4.25** at 100 ˚C to afford **4.26** (66% yield over three steps from alkynyl benzyl alcohol **4.9b**).

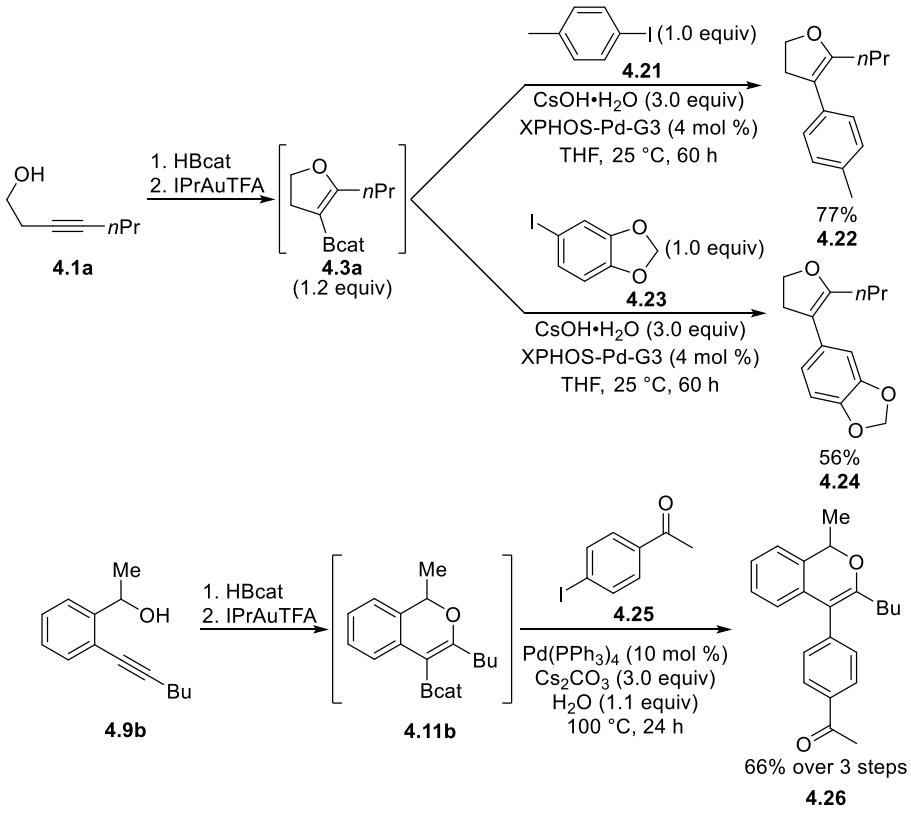

Scheme 4.7. Downstream Functionalization

Conclusions

A method has been developed for preparing 3-borylated dihydrofurans and 4-borylated isochromenes via an oxyboration reaction that generates exclusively one regioisomer, in contrast and/or compliment to alternative C–H activation routes. The method can be scaled, and generates borylated heterocycles suitable for downstream functionalization, as highlighted in the Suzuki cross-coupling of the catechol boronates. The oxyboration reaction toward borylated isochromenes can also harness the corresponding ketones instead of benzyl alcohols as substrates. The method provides a useful tool to access functionalized, regioisomerically pure borylated dihydrofurans and isochromenes as building blocks for organic synthesis.

References

(1) Tu, K. N.; Gao, C.; Blum, S. A. *J. Org. Chem.* **2018**, *83*, 11204–11217.
(2) Godula, K.; Sames, D. *Science* **2006**, *312*, 67–72.
(3) Welsch, M. E.; Snyder, S. A.; Stockwell, B. R. *Curr. Opin. Chem. Biol.* **2010**, *14*, 347–361.

(4) Larsen, M. A.; Hartwig, J. F. *J. Am. Chem. Soc.* **2014**, *136*, 4287–4299.
(5) Hirner, J. J.; Faizi, D. J.; Blum, S. A. *J. Am. Chem. Soc.* **2014**, *136*, 4740–4745.
(6) Chong, E.; Blum, S. A. *J. Am. Chem. Soc.* **2015**, *137*, 10144–10147.
(7) Tu, K. N.; Hirner, J. J.; Blum, S. A. *Org. Lett.* **2016**, *18*, 480–483.
(8) Faizi, D. J.; Issaian, A.; Davis, A. J.; Blum, S. A. *J. Am. Chem. Soc.* **2016**, *138*, 2126–2129.
(9) Faizi, D. J.; Davis, A. J.; Meany, F. B.; Blum, S. A. *Angew. Chem. Int. Ed.* **2016**, *55*, 14286–14290.
(10) Issaian, A.; Tu, K. N.; Blum, S. A. *Acc. Chem. Res.* **2017**, *50*, 2598–2609.
(11) Warner, A. J.; Lawson, J. R.; Fasano, V.; Ingleson, M. J. *Angew. Chem. Int. Ed.* **2015**, *54*, 11245–11249.
(12) Warner, A. J.; Churn, A.; McGough, J. S.; Ingleson, M. J. *Angew. Chem. Int. Ed.* **2017**, *56*, 354–358.
(13) Kikuchi, T.; Takagi, J.; Isou, H.; Ishiyama, T.; Miyaura, N. *Chem. Asian J.* **2008**, *3*, 2082–2090.
(14) Kikuchi, T.; Takagi, J.; Ishiyama, T.; Miyaura, N. *Chem. Lett.* **2008**, *37*, 664–665.
(15) Green, S. *Nature* **1968**, *220*, 931–932.
(16) Jacobi, P. A.; Selnick, H. G. *J. Org. Chem.* **1990**, *55*, 202–209.
(17) Koike, T.; Takai, T.; Hoashi, Y.; Nakayama, M.; Kosugi, Y.; Nakashima, M.; Yoshikubo, S.; Hirai, K.; Uchikawa, O. *J. Med. Chem.* **2011**, *54*, 4207–4218.
(18) Kilroy, T. G.; O'Sullivan, T. P.; Guiry, P. J. *Eur. J. Org. Chem.* **2005**, *2005*, 4929–4949.
(19) Shi, G. Q.; Dropinski, J. F.; Zhang, Y.; Santini, C.; Sahoo, S. P.; Berger, J. P.; MacNaul, K. L.; Zhou, G.; Agrawal, A.; Alvaro, R.; Cai, T.; Hernandez, M.; Wright, S. D.; Moller, D. E.; Heck, J. V.; Meinke, P. T. *J. Med. Chem.* **2005**, *48*, 5589–5599.
(20) Freire, C. P. V.; Ferreira, S. B.; de Oliveira, N. S. M.; Matsuura, A. B. J.; Gama, I. L.; da Silva, F. de C.; de Souza, M. C. B. V.; Lima, E. S.; Ferreira, V. F. *Medchemcomm* **2010**, *1*, 229–232.
(21) Matsuya, Y.; Suzuki, N.; Kobayashi, S.-Y.; Miyahara, T.; Ochiai, H.; Nemoto, H. *Bioorg. Med. Chem.* **2010**, *18*, 1477–1481.
(22) Lipshutz, B. H. *Chem. Rev.* **1986**, *86*, 795–819.
(23) Mancuso, R.; Mehta, S.; Gabriele, B.; Salerno, G.; Jenks, W. S.; Larock, R. C. *J. Org. Chem.* **2010**, *75*, 897–901.
(24) Varela-Fernández, A.; González-Rodríguez, C.; Varela, J. A.; Castedo, L.; Saá, C. *Org. Lett.* **2009**, *11*, 5350–5353.
(25) Tomás-Mendivil, E.; Starck, J.; Ortuno, J.-C.; Michelet, V. *Org. Lett.* **2015**, *17*, 6126–6129.
(26) Wang, W.; Li, T.; Milburn, R.; Yates, J.; Hinnant, E.; Luzzio, M. J.; Noble, S. A.; Attardo, G. *Bioorg. Med. Chem. Lett.* **1998**, *8*, 1579–1584.
(27) Harborne, J. B.; Girija, A. R.; Devi, H. M.; Lakshmi, N. K. M. *Phytochemistry* **1983**, *22*, 2741–2742.
(28) Kanokmedhakul, S.; Kanokmedhakul, K.; Nasomjai, P.; Louangsysouphanh, S.; Soytong, K.; Isobe, M.; Kongsaeree, P.; Prabpai, S.; Suksamrarn, A. *J. Nat. Prod.* **2006**, *69*, 891–895.
(29) Wang, C.; Wei, G.; Yang, X.; Yao, H.; Jiang, J.; Liu, J.; Shen, M.; Wu, X.; Xu, J. *Org. Biomol. Chem.* **2014**, *12*, 7338–7344.
(30) Fu, R.; Yan, T.; Wang, Q.; Guo, Q.; Yao, H.; Wu, X.; Li, Y. *Vascul. Pharmacol.* **2012**, *57*, 105–112.
(31) Fu, R.; Wang, Q.; Guo, Q.; Xu, J.; Wu, X. *Vascul. Pharmacol.* **2013**, *58*, 78–86.
(32) Fu, R.; Chen, Z.; Wang, Q.; Guo, Q.; Xu, J.; Wu, X. *Atherosclerosis* **2011**, *219*, 40–48.

(33) Qian, H.; Huang, W. L.; Wu, X. M.; Zhang, H. Bin; Zhou, J. P.; Ye, W. C. *Chin. Chem. Lett.* **2007**, *18*, 1227–1230.
(34) Miyaura, N.; Suzuki, A. *Chem. Rev.* **1995**, *95*, 2457–2483.
(35) Roy, D.; Uozumi, Y. *Adv. Synth. Catal.* **2018**, *360*, 602–625.
(36) Faizi, D. J.; Nava, N. A.; Al-Amin, M.; Blum, S. A. *Org. Synth.* **2016**, *93*, 228–244.
(37) Wishart, D. S.; Knox, C.; Guo, A. C.; Cheng, D.; Shrivastava, S.; Tzur, D.; Gautam, B.; Hassanali, M. *Nucleic Acids Res.* **2008**, *36*, D901–D906.
(38) Yuan, Y.; Lee, R. E.; Besra, G. S.; Belisle, J. T.; Barry, C. E. *Proc. Natl. Acad. Sci.* **1995**, *92*, 6630–6634.
(39) George, K. M.; Yuan, Y.; Sherman, D. R.; Barry, C. E. *J. Biol. Chem.* **1995**, *270*, 27292–27298.
(40) Meanwell, N. A. *J. Med. Chem.* **2011**, *54*, 2529–2591.
(41) Salaün, J. In *Small ring compounds in organic synthesis VI*; Springer, 2000; pp 1–67.
(42) Talele, T. T. *J. Med. Chem.* **2016**, *59*, 8712–8756.
(43) Takagi, J.; Takahashi, K.; Ishiyama, T.; Miyaura, N. *J. Am. Chem. Soc.* **2002**, *124*, 8001–8006.
(44) Issaian, A.; Faizi, D. J.; Bailey, J. O.; Mayer, P.; Berionni, G.; Singleton, D. A.; Blum, S. A. *J. Org. Chem.* **2017**, *82*, 8165–8178.
(45) Nogushi, H.; Hojo, K.; Suginome, M. *J. Am. Chem. Soc.* **2007**, *129*, 758–759.
(46) Yuan, K.; Wang, S. *Org. Lett.* **2017**, *19*, 1462–1465.
(47) Geri, J. B.; Szymczak, N. K. *J. Am. Chem. Soc.* **2017**, *139*, 9811–9814.
(48) Männig, D.; Nöth, H. *Angew. Chem. Int. Ed.* **1985**, *24*, 878–879.
(49) Terada, M.; Li, F.; Toda, Y. *Angew. Chem. Int. Ed.* **2014**, *53*, 235–239.
(50) Maluenda, I.; Navarro, O. *Molecules* **2015**, *20*, 7528–7557.
(51) Thomas, A. A.; Zahrt, A. F.; Delaney, C. P.; Denmark, S. E. *J. Am. Chem. Soc.* **2018**, *140*, 4401–4416.

Experimental

General Methods

All reagents were used as received from commercial sources unless otherwise stated. 1,2-Dimethoxylethane was purchased from Sigma–Aldrich in a Sigma–Aldrich Sure/Seal™ bottle and used without further purification. Tetrahydrofuran and triethylamine were dried by passing through an alumina column under argon pressure on a push still solvent system. Chloroform was dried over K_2CO_3,[1] degassed using three freeze-pump-thaw cycles, and vacuum transferred before use. Toluene-d_8 and C_6D_6 were dried over CaH_2, degassed using three freeze-pump-thaw cycles, and vacuum transferred before use. Catecholborane[1] was degassed using three freeze-pump-thaw cycles, and vacuum transferred before use. Ozone was generated by a ClearWater Tech, LLC M-1500 ozone generator. Cesium carbonate was dried by heating at ca. 300 ˚C under vacuum (ca. 30 mTorr) for ca. 12 h and stored in a N_2-filled glovebox. Manipulations were performed in a glovebox under nitrogen atmosphere unless otherwise noted. Analytical thin layer chromatography (TLC) was performed using Merck F_{250} plates and visualized under UV irradiation at 254 nm, or using a basic aqueous solution of potassium permanganate. Flash chromatography was conducted using a Teledyne Isco Combiflash® R_f 200 Automatic Flash Chromatography System, and Teledyne Isco Redisep® 35– 70 μm silica gel. All proton and carbon nuclear magnetic resonance (^{1}H and ^{13}C) spectra were recorded on a Bruker DRX-400 spectrometer, Bruker DRX-500 spectrometer outfitted with a cryoprobe, or a Bruker AVANCE-600 spectrometer. Boron nuclear magnetic resonance (^{11}B NMR) spectra were recorded on a Bruker AVANCE-600 or on a Bruker DRX-500 spectrometer. Fluorine nuclear magnetic resonance (^{19}F NMR) spectra were recorded on a Bruker DRX-400 spectrometer or on a Bruker AVANCE-600 spectrometer. All coupling constants were measured in Hertz (Hz). Chemical shifts were reported in ppm and referenced to the residual protiated solvent peak (δ_H = 7.26 ppm for $CDCl_3$, δ_H = 2.08 ppm for d_8-toluene, δ_H =

7.16 ppm for C_6D_6 in ^1H NMR spectroscopy experiments; δ_C = 77.16 ppm for $CDCl_3$, δ_C = 20.43 ppm for *d*$_8$-toluene, δ_C = 128.06 ppm for C_6D_6 in ^{13}C NMR spectroscopy experiments), except compounds with Bdan where chemical shifts were reported in ppm and referenced to TMS (δ_H = 0.00 ppm). ^{11}B NMR and ^{19}F NMR spectroscopy experiments were referenced to the absolute frequency of 0 ppm in the ^1H dimension according to the Xi scale. High-resolution mass spectrometry (HRMS (ESI-TOF)) data were obtained at the University of California, Irvine.

Synthetic Procedures

General Experimental Procedure A for the Synthesis of Alkynols 4.1c–4.1g.

Alkynols were prepared according to a literature procedure, repeated here for convenience and clarity.[2] Using a standard Schlenk line, to a flame-dried round bottom flask was added zinc dust (1.63 g, 25.0 mmol, 5.00 equiv) and I_2 (1.27 g, 5.00 mmol, 1.00 equiv). The flask was capped with septum and placed under dynamic N_2. Then aldehyde (5.00 mmol, 1.00 equiv), and propargyl bromide (6.00 mmol, 1.20 equiv) in dry THF (50 mL) was added via syringes at 25 °C. The resulting reaction mixture was sonicated at room temperature for 4 h. The reaction was quenched with sat. ammonium chloride (1 × 20 mL). The aqueous layer was extracted with EtOAc (1 × 30 mL). The combined organic layers were washed with brine (1 × 30 mL), dried over anhydrous Na_2SO_4, filtered through filter paper, and concentrated in vacuo. The resulting crude oil was purified by silica gel flash column chromatography using an elution gradient from 100% hexanes to 10% EtOAc in hexanes. Product-containing fractions were identified by TLC, combined and concentrated in vacuo to afford **4.1**.

General Experimental Procedure B for the Synthesis of Alkynols 4.1h–4.1j.

Alkynols were prepared according to a literature procedure, repeated here for convenience and clarity.[3] Using a standard Schlenk line, to a flame-dried round bottom flask was added terminal alkynol (0.450 mL, 6.00 mmol, 1.20 equiv) in dry THF (35 mL) via syringe, and cooled to -78 °C under dynamic N_2 atmosphere. To this cooled solution was added *n*-butyllithium (1.60 M solution in hexane) (7.8 mL, 13 mmol, 2.5 equiv) dropwise via syringe. The resulting suspension was stirred at –78 °C for 1 h, followed by addition of a solution of dry $ZnBr_2$ (2.82 g, 12.5 mmol, 2.50 equiv) in dry THF (10 mL) via syringe. The mixture was stirred at –78 °C for 10 min, then warmed to 25 °C. The catalyst Pd(DPEphos)Cl_2 (35.8 mg, 0.0500 mmol, 1.00 mol%) and benzyl bromide (5.00 mmol, 1.00 equiv) were added to the clear reaction mixture via syringe at 25 °C and stirred at 40 °C for 18 h. The reaction was quenched with 1.0 M hydrochloric acid (1 × 10 mL). The aqueous layer was extracted with ether (2 × 20 mL). The combined organic layers were washed with sat. sodium bicarbonate (1 × 15 mL), dried over anhydrous Na_2SO_4, filtered through filter paper, and concentrated in vacuo. The resulting crude oil was purified by silica gel flash column chromatography using an elution gradient from 100% hexanes to 30% EtOAc in hexanes. Product-containing fractions were identified by TLC, combined and concentrated in vacuo to afford **4.1**.

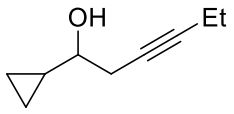

4.1c

1-cyclopropyl-3-hexyn-1-ol ***(4.1c)*** was prepared using procedure A and obtained as light yellow oil (199 mg, 29% yield). TLC (20% EtOAc/hexanes): R_f = 0.27, visualized by UV absorbance. ^{1}H NMR (d_8-toluene, 500 MHz): δ 2.94–2.89 (m, 1H), 2.36–2.26 (m, 2H), 1.97 (qt, *J* = 7.5, 2.5 Hz, 2H), 1.51 (d, *J* = 4.0 Hz, 1H), 0.97 (t, *J* = 7.5 Hz, 3H), 0.83–0.77 (m, 1H), 0.28– 0.26 (m, 2H), 0.24–0.21 (m, 1H), 0.13–0.11 (m, 1H). ^{13}C{^{1}H}NMR ($CDCl_3$, 125 MHz): δ 84.0, 76.6, 73.8, 28.3,

17.0, 14.4, 12.7, 2.4. HRMS (ESI-TOF) *m/z* calcd for $C_9H_{14}ONa$ ([M+Na]+) 161.0942, found 161.0944.

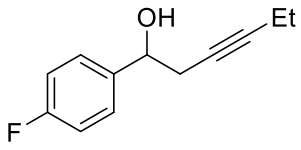

4.1d

1-(4-fluorophenyl)-3-hexyn-1-ol ***(4.1d)*** was prepared using procedure A and obtained as light yellow oil (303 mg, 32% yield). TLC (20% EtOAc/hexanes): R_f = 0.22, visualized by UV absorbance. ^{1}H NMR (d_8-toluene, 500 MHz): δ 7.03–7.00 (m, 2H), 6.77–6.73 (m, 2H), 4.44–4.41 (m, 1H), 2.33–2.32 (m, 2H), 1.93–1.88 (m, 2H), 1.82 (bs, 1H), 0.91 (td, *J* = 7.4, 3.0 Hz, 3H). ^{13}C{^{1}H}NMR (d_8-toluene, 150 MHz): δ 162.2 (d, *J* = 93.4 Hz), 139.2, 127.4 (d, *J* = 8.1 Hz), 114.7 (d, *J* = 21.2 Hz), 84.3, 75.6, 71.8, 30.1, 13.9, 12.3. ^{19}F{^{1}H}NMR (d_8-toluene, 565 MHz): δ –115.2. HRMS (ESI-TOF) *m/z* calcd for $C_{12}H_{12}FO$ ([M-H]-) 191.0872, found 191.0868.

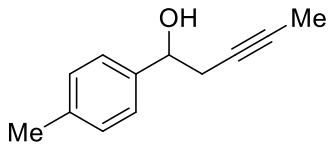

4.1e

1-(4-methylphenyl)-3-pentyn-1-ol ***(4.1e)*** was prepared using procedure A and obtained as clear oil (175 mg, 20% yield). ^{1}H NMR ($CDCl_3$, 600 MHz): δ 7.27 (d, *J* = 7.7 Hz, 2H), 7.16 (d, *J* = 7.7 Hz, 2H), 4.78 (m, 1H), 2.59–2.52 (m, 2H), 2.34 (s 3H), 1.81 (s, 3H). This spectrum is in agreement with previously reported spectral data.[4]

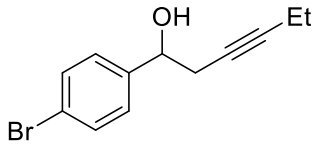

4.1f

1-(4-bromophenyl)-3-hexyn-1-ol ***(4.1f)*** was prepared using procedure A and obtained as light yellow oil (473 mg, 37% yield). TLC (20% EtOAc/hexanes): R_f = 0.29, visualized by UV absorbance. ^{1}H NMR ($CDCl_3$, 600 MHz): δ 7.47 (d, *J* = 8.4 Hz, 2H), 7.26 (d, *J* = 8.4 Hz, 2H), 4.79–4.76 (m, 1H), 2.62–2.50 (m, 2H), 2.44 (d, *J* = 3.0 Hz, 1H), 2.18 (qt, *J* = 7.2, 2.4 Hz, 2H), 1.12 (t, *J* = 7.8 Hz, 3H). ^{13}C{^{1}H}NMR ($CDCl_3$, 150 MHz): δ 141.9, 131.6, 127.7, 121.7, 85.5, 75.0, 72.1, 30.2, 14.2, 12.5. HRMS (ESI-TOF) *m/z* calcd for $C_{12}H_{12}BrO$ ([M-H]-) 251.0072, found 251.0081.

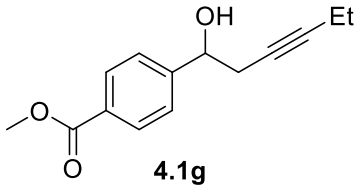

4.1g

1-(methyl-4-formylphenyl)-3-hexyn-1-ol ***(4.1g)*** was prepared using procedure A and obtained as yellow oil (330 mg, 28% yield). TLC (20% EtOAc/hexanes): R_f = 0.15, visualized by UV absorbance. ^{1}H NMR (d_8-toluene, 500 MHz): δ 8.04–8.01 (m, 2H), 7.18–7.16 (m, 2H), 4.46 (s, 1H), 3.51 (t, *J* = 2.5 Hz, 3H), 2.34–2.33 (m, 2H), 1.91–1.87 (m, 3H), 0.91 (t, *J* = 3.0 Hz, 3H). ^{13}C{^{1}H}NMR (d_8-toluene, 125 MHz): δ 171.1, 153.4, 134.8, 134.7, 130.8, 89.7, 80.4, 77.1, 56.2, 35.1, 19.1, 17.4. HRMS (ESI-TOF) *m/z* calcd for $C_{14}H_{16}O_3Na$ ([M+Na]+) 255.0997, found 255.0998.

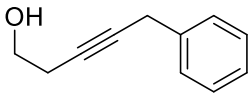

4.1h

5-phenyl-3-hexyn-1-ol ***(4.1h)*** was prepared using procedure B and obtained as yellow oil (129 mg, 16% yield). TLC (30% EtOAc/hexanes): R_f = 0.33, visualized by $KMnO_4$ stain solution. ^{1}H NMR (d_8-toluene, 500 MHz): δ 7.18 (d, *J* = 7.5 Hz, 2H), 7.11–7.10 (m, 2H), 7.02 (s, 1H), 3.36 (t, *J* = 7.0 Hz, 2H), 3.31 (s, 2H), 2.17–2.13 (m, 2H). ^{13}C{^{1}H}NMR (d_8-toluene, 125 MHz): δ 137.1, 137.2, 126.7, 124.7, 79.9, 79.5, 61.5, 25.2, 23.5. HRMS (ESI-TOF) *m/z* calcd for $C_{11}H_{12}ONa$ ([M+Na]+) 183.0786, found 183.0783.

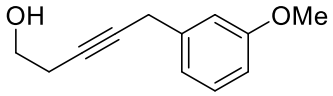

4.1i

5-(m-anisyl)-3-hexyn-1-ol ***(4.1i)*** was prepared using procedure B and obtained as yellow oil (179 mg, 19% yield). TLC (30% EtOAc/hexanes): R_f = 0.18, visualized by KMnO4 stain solution. ^{1}H NMR (C_6D_6, 600 MHz): δ 7.08 (t, *J* = 7.8 Hz, 1H), 6.98 (s, 1H), 6.90 (d, *J* = 7.8 Hz, 1H), 6.68 (d, *J* = 7.8 Hz, 1H), 3.39–3.33 (m, 7H), 2.19–2.16 (m, 2H). ^{13}C{^{1}H}NMR (C_6D_6, 150 MHz): δ 160.5, 139.2, 129.7, 120.5, 114.1, 112.3, 79.9, 79.7, 61.4, 54.7, 25.4, 23.5. HRMS (ESI-TOF) *m/z* calcd for $C_{12}H_{14}O_2Na$ ([M+Na]+) 213.0892, found 213.0894.

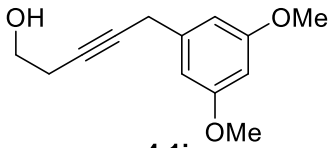

4.1j

5-(3,5-dimethoxyphenyl)-3-hexyn-1-ol ***(4.1j)*** was prepared using procedure B and obtained as yellow solid (582 mg, 53% yield). TLC (30% EtOAc/hexanes): R_f = 0.15, visualized by $KMnO_4$

stain solution. ^{1}H NMR (d_8-toluene, 600 MHz): δ 6.53 (d, J = 1.8 Hz, 2H), 6.35 (s, 1H), 3.38–3.36 (m, 8H), 3.32 (s, 2H), 2.17–2.14 (m, 2H). ^{13}C{^{1}H}NMR (d_8-toluene, 125 MHz): δ 161.6, 139.8, 106.4, 104.7, 99.0, 79.8, 79.6, 61.5, 54.7, 25.5, 23.6. HRMS (ESI-TOF) *m/z* calcd for $C_{13}H_{16}O_3Na$ ([M+Na]+) 243.0997, found 243.0996.

Optimization of direct oxyboration

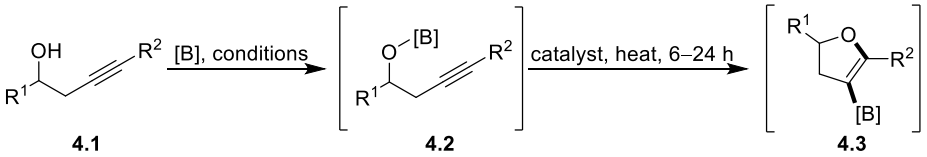

4.1 **4.2** **4.3**

Boric ester 4.2. The reaction was performed inside an N_2-filled glovebox. A 1-dram vial was charged with a solution of **4.1** (0.400 mmol, 1.00 equiv) in d_8-toluene (0.10 mL). To this solution was added a boron reagent (0.400 mmol, 1.00 equiv) at 25 °C. The reaction mixture was stirred for 30–60 min, then transferred to a J. Young tube and monitored by ^{1}H NMR spectroscopy to identify completion of the reaction to afford **4.2**, which was used directly in the screen of reaction conditions without further purification.

Boronic ester 4.3. Catalyst and additive were dissolved in d_8-toluene (0.20 mL) in a vial and transferred to the J. Young tube containing **4.2** via syringe. The vial was rinsed with d_8-toluene (0.10 mL) and this rinse was added to the J. Young tube. The tube was then capped and removed from the glovebox. The tube was heated in a preheated oil bath at the temperature listed in Table SI-4.1. After heating for the indicated time, the progress of the reaction was determined by ^{1}H and ^{11}B NMR spectroscopy. Percent conversion of desired product was calculated as the ratio of product over the sum of product and reactant.

First, a variety of gold catalysts with different ligands and counterions attached were investigated, and IPrAuTFA (entry 1, Table S4.1) was found to be the optimal catalyst, giving the highest conversion to catechol boronates **4.3** and producing less byproducts than when IPrAuCl/$AgBF_4$ (entry 10, Table S4.1) was used.

Table S4.1: Optimization of Oxyboration Reaction towards Borylated Dihydrofurans **4.3** with [B] = Bcat and R_2 = *p*-MeC_6H_4 (**SI-4.1**): Catalyst Screening

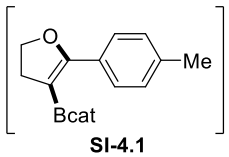

SI-4.1

Entry	[B] reagent	Conc. (M)	Catalyst	Loading (mol %)	Temp (°C)	Conversion to **SI-4.1** (%)	Time (h)
1	HBcat	1.0 M	IPrAuTFA	2.5	40 °C	55%	20 h
2	HBcat	1.0 M	IPrAuOAc	2.5	40 °C	trace	20 h
3	HBcat	1.0 M	IPrAuOTs	2.5	40 °C	trace	20 h
4	HBcat	1.0 M	IPrAuOTf	2.5	40 °C	decomposition	20 h
5	HBcat	1.0 M	$IPrAuNTf_2$	2.5	40 °C	decomposition	20 h
6	HBcat	1.0 M	IPrAuCl $AgBF_4$	2.5 2.5	40 °C	24%	18 h
7	HBcat	1.0 M	IPrAuCl $AgSbF_6$	2.5 2.5	40 °C	decomposition	18 h
8	HBcat	1.0 M	(CAAC)AuCl AgCl	2.5 2.5	40 °C	44%	18 h
9	HBcat	1.0 M	(CAAC)AuCl $AgBF_4$	2.5 2.5	40 °C	trace	18 h
10	HBcat	1.0 M	IPrAuCl $AgBF_4$	5.0 5.0	40 °C	57%	18 h
11	HBcat	1.0 M	IPrAuCl $AgBF_4$	7.5 7.5	40 °C	32%	22 h
12	HBcat	1.0 M	AgTFA	5.0	40 °C	no reaction	23 h
13	HBcat	1.0 M	$AgBF_4$	2.5	40 °C	no reaction	23 h
14	HBcat	1.0 M	IPrCuTFA	5.0	40 °C	no reaction	21 h

We also studied different amounts of additives, concentrations, IPrAuTFA catalyst loadings, reaction temperatures (Table S4.2), and found the optimal conditions in entry 7 (1.0 M reaction

concentration, 2.5 mol% catalyst, no additives, and 40 °C). However, we were not able to achieve full conversion of starting material boric ester **4.2** to boronic ester **4.3**. The reaction stopped at approximately half way even after additional catalyst added (entry 12, Table S4.2), and the remaining starting material started to decompose. We hypothesized that the aryl substituent on R_2 might play a role in hindering full conversion to boronic ester **4.3**. For additional optimization, the substrate was changed to alkyl substitution (Table S4.3).

Table S4.2: Optimization of Oxyboration Reaction towards Borylated Dihydrofurans **4.3** with [B] = Bcat and R_2 = *p*-MeC_6H_4 (**SI-4.1**): Concentration, Temperature, Catalyst Loading Screenings

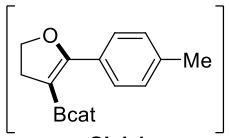

SI-4.1

Entry	[B] reagent	Conc. (M)	Catalyst	Loading (mol %)	Temp (°C)	Conversion to **SI-4.1** (%)	Time (h)
1	NaH, ClBcat	0.4 M	IPrAuTFA NaTFA	5.0 25	110 °C	28%	19 h
2	NaH, ClBcat	0.4 M	IPrAuTFA NaTFA	5.0 15	110 °C	25%	19 h
3	HBcat	0.4 M	IPrAuTFA NaTFA	5.0 25	110 °C	30%	19 h
4	HBcat	1.0 M	IPrAuTFA	2.5	110 °C	33%	20 h
5	HBcat	1.0 M	IPrAuTFA	2.5	50 °C	53%	20 h
6	HBcat	1.0 M	IPrAuTFA	2.5	60 °C	48%	20 h
7	**HBcat**	**1.0 M**	**IPrAuTFA**	**2.5**	**40 °C**	**55%**	**20 h**
8	HBcat	1.0 M	IPrAuTFA	2.5	25 °C	29%	26 h
9	HBcat	10 M	IPrAuTFA	2.5	40 °C	30%	25 h
10	HBcat	5.0 M	IPrAuTFA	2.5	40 °C	53%	44 h
11	HBcat	0.5 M	IPrAuTFA	2.5	40 °C	48%	43 h
12	HBcat	1.0 M	IPrAuTFA	5.0	40 °C	50%	18 h
13	HBcat	1.0 M	IPrAuTFA	1.3	40 °C	23%	22 h

Table S4.3: Optimization of Oxyboration Reaction with Bcat (R^2 = *n*-C_3H_7)

Entry	[B] reagent	Conc. (M)	Catalyst	Loading (mol %)	Temp (°C)	Conversion (%)	Time (h)
1	HBcat	1.0 M	IPrAuTFA	2.5	40 °C	98%	20 h
2	HBcat	0.5 M	IPrAuTFA	2.5	40 °C	87%	22 h
3	HBcat	1.5 M	IPrAuTFA	2.5	40 °C	92%	22 h
4	HBcat	1.0 M	None	NA	40 °C	no reaction	27 h
5	HBpin	1.0 M	IPrAuTFA	2.5	40 °C	no reaction	27 h

Attempt at formal oxyboration

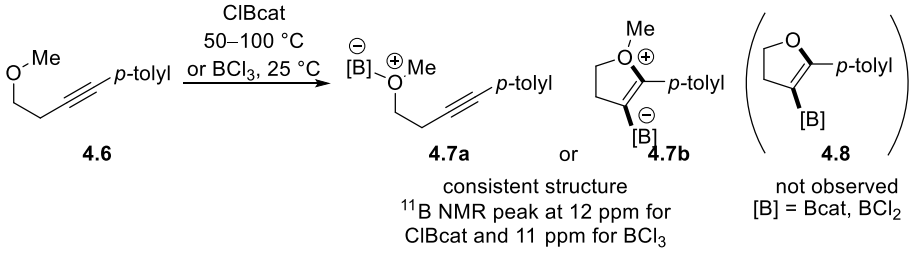

In an N_2-filled glovebox, alkynol **4.6** (69.6 mg, 0.400 mmol, 1.00 equiv) was dissolved in d_8-toluene (0.1 mL) in a 1-dram vial. B-chlorocatecholborane (86.0 mg, 0.560 mmol, 1.40 equiv) was dissolved in d_8-toluene (0.1 mL) in a separate 1-dram vial and transferred via pipette to the first vial containing **4.6**. The reaction mixture was then transferred into a J. Young NMR tube. The original vial was rinsed with d_8-toluene (0.2 mL) and the rinse was added to the same J. Young NMR tube, which was sealed and removed from glovebox. Reaction progress was determined by ^{1}H NMR spectroscopy (600 MHz, d_8-toluene) at t= 0 h and then heated to 50 °C. After 24 h, the J. Young tube was cooled down to 25 °C and ^{1}H NMR spectroscopy (600 MHz, d_8-toluene) was taken again. A species containing a tetracoordinated boron was observed, as depicted in **4.7a** and **4.7b**, due to an ^{11}B NMR spectroscopy signal at 11–12 ppm.

General procedure NMR conversions using internal standard.

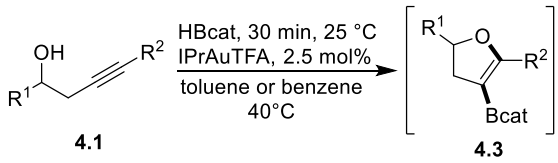

4.1 **4.3**

In an N_2-filled glovebox, alkynol **4.1** (0.40 mmol, 1.0 equiv) and phenanthrene (3–5 mg, mass was recorded accurately each time) were dissolved in d_8-toluene (0.1 mL) or C_6D_6 (0.1 mL) in a 1-dram vial equipped with stir bar. Catecholborane (42.7 µL, 0.400 mmol, 1.00 equiv) was added via gastight syringe to this solution. The resulting solution was stirred at room temperature for 0.5 h. The solution was then transferred to a vial containing the catalyst IPrAuTFA (7.0 mg, 0.0025 mmol, 2.5 mol%). The original vial was rinsed with d_8-toluene (0.2 mL) or C_6D_6 (0.2 mL) and the rinse was added to the new vial. This mixture was then transferred into a J. Young NMR tube, which was sealed and removed from the glove box. Reaction progress was monitored by ^{1}H NMR spectroscopy (600 MHz, d_8-toluene) or (600 MHz, C_6D_6) of **4.3** using the internal phenanthrene standard. The table below showed the NMR spectroscopy yield calculated using this method.

Table S4.4: ^{1}HNMR spectroscopy yield of borylated dihydrofurans **4.3**

	R_1	R_2	NMR yield (%)	Time (h)	Temperature (°C)
4.3a	H	*n*-Pr	95%	20 h	40 °C
4.3b	Me	Et	70%	20 h	40 °C
4.3c	Cpr	Et	98%	20 h	40 °C
4..3d	4-FPh	Et	99%	20 h	40 °C
4.3e	4-MePh	Me	86%	20 h	40 °C
4.3f	4-BrPh	Et	97%	20 h	40 °C
4.3g	4-MeOC(O)Ph	Et	92%	20 h	40 °C
4.3h	H	CH_2Ph	60%	20 h	40 °C
4.3i	H	CH_2-(3-MeO)Ph	72%	20 h	40 °C
4.3j	H	CH_2-(3,5-MeO)Ph	89%	20 h	40 °C

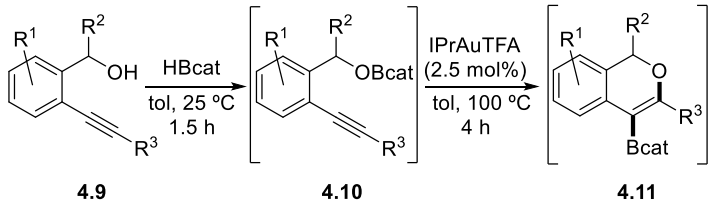

4.9 **4.10** **4.11**

This optimization study was conducted by graduate student Chao Gao.

In an N_2-filled glovebox, to a one-dram vial ("substrate vial") containing alkynyl benzylic alcohols (**4.9**) (0.400 mmol, 1.0 equiv) was added HBcat (42.6 µL, 0.400 mmol, 1.0 equiv) with a gastight syringe, followed by rinsing walls of the substrate vial with 0.05 mL d_8-toluene, and the resulting solution was left in the glovebox uncapped to allow release of H_2 gas at 25 ˚C for 1.5 h. Then, the resulting substrate solution was transferred to a separate one-dram vial ("reaction vial") containing IPrAuTFA (7.0 mg, 0.010 mmol, 2.5 mol %) and a stir bar, followed by rinsing the substrate vial with 0.35 mL d_8-toluene, and the rinse was combined with the reaction solution in the reaction vial. Then, the reaction vial was capped, and the reaction mixture was heated to 100 ˚C (or 120 ˚C for **4.10e**) and stirred at this temperature for 4 h (18 h for **4.10e**, and 19 h for **4.10g**). The resulting solution was cooled to 25 ˚C, before placing the reaction containing vial on a balance in the glovebox. Then, the weight of the reaction vial (without the cap) and reaction solution was tared, and phenanthrene (3–5 mg, mass was recorded accurately each time) was directly added to the reaction solution to prepare a homogeneous reaction solution with phenanthrene as an internal standard. ^{1}H NMR spectroscopy was performed to analyze the homogeneous solution to determine the NMR yield of compound **4.11**. The table below shows the NMR spectroscopy yield calculated using this method:

Table S4.5: ^{1}H NMR spectroscopy yield of 4-borylated isochromenes **4.11**

	R^1	R^2	R^3	NMR yield (%)	Time (h)	Temperature (°C)
4.11a	H	H	Bu	94%	4 h	100 °C
4.11c	H	Me	$(CH_2)_3Cl$	89%	4 h	100 °C
4.11e	H	CF_3	Bu	98%	18 h	120 °C
4.11f	*m*-F	Me	Bu	93%	4 h	100 °C
4.11g	*p*-Cl	Me	Bu	81%	19 h	100 °C

General Experimental Procedure for the Synthesis of pinacol boronates 4.4.

In an N_2-filled glovebox, alkynol **4.1** (0.40 mmol, 1.0 equiv) was dissolved in 0.1 mL toluene or benzene in a 1-dram vial equipped with stir bar. Catecholborane (42.7 μL, 0.400 mmol, 1.00 equiv) was added via gastight syringe to this solution. The resulting solution was left uncapped to allow the release of H_2 gas and stirred at room temperature for 0.5 h, then transferred via pipet to a 1-dram vial containing the catalyst IPrAuTFA (7.0 mg, 0.010 mmol, 2.5 mol%). The first vial was rinsed with toluene (3 × 0.10 mL) and transferred to the reaction mixture. The vial with the resulting suspension was capped and the solution was stirred on a preheated hot plate at 40 °C over an appropriate time as determined by the NMR spectroscopy yield study.

The reaction vial was cooled to room temperature and a solution of pinacol (142 mg, 1.20 mmol, 3.00 equiv) in anhydrous Et_3N (0.84 mL, 6.00 mmol, 15.0 equiv) was added. The resulting solution was stirred at 25 °C for 1 h. The vial containing the reaction mixture was then removed from the glovebox. Volatiles were removed in vacuo. The resulting light brown oil was purified by silica gel chromatography using an elution gradient from 100% hexanes to 10% EtOAc in hexanes. Solvents were removed in vacuo to afford the desired pinacol boronate **4.4**. All of the pinacol

boronates **4.4a**–**4.4j** are missing one carbon signal in their corresponding ^{13}C NMR spectroscopy data. This carbon atom is assigned to the carbon in the newly formed C–B σ-bond. This is expected due to the quadrupolar relaxation of boron.[5]

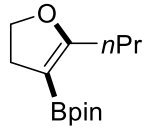

4.4a

*Pinacol boronate (**4.4a**)* was obtained as colorless oil using C_6D_6 as solvent (81 mg, 85% yield). TLC (20% EtOAc/hexanes): R_f = 0.71, visualized by UV absorbance. ^1H NMR ($CDCl_3$, 600 MHz): δ 4.28 (t, *J* = 9.6 Hz, 2H), 2.69 (t, *J* = 9.0 Hz, 2H), 2.42 (t, *J* = 7.2 Hz, 2H), 1.52 (sextet, *J* = 7.2 Hz, 2H), 1.25 (s, 12H), 0.90 (t, *J* = 7.2 Hz, 3H). $^{13}C\{^1H\}$NMR ($CDCl_3$, 150 MHz): δ 172.5, 82.6, 70.6, 32.0, 29.8, 24.9, 20.9, 13.7. $^{11}B\{^1H\}$NMR ($CDCl_3$, 192 MHz): δ 30.2 (s). HRMS (ESI-TOF) *m/z* calcd for $C_{13}H_{24}BO_3$ ([M+H]+) 239.1819, found 239.1824.

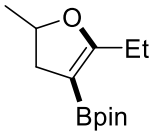

4.4b

*Pinacol boronate (**4.4b**)* was obtained as colorless oil using C_6D_6 as solvent (61 mg, 64% yield). TLC (20% EtOAc/hexanes): R_f = 0.75, visualized by UV absorbance. ^1H NMR ($CDCl_3$, 600 MHz): δ 4.68–4.63 (m, 1H), 2.82 (dd, *J* = 14, 9.6 Hz, 1H), 2.43–2.41 (m, 2H), 2.28 (dd, *J* = 14, 7.2 Hz, 1H), 1.29 (d, *J* = 6.6 Hz, 3H), 1.24 (s, 12H), 1.07 (t, *J* = 7.2 Hz, 3H). $^{13}C\{^1H\}$NMR (CDC_{l3}, 150 MHz): δ 173.1, 82.5, 78.6, 39.2, 25.0, 24.9, 22.0, 21.7, 12.4. $^{11}B\{^1H\}$NMR ($CDCl_3$, 192 MHz): δ 30.1 (s). HRMS (ESI-TOF) *m/z* calcd for $C_{13}H_{23}BO_3$ ([M]+) 238.1743, found 238.1743.

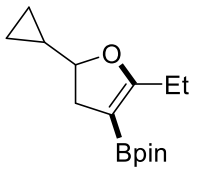

4.4c

*Pinacol boronate (**4.4c**)* was obtained as colorless oil using toluene as solvent (81 mg, 77% yield). TLC (20% EtOAc/hexanes): R_f = 0.57, visualized by UV absorbance. ^{1}H NMR ($CDCl_3$, 600 MHz): δ 4.00–3.99 (m, 1H), 2.78 (t, *J* = 11 Hz, 1H), 2.52–2.51 (m, 1H), 2.44–2.43 (m, 2H), 1.25 (s, 12H), 1.08 (s, 4H), 0.55 (s, 1H), 0.47 (s, 1H), 0.38 (s, 1H), 0.24 (s, 1H). ^{13}C{^{1}H}NMR ($CDCl_3$, 150 MHz): δ 173.3, 86.5, 82.5, 27.3, 24.98, 24.95, 21.7, 16.0, 12.6, 3.3, 1.3. ^{11}B{^{1}H}NMR ($CDCl_3$, 192 MHz): δ 30.1 (s). HRMS (CI-TOF) *m/z* calcd for $C_{15}H_{25}BO_3$ ($[M]^+$) 264.1900, found 264.1889.

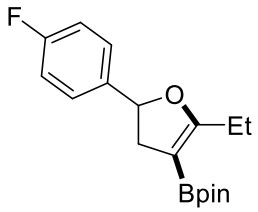

4.4d

*Pinacol boronate (**4.4d**)* was obtained as light yellow oil using toluene as solvent (97 mg, 76% yield). TLC (20% EtOAc/hexanes): R_f = 0.53, visualized by UV absorbance. ^{1}H NMR ($CDCl_3$, 600 MHz): δ 7.29 (t, *J* = 6.6 Hz, 2H), 7.02 (t, *J* = 8.7 Hz, 2H), 5.48 (t, *J* = 9.3 Hz, 1H), 3.16 (dd, *J* = 14.4, 10.8 Hz, 1H), 2.66 (dd, *J* = 14.4, 7.8 Hz, 1H), 2.55–2.50 (m, 2H), 1.25 (d, *J* = 3.0 Hz, 12H), 1.15 (t, *J* = 7.8 Hz, 3H). ^{13}C{^{1}H}NMR ($CDCl_3$, 150 MHz): δ 173.1, 163.1, 161.5, 139.4, 127.4, 115.4, 82.7, 82.5, 40.8, 25.0, 21.7, 12.5. ^{11}B{^{1}H}NMR ($CDCl_3$, 192 MHz): δ 29.6 (s). ^{19}F{^{1}H}NMR ($CDCl_3$, 565 MHz): δ –115.4. HRMS (CI-TOF) *m/z* calcd for $C_{18}H_{24}BFO_3$ ($[M]^+$) 318.1806, found 318.1804.

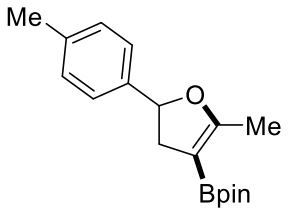

4.4e

*Pinacol boronate (**4.4e**)* was obtained as light yellow oil using toluene as solvent (97 mg, 66% yield). TLC (20% EtOAc/hexanes): R_f = 0.57, visualized by UV absorbance. ^{1}H NMR (d_8-toluene, 600 MHz): δ 7.05–7.01 (m, 3H), 6.86 (d, *J* = 7.2 Hz, 1H), 5.38 (dd, *J* = 10.2, 8.4 Hz, 1H), 3.23 (ddd, *J* = 15, 10.2, 1.8 Hz, 1H), 2.87 (ddd, *J* = 15, 8.4, 1.8 Hz, 1H), 2.25 (t, *J* = 1.8 Hz, 1H), 1.09 (d, *J* = 6.6 Hz, 12H). ^{13}C{^{1}H}NMR (d_8-toluene, 150 MHz): δ 168.8, 143.9, 137.9, 128.6, 128.3, 126.6, 123.0, 83.8, 82.5, 41.4, 25.0, 24.9, 21.3, 14.4. ^{11}B{^{1}H}NMR (d_8-toluene, 192 MHz): δ 30.3 (s). HRMS (ESI-TOF) *m/z* calcd for $C_{18}H_{25}BO_3Na$ ([M+Na]$^+$) 323.1798, found 323.1788.

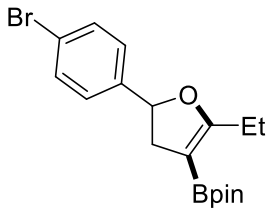

4.4f

*Pinacol boronate (**4.4f**)* was obtained as light yellow oil using toluene as solvent (125 mg, 82% yield). TLC (20% EtOAc/hexanes): R_f = 0.54, visualized by UV absorbance. ^{1}H NMR ($CDCl_3$, 600 MHz): δ 7.46 (d, *J* = 8.4 Hz, 2H), 7.20 (t, *J* = 8.4 Hz, 2H), 5.46 (t, *J* = 9.0 Hz, 1H), 3.18 (dd, *J* = 15, 10.8 Hz, 1H), 2.64 (dd, *J* = 14.4, 7.8 Hz, 1H), 2.58–2.48 (m, 2H), 1.25 (d, *J* = 3.6 Hz, 12H), 1.15 (t, *J* = 7.8 Hz, 3H). ^{13}C{^{1}H}NMR ($CDCl_3$, 150 MHz): δ 173.0, 142.7, 131.7, 127.4, 121.3, 82.7, 82.3, 40.8, 25.0, 21.6, 12.5. ^{11}B{^{1}H}NMR ($CDCl_3$, 192 MHz): δ 30.0 (s). HRMS (CI-TOF) *m/z* calcd for $C_{18}H_{24}BBrO_3$ ([M]$^+$) 380.0987, found 380.0981.

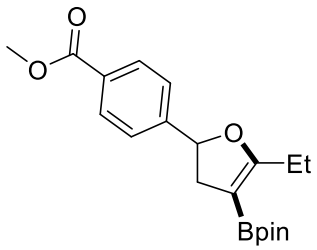

4.4g

*Pinacol boronate (**4.4g**)* was obtained as colorless oil using toluene as solvent (102 mg, 72% yield). TLC (20% EtOAc/hexanes): R_f = 0.51, visualized by UV absorbance. ^{1}H NMR ($CDCl_3$, 600 MHz): δ 8.01 (d, *J* = 7.8 Hz, 2H), 7.38 (t, *J* = 7.2 Hz, 2H), 5.55 (t, *J* = 8.4 Hz, 1H), 3.91 (s, 3H), 3.22 (t, *J* = 12.6 Hz, 1H), 2.66 (dd, *J* = 14.4, 7.8 Hz, 1H), 2.60–2.51 (m, 2H), 1.24 (d, *J* = 3.6 Hz, 12H), 1.17 (t, *J* = 7.8 Hz, 3H). ^{13}C{^{1}H}NMR ($CDCl_3$, 150 MHz): δ 173.0, 167.1, 148.9, 130.0, 129.3, 125.4, 82.7, 82.4, 52.2, 40.9, 31.7, 25.0, 22.8, 21.7, 14.3, 12.5. ^{11}B{^{1}H}NMR ($CDCl_3$, 192 MHz): δ 29.7 (s). HRMS (ESI-TOF) *m/z* calcd for $C_{20}H_{28}BO_5$ ($[M+H]^+$) 359.2034, found 359.2036.

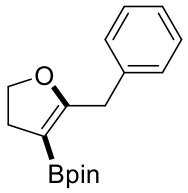

4.4h

*Pinacol boronate (**4.4h**)* was obtained as white solid using toluene as solvent (59 mg, 53% yield). TLC (40% DCM/hexanes): R_f = 0.26, visualized by UV absorbance. ^{1}H NMR (C_6D_6, 500 MHz): δ 7.51 (d, *J* = 7.5 Hz, 2H), 7.20 (t, *J* = 7.5 Hz, 2H), 7.07 (t, *J* = 7.5 Hz, 1H), 4.02 (s, 2H), 3.92 (t, *J* = 9.5 Hz, 2H), 2.67 (t, *J* = 9.5 Hz, 2H), 1.12 (s, 12H). ^{13}C{^{1}H}NMR (C_6D_6, 125 MHz): δ 171.4, 139.1, 129.4, 128.6, 126.6, 82.7, 70.8, 35.0, 32.3, 25.0. ^{11}B{^{1}H}NMR (C_6D_6, 192 MHz): δ 30.5 (s). HRMS (ESI-TOF) *m/z* calcd for $C_{17}H_{23}BO_3Na$ ($[M+Na]^+$) 309.1641, found 309.1645.

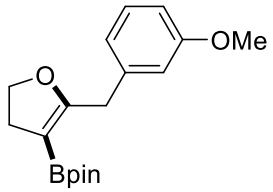

4.4i

*Pinacol boronate (**4.4i**)* was obtained as colorless oil using toluene as solvent (79 mg, 63% yield). TLC (30% EtOAc/hexanes): R_f = 0.52, visualized by UV absorbance. ^{1}H NMR (C_6D_6, 600 MHz): δ 7.21–7.13 (m, 3H), 6.71 (d, *J* = 7.8 Hz, 1H), 4.01 (s, 2H), 3.95–3.91 (m, 2H), 3.36 (d, *J* = 1.8 Hz, 3H), 2.68 (t, *J* = 9.6 Hz, 2H), 1.13 (d, *J* = 2.4 Hz, 12H). ^{13}C{^{1}H}NMR (C_6D_6, 150 MHz): δ 171,4. 160.4, 140.6, 129.5, 121.9, 115.4, 112.2, 82.7, 70.8, 54.7, 35.0, 32.3, 25.0. ^{11}B{^{1}H}NMR (C_6D_6, 192 MHz): δ 30.4 (s). HRMS (ESI-TOF) *m/z* calcd for $C_{18}H_{25}BO_4Na$ ([M+Na]$^+$) 339.1747, found 339.1735.

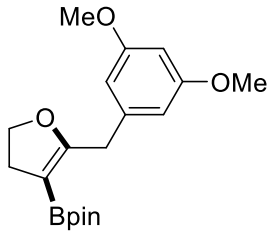

4.4j

*Pinacol boronate (**4.4j**)* was obtained as yellow solid using toluene as solvent (91 mg, 66% yield). TLC (40% DCM/hexanes): R_f = 0.22, visualized by UV absorbance. ^{1}H NMR (C_6D_6, 600 MHz): δ 6.49 (d, *J* = 2.0 Hz, 2H), 6.32 (t, *J* = 2.0 Hz, 1H), 4.28 (t, *J* = 9.5 Hz, 2H), 3.77 (s, 6H), 3.71 (s, 2H), 2.71 (t, *J* = 9.5 Hz, 2H), 1.28 (s, 12H). ^{13}C{^{1}H}NMR ($CDCl_3$, 150 MHz): δ 170.2, 160.8, 140.8, 107.0, 98.7, 82.8, 71.0, 55.4, 34.7, 31.8, 25.0. ^{11}B{^{1}H}NMR ($CDCl_3$, 192 MHz): δ 30.0 (s). HRMS (ESI-TOF) *m/z* calcd for $C_{19}H_{27}BO_5Na$ ([M+Na]$^+$) 369.1853, found 369.1866.

Gram-scale preparation of 4.4a. The gram-scale oxyboration reaction was conducted in a 100-mL bomb equipped with a stir bar in a N_2-filled glovebox. A flame-dried 100-mL bomb with a stir bar was charged with alkynol **4.1a** (0.672 g, 6.00 mmol, 1.00 equiv) together with C_6D_6 (4.6 mL) was added via syringe. To the resulting rapidly stirring suspension was added catecholborane (0.64 mL, 6.0 mmol, 1.0 equiv) via syringe. The bomb was sealed, and the suspension was stirred at room temperature for 30 min. The bomb was removed from the glovebox and placed in a preheated oil bath at 40 °C until full consumption of starting materials was achieved (18 h). This time was chosen based on the time required for conversion on the NMR scale. The bomb was moved inside the N_2-filled glovebox. Pinacol (2.12 g, 18.0 mmol, 3.00 equiv) was dissolved in anhydrous Et_3N (2.5 mL, 18 mmol, 3.0 equiv). The resulting solution was added to the above reaction mixture via syringe, and the resulting suspension was stirred at 25 °C for 1 h inside the N_2-filled glovebox. The bomb was then removed from the glovebox. Volatiles were removed in vacuo. The resulting light brown oil was purified by silica gel chromatography using an elution gradient from 100% hexanes to 10% EtOAc. Solvents were removed in vacuo to afford the desired pinacol boronate **4.4a** as a light yellow oil (1.42 g, 75% yield). Spectral data were identical to those previously obtained for this compound.

Unsuccessful Substrates for the formation of oxyboration product 4.3.

a. Incomplete conversion to boronic ester **4.3**

R^2 group is in conjugation to the alkyne

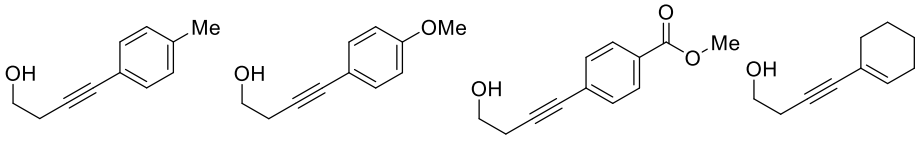

Electron-poor R^2 groups

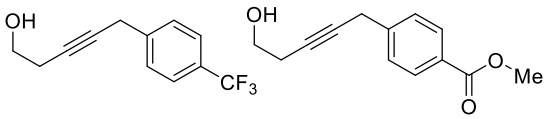

b. No conversion to boronic ester **4.3**

The reaction did not work when R^1 was strongly electron-rich or electron-poor groups, pyridyl and terminal alkyne.

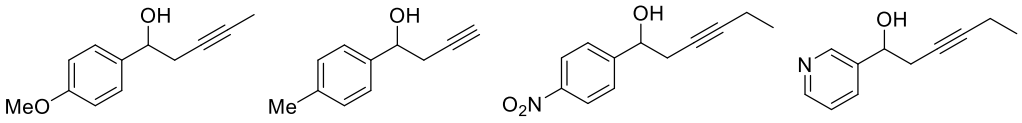

Downstream Functionalization Study of Borylated Dihydrofurans

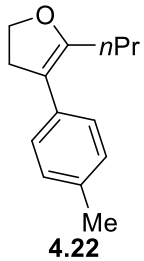

4.22

*5-propyl-4-(p-tolyl)-2,3-dihydrofuran (**4.22**)* Compound **4.3a** was prepared according to the procedure described above, except for the isolation step, and stored in a vial in d_8-toluene inside the N_2-filled glovebox without purification. The concentration of the solution of **4.3a** was calculated by ^{1}H NMR spectroscopy using an internal standard. Phenanthrene as internal standard (4.5 mg, 0.025 mmol) was dissolved in d_8-toluene (0.4 mL) in a 1-dram vial. To this solution was added a small aliquot of **4.3a** in d_8-toluene (10. μL) using gas-tight syringe. The mixture was then

transferred to a J. Young tube and removed from glovebox. The concentration of the stock solution of **4.3a** was calculated based on the integration ratio between the known phenanthrene and the unknown stock solution using ^{1}H NMR spectroscopy. This solution was used in the next step.

The cross-coupling procedure was adapted from a literature procedure.[6] In a N_2-filled glovebox, to a one-dram vial ("reaction vial") containing 4-iodotoluene (43.6 mg, 0.200 mmol, 1.0 equiv) was added CsOH•H_2O (100.8 mg, 0.6002 mmol, 3.0 equiv) and **4.3a** from the stock solution above (0.240 mmol, 1.2 equiv) via gas-tight syringe. XPHOS-Pd-G3 (6.8 mg, 0.0080 mmol, 0.040 equiv) was dissolved in THF (0.1 mL) and transferred via pipet to the reaction vial. The vial containing the Pd catalyst was rinsed with THF (0.1 mL) and the rinse was also added via pipet to the reaction vial. A stir bar was added to the reaction vial. The vial was capped and the solution was stirred at 25 °C for 2.5 d. Then the reaction vial was removed from glovebox and solution was diluted with Et_2O (1 mL). The reaction mixtued was filtered through a pad of Celite®. The reaction vial and the Celite® were rinsed with Et_2O (2 mL). The filtrate was concentrated in vacuo, and purified by flash chromatography (30% DCM in hexane) to afford a colorless oil (31 mg, 77% yield). TLC (40% DCM/hexanes): R_f = 0.53, visualized by UV absorbance. ^{1}H NMR ($CDCl_3$, 500 MHz): δ 7.13 (m, 4H), 4.34 (t, *J* = 9.0 Hz, 2H), 3.00 (t, *J* = 9.0 Hz, 2H), 2.36 (t, *J* = 8.0 Hz, 2H), 2.33 (s, 3H), 1.62 (sext, *J* = 7.5 Hz, 2H), 0.96 (t, *J* = 7.5 Hz, 3H). ^{13}C{^{1}H}NMR ($CDCl_3$, 125 MHz): δ 154.1, 134.9, 133.4, 129.1, 126.3, 108.2, 68.0, 34.2, 29.3, 21.2, 20.7, 14.1. HRMS (CI-TOF) *m/z* calcd for $C_{14}H_{18}O$ ($[M]^+$) 202.1358, found 202.1355.

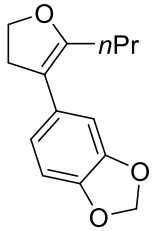

4.24

*5-(2-propyl-4,5-dihydrofuran-3-yl)benzo[d][1,3]dioxole (**4.24**)*: Compound **4.3a** was prepared according to the procedure described above, except for the isolation step, and stored in a vial in d_8-toluene inside the N_2-filled glovebox without purification. The concentration of the solution of **4.3a** was calculated by ^{1}H NMR spectroscopy using an internal standard. Phenanthrene as internal standard (4.5 mg, 0.025 mmol) was dissolved in d_8-toluene (0.4 mL) in a 1-dram vial. To this solution was added a small aliquot of **4.3a** in d_8-toluene (10. μL) using gas-tight syringe. The mixture was then transferred to a J. Young tube and removed from glovebox. The concentration of the stock solution of **4.3a** was calculated based on the integration ratio between the known phenanthrene and the unknown stock solution using ^{1}H NMR spectroscopy. This solution was used in the next step.

The cross-coupling procedure was adapted from a literature procedure.[6] In a N_2-filled glovebox, to a one-dram vial ("reaction vial") containing **4.23** (49.6 mg, 0.200 mmol, 1.0 equiv) was added CsOH•H_2O (100.8 mg, 0.6002 mmol, 3.0 equiv) and **4.3a** from the stock solution above (0.240 mmol, 1.2 equiv) via gas-tight syringe. XPHOS-Pd-G3 (6.8 mg, 0.0080 mmol, 0.040 equiv) was dissolved in THF (0.1 mL) and transferred via pipet to the reaction vial. The vial containing the Pd catalyst was rinsed with THF (0.1 mL) and the rinse was also added via pipet to the reaction vial. A stir bar was added to the reaction vial. The vial was capped and the solution was stirred at 25 °C for 2.5 d. Then the reaction vial was removed from glovebox and solution was diluted with Et_2O (1 mL). The reaction mixture was filtered through a pad of Celite®. The reaction vial and the Celite® were rinsed with Et_2O (2 mL). The filtrate was concentrated in vacuo and purified by flash chromatography (30% DCM in hexane) to afford a colorless oil (26 mg, 56% yield). TLC (40% DCM/hexanes): R_f = 0.45, visualized by UV absorbance. ^{1}H NMR ($CDCl_3$, 500 MHz): δ 6.78 (d, *J* = 8.0 Hz, 1H), 6.74 (d, *J* = 1.5 Hz, 1H), 6.68 (dd, *J* = 8.0, 1.5 Hz, 1H), 5.94 (s, 2H), 4.32 (t, *J* =

9.5 Hz, 2H), 2.96 (t, *J* = 9.5 Hz, 2H), 2.33 (t, *J* = 7.5 Hz, 2H), 1.60 (sext, *J* = 7.5 Hz, 2H), 0.96 (t, *J* = 7.5 Hz, 3H). $^{13}C\{^{1}H\}$NMR ($CDCl_3$, 125 MHz): δ 154.1, 134.9, 133.4, 129.1, 126.3, 108.2, 68.0, 34.2, 29.3, 21.2, 20.7, 14.1. HRMS (ESI-TOF) *m/z* calcd for $C_{14}H_{17}O_3$ ($[M+H]^+$) 233.1178, found 233.1181.

The following experiments were conducted by graduate student Chao Gao.

Genral Experimental Procedure C for the preparation of 2-alkynyl benzyl and 2′-Alkynyl benzyl alcohols (9a, 9i).[7]

A 100 mL flame-dried and septum-capped round bottom flask was prepared and filled with N_2 on a Schlenk line. Then, 2-iodobenzyl alcohol (1.17 g, 5.00 mmol, 1.00 equiv), $PdCl_2(PPh_3)_2$ (0.175 g, 0.250 mmol, 5.00 mol %), and CuI (95.0 mg, 0.500 mmol, 10.0 mol %) were quickly placed, respectively, into the 100 mL round bottom flask after the septum was briefly removed. Then, the system was capped with the septum again, followed by vacuumed on high vacuum for ca. 5 min. Then, the system was refilled with N_2 on a Schlenk line. Then, tetrahydrofuran (25 mL) was added via a syringe under N_2 on the Schlenk line to make a homogeneous solution. Then, the N_2 inlet from the Schlenk line was replaced with a N_2-filled balloon, which was kept connected to the reaction round bottom flask until the end of this reaction. To the resulting solution Et_3N (1.4 mL, 10. mmol, 2.0 equiv) was added via a syringe. The resulting solution was cooled to 0 ˚C in an ice bath. At 0 ˚C, alkyne (7.5 mmol, 1.5 equiv) was added dropwise via a syringe, followed by warming of the resulting solution to 25 ˚C. The reaction solution was stirred at 25 ˚C under N_2 for 18 h or until all aryl iodide was consumed as shown by TLC. The reaction was quenched with saturated NH_4Cl(aq) (20 mL), and the resulting organic layer was washed with brine (10 mL). The aqueous layer was extracted with EtOAc (3 × 10 mL), and the combined organic layers were dried

over $MgSO_4$, and then filtered through a Celite® plug (Celite® in a medium glass frit funnel). The filtrate was concentrated in vacuo. The crude product was purified by silica gel flash column chromatography.

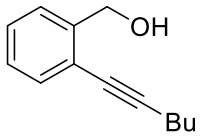

4.9a

*(2-(hex-1-yn-1-yl)phenyl)methanol (**4.9a**):* Prepared according to general procedure C, and purified by flash column chromatography (silica, 15% EtOAc in hexane) to afford a brown liquid (0.80 g, 85% yield). ^{1}H NMR ($CDCl_3$, 500 MHz): δ 7.44–7.33 (m, 2H), 7.32–7.18 (m, 2H), 4.79 (d, *J* = 6.3 Hz, 2H), 2.46 (t, *J* = 7.1 Hz, 2H), 2.07 (s, 1H), 1.66–1.56 (m, 2H), 1.55–1.44 (m, 2H), 0.96 (t, *J* = 7.3, 1.2 Hz, 3H). This spectrum is in agreement with previously reported spectral data.[7]

General Experimental Procedure D for the preparation of 2-alkynyl benzyl and 2′-Alkynyl benzyl alcohols (**4.9b**–**d**, **4.9f**).[7,8]

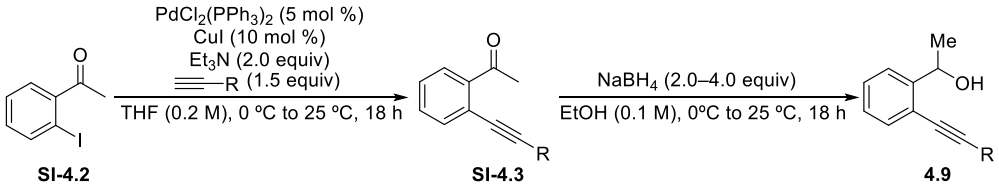

SI-4.2 **SI-4.3** **4.9**

A 100 mL flame-dried and septum-capped round bottom flask containing a stir bar was prepared and filled with N_2 on a Schlenk line. Then 2′-iodoacetophenone (1.0 equiv), $PdCl_2(PPh_3)_2$ (5 mol%), and CuI (10 mol%) were placed, respectively, to the 100 mL round bottom flask after the septum was briefly removed. Then, the system was capped again with the septum and vacuumed with a high vacuum. Then, the system was refilled with N_2 on a Schlenk line. Tetrahydrofuran (0.2 M) was added under N_2 on the Schlenk line via a syringe. Then, the N_2 inlet

from the Schlenk line was replaced with a N_2-filled balloon, which was kept connected to the reaction round bottom flask until the end of this reaction. To the resulting solution Et_3N (2.0 equiv) was added. The resulting solution was cooled to 0 ˚C in an ice bath. At 0 ˚C, alkyne (1.5 equiv) was added dropwise, followed by warming of the resulting solution to 25 ˚C. The reaction solution was stirred at 25 ˚C under N_2 for 18 h or until all aryl iodide was consumed as shown by TLC (ca. 10% EtOAc in hexane). The reaction was quenched with saturated NH_4Cl(aq) (20 mL), and the resulting organic layer was washed with brine (10 mL). The aqueous layer was extracted with EtOAc (3 × 10 mL), and the combined organic layers were dried over $MgSO_4$, and then filtered through a Celite® plug (Celite® in a medium glass frit funnel). The filtrate was concentrated in vacuo. The crude product was purified by silica gel flash column chromatography to afford 2′-alkynylacetophenones. 2′-Alkynylacetophenone (1.0 equiv) was placed into a flame-dried 100 mL round bottomed flask with a stir bar. Then, the round bottom flask was capped with a septum, and the system was vacuumed under high vacuum. Then, the system was refilled with N_2 on a Schlenk line. Under N_2 on the Schlenk line, EtOH was added via a syringe to produce a 0.1 M solution. The resulting solution was cooled to 0 ˚C. At 0 ˚C, $NaBH_4$ (2.0–4.0 equiv) was added, and the reaction was stirred at 0 ˚C for 10 min. Then, the N_2 inlet from the Schlenk line was replaced with a N_2-filled balloon, which was kept connected to the reaction round bottom flask until the end of this reaction. The reaction was then warmed to 25 ˚C and stirred at this temperature under N_2 18 h before it was quenched with saturated NH_4Cl(aq) (20 mL), and the resulting organic layer was washed with brine (20 mL). Then, the aqueous layer was extracted with EtOAc (3 × 10 mL), followed by combining all organic layers. The combined organic layers were then dried over $MgSO_4$, and then filtered through a Celite® plug (Celite® in a medium glass frit funnel), and the

filtrate was concentrated in vacuo to afford the crude product, which was then purified by flash column chromatography as described separately for each substrate below.

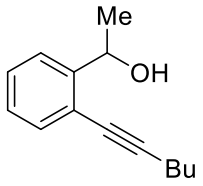

4.9b

*-(2-(hex-1-yn-1-yl)phenyl)ethan-1-ol (**4.9b**):* Prepared according to general procedure D (4.0 equiv $NaBH_4$ used), and purified by flash column chromatography (silica, 10% EtOAc in hexane) to afford a light yellow liquid (0.92 g, 91% yield). ^{1}H NMR ($CDCl_3$, 500 MHz): δ 7.48 (d, *J* = 7.9 Hz, 1H), 7.38 (d, *J* = 7.7 Hz, 1H), 7.30 (t, *J* = 7.6 Hz, 1H), 7.19 (t, *J* = 7.6 Hz, 1H), 5.29 (t, *J* = 5.7 Hz, 1H), 2.46 (t, *J* = 7.1 Hz, 2H), 2.19 (d, *J* = 4.1 Hz, 1H), 1.66–1.57 (m, 2H), 1.54–1.44 (m, 5H), 0.96 (t, *J* = 7.3 Hz, 3H). This spectrum is in agreement with previously reported spectral data.[9]

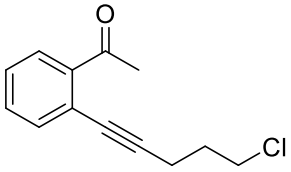

SI-4.3c

*1-(2-(6-chlorohex-1-yn-1-yl)phenyl)ethan-1-one (**SI-4.3c**):* Prepared according to general procedure D, and purified by flash column chromatography (silica, 15% EtOAc in hexane) to afford an orange oil (0.61 g, 93% yield). The molecular structure was shown in the Supporting Information. ^{1}H NMR ($CDCl_3$, 600 MHz): δ 7.69–7.65 (m, 1H), 7.49 (dd, *J* = 7.6, 1.4 Hz, 1H), 7.41 (td, *J* = 7.6, 1.4 Hz, 1H), 7.35 (td, *J* = 7.6, 1.4 Hz, 1H), 3.74 (t, *J* = 6.3 Hz, 2H), 2.72–2.64 (m, 5H), 2.13–2.05 (m, 2H). ^{13}C{^{1}H}NMR ($CDCl_3$, 151 MHz): δ 200.7, 141.1, 134.3, 131.3, 128.6,

127.9, 122.1, 94.3, 80.7, 43.8, 31.3, 30.0, 17.3. HRMS (ESI-TOF) m / z calcd for $C_{13}H_{14}ClO$ ($[M+H]^+$) 221.0733, found 221.0738.

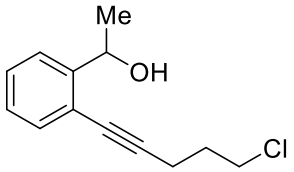

4.9c

*1-(2-(6-chlorohex-1-yn-1-yl)phenyl)ethan-1-ol (**4.9c**):* Prepared according to general procedure D (4.0 equiv $NaBH_4$ used), and purified by flash column chromatography (silica, 20% EtOAc in hexane) to afford a light yellow liquid (0.45 g, 68% yield). ^{1}H NMR ($CDCl_3$, 600 MHz): δ 7.50 (d, *J* = 7.8 Hz, 1H), 7.38 (d, *J* = 7.6, 1H), 7.32 (t, *J* = 7.5, 1H), 7.20 (td, *J* = 7.5, 1.3 Hz, 1H), 5.29 (q, *J* = 6.1 Hz, 1H), 3.72 (t, *J* = 6.9, 2H), 2.66 (t, *J* = 6.8 Hz, 2H), 2.28–1.98 (m, 3H), 1.51 (d, *J* = 6.6 Hz, 3H). ^{13}C{^{1}H}NMR ($CDCl_3$, 151 MHz): δ 147.4, 132.5, 128.5, 127.1, 124.7, 120.8, 93.3, 79.4, 68.6, 43.8, 31.5, 24.0, 17.2. HRMS (ESI-TOF) m / z calcd for $C_{13}H_{15}ClONa$ ($[M+Na]^+$) 245.0709, found 245.0700.

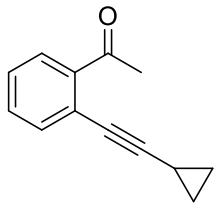

SI-4.3d

*1-(2-(cyclopropylethynyl)phenyl)ethan-1-one (**SI-4.3d**):* Prepared according to general procedure D, and purified by flash column chromatography (silica, 10% EtOAc in hexane) to afford a yellow oil (0.34 g, 93% yield). The molecular structure was shown in the Supporting Information. ^{1}H NMR ($CDCl_3$, 500 MHz): δ 7.66 (ddd, *J* = 7.5, 1.5, 0.5 Hz, 1H), 7.48–7.43 (m, 1H), 7.42–7.35 (m,

1H), 7.35–7.24 (m, 1H), 2.70 (s, 3H), 1.50 (tt, *J* = 8.2, 5.0 Hz, 1H), 0.95–0.80 (m, 4H). This spectrum is in agreement with previously reported spectral data.[10]

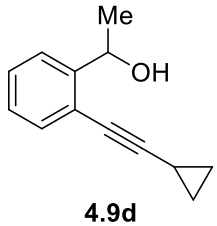

4.9d

*1-(2-(cyclopropylethynyl)phenyl)ethan-1-ol (**4.9d**):* Prepared according to general procedure D (2.0 equiv $NaBH_4$ used), and purified by flash column chromatography (silica, 15% EtOAc in hexane) to afford a yellow liquid (0.27 g, 76% yield). ^{1}H NMR ($CDCl_3$, 500 MHz): δ 7.46 (dd, *J* = 7.9, 1.2 Hz, 1H), 7.35 (dd, *J* = 7.7, 0.8 Hz, 1H), 7.28 (t, *J* = 7.6 Hz, 1H), 7.21–7.13 (m, 1H), 5.29–5.21 (m, 1H), 2.16 (d, *J* = 4.2 Hz, 1H), 1.53–1.44 (m, 4H), 0.94–0.85 (m, 2H), 0.87–0.75 (m, 2H). ^{13}C{^{1}H}NMR ($CDCl_3$, 151 MHz): δ 147.5, 132.5, 128.2, 127.1, 124.7, 121.2, 98.9, 73.5, 68.7, 23.8, 8.9, 0.4. HRMS (ESI-TOF) m / z calcd for $C_{13}H_{14}ONa$ ($[M+Na]^+$) 209.0942, found 209.0937.

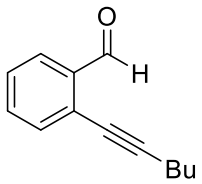

SI-4.5

*2-(hex-1-yn-1-yl)benzaldehyde (**SI-4.5**):* was prepared according to general procedure D, and purified by flash column chromatography (silica, 10% EtOAc in hexane) to afford a yellow liquid (0.40 g, 86% yield). The molecular structure was shown in the Supporting Information. ^{1}H NMR ($CDCl_3$, 500 MHz): δ 10.54 (s, 1H), 7.89 (d, *J* = 7.7 Hz, 1H), 7.58–7.44 (m, 2H), 7.38 (t, *J* =

7.3 Hz, 1H), 2.49 (t, *J* = 7.1 Hz, 2H), 1.68–1.58 (m, 2H), 1.56–1.44 (m, 2H), 0.97 (t, *J* = 7.4, 1.6 Hz, 3H). This spectrum is in agreement with previously reported spectral data.[11]

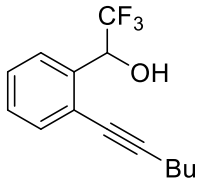

4.9e

*2,2,2-trifluoro-1-(2-(hex-1-yn-1-yl)phenyl)ethan-1-ol (**4.9e**):* Prepared according to a modified reported procedure.[12] In a N_2-filled glovebox, 2-(hex-1-yn-1-yl)benzaldehyde (**SI-4.5**, 0.400 g, 2.15 mmol, 1.0 equiv) was dissolved into DME (10.8 mL, 0.200 M) in a flame-dried 100 mL round bottomed flask, followed by addition of CsF (0.163 g, 1.07 mmol, 0.50 equiv) and a stir bar. Then, the reaction flask was capped with a septum, and removed from the glovebox. The resulting solution was cooled to 0 ˚C under N_2 on a Schlenk line. Then, $TMSCF_3$ (0.32 mL, 2.2 mmol, 1.0 equiv) was added dropwise via a syringe, and the reaction was warmed to 25 ˚C and stirred under N_2 on the Schlenk line. Upon the full consumption of the starting material (ca. 17 h) as shown by TLC (ca. 10% EtOAc in hexane), the reaction was quenched by adding 10% HCl(aq) (10 mL), and the aqueous layer was extracted with EtOAc (3 × 10 mL). The organic layers were combined and dried over $MgSO_4$. The drying agent was then removed via filtration through a Celite® plug (Celite® in a medium glass frit funnel), and the filtrate was concentrated in vacuo. The residue was purified via a flash column chromatography (silica, 10% EtOAc in hexane) to afford a yellow oil (0.37 g, 68% yield). ^{1}H NMR ($CDCl_3$, 500 MHz): δ 7.59–7.53 (m, 1H), 7.45 (dd, *J* = 7.0, 2.1 Hz, 1H), 7.39–7.28 (m, 2H), 5.63–5.54 (m, 1H), 2.85 (d, *J* = 5.8 Hz, 1H), 2.45 (t, *J* = 7.1 Hz, 2H), 1.66–1.43 (m, 4H), 0.96 (t, *J* = 7.3 Hz, 3H). ^{13}C{^{1}H}NMR ($CDCl_3$, 151 MHz): δ 135.4, 132.7, 129.2, 128.1, 127.5, 125.6, 123.9, 96.5, 77.7, 71.0 (q, *J* = 32 Hz), 30.8, 22.1, 19.3,

13.7. $^{19}F\{^{1}H\}$NMR ($CDCl_3$, 565 MHz): δ -77.74 (d, *J* = 6.8 Hz). HRMS (ESI-TOF) m / z calcd for $C_{14}H_{14}F_3O$ ($[M-H]^-$) 255.0997, found 255.0999.

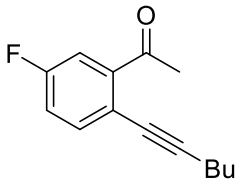

SI-4.3f

*1-(5-fluoro-2-(hex-1-yn-1-yl)phenyl)ethan-1-one (**SI-4.3f**):* Prepared according to general procedure D, and purified by flash column chromatography (silica, 5% EtOAc in hexane) to afford a brown liquid (0.47 g, 71% yield). The molecular structure was shown in the Supporting Information. ^{1}H NMR ($CDCl_3$, 500 MHz): δ 7.46 (dd, *J* = 8.6, 5.5 Hz, 1H), 7.36–7.33 (m, 1H), 7.12–7.09 (m, 1H), 2.73 (s, 3H), 2.45 (t, *J* = 7.1 Hz, 2H), 1.64–1.52 (m, 2H), 1.54–1.42 (m, 2H), 0.93 (t, *J* = 7.2 Hz, 3H). This spectrum is in agreement with previously reported spectral data.[13]

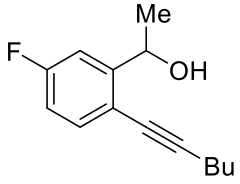

4.9f

*1-(5-fluoro-2-(hex-1-yn-1-yl)phenyl)ethan-1-ol (**4.9f**):* Prepared according to general procedure D (2.0 equiv $NaBH_4$ used), and purified by flash column chromatography (silica, 10% EtOAc in hexane) to afford a yellow oil (0.36 g, 76% yield). ^{1}H NMR ($CDCl_3$, 500 MHz): δ 7.34 (dd, *J* = 8.5, 5.7 Hz, 1H), 7.22 (dd, *J* = 9.9, 2.8 Hz, 1H), 6.87 (td, *J* = 8.3, 2.7 Hz, 1H), 5.32–5.22 (m, 1H), 2.44 (t, *J* = 7.0 Hz, 2H), 2.11 (d, *J* = 4.0 Hz, 1H), 1.65–1.55 (m, 2H), 1.55–1.43 (m, 5H), 0.96 (t, *J* = 7.3 Hz, 3H). $^{13}C\{^{1}H\}$NMR ($CDCl_3$,151 MHz): δ 162.6 (d, *J* = 248 Hz), 150.3 (d, *J* = 7 Hz), 134.1 (d, *J* = 8 Hz), 117 (d, *J* = 3 Hz), 114 (d, *J* = 22 Hz), 112.1 (d, *J* = 23 Hz), 95.3, 77.4, 68.4,

30.9, 23.8, 22.2, 19.30, 13.7. $^{19}F\{^{1}H\}$NMR ($CDCl_3$, 565 MHz): δ -111.08– -111.23 (m). HRMS (ESI-TOF) m / z calcd for $C_{14}H_{17}FONa$ ([M+Na]$^+$) 243.1161, found 243.1167.

Preparation of precursor to 9g

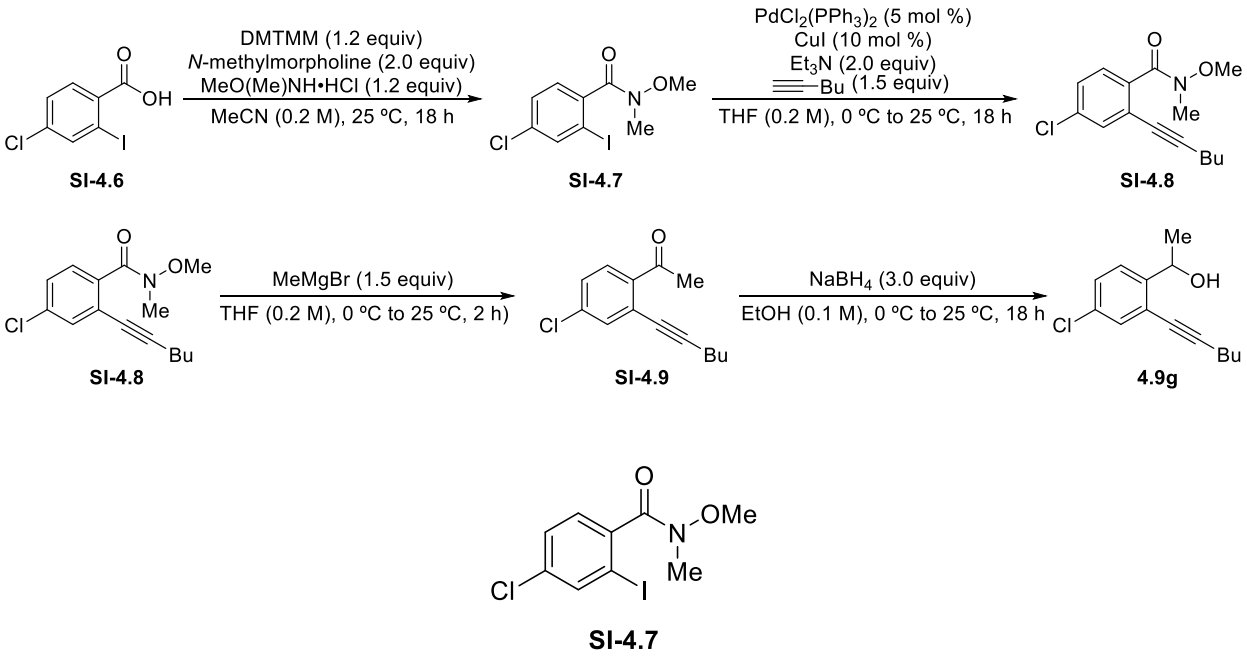

SI-4.7

*4-Chloro-2-iodo-N-methoxy-N-methylbenzamide (**SI-4.7**):* was prepared according to a modified reported procedure.[14] The molecular structure was shown in the Supporting Information. A 100-mL flame-dried septum-capped round bottom flask containing a stir bar was prepared. Then, 4-chloro-2-iodobenzoic acid (**SI-4.6)** (1.41 g, 5.00 mmol, 1.0 equiv) was placed in the 100 mL round bottom flask, followed by capping the system with a septum. Then, the system was vacuumed under high vacuum, and refilled with N_2 on a Schlenk line. Then, MeCN (21 mL, 0.2 M) was added under N_2 under N_2 on the Schlenk line. To the resulting solution, 4-(4,6-dimethoxy-1,3,5-triazin-2-yl)-4-methyl-morpholinium chloride (DMTMM; 1.66 g, 6.00 mmol, 1.2 equiv), *N*-methylmorpholine (1.0 mL, 10.0 mmol, 2.0 equiv), and MeO(Me)NH•HCl (0.585 g, 6.0 mmol, 1.2 equiv) were quickly added, respectively, under N_2 on the Schlenk line at 25 ˚C after the septum

was briefly removed. Once the addition of chemicals was done, the septum was quickly returned. Then, the resulting mixture was stirred at 25 ˚C under N_2 with a N_2-filled balloon for 18 h. Then, the solvent was removed in vacuo, and the resulting residue was dissolved in EtOAc (20 mL). The new solution was washed with 1 M HCl(aq) (1 × 20 mL), deionized H_2O (1 × 15 mL), and brine (1 × 15 mL). The aqueous phases were combined and extracted with EtOAc (1 × 15 mL), followed by combining all resulting organic phases. The combined organic phases were then dried over $MgSO_4$, and then filtered through a Celite® plug (Celite® in a medium glass frit funnel). The filtrate was concentrated in vacuo to afford the crude product, which was purified by flash column chromatography (40% EtOAc in hexane) to afford a light yellow oil (1.5 g, 93%). ^{1}H NMR ($CDCl_3$, 500 MHz): δ 7.84 (d, J = 2.0 Hz, 1H), 7.37 (dd, *J* = 8.2, 2.0 Hz, 1H), 7.19 (d, *J* = 8.2 Hz, 1H), 4.98–2.47 (m, 6H). This spectrum is in agreement with previously reported spectral data.[15]

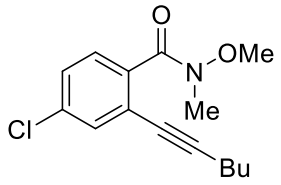

SI-4.8

*4-chloro-2-(hex-1-yn-1-yl)-N-methoxy-N-methylbenzamide (**SI-4.8**):* was prepared according to general procedure D from **SI-4.7**, and purified by flash column chromatography (silica, 30% EtOAc in hexane) to afford a brown oil (1.2 g, 92% yield). The molecular structure was shown in the Supporting Information. ^{1}H NMR ($CDCl_3$, 600 MHz): δ 7.41 (d, *J* = 2.0 Hz, 1H), 7.33–7.20 (m, 2H), 3.41 (br d, *J* = 109.2 Hz, 6H), 2.40 (dd, *J* = 7.4, 6.7 Hz, 2H), 1.61–1.52 (m, 2H), 1.50–1.36 (m, 2H), 0.93 (td, *J* = 7.3, 0.7 Hz, 3H). ^{13}C{^{1}H}NMR ($CDCl_3$, 125 MHz): δ 168.5, 136.4, 134.0, 131.2, 127.1, 122.7, 95.1, 76.5, 60.5, 31.8, 30.0, 21.3, 18.5, 13.0. HRMS (ESI-TOF) m / z calcd for $C_{15}H_{19}ClNO_2$ ($[M+H]^+$) 280.1104, found 280.1100.

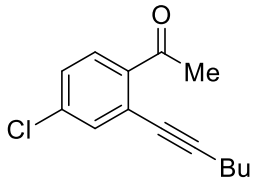

SI-4.9

*1-(4-chloro-2-(hex-1-yn-1-yl)phenyl)ethan-1-one (**SI-4.9**):* was prepared according to a modified literature procedure.[16] The molecular structure was shown in the Supporting Information. To a solution of **SI-4.8** (1.19 g, 4.25 mmol, 1.0 equiv) in dry THF (21 mL, 0.2 M) in a 100 mL flame-dried septum-capped round bottom flask with a stir bar was added MeMgBr (2.1 mL of a 3.0 M Et_2O solution, 6.37 mmol, 1.5 equiv), dropwise via a syringe at 0 ˚C under N_2 on a Schlenk line. The resulting solution was warmed to 25 ˚C, and stirred at this temperature for 2.0 h under N_2 on the Schlenk line. Then, the reaction was quenched with saturated NH_4Cl(aq) (20 mL). The resulting organic layer was washed with brine (20 mL). Then, the aqueous layer was extracted with EtOAc (3 × 15 mL), followed by combining all organic layers. The combined organic layers were then dried over $MgSO_4$, and then filtered through a Celite® plug (Celite® in a medium glass frit funnel), and the filtrate was concentrated in vacuo to afford the crude product, which was then purified by flash column chromatography (10% EtOAc in hexane) to afford a yellow oil (0.73 g, 73%). ^{1}H NMR ($CDCl_3$, 500 MHz): δ 7.63 (d, *J* = 8.4 Hz, 1H), 7.47 (d, *J* = 2.1 Hz, 1H), 7.29 (dd, *J* = 8.4, 2.1 Hz, 1H), 2.70 (s, 3H), 2.46 (t, *J* = 7.1 Hz, 2H), 1.77–1.57 (m, 2H), 1.52–1.41 (m, 2H), 0.95 (t, *J* = 7.3 Hz, 3H). ^{13}C{^{1}H}NMR ($CDCl_3$, 126 MHz): δ 200.0, 139.2, 137.5, 133.8, 130.1, 128.0, 124.5, 98.6, 79.0, 30.5, 30.2, 22.2, 19.5, 13.7. HRMS (ESI-TOF) m / z calcd for $C_{14}H_{15}ClONa$ ($[M+Na]^+$) 257.0709, found 257.0711.

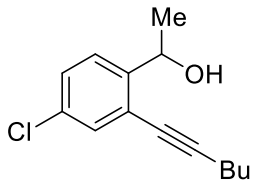

4.9g

*1-(4-chloro-2-(hex-1-yn-1-yl)phenyl)ethan-1-ol (**4.9g**)***:*** Prepared according to general procedure D from **SI-4.9** (3.0 equiv $NaBH_4$ used), and purified by flash column chromatography (silica, 10% EtOAc in hexane) to afford a colorless oil (0.62 g, 84% yield). ^{1}H NMR ($CDCl_3$, 500 MHz): δ 7.43 (d, *J* = 8.4 Hz, 1H), 7.35 (d, *J* = 2.3 Hz, 1H), 7.31–7.21 (m, 1H), 5.25 (qd, *J* = 6.4, 3.4 Hz, 1H), 2.45 (t, *J* = 7.1 Hz, 2H), 2.09 (d, *J* = 3.8 Hz, 1H), 1.69–1.55 (m, 2H), 1.53–1.42 (m, 5H), 0.96 (t, *J* = 7.3 Hz, 3H). ^{13}C{^{1}H}NMR ($CDCl_3$, 126 MHz): δ 145.9, 132.6, 132.0, 128.3, 126.2, 123.0, 97.1, 77.3, 68.2, 30.8, 24.0, 22.2, 19.4, 13.7. HRMS (ESI-TOF) m / z calcd for $C_{14}H_{17}ClONa$ ($[M+Na]^+$) 259.0865, found 259.0868.

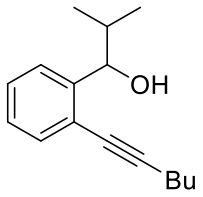

4.9h

1-(2-(hex-1-yn-1-yl)phenyl)-2-methylpropan-1-ol (**4.9h**): Prepared according to reported procedure.[16] A solution of **SI-4.5** (0.452 g, 2.43 mmol, 1.00 equiv) in dry THF (4.8 mL, 0.50 M) in a 100 mL flame-dried septum-capped round bottom flask equipped with a star bar was cooled to 0 ˚C under N_2 on a Schlenk line. To the cooled solution, ^{i}PrMgBr (2.9 mL of a 1.0 M THF solution, 2.9 mmol, 1.2 equiv) was added dropwise at 0 ˚C via a syringe. The resulting solution was warmed to 25 ˚C, and stirred at this temperature for 2.0 h under N_2. Then, the reaction was quenched with saturated NH_4Cl(aq) (20 mL), and the resulting organic layer was washed with

brine (20 mL). Then, the aqueous layer was extracted with EtOAc (3 × 10 mL), followed by combining all organic layers. The combined organic layers were then dried over $MgSO_4$, and then filtered through a Celite® plug (Celite® in a medium glass frit funnel), and the filtrate was concentrated in vacuo to afford the crude product, which was then purified by flash column chromatography (15% EtOAc in hexane) to afford a yellow oil (0.12 g, 21%). ^{1}H NMR ($CDCl_3$, 600 MHz): δ 7.44–7.39 (m, 1H), 7.37 (dd, *J* = 7.7, 1.3 Hz, 1H), 7.32–7.26 (m, 1H), 7.18 (td, *J* = 7.6, 1.4 Hz, 1H), 4.84 (dd, *J* = 6.6, 4.7 Hz, 1H), 2.45 (t, *J* = 7.0 Hz, 2H), 2.18–2.06 (m, 1H), 2.03 (dd, *J* = 4.8, 0.7 Hz, 1H), 1.71–1.56 (m, 2H), 1.53–1.43 (m, 2H), 1.00 (d, *J* = 6.7 Hz, 2H), 0.96 (t, *J* = 7.3 Hz, 3H), 0.88 (d, *J* = 6.9 Hz, 3H). ^{13}C{^{1}H}NMR ($CDCl_3$, 151 MHz): δ 145.6, 132.4, 127.8, 126.9, 126.4, 122.0, 95.6, 78.9, 77.8, 34.7, 31.0, 22.2, 19.7, 19.4, 17.8, 13.8. HRMS (ESI-TOF) m / z calcd for $C_{16}H_{22}ONa$ ([M+Na]$^+$) 253.1568, found 253.1563.

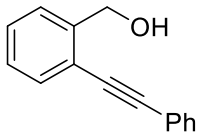

4.9i

*(2-(phenylethynyl)phenyl)methanol (**4.9i**):* Prepared according to general procedure C, and purified by flash column chromatography (silica, 15% EtOAc in hexane) to afford a light yellow solid, and the resulting solid was further purified with hot hexane (ca. 40–60 ˚C, ca. 3 mL) to afford a white solid (0.58 g, 56% yield). ^{1}H NMR ($CDCl_3$, 500 MHz): δ 7.61–7.45 (m, 4H), 7.42–7.34 (m, 4H), 7.30 (t, *J* = 7.3 Hz, 1H), 4.93 (d, *J* = 6.5 Hz, 2H), 2.07 (t, *J* = 6.4 Hz, 1H). This spectrum is in agreement with previously reported spectral data.[7]

Optimization of oxyboration reaction conditions.

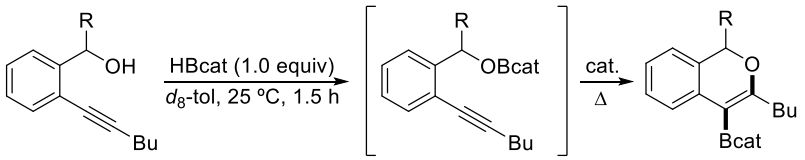

R = H, **4.9a**
R = Me, **4.9b**

R = H, **4.10a**
R = Me, **4.10b**

R = H, **4.11a**
R = Me, **4.11b**

Boric ester substrate 4.10. The reaction was performed inside a N_2-filled glovebox. 2′-Alkynyl benzyl alcohol (**4.9**) (0.400 mmol, 1.00 equiv), HBcat (0.400 mmol, 1.00 equiv), d_8-toluene (0.05 mL), and a stir bar was added to a one-dram vial. The resulting solution was kept uncapped to allow the release of H_2 gas at 25 ˚C to afford intermediate **4.10** in solution. ^{1}H NMR spectroscopy showed the reaction be complete after 1.5 h. (The solution of **4.10** was diluted to a 1 M solution by adding extra 0.35 mL d_8-toluene and transferred to a J. Young tube before acquiring the ^{1}H NMR spectroscopy.)

Boronic ester 4.11. A catalyst solution for screening was prepared by dissolving catalyst into d_8-toluene (0.15 mL) in another one-dram vial. Then, the boric ester **4.10** (prepared according to the above protocol without the dilution step and used without purification) and catalyst solutions were mixed and transferred into a J. Young tube, followed by rinsing the two vials with d_8-toluene (0.1 mL for each vial). Both rinses were combined and transferred into the J. Young tube. The tube was sealed and removed from the box. After heating for the indicated time, the progress of the reaction was determined by ^{1}H and ^{11}B NMR spectroscopy.

Table S4.6. Catalyst screening

Entry	R	Catalyst	Temp. (˚C)	Cat. Loading (mol%)	Cyclization Time (h)	Conv. (%)[a]
1	H	PPh_3AuTFA	80	5.0	46	0
2	H	PPh_3AuOTf	80	5.0	25	0
3	H	PPh_3AuSbF_6	80	5.0	32	0
4	H	PPh_3AuPF_5	80	5.0	32	0
5	H	(CAAC)AuTFA	100	5.0	20	63
6	H	$PicAuCl_2$	100	5.0	8	0
7	H	IPrCuOTf	100	5.0	8	0
8	H	$IPr^{*OMe}AuTFA$	80	5.0	15	0
9	H	$IPr^{Me}AuTFA$	80	5.0	10	78
10	H	$IPr^{Me}AuOTf$	80	5.0	12	0[b]
11	H	IPrAuTFA	80	5.0	10	91
12	Me	IPrAuTFA	80	5.0	10	87
13	Me	IPrAuTFA	100	5.0	3	88
14	Me	IPrAuTFA	100	2.5	4	86
15	Me	None	100	N/A	48	0

[a] Calculated through ratio of products to starting material in ^1H NMR spectra; [b] Only protodeborylated product observed.

Experimental results showed that gold(I) catalysts bearing phosphine L-type ligands did not offer catalytic activity (Table S4.6, entries 1–4), and gold (III) catalyst did not offer desired activity, either (Table S4.6, entry 6). Then, more thermally robust carbene L-type ligands were explored. Cyclic (alkyl)(amino)carbene (CAAC) gave 63% conversion to the desired product at 100 ˚C with 5 mol % catalyst loading (Table S4.6, entry 5). With this result in hand, other types of carbene ligands and different metal centers were studied (Table S4.6, entry 7–13), and it was found that IPrAuTFA could offer as high as 91% conversion to the desired product at 80 ˚C with 5 mol % catalyst loading (Table S4.6, entries 7–12). The borylative cyclization was further optimized to 100 ˚C with 2.5 mol % of this catalyst for 4 h (Table S4.6, entry 14).

2. Optimization of isolation method.

General Remarks:

To test the stability of the products at ambient conditions, the isolated products (oil, foam, or solid) were stored in capped dram vials under ambient conditions, and samples were analyzed periodically by dissolving the full sample in $CDCl_3$ and analyzed by ^1H NMR spectroscopy periodically to monitor the decomposition of the final products. After each analysis, the sample used for ^1H NMR spectroscopy was recovered by removing the $CDCl_3$ in vacuo and storing it in a capped dram vial under ambient conditions.

Attempted Isolation of oxyboration product 4.11a with KHF_2

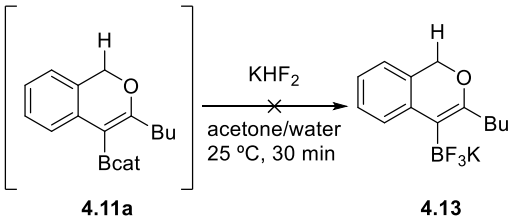

4.11a **4.13**

Compound **4.11a** was prepared according to general procedure E. Then, the titled isolation method was then performed.

The attempted isolation of the BF_3K salt was performed according to a similar reported procedure.[17] The reaction solution of **4.11a** was transferred to a 25 mL Schlenk tube charged with a stir bar in the glovebox, and the Schlenk tube was sealed and removed from the glovebox. The Schlenk tube was connected to a vacuum line, and the solvent was removed in vacuo. Then, the system was filled with N_2. Acetone (3.6 mL, 0.11 M) was added via a syringe under N_2 atmosphere. Separately, KHF_2 (0.11 g, 1.4 mmol, 3.5 equiv) was dissolved in deionized H_2O (1.2 mL, 1.2 M), and this KHF_2 (aq) was then added to the reaction Schlenk tube via a syringe under N_2 on a Schlenk line. Then, the Schlenk tube was sealed to maintain the internal N_2 atmosphere, and the reaction was stirred at 25 ˚C for 30 min before removing the solvents in vacuo. To the resulting residue,

Et_2O (3 mL) was added and subsequently subjected to high vacuum for 30 min to remove residue solvent. The resulting solid was then washed with Et_2O (4 × 3 mL), and the potential product was extracted with acetone (4 × 3 mL) from the residue, which was not soluble in acetone. Then, all acetone extracts were combined and concentrated in vacuo to afford a white solid. This white solid was analyzed by ^{1}H NMR, ^{13}C NMR, ^{11}B NMR, and ^{19}F NMR spectroscopy, and the desired product **4.13** was not observed. The non-acetone-soluble residue was dissolved in D_2O and analyzed by ^{1}H NMR, ^{13}C NMR, ^{11}B NMR, and ^{19}F NMR spectroscopy, and the desired product **4.13** was not observed, again.

Isolation of oxyboration product 4.11a with pinacol

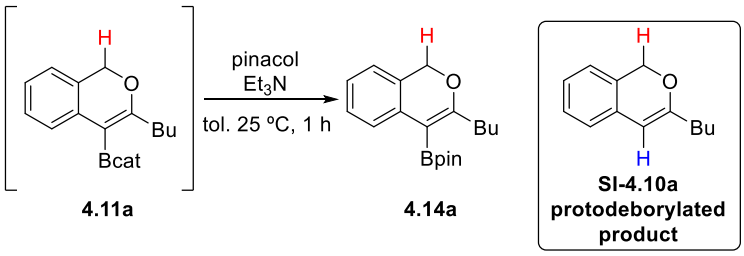

4.11a **4.14a**

An ^{1}H NMR spectrum was taken again for the product **4.14a** 18 h after the product was made and stored in oil state under ambient conditions (the ^{1}H NMR sample was prepared in the same concentration as the previous ^{1}H NMR sample), and it was found that significant amount of product decomposed into unknown compounds. (Approximately 30% of the product decomposed. This value was roughly estimated by comparing relative intensities of desired product in the new ^{1}H NMR spectrum and the previous ^{1}H NMR spectrum.) The spectrum of the decomposed compounds did not match the spectrum of the protodeborylated product (**SI-4.10a**).

Isolation of oxyboration product 4.11b with pinacol

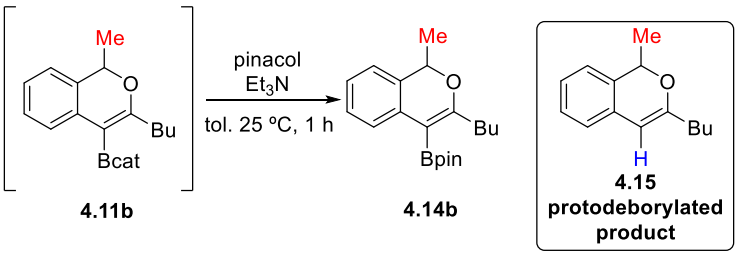

An ^{1}H NMR spectrum was taken again for the product 1 d after the product was made and stored in oil state under ambient conditions, and no discernable decomposition was observed. An ^{1}H NMR spectrum was taken again for the product after 2 d after the product was made and stored in oil state under ambient conditions, and only a trace amount of decomposed product was observed. The spectrum of the decomposed product matched the spectrum of the protodeborylated product (**4.15**). An ^{1}H NMR was taken again for the product 5 d after the product was made and stored in oil state under ambient conditions, and significant amount (approximately 30%; calculated through ratio of **4.14b** to **4.15** in ^{1}H NMR spectrum) of product had decomposed, and the spectrum of the decomposed product matched the spectra of the protodeborylated product (**4.15**). This was the only decomposition product observed, according to the mass balance. Thus, isolation through this method was not promising for long-term stability, even though the methylated version (R^2 = Me) was somewhat more stable than the non-methylated version (R^2 = H).

Isolation of oxyboration products 4.11a and 4.11b with 1,8-diaminonaphthalene

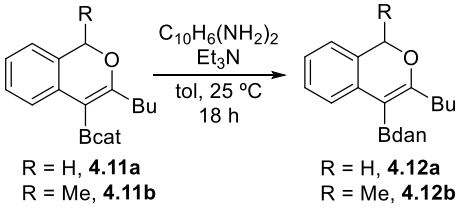

R = H, **4.11a**
R = Me, **4.11b**

R = H, **4.12a**
R = Me, **4.12b**

Compounds **4.11a** and **4.11b** was prepared and isolated according to general procedure E.

In a N_2-filled glovebox, 1,8-diaminonaphthalene (126 mg, 0.800 mmol, 2.0 equiv) and Et_3N (0.84 mL, 6.0 mmol, 15. equiv) was added to **4.11a** or **4.11b** in a one-dram vial. The vial used for weighting 1,8-diaminonaphthalene was rinsed with 0.20 mL toluene, and the resulting solution was combined with the reaction solution, followed by capping the reaction vial. The reaction was stirred at 25 ˚C for 18 h. Upon completion of isolation as checked by TLC (ca. 30% DCM in hexane), the reaction vial was taken out from the glovebox, and the reaction was quenched with saturated NH_4Cl(aq) (5 mL). Then, the resulting organic layer was washed with brine (5 mL). The aqueous layer was then extracted with EtOAc (3 × 5 mL), followed by combining all organic layers. The combined organic layers were then dried over $MgSO_4$, and then filtered through a Celite® plug (Celite® in an M glass frit funnel), and the filtrate was concentrated in vacuo to afford the crude product, which was then purified by flash column chromatography (**4.12a**: 35% DCM in hexane; **4.12b**: 25% DCM in hexane).

To compare stability as a solid and when in solution, an ^{1}H NMR spectrum of a freshly made **4.12b** sample was taken again for the product 4.5 months after the product was made and stored as a solid, and no decomposition was observed. However, the color of the solid product turned from white to purple. A separate batch of **4.12b** was also made and stored in $CDCl_3$ as a solution, and protodeborylation product (**4.15**) was observed after 3 d by ^{1}H NMR spectroscopy. This was the only decomposed product observed.

An ^{1}H NMR spectrum of a freshly made **4.12a** sample was taken again for the product 4.5 months after the product was made and stored as a foam, and no decomposition was observed. However,

the color of the foam product turned from white to purple. The comparison experiment where the product was stored in $CDCl_3$ was not conducted.

General Experimental Procedure E for the Synthesis of pinacol boronates 4.12.

In a N_2-filled glovebox, to a one-dram vial containing alkynyl benzylic alcohols (0.400 mmol, 1.0 equiv) was added HBcat (42.6 µL, 0.400 mmol, 1.0 equiv), followed by rinsing walls of the vial with 0.05 mL toluene, and the resulting solution was left in the glovebox uncapped to allow the release of H_2 gas at 25 ˚C for 1.5 h. Then, the resulting substrate solution was transferred to a separate one-dram vial containing IPrAuTFA (7.0 mg, 0.010 mmol, 2.5 mol %) and a stir bar, followed by rinsing the first one-dram vial with 3.5 mL toluene, and the rinse was combined with the reaction solution in the second one-dram vial. The reaction vial was capped. Then, the reaction mixture was heated to 100 ˚C (or 120 ˚C for **4.10e**) with stirring at this temperature for 4 h (18 h for **4.10e**, and 19 h for **4.10g**). The resulting solution was cooled to 25 ˚C, followed by addition of 1,8-diaminonaphthalene (126 mg, 0.800 mmol, 2.0 equiv) and Et_3N (0.84 mL, 6.0 mmol, 15 equiv). The vial used for weighting 1,8-diaminonaphthalene was rinsed with 0.20 mL toluene, and the resulting solution was combined with the reaction solution, followed by capping the reaction vial again. The reaction was stirred at 25 ˚C for 18 h. Once the isolation reaction was done as determined by TLC (20–40% DCM in hexane), the reaction vial was removed from the glovebox, and the reaction was quenched with saturated NH_4Cl(aq) (5 mL). Then, the resulting organic layer was washed with brine (5 mL). The aqueous layer was then extracted with EtOAc (3 × 5 mL), followed by combining all organic layers. The combined organic layers were then dried over $MgSO_4$, which was then filtered with a Celite® plug (Celite® in an M glass frit funnel), and the filtrate was concentrated in vacuo to afford the crude product, which was then purified by flash column chromatography.

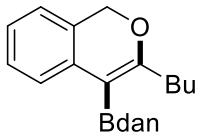

4.12a

2-(3-butyl-1H-isochromen-4-yl)-2,3-dihydro-1H-naphtho[1,8-de][1,3,2]diazaborinine ***(4.12a)****:* Prepared according to general procedure E, and purified by flash column chromatography (silica, 35% DCM in hexane) to afford a white foam (0.048 g, 34% yield). ^{1}H NMR ($CDCl_3$, 500 MHz): δ 7.23–7.12 (m, 5H), 7.09 (dd, *J* = 8.4, 1.1 Hz, 2H), 7.06–7.01 (m, 1H), 6.35 (dd, *J* = 7.2, 1.1 Hz, 2H), 5.84 (s, 2H), 5.06 (s, 2H), 2.56–2.20 (m, 2H), 1.61 (tt, *J* = 8.9, 6.8 Hz, 2H), 1.40 (dq, *J* = 14.7, 7.4 Hz, 2H), 0.94 (t, *J* = 7.3 Hz, 3H). ^{13}C{^{1}H}NMR ($CDCl_3$, 151 MHz): δ 161.4, 141.3, 136.5, 133.9, 128.3, 127.7, 127.7, 125.9, 124.1, 123.7, 119.9, 117.9, 106.0, 68.6, 34.3, 30.5, 29.8, 22.6, 14.1. ^{11}B{^{1}H}NMR ($CDCl_3$, 193 MHz): δ 30.21. HRMS (ESI-TOF) m / z calcd for $C_{23}H_{24}BN_2O$ ($[M+H]^+$) 355.1986, found 355.1979.

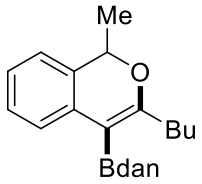

4.12b

2-(3-butyl-1-methyl-1H-isochromen-4-yl)-2,3-dihydro-1H-naphtho[1,8-de][1,3,2]diazaborinine ***(4.12b)****:* Prepared according to general procedure E, and purified by flash column chromatography (silica, 25% DCM in hexane) to afford a white solid (0.114 g, 78% yield). ^{1}H NMR ($CDCl_3$, 600 MHz): δ 7.20–7.11 (m, 6H), 7.08 (d, *J* = 8.2 Hz, 1H), 7.05 (d, *J* = 7.2 Hz, 1H), 6.35 (d, *J* = 7.2 Hz, 2H), 5.83 (s, 2H), 5.20 (q, *J* = 6.5 Hz, 1H), 3.05–2.12 (m, 2H), 1.70–1.58 (m, 5H), 1.49–1,35 (m, 2H), 0.94 (t, *J* = 7.3 Hz, 3H). ^{13}C{^{1}H}NMR ($CDCl_3$, 151 MHz): δ 159.6, 141.4, 136.5,

133.1, 132.1, 127.9, 127.6, 126.0, 124.0, 123.5, 119.9, 117.9, 106.0, 73.6, 34.5, 30.3, 22.6, 20.0, 14.1. $^{11}B\{^{1}H\}$NMR ($CDCl_3$, 193 MHz): δ 30.05. HRMS (ESI-TOF) m / z calcd for $C_{24}H_{25}BN_2O$ ($[M]^+$) 368.2065, found 368.2066.

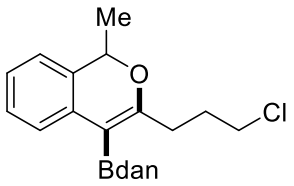

4.12c

*2-(3-(3-chloropropyl)-1-methyl-1H-isochromen-4-yl)-2,3-dihydro-1H-naphtho[1,8-de][1,3,2]diazaborinine (**4.12c**):* Prepared according to general procedure E, and purified by flash column chromatography (silica, 25% DCM in hexane) to afford a white solid (0.098 g, 63% yield). ^{1}H NMR ($CDCl_3$, 600 MHz): δ 7.23–7.13 (m, 5H), 7.08 (dd, *J* = 15.2, 6.9 Hz, 3H), 6.36 (d, *J* = 7.3 Hz, 2H), 5.93 (s, 2H), 5.22 (q, *J* = 6.6 Hz, 1H), 3.63 (t, *J* = 5.8 Hz, 2H), 2.62–2.50 (m, 2H), 2.19–2.07 (m, 2H), 1.63 (d, *J* = 6.8 Hz, 3H). $^{13}C\{^{1}H\}$NMR ($CDCl_3$, 151 MHz): δ 157.3, 141.3, 136.4, 132.8, 132.1, 128.0, 127.7, 126.4, 124.3, 123.5, 119.9, 117.9, 106.0, 73.7, 44.5, 31.6, 30.3, 19.9. $^{11}B\{^{1}H\}$NMR ($CDCl_3$, 193 MHz): δ 30.01. HRMS (ESI-TOF) m / z calcd for $C_{23}H_{22}BClN_2ONa$ ($[M+Na]^+$) 411.1416, found 411.1403.

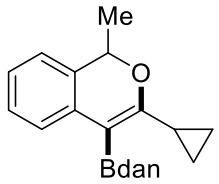

4.12d

*2-(3-cyclopropyl-1-methyl-1H-isochromen-4-yl)-2,3-dihydro-1H-naphtho[1,8-de][1,3,2]diazaborinine (**4.12d**):* Prepared according to general procedure E, and purified by flash

column chromatography (silica, 25% DCM in hexane) to afford a white foam (0.086 g, 61% yield). ^{1}H NMR ($CDCl_3$, 500 MHz): δ 7.22–7.10 (m, 5H), 7.07 (dd, *J* = 8.3, 1.0 Hz, 2H), 7.02 (d, *J* = 7.4 Hz, 1H), 6.36 (dd, *J* = 7.3, 1.1 Hz, 2H), 5.94 (s, 2H), 5.09 (q, *J* = 6.5 Hz, 1H), 1.89–1.80 (m, 1H), 1.54 (d, *J* = 6.5 Hz, 3H), 1.03–0.92 (m, 2H), 0.76–0.61 (m, 2H). ^{13}C{^{1}H}NMR ($CDCl_3$, 151 MHz): δ 158.8, 141.5, 136.5, 133.4, 132.1, 128.0, 127.7, 125.6, 123.5, 123.4, 119.9, 117.9, 106.0, 73.6, 29.9, 19.6, 14.3, 5.9, 5.2. ^{11}B{^{1}H}NMR ($CDCl_3$, 193 MHz): δ 30.23. HRMS (ESI-TOF) m / z calcd for $C_{23}H_{21}BN_2O$ ([M]$^{+}$) 352.1751, found 352.1741.

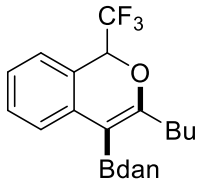

4.12e

*2-(3-butyl-1-(trifluoromethyl)-1H-isochromen-4-yl)-2,3-dihydro-1H-naphtho[1,8-de][1,3,2]diazaborinine (**4.12e**):* Prepared according to general procedure E, and purified by flash column chromatography (silica, 25% DCM in hexane) to afford a white foam (0.119 g, 70% yield). ^{1}H NMR ($CDCl_3$, 500 MHz): δ 7.23 (t, *J* = 7.6 Hz, 1H), 7.16 (d, *J* = 7.6 Hz, 2H), 7.10 (dd, *J* = 9.3, 6.2 Hz, 3H), 7.05 (d, *J* = 8.4 Hz, 2H), 6.29 (d, *J* = 7.4 Hz, 2H), 5.73 (s, 2H), 5.45 (q, *J* = 7.6 Hz, 1H), 2.59–2.15 (m, 2H), 1.79–1.49 (m, 2H), 1.42–1.24 (m, 2H), 0.90 (t, *J* = 7.4 Hz, 3H). ^{13}C{^{1}H}NMR ($CDCl_3$, 151 MHz): δ 157.8, 141.1, 136.4, 133.1, 130.1, 127.8, 127.1, 126.4, 124.9, 123.0, 120.6, 120.0, 118.1, 106.2, 74.5 (q, *J* = 32 Hz), 34.22, 29.87, 22.41, 14.03. ^{11}B{^{1}H}NMR ($CDCl_3$, 193 MHz): δ 29.59. ^{19}F NMR ($CDCl_3$, 565 MHz): δ –78.48 (d, *J* = 7.3 Hz). HRMS (ESI-TOF) m / z calcd for $C_{24}H_{22}BF_3N_2O$ ([M]$^{+}$) 422.1782, found 422.1792.

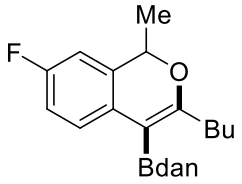

4.12f

*2-(3-butyl-7-fluoro-1-methyl-1H-isochromen-4-yl)-2,3-dihydro-1H-naphtho[1,8-de][1,3,2]diazaborinine (**4.12f**):* Prepared according to general procedure E, and purified by flash column chromatography (silica, 25% DCM in hexane) to afford a white solid (0.120 g, 77% yield). ^{1}H NMR ($CDCl_3$, 600 MHz): δ 7.17 (td, *J* = 7.8, 2.0 Hz, 2H), 7.14–7.09 (m, 3H), 6.87 (tt, *J* = 8.6, 2.3 Hz, 1H), 6.79 (dt, *J* = 9.1, 2.4 Hz, 1H), 6.37 (dd, *J* = 7.2, 1.8 Hz, 2H), 6.02–5.73 (m, 2H), 5.16 (q, *J* = 6.5 Hz, 1H), 2.40–2.31 (m, 2H), 1.75–1.53 (m, 5H), 1.45–1.37 (m, 2H), 1.00 (t, *J* = 7.4 Hz 3H). ^{13}C{^{1}H}NMR ($CDCl_3$, 151 MHz): δ 161.3 (d, *J* = 245 Hz), 158.7 (d, *J* = 2 Hz), 141.2, 136.3, 134.1 (d, *J* = 7 Hz), 129.2 (d, *J* = 3 Hz), 127.7, 125.4 (d, *J* = 7.6 Hz), 119.8, 117.9, 114.3 (d, *J* = 21 Hz), 110.7 (d, *J* = 23 Hz), 106.0, 73.1 (d, *J* = 2 Hz), 34.3, 30.2, 22.5, 19.6, 14.2. ^{11}B{^{1}H}NMR ($CDCl_3$, 193 MHz): δ 30.29. ^{19}F{^{1}H}NMR ($CDCl_3$, 565 MHz): δ –115.93– –116.15 (m). HRMS (ESI-TOF) m / z calcd for $C_{24}H_{24}BFN_2O$ ([M]$^{+}$) 386.1970, found 386.1966.

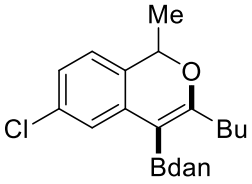

4.12g

*2-(3-butyl-6-chloro-1-methyl-1H-isochromen-4-yl)-2,3-dihydro-1H-naphtho[1,8-de][1,3,2]diazaborinine (**4.12g**):* Prepared according to general procedure E, and purified by flash column chromatography (silica, 25% DCM in hexane) to afford a white solid (0.108 g, 67% yield). ^{1}H NMR ($CDCl_3$, 600 MHz): δ 7.17 (t, *J* = 7.8 Hz, 2H), 7.11 (dd, *J* = 7.0, 2.5 Hz, 4H), 6.96 (d,

J = 8.4 Hz, 1H), 6.38 (d, *J* = 7.2 Hz, 2H), 5.83 (s, 2H), 5.17 (q, *J* = 6.5 Hz, 1H), 2.35 (tt, *J* = 9.9, 5.0 Hz, 2H), 1.79–1.52 (m, 5H), 1.39 (sext, *J* = 7.4 Hz, 2H), 0.94 (t, *J* = 7.3 Hz, 3H). $^{13}C\{^{1}H\}$NMR ($CDCl_3$, 151 MHz): δ 160.9, 141.2, 136.4, 135.1, 133.6, 130.2, 127.8, 125.7, 124.7, 123.7, 119.9, 118.1, 106.2, 73.3, 34.5, 30.2, 22.5, 19.9, 14.2. $^{11}B\{^{1}H\}$NMR ($CDCl_3$, 193 MHz): δ 30.09. HRMS (ESI-TOF) m / z calcd for $C_{24}H_{24}BClN_2O$ ($[M]^+$) 402.1674, found 402.1677.

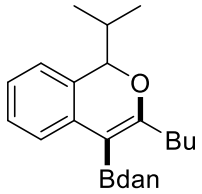

4.12h

*2-(3-butyl-1-isopropyl-1H-isochromen-4-yl)-2,3-dihydro-1H-naphtho[1,8-de][1,3,2]diazaborinine (**4.12h**):* Prepared according to general procedure E, and purified by flash column chromatography (silica, 25% DCM in hexane) to afford a white solid (0.108 g, 67% yield). ^{1}H NMR ($CDCl_3$, 600 MHz): δ 7.13–7.05 (m, 5H), 7.03 (d, *J* = 8.3 Hz, 2H), 6.93 (d, *J* = 7.3 Hz, 1H), 6.27 (d, *J* = 7.2 Hz, 2H), 5.74 (s, 2H), 4.76 (d, *J* = 6.6 Hz, 1H), 2.33 (td, *J* = 7.3, 4.1 Hz, 2H), 2.27–2.18 (m, 1H), 1.70–1.52 (m, 2H), 1.44–1.29 (m, 2H), 1.07 (d, *J* = 6.7 Hz, 3H), 0.97–0.83 (m, 6H). $^{13}C\{^{1}H\}$NMR ($CDCl_3$, 151 MHz): δ 159.4, 141.4, 136.4, 133.4, 129.4, 127.8, 127.7, 125.5, 125.3, 124.0, 119.9, 117.8, 106.0, 82.8, 34.7, 31.3, 30.2, 22.6, 19.4, 18.1, 14.1. $^{11}B\{^{1}H\}$NMR ($CDCl_3$, 193 MHz): δ 29.93. HRMS (ESI-TOF) m / z calcd for $C_{26}H_{30}BN_2O$ ($[M+H]^+$) 397.2456, found 397.2425.

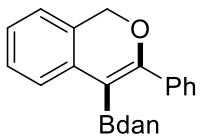

4.12i

2-(3-phenyl-1H-isochromen-4-yl)-2,3-dihydro-1H-naphtho[1,8-de][1,3,2]diazaborinine ***(4.12i)****:* Prepared according to general procedure E, and purified by flash column chromatography (silica, 10% EtOAc in hexane) to afford a white solid (0.036 g, 24% yield). ^{1}H NMR ($CDCl_3$, 600 MHz): δ 7.87–7.78 (m, 2H), 7.45 (dd, *J* = 7.6, 1.3 Hz, 1H), 7.42–7.36 (m, 3H), 7.35–26 (m, 3H), 7.25–7.15 (m, 2H), 7.13 (d, *J* = 8.2 Hz, 2H), 6.31 (d, *J* = 7.1 Hz, 2H), 5.83 (s, 2H), 5.29 (s, 2H). ^{13}C{^{1}H}NMR ($CDCl_3$, 151 MHz): δ 157.9, 141.1, 136.4, 136.3, 134.0, 129.2, 128.5, 128.4, 128.4, 128.2, 127.7, 127.7, 126.7, 124.4, 124.2, 119.8, 117.9, 106.1, 68.9. ^{11}B{^{1}H}NMR ($CDCl_3$, 193 MHz): δ 30.30. HRMS (ESI-TOF) m / z calcd for $C_{25}H_{19}BN_2O$ ($[M]^+$) 374.1595, found 374.1586.

Unsuccessful Substrates for the formation of oxyboration product 4.11

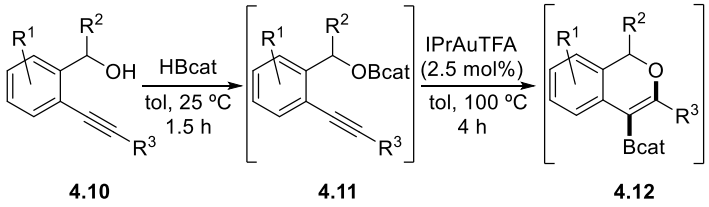

4.10 **4.11** **4.12**

Incomplete conversion to boronic ester (**4.11**)

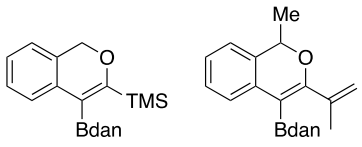

Electron rich, in conjugation, or sterically bulky R^3 reduced the cyclization efficiency significantly.

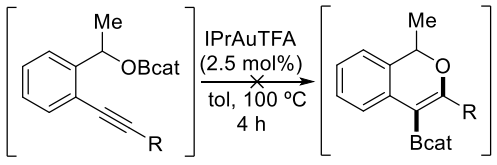

4.10 **4.11**

No conversion to boronic ester (**4.11**) from boric ester (**4.10**) observed

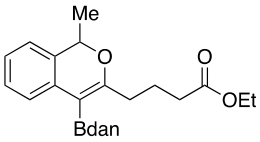

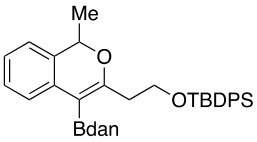

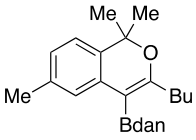

Groups that can coordinate to boron species and/or tetrasubstituted benzylic carbon shut down the cyclization completely.

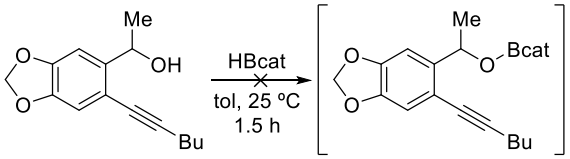

4.9 **4.10**

2′-Alkynyl benzyl alcohol (**4.9**) decomposed upon attempted conversion to boric ester (**4.10**).

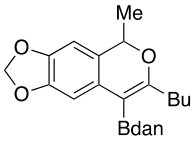

Acetal was fragile to decomposition.

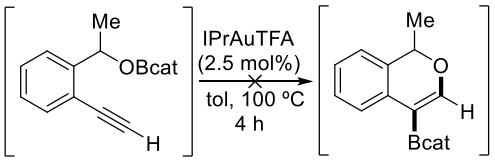

4.10 **4.11**

Boric ester (**4.10**) decomposed in reaction to boronic ester (**4.11**).

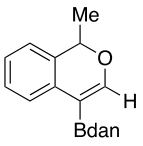

^{1}H NMR spectroscopy showed that boric ester (**4.10**) decomposed into unidentifiable products in reaction to boronic ester (**4.11**). We did not have information to determine the decomposition occurred to the boric ester (**4.10**) before cyclization to boronic ester (**4.11**), or if the decomposition occurred to the boronic ester (**4.11**) after cyclization was done, or a combination of the two scenarios.

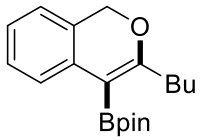

4.14a

*3-butyl-4-(4,4,5,5-tetramethyl-1,3-dioxolan-2-yl)-1H-isochromene(**4.14a**):* Prepared according to a literature procedure from compound **4.11a**.[18] Compound **4.11a** was prepared according to general procedure E. In a N_2-filled glovebox, pinacol (0.142 g, 1.20 mmol, 3.0 equiv) was dissolved into Et_3N (0.84 mL, 3.0 mmol, 15 equiv), and the resulting solution was transferred to **4.11a**. The resulting reaction solution was capped and stirred in the glovebox for 1 h at 25 ˚C. Then, the reaction vial was removed from the glovebox, and the solvent was removed in vacuo. The resulting residue was purified by flash chromatography (15% DCM in hexane) to afford a yellow oil (0.070 g, 56% yield). ^{1}H NMR ($CDCl_3$, 500 MHz): δ 7.69 (d, *J* = 7.8 Hz, 1H), 7.29–7.21 (m, 1H), 7.15–7.08 (m, 1H), 6.99 (d, *J* = 7.4 Hz, 1H), 4.98 (s, 2H), 2.63 (t, *J* = 7.6 Hz, 2H), 1.67–1.57 (m, 2H), 1.46–1.32 (m, 2H), 1.38 (s, 12H), 0.97 (t, *J* = 7.4 Hz, 3H). ^{13}C{^{1}H}NMR ($CDCl_3$, 126 MHz): δ 170.8, 133.9, 128.1, 127.6, 125.4, 124.6, 123.6, 83.0, 68.9, 33.5, 31.2, 25.0, 22.68, 14.1. ^{11}B{^{1}H}NMR ($CDCl_3$, 160 MHz): δ 31.75.

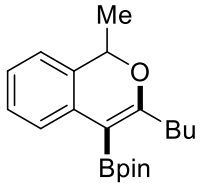

4.14b

2-(3-butyl-1-methyl-1H-isochromen-4-yl)-4,4,5,5-tetramethyl-1,3,2-dioxaborolane ***(4.14b)****:* Prepared according to a literature procedure from compound **4.11b**.[18] Compound **4.11b** was prepared according to general procedure E. In a N_2-filled glovebox, pinacol (70.9 mg, 0.600 mmol, 3.0 equiv) was dissolved into Et_3N (0.42 mL, 3.0 mmol, 15 equiv), and the resulting solution was transferred to **4.11b**. The resulting reaction solution was stirred in the glovebox for 1 h at 25 ˚C. Then, the reaction vial was removed from the glovebox, and the solvent was removed in vacuo. The resulting residue was purified by flash chromatography (5% to 100% DCM in hexane) to afford a yellow oil (22.3 mg, 34% yield). ^{1}H NMR ($CDCl_3$, 600 MHz): δ 7.65 (dd, *J* = 7.9, 1.1 Hz, 1H), 7.20 (td, *J* = 7.6, 1.4 Hz, 1H), 7.11 (td, *J* = 7.4, 1.2 Hz, 1H), 6.98 (d, *J* = 7.4 Hz, 1H), 5.09 (q, *J* = 6.5 Hz, 1H), 2.73–2.44 (m, 2H), 1.65–1.53 (m, 5H), 1.44–1.30 (m, 14H), 0.94 (t, *J* = 7.4 Hz, 3H). ^{13}C{^{1}H}NMR ($CDCl_3$, 151 MHz): δ 169.0, 133.2, 132.0, 127.8, 125.5, 124.9, 122.9, 83.0, 74.0, 33.7, 30.9, 25.0, 22.7, 19.6, 14.1. ^{11}B{^{1}H}NMR ($CDCl_3$, 193 MHz): δ 31.37.

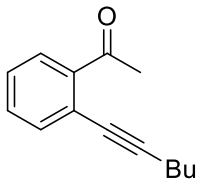

4.16

1-(2-(hex-1-yn-1-yl)phenyl)ethan-1-one ***(4.16)****:* Prepared according to general procedure D, and purified by flash column chromatography (silica, 10% EtOAc in hexane) to afford a brown oil (0.92 g, 92% yield). ^{1}H NMR ($CDCl_3$, 500 MHz): δ 7.68–7.62 (m, 1H), 7.48 (dd, *J* = 7.6, 1.4 Hz,

1H), 7.39 (td, *J* = 7.5, 1.5 Hz, 1H), 7.32 (td, *J* = 7.6, 1.4 Hz, 1H), 2.72 (s, 3H), 2.46 (t, *J* = 7.1 Hz, 2H), 1.66–1.56 (m, 2H), 1.54–1.43 (m, 2H), 0.95 (t, *J* = 7.3 Hz, 3H). $^{13}C\{^{1}H\}$NMR ($CDCl_3$, 151 MHz): δ 201.3, 141.2, 134.1, 131.2, 128.4, 127.7, 122.6, 97.0, 79.8, 30.7, 30.2, 22.2, 19.6, 13.8. HRMS (ESI-TOF) m / z calcd for $C_{14}H_{16}ONa$ ($[M+Na]^+$) 223.1099, found 223.1096.

Structure elucidation. Oxyboration was performed according to general procedure E, except the isolation portion in the general procedure E was not conducted. Instead, after cyclization, 1 M HCl(aq) (10 mL) was used to quench the reaction and to protodeborate the product in situ. Then, the organic layer was washed with brine (1 × 15 mL), and all aqueous layers were combined and extracted with EtOAc (3 × 5 mL). The organic layers were combined. The combined organic phases were then dried over $MgSO_4$, and then filtered through a Celite® plug (Celite® in a medium glass frit funnel), and the filtrate was concentrated in vacuo to afford the crude product. An ^{1}H NMR spectrum of the crude reaction mixture showed only one regioisomer of product. The crude product was then purified by flash column chromatography (15% EtOAc in hexane) to afford a light yellow oil (0.041 g, 50%). ^{1}H NMR ($CDCl_3$, 500 MHz): δ 7.17 (td, *J* = 7.4, 1.3 Hz, 1H), 7.11 (td, *J* = 7.5, 1.4 Hz, 1H), 6.99 (d, *J* = 7.3 Hz, 1H), 6.92 (dd, *J* = 7.4, 1.3 Hz, 1H), 5.61 (s, 1H), 5.20 (q, *J* = 6.5 Hz, 1H), 2.18 (t, *J* = 7.5 Hz, 2H), 1.81–1.49 (m, 5H), 1.46–1.34 (m, 2H), 0.94 (t, *J* = 7.3 Hz, 3H). $^{13}C\{^{1}H\}$NMR ($CDCl_3$, 126 MHz): δ 157.2, 131.8, 131.4, 127.8, 125.8, 123.3, 122.7, 100.3, 74.1, 33.7, 29.2, 22.5, 19.9, 14.1. This spectrum was in agreement with previously reported spectral data for **4.15** by a different laboratory.[19]

For further analysis, likely compound **4.15** (or perhaps **4.17**) (0.0408 g, 0.200 mmol, 1.0 equiv) made in the previous step was dissolved in DCM (2.5 mL, 0.08 M) in a one dram vial with a stir bar, and the resulting solution was cooled to –78 ˚C. Then, O_3 was passed through the cooled solution until the solution became dark blue (ca. 5 min.). To the resulting dark blue solution, a

solution of PPh_3 (0.0682 g, 0.260 mmol, 1.3 equiv) in DCM (0.7 mL, 0.4 M) as a quench was added dropwise at –78 ˚C, and the resulting solution was stirred at 25 ˚C for 3 h. Then, the solvent was removed in vacuo, and the resulting residue was purified by flash column chromatography (5% EtOAc in hexane) to afford a transparent oil (0.022 g, 47%). ^{1}H NMR ($CDCl_3$, 500 MHz): δ 10.27 (s, 1H), 7.90–7.76 (m, 1H), 7.66–7.54 (m, 2H), 7.46 (ddd, *J* = 7.4, 6.1, 2.5 Hz, 1H), 6.67 (q, *J* = 6.6 Hz, 1H), 2.35 (td, *J* = 7.6, 3.6 Hz, 2H), 1.77–1.49 (m, 5H), 1.44–1.29 (m, 2H), 0.91 (t, *J* = 7.4 Hz, 3H). ^{13}C{^{1}H}NMR ($CDCl_3$, 126 MHz): δ 192.5, 172.9, 144.8, 134.2, 133.1, 132.7, 128.0, 126.1, 68.7, 34.4, 27.1, 22.9, 22.4, 13.8. HRMS (ESI-TOF) m / z calcd for $C_{14}H_{18}O_3Na$ ($[M+Na]^+$) 257.1154, found 257.1154. These spectra indicated the product to be **4.18**, and ^{1}H NMR spectral information of both the crude and purified fractions did not match previously reported spectra of **4.19**[20] or **4.20**[21]. It was concluded that the only product was **4.18**.

Hydroboration-Oxyboration. In a N_2-filled glovebox, to a one-dram vial containing **4.16** (0.0801 g, 0.400 mmol, 1.0 equiv) was added HBcat (85.2 µL, 0.800 mmol, 2.0 equiv) and a stir bar. The walls of the vial were rinsed with 0.05 mL toluene, and the vial was capped. Then, the resulting solution was heated at 50 ˚C for 5.0 h with stirring. Then, the resulting solution was concentrated under high vacuum (ca. 10 mTorr) for 1.5 h at 25 ˚C in the glovebox. This process completed the hydroboration step.

In a separate one-dram vial in the glovebox, IPrAuTFA (7.0 mg, 0.010 mmol, 2.5 mol %) was dissolved into 0.4 mL toluene, and the resulting catalyst solution was transferred into the substrate vial containing the hydroboration product, and a stir bar was added. The reaction vial was then capped. The reaction mixture was heated to 100 ˚C with stirring for 4 h. This process completed the oxyboration step.

In order to replace Bcat with Bdan, the resulting solution was cooled to 25 ˚C, followed by addition of 1,8-diaminonaphthalene (126 mg, 0.800 mmol, 2.0 equiv) and Et_3N (0.84 mL, 6.0 mmol, 15 equiv). The vial used for weighting 1,8-diaminonaphthalene was rinsed with 0.20 mL toluene, and the rinse was combined with the reaction solution. The reaction vial was capped again, and the reaction was stirred at 25 ˚C for 18 h. Once the exchange reaction was done, the reaction vial was removed from the glovebox, and the reaction mixture was quenched with saturated NH_4Cl(aq) (5 mL). The resulting organic layer was washed with brine (5 mL). Then, the aqueous layer was extracted with EtOAc (3 × 5 mL), followed by combining all organic layers. The combined organic layers were then dried over $MgSO_4$, and then filtered through a Celite® plug (Celite® in an M glass frit funnel), and the filtrate was concentrated in vacuo to afford the crude product, which was then purified by flash column chromatography (silica, 25% DCM in hexane) to afford a white solid (0.100 g, 68% yield). ^{1}H NMR spectroscopic data matched that previously obtained from **4.12b** (see above).

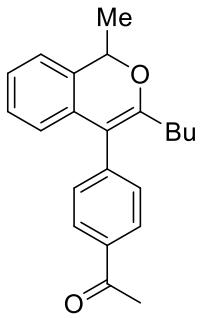

4.26

*1-(4-(3-butyl-1-methyl-1H-isochromen-4-yl)phenyl)ethan-1-one (**4.26**):* First, intermediate **4.11b** was prepared according to general procedure E from **4.9b** (0.040 g, 0.20 mmol, 1.0 equiv) (with the exception that no isolation was performed). Instead of isolation, once **4.11b** was prepared in

the glovebox, the reaction solution was cooled to 25 ˚C and transferred into a one dram vial ("reaction vial") containing $Pd(PPh_3)_4$ (23.1 mg, 0.0200 mmol, 10. mol %), Cs_2CO_3 (0.196 g, 0.600 mmol, 3.0 equiv), and a stir bar. Compound 1-(4-iodophenyl)ethan-1-one **4.25** (0.591 g, 0.240 mmol, 1.2 equiv) was dissolved in 0.15 mL toluene, and the resulting solution was transferred to the reaction vial. Then, the vials for **4.11b** and **4.25** were each rinsed with 0.5 mL toluene, and all the rinses were combined into the reaction vial. The reaction vial was capped with a cap with a septum and sealed with black tape before it was taken out from the glovebox. Outside the glovebox, deionized water (4.0 µL, 0.22 mmol, 1.1 equiv) was quickly added via a 10 µL airtight syringe, followed by hearting the resulting solution to 100 ˚C and stirred at this temperature vigorously (to ensure mixing of the water droplet) for 24 h. Then, the reaction was quenched with aqueous saturated NH_4Cl (5 mL). The resulting organic layer was washed with brine (5 mL). Then, the aqueous layer was extracted with EtOAc (3 × 5 mL), followed by combining all organic layers. The combined organic layers were then dried over $MgSO_4$, and then filtered through a Celite® plug (Celite® in an M glass frit funnel), and the filtrate was concentrated in vacuo to afford the crude product, which was then purified by flash column chromatography (silica, 4% EtOAc in hexane) to afford a light yellow oil (0.042 g, 66%) ^{1}H NMR ($CDCl_3$, 600 MHz): δ 8.02 (d, *J* = 7.9 Hz, 2H), 7.36 (d, *J* = 7.9 Hz, 2H), 7.15 (t, *J* = 7.4 Hz, 1H), 7.12–7.05 (m, 2H), 6.53 (d, *J* = 7.7 Hz, 1H), 5.27 (q, *J* = 6.5 Hz, 1H), 2.66 (s, 3H), 2.14–2.03 (m, 2H), 1.67 (d, *J* = 6.5 Hz, 3H), 1.59–1.42 (m, 2H), 1.31–1.20 (m, 2H), 0.81 (t, *J* = 7.3 Hz, 3H). $^{13}C\{^1H\}$NMR ($CDCl_3$, 126 MHz): δ 198.0, 153.8, 142.9, 135.9, 132.4, 131.9, 131.7, 128.7, 127.7, 126.3, 123.2, 122.4, 113.7, 73.6, 31.3, 29.7, 26.8, 22.5, 19.9, 14.0. HRMS (ESI-TOF) m / z calcd for $C_{22}H_{24}O_2Na$ ($[M+Na]^+$) 343.1674, found 343.1671.

References for Experimental Section

(1) Perrin, D. D.; Armarego, W. L. F. In *Purification of Laboratory Chemicals*; Elsevier, 2017; pp 95–634.
(2) Iafe, R. G.; Chan, D. G.; Kuo, J. L.; Boon, B. A.; Faizi, D. J.; Saga, T.; Turner, J. W.; Merlic, C. A. *Org. Lett.* **2012**, *14*, 4282–4285.
(3) Qian, M.; Negishi, E. I. *Tetrahedron Lett.* **2005**, *46*, 2927–2930.
(4) Li-Jun, Z.; Xue-Sheng, M.; Yao-Zeng, H. *J. Organomet. Chem.* **1994**, *471*, 77–85.
(5) Akitt, J. W. *J. Magn. Reson.* **1970**, *3*, 411–414.
(6) Thomas, A. A.; Zahrt, A. F.; Delaney, C. P.; Denmark, S. E. *J. Am. Chem. Soc.* **2018**, *140*, 4401–4416.
(7) Hiroya, K.; Jouka, R.; Kameda, M.; Yasuhara, A.; Sakamoto, T. *Tetrahedron* **2001**, *57*, 9697–9710.
(8) Schulte, B.; Fröhlich, R.; Studer, A. *Tetrahedron* **2008**, *64*, 11852–11859.
(9) Wang, C.; Yang, J.; Cheng, X.; Li, E.; Li, Y. *Tetrahedron Lett.* **2012**, *53*, 4402–4404.
(10) Mora-Radó, H.; Bialy, L.; Czechtizky, W.; Méndez, M.; Harrity, J. P. A. *Angew. Chem. Int. Ed.* **2016**, *55*, 5834–5836.
(11) Yanada, R.; Hashimoto, K.; Tokizane, R.; Miwa, Y.; Minami, H.; Yanada, K.; Ishikura, M.; Takemoto, Y. *J. Org. Chem.* **2008**, *73*, 5135–5138.
(12) Fan, Y. C.; Kwon, O. *Org. Lett.* **2012**, *14*, 3264–3267.
(13) Das, A.; Liao, H.-H.; Liu, R.-S. *J. Org. Chem.* **2007**, *72*, 9214–9218.
(14) Nakao, A.; Hayakawa, M. *Jpn. Kokai Tokkyo Koho* **2013**, *JP 2013-21*, 17 Oct 2013.
(15) Jithunsa, M.; Ueda, M.; Miyata, O. *Org. Lett.* **2011**, *13*, 518–521.
(16) Zhang, F.; Qin, Z.; Kong, L.; Zhao, Y.; Liu, Y.; Li, Y. *Org. Lett.* **2016**, *18*, 5150–5153.
(17) Hirner, J. J.; Faizi, D. J.; Blum, S. A. *J. Am. Chem. Soc.* **2014**, *136*, 4740–4745.
(18) Chong, E.; Blum, S. A. *J. Am. Chem. Soc.* **2015**, *137*, 10144–10147.
(19) Tomás-Mendivil, E.; Starck, J.; Ortuno, J.-C.; Michelet, V. *Org. Lett.* **2015**, *17*, 6126–6129.
(20) Kawaguchi, S.; Nakamura, K.; Yamaguchi, K.; Sato, Y.; Gonda, Y.; Nishioka, M.; Sonoda, M.; Nomoto, A.; Ogawa, A. *Eur. J. Org. Chem.* **2017**, *2017*, 5343–5346.
(21) Xu, M.-Y.; Pei, X.-Q.; Wu, Z.-L. *J. Mol. Catal. B Enzym.* **2014**, *108*, 64–71.

Chapter 5

Copper-Catalyzed Aminoboration from Hydrazones to Generate Borylated Pyrazoles

Abstract: Herein we report an aminoboration reaction that employs inexpensive, commercially available $Cu(OTf)_2$ as an effective catalyst in the direct addition of B–N σ bonds to C–C π bonds, genetating borylated pyrazoles, which are useful building blocks for drug discovery. By nature of the mechanism, the reaction produces exclusively one regioisomer and tolerates groups incompatible with alternative lithiation/borylation and iridium-catalyzed C–H activation/borylation methods. The reaction can be scaled up and the resulting isolable pyrazole pinacol boronates can be further functionalized through palladium-catalyzed Suzuki cross-coupling reactions. I initiated this project and worked with an undergraduate student Scott Kim, whose contribution is noted in the experimental section.

Introduction

Aminoboration of alkynes by B–N σ bond addition would be a useful synthetic method to provide alternative routes to borylated *N*-heterocycles that can be further functionalized through metal-catalyzed cross-coupling reactions.[1] Yet there were only limited reports of direct addition of B–N σ bonds to C–C π bonds prior to a report by our group in 2015, demonstrating this aminoboration strategy for the synthesis of borylated indoles.[2] That reaction employed a precious-metal catalyst IPrAuTFA. Replacement of this precious-metal catalyst with an Earth-abundant metal catalyst is however desirable from cost and sustainability standpoints.

Subsequent to our report, there were two additional reports of aminoboration reactions[3,4] in which boron trichloride was used to activate the C–C π bonds toward cyclization without a catalyst. However, due to its highly reactivity, boron trichloride might not tolerate other active sites on the same substrate. We herein report the first example of copper as a catalyst in the direct addition of B–N σ bonds to C–C π bonds. Cost effective $Cu(OTf)_2$ is an efficient catalyst obviating the need for complicated organic ligands, further reducing catalyst cost and increasing availability.

This catalyst promotes borylative cyclization of hydrazones, a substrate that proved unavailable to BCl_3 cyclization.

This aminoboration method is tolerant of a variety of functional groups and generates exclusively the 4-borylated regioisomer in one synthetic step, without the need to preform the heterocyclic core. Products of this reaction are building blocks toward potent medicinal scaffolds that exhibit a full spectrum of biological activities, such as antimicrobial,[5] antifungal,[6] antiinflammatory,[7] anticancer,[8] and many others.[9] Pyrazoles are present in several FDA-approved drugs, for example celecoxib (Celebrex),[10] sildenafil citrate (Viagra),[11] tepoxalin (Zubrin),[12] and also in pesticides.[13] Currently, borylated pyrazoles can be accessed through [3+2] cycloaddition/retrocycloaddition of sydnones (Scheme 5.1a),[14] or Ir-catalyzed borylation of pyrazoles (Scheme 5.1b).[15] However, these methods are limited due to poor regioselectivity. Alternatively, a sequential lithiation/borylation of 4-bromopyrazoles[16] has been used to access 4-borylated pyrazoles (Scheme 5.1c), but this method does not tolerate bromides and electrophilic functional groups.

On the basis of our previous borylative heterocyclization reactions,[2,17–22] we hypothesized that an analogous route to borylated pyrazoles from hydrazones **5.1** may be amenable to a direct borylation pathway.[22] The aminoboration reaction developed here is an one-pot procedure starting from readily available hydrazones and does not require isolation of synthetic intermediates (Scheme 5.1d).

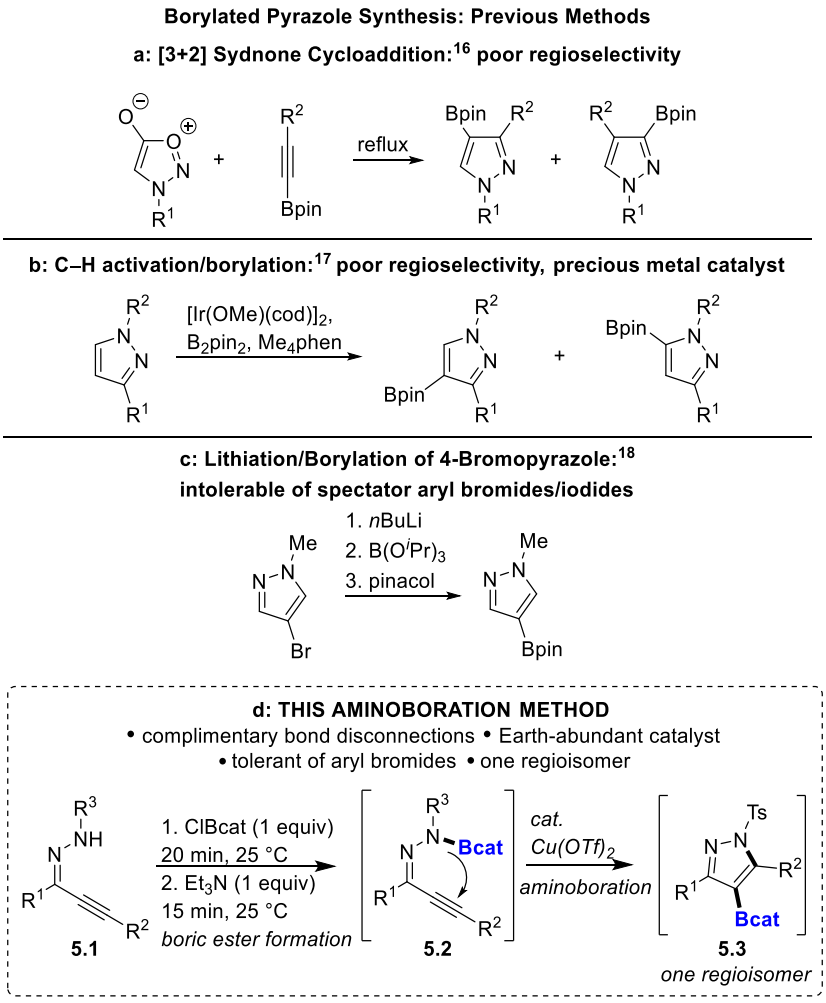

Scheme 5.1. Comparison of previous methods (**a**–**c**) and **d**) this aminoboration method

Results and Discussions

The reaction was developed through a series of optimization studies. We first investigated the formation of the requisite B–N σ bond (eq 5.1, Table 5.1) through the screening of different boron sources and bases using phenyl hydrazone (R^3 = Ph) and tosyl hydrazone (R^3 = Ts) as initial nitrogen substitution patterns. In contrast to oximes, which could be readily deprotonated by catecholboranr (HBcat) due to their lower pK_a value, hydrazones **5.1** could not be deprotonated by HBcat,[18,23] even at elevated temperature (Table 5.1, entries 1, 4, and 6). When the inorganic base sodium hydride was attempted together with *B*-chlorocatecholborane (ClBcat) and R = Ph,[2,17] no

change in the reaction mixture was detected by ^{1}H and ^{11}B NMR spectroscopy (Table 5.1, entries 2 and 7), probably due to the insolubility of sodium hydride in toluene. We decided to turn to triethylamine as our base of choice with the aim to improve solubility. With this base, boric ester **5.2** was formed when R = Ph, however starting material **5.1** was not consumed completely, and many byproducts were also formed duing this process. The stronger electron withdrawing properties of the tosyl group (R^3 = Ts) rendered its corresponding hydrazone more prone to deprotonation, resulting in formation of the amino boric ester **5.2** possessing the desired B–N σ bond at room temperature with complete consumption of **5.1** (Table 5.1, entries 8). These conditions were promising. The byproduct of this reaction, triethylammonium chloride was removed from the reaction mixture by filtration. However, its sparing solubility in toluene provided an acidic proton possibly responsible for protodeborylation of **5.3a** to form **5.3a′**. Therefore, different organic and inorganic bases were then investigated to minimize this undesired process (Table 5.1, entries 9–15), but Et_3N remained the optimal base. Attempted activation of the C–C π bond toward borylative cyclization by boron trichloride[3,4] did not yield desired product (Table 5.1, entry 3).

We next targeted the aminoboration step for optimization. A series of gold and copper catalysts with varying oxidation states, counterions, and ligands were examined with **5.1a** as the model substrate. Previously, our group developed oxyboration and aminoboration methods with IPrAuTFA as the optimal catalyst.[2,17,18,23] However, when IPrAuTFA was used in this reaction, only a trace amount of **5.3a** was observed by ^{1}H and ^{11}B NMR spectroscopy (Table 5.2, entry 1). We switched to study Cu(I) and Cu(II) catalysts due to an initial unpublished hit in the oxyboration study of borylated isoxazoles,[18] and found the inexpensive and commercially available $Cu(OTf)_2$ to be the optimal catalyst, with 70% conversion to **5.3a** at 40 °C in 24 h (Table 5.2, entries 2–5).

A control experiment without a catalyst was performed at 40 °C; after no conversion to product was observed at 24 h, then the reaction was heated to 110 °C (Table 5.2, entry 6). This control reaction at elevated temperature produced only trace amounts (< 5%) of boronate **5.3**, confirming the vital role of the catalyst.

Table 5.1. Optimization study for the formation of amino boric ester **5.2**[a]

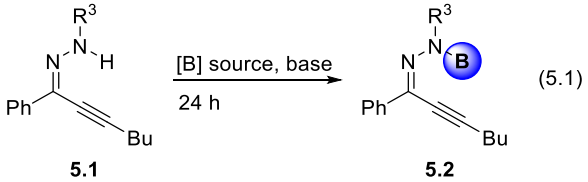

5.1 **5.2**

Entry	R^3	[B] Source	Base	T (°C)	Results
1	Ph	HBcat	None	50	No B–N bond formed
2	Ph	ClBcat	NaH	50–100	No B–N bond formed, protonated pyrazole as major product
3	Ph	BCl_3	None	23	No B–N bond formed
4	Ph	HBcat	None	110	No B–N bond formed
5	Ph	ClBcat	Et_3N	23	B–N bond formed, not clean
6	Ts	HBcat	None	80	No B–N bond formed, 10% protonated pyrazole formed
7	Ts	ClBcat	NaH	80–110	No B–N bond formed
8	**Ts**	**ClBcat**	**Et_3N**	**23**	**80% conversion**
9	Ts	ClBcat	Et_2NH	23	No B–N bond formed
10	Ts	ClBcat	$NaHCO_3$	23	No B–N bond formed
11	Ts	ClBcat	pyridine	23	No B–N bond formed
12	Ts	ClBcat	2,6-lutidine	23	15% conversion
13	Ts	ClBcat	2,6-tert-lutidine	23	No B–N bond formed
14	Ts	ClBcat	DMAP	23	No B–N bond formed
15	Ts	ClBcat	DBU	23	No B–N bond formed

[a]Reactions were carried out on a 0.10 mmol scale.

Table 5.2. Optimization study for the formation of borylated pyrazole **5.3a**

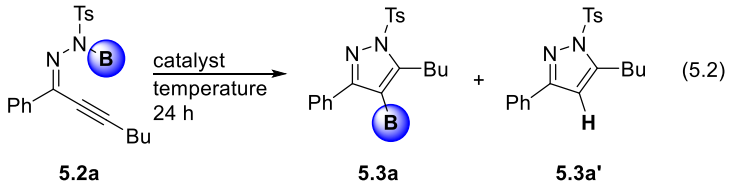

Entry	Catalyst	Cat. loading (% mol)	Base	T (°C)	Percent conversion[a] to **5.3a**
1	IPrAuTFA	5	Et_3N	80	trace
2	IPrCuTFA	5	Et_3N	40	0
3	CuI	5	Et_3N	40	20
4	$Cu(OAc)_2$	5	Et_3N	40	24
5	**$Cu(OTf)_2$**	**5**	**Et_3N**	**40**	**70**
6	None	N/A	Et_3N	40–110	trace

Reactions were carried out on a 0.10 mmol scale. [a]Percent conversion was determined based on the amount of desired product formed with respect to the amounts of starting material and byproduct **5.3a'**.

Under the optimized reaction conditions (Table 5.2, entry 5), the substrate scope was examined (Scheme 5.2). Previously unreported pyrazole catechol boronic esters **5.3a–5.3k** were generated and then transesterified to afford bench-stable and silica-gel-column-chromatography-stable pyrazole pinacol boronic esters **5.4a–5.4k**. In Table **5.3**, the numbers inside the parentheses denotes the ^{1}H NMR spectroscopy yields of pyrazole catechol boronic esters **5.3** relative to phenanthrene as internal standard. The numbers outside the parentheses correspond to the isolated yields of **5.4**.

The aminoboration reaction provided **5.4** in moderate-to-good ^{1}H NMR spectroscopy and isolated yields. The reaction was compatible with a variety of electron-rich (**5.1b** and **5.1k**) and electron-poor (**5.1h)** aryl substituents in R^1 and R^2. Aliphatic substitution (**5.1c**, **5.1g** and **5.1j**) and heteroaryl (**5.1e** and **5.1f**) were also tolerated with the reaction conditions. Thiophene-substituted **5.4e** and **5.4f** demonstrated the complementary bond disconnections that avoided potential competing ortho borylation of the thiophene[24] under the alternative lithiation/borylation method

(73% and 80% ^{1}H NMR yields of **5.3e** and **5.3f**, respectively, and 60% and 74% isolated yields of **5.4e** and **5.4f**, respectively).

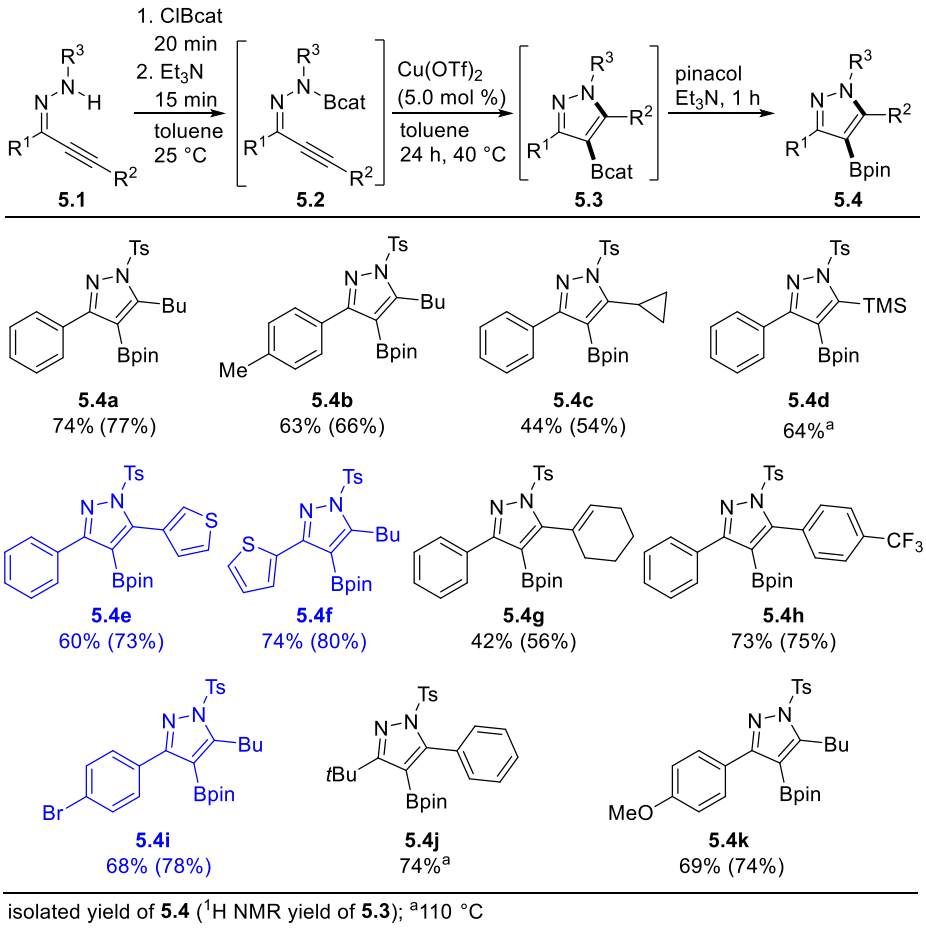

isolated yield of **5.4** (^{1}H NMR yield of **5.3**); ^{a}110 °C

Scheme 5.2. Reaction substrate scope

In addition, aryl bromide **5.1i** smoothly undergoes aminoboration to produce borylated pyrazole **5.3i** (78% ^{1}H NMR yield, 68% isolated yield of **5.4i**). Aryl bromides would not be tolerated under an alternative lithiation/borylation sequence[16] because of competitive lithium–halogen exchange. Substrates **5.1d** and **5.1j** required elevated reaction temperature (110 °C), which may be caused by steric hindrance from the *tert*-butyl and the silyl groups.

We propose a plausible catalytic cycle for the copper-catalyzed aminoboration reaction in Scheme 5.3. The Lewis acidic $Cu(OTf)_2$ activates the C–C π bond[25,26] to form intermediate **5.5**, to which the N–B σ bond is subsequently added to generate intermediate **5.6**, which then separates

into a neutral organocopper intermediate **5.7** and electrophilic boron intermediate **5.8**. The organocopper intermediate is primed for transmetalation with **5.**8 in the next step to produce the desired boronate **5.3** and regenerate $Cu(OTf)_2$, showcasing an early example of organocopper-to-boron of transmetalation reaction. Organocopper-to-boron transmetalation is not well-established but the reverse reaction from organoboron-to-copper is better studied.[27,28]

The viability of copper catalysis in this reaction was considered further. Interestingly, this direct borylative heterocyclization did not proceed with IPrAuTFA as the catalyst, in contrast to four examples of oxyboration and aminoboration to make borylated benzofurans,[17] indoles,[2] isoxazoles,[18] and dihydrofurans.[23] The origin of this difference remains unclear. In an unpublished result from borylated isoxazoles,[18] we found that $Cu(OTf)_2$ could also catalyze this oxyboration, albeit with much slower rate than IPrAuTFA. Isoxazoles and pyrazoles are the only two substrate classes from this set that contain two consecutive heteroatoms in each of their core structures. This structural similarity may play a role in their susceptibility towards copper catalysis. We hypothesize that copper might coordinate to the far-left nitrogen atom (highlighted in a red box, Scheme 5.3) and activate the system toward B–N σ bond addition across the C–C π bond (shown in alternative intermediate **5.9**).

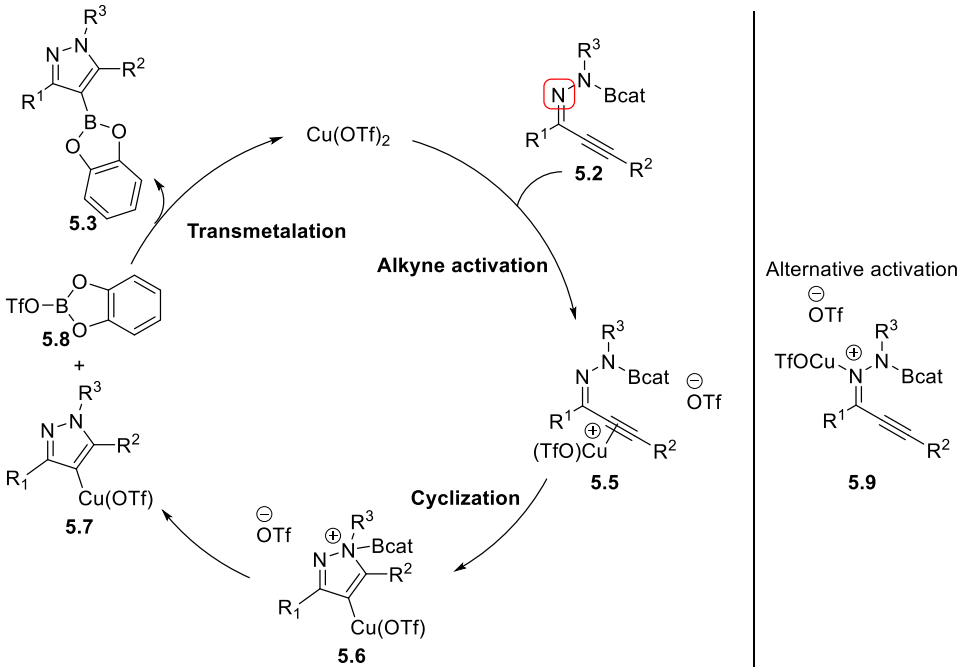

Scheme 5.3. Proposed mechanisms for Cu(II)-catalyzed aminoboration reaction

Synthetic Utility. The scale-up experiment of the aminoboration reaction of **5.1f** was successful to afford 816 mg of pinacol boronate **5.4f** on a 3 mmol scale (eq 5.3). This convenient scalability demonstrates the efficiency of the method, in which large quantities of these heterocyclic boronic ester building blocks could be prepared for multistep downstream syntheses.

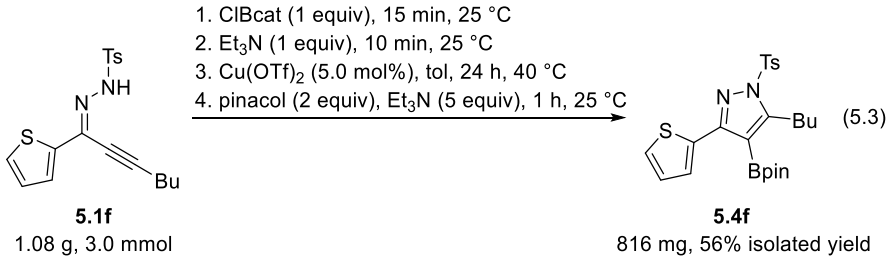

Conclusion

A new copper-catalyzed aminoboration reaction to generate borylated pyrazoles was developed. The reaction tolerates functional groups that are incompatible with alternative methods and produces only one regioisomer. This is the first report of Earth-abundant copper as the catalyst

in direct borylative heterocyclization reactions. No complicated organic ligands are needed to attenuate the catalyst reactivity, with $Cu(OTf)_2$ as the optimal catalyst. The reaction was scaled up successfully, highlighting the cost-effective route towards the synthesis of borylated pyrazoles, an important core structure in drug discovery. Further mechanistic studies, including competition experiments are underway to aid in better understanding of the reaction mechanism and the origin of its catalyst selectivity.

References

(1) Takagi, J.; Takahashi, K.; Ishiyama, T.; Miyaura, N. *J. Am. Chem. Soc.* **2002**, *124*, 8001–8006.
(2) Chong, E.; Blum, S. A. *J. Am. Chem. Soc.* **2015**, *137*, 10144–10147.
(3) Warner, A. J.; Lawson, J. R.; Fasano, V.; Ingleson, D. M. J. *Angew. Chem. Int. Ed. Engl.* **2015**, *54*, 11245.
(4) Lv, J.; Zhao, B.; Liu, L.; Han, Y.; Yuan, Y.; Shi, Z. *Adv. Synth. Catal.* **2018**, *360*, 4054–4059.
(5) Beyzaei, H.; Motraghi, Z.; Aryan, R.; Zahedi, M. M.; Samzadeh-Kermani, A. *Acta Chim. Slov.* **2017**, *64*, 911–918.
(6) Huo, X. Y.; Guo, L.; Chen, X. F.; Zhou, Y. T.; Zhang, J.; Han, X. Q.; Dai, B. *Molecules* **2018**, *23*, 1–11.
(7) Surendra Kumar, R.; Arif, I. A.; Ahamed, A.; Idhayadhulla, A. *Saudi J. Biol. Sci.* **2016**, *23*, 614–620.
(8) Kumari, S.; Paliwal, S.; Chauhan, R. *Synth. Commun.* **2014**, *44*, 1521–1578.
(9) Naim, M. J.; Alam, O.; Nawaz, F.; Alam, M. J.; Alam, P. *J. Pharm. Bioallied Sci.* **2016**, *8*, 2–17.
(10) Penning, T. D.; Talley, J. J.; Bertenshaw, S. R.; Carter, J. S.; Collins, P. W.; Docter, S.; Graneto, M. J.; Lee, L. F.; Malecha, J. W.; Miyashiro, J. M.; et al. *J. Med. Chem.* **1997**, *40*, 1347–1365.
(11) Dale, D. J.; Dunn, P. J.; Golightly, C.; Hughes, M. L.; Levett, P. C.; Pearce, A. K.; Searle, P. M.; Ward, G.; Wood, A. S. *Org. Process Res. Dev.* **2000**, *4*, 17–22.
(12) Abdel-Magib, A. F.; Harris, B.; Maryanoff, C. A. WO 01/09102 A2, 2001.
(13) Wu, J.; Song, B.-A.; Hu, D.-Y.; Yue, M.; Yang, S. *Pest Manag. Sci.* **2012**, *68*, 801–810.
(14) Browne, D. L.; Helm, M. D.; Plant, A.; Harrity, J. P. A. *Angew. Chem. Int. Ed.* **2007**, *46*, 8656–8658.
(15) Larsen, M. A.; Hartwig, J. F. *J. Am. Chem. Soc.* **2014**, *136*, 4287–4299.
(16) Mullens, P. R. *Tetrahedron Lett.* **2009**, *50*, 6783–6786.
(17) Hirner, J. J.; Faizi, D. J.; Blum, S. A. *J. Am. Chem. Soc.* **2014**, *136*, 4740–4745.
(18) Tu, K. N.; Hirner, J. J.; Blum, S. A. *Org. Lett.* **2016**, *18*, 480–483.
(19) Johnson, J. S.; Chong, E.; Tu, K. N.; Blum, S. A. *Organometallics* **2016**, *35*, 655–662.
(20) Faizi, D. J.; Issaian, A.; Davis, A. J.; Blum, S. A. *J. Am. Chem. Soc.* **2016**, *138*, 2126–2129.
(21) Faizi, D. J.; Davis, A. J.; Meany, F. B.; Blum, S. A. *Angew. Chem. Int. Ed.* **2016**, *55*, 14286–

14290.
(22) Issaian, A.; Tu, K. N.; Blum, S. A. *Acc. Chem. Res.* **2017**, *50*, 2598–2609.
(23) Tu, K. N.; Gao, C.; Blum, S. A. *J. Org. Chem.* **2018**, *83*, 11204–11217.
(24) Comins, D. L.; Killpack, M. O. *J. Org. Chem.* **1987**, *52*, 104–109.
(25) da Silva, V. D.; de Faria, B. M.; Colombo, E.; Ascari, L.; Freitas, G. P. A.; Flores, L. S.; Cordeiro, Y.; Romão, L.; Buarque, C. D. *Bioorg. Chem.* **2019**, *83*, 87–97.
(26) Suero, M. G.; Bayle, E. D.; Collins, B. S. L.; Gaunt, M. J. *J. Am. Chem. Soc* **2013**, *135*, 5335.
(27) Yang, C.-T.; Zhang, Z.-Q.; Liu, Y.-C.; Liu, L. *Angew. Chem. Int. Ed.* **2011**, *50*, 3904–3907.
(28) Ding, S.; Xu, L.; Li, P. *ACS Catal.* **2016**, *6*, 1329–1333.

Experimental

General Methods

All reagents were used as received from commercial sources unless otherwise stated. Tetrahydrofuran and triethylamine were dried by passing through an alumina column under argon pressure on a push still solvent system. Toluene-d_8 was dried over CaH_2, degassed using three freeze-pump-thaw cycles, and vacuum transferred before use. *B*-chlorocatecholborane was purchased from TCI Chemicals and used inside a N_2-filled glovebox without further purification. Manipulations were performed in a glovebox under nitrogen atmosphere unless otherwise noted. Analytical thin layer chromatography (TLC) was performed using Merck F_{250} plates and visualized under UV irradiation at 254 nm or using a basic aqueous solution of potassium permanganate. Flash chromatography was conducted using a Teledyne Isco Combiflash® R_f 200 Automatic Flash Chromatography System, and Teledyne Isco Redisep® 35– 70 μm silica gel. All proton and carbon nuclear magnetic resonance (^{1}H and ^{13}C) spectra were recorded on a Bruker DRX-400 spectrometer, Bruker DRX-500 spectrometer outfitted with a cryoprobe, or a Bruker AVANCE-600 spectrometer. Boron nuclear magnetic resonance (^{11}B NMR) spectra were recorded on a Bruker AVANCE-600 spectrometer. Fluorine nuclear magnetic resonance (^{19}F NMR) spectra were recorded on a Bruker AVANCE-600 spectrometer. All coupling constants were measured in Hertz (Hz). Chemical shifts were reported in ppm and referenced to the residual protiated solvent peak (δ_H = 7.26 ppm for $CDCl_3$ in ^{1}H NMR spectroscopy experiments; δ_C = 77.16 ppm for $CDCl_3$ in ^{13}C NMR spectroscopy experiments). ^{11}B NMR and ^{19}F NMR spectroscopy experiments were referenced to the absolute frequency of 0 ppm in the ^{1}H dimension according to the Xi scale. High-resolution mass spectrometry (HRMS (ESI-TOF)) data were obtained at the University of California, Irvine.

Synthetic Procedures

Preparation of alkynyl ketones SI-5.2a–k was performed by undergraduate student Scott Kim. General procedure.

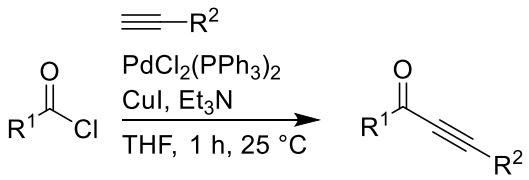

SI-5.1 **SI-5.2**

Ketones were prepared according to a literature procedure.[1] Using standard Schlenk line, to a flame-dried round bottom flask equipped with stir bar under N_2 atmosphere was added acid chloride **SI-5.1** (5.0 mmol, 1.0 equiv), $PdCl_2(PPh_3)_2$ (70. mg, 0.20 mmol, 2.0 mol%), CuI (38 mg, 0.40 mmol, 4.0 mol %), Et_3N (0.70 mL, 5.0 mmol, 1.0 equiv), and alkyne (5.0 mmol, 1.0 equiv) in dry THF (25 mL) at 25 °C. The resulting reaction mixture was stirred at room temperature under dynamic N_2 and monitored by TLC until starting materials were completely consumed (t = ~1 h). The reaction was quenched with saturated ammonium chloride (20 mL). The aqueous layer was extracted with EtOAc (3 × 20 mL). The combined organic layers were washed with brine (20 mL), dried over $MgSO_4$, filtered, and concentrated in vacuo. The resulting crude solid was purified by silica gel flash column chromatography using an elution gradient from 100% hexanes to 20% EtOAc in hexanes. Product-containing fractions were combined and concentrated in vacuo to afford **SI-5.2**.

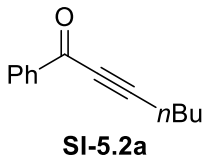

SI-5.2a

1-phenylhept-2-yn-1-one (SI-5.2a) was obtained as yellow oil on a 20 mmol scale of starting material (3.314 g, 89% isolated yield). TLC (20% EtOAc/hexanes): R_f = 0.50, visualized by UV absorbance. ^{1}H NMR ($CDCl_3$, 600 MHz): δ 8.14–8.13 (m, 2H), 7.61–7.58 (m, 1H), 7.49–7.46 (m, 2H), 2.51 (t, *J* = 7.2 Hz, 2H), 1.67 (quintet, *J* = 7.2 Hz, 2H), 1.51 (sextet, *J* = 7.2 Hz, 2H), 0.97 (t, *J* = 7.2 Hz, 3H). This spectrum is in agreement with previously reported spectral data.[2]

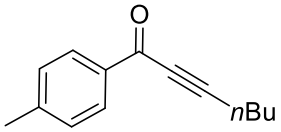

SI-5.2b

1-(4-Methylphenyl)hept-2-yn-1-one (SI-5.2b) was obtained as orange oil at 40 °C (0.872 g, 87% isolated yield). TLC (20% EtOAc/hexanes): R_f = 0.47, visualized by UV absorbance. ^{1}H NMR ($CDCl_3$, 600 MHz): δ 8.02 (d, *J* = 8.4 Hz, 2H), 7.27 (d, *J* = 8.4 Hz, 2H), 2.50 (t, *J* = 7.2 Hz, 2H), 2.50 (s, 3H), 1.66 (t, *J* = 7.2 Hz, 2H), 1.50 (sextet, *J* = 7.2 Hz, 2H), 0.96 (t, *J* = 7.2 Hz, 3H). This spectrum is in agreement with previously reported spectral data.[3]

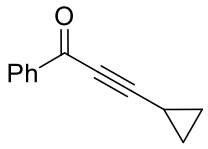

SI-5.2c

3-cyclopropyl-1-phenylprop-2-yn-1-one (SI-5.2c) was obtained as yellow oil (0.744 g, 87% isolated yield). TLC (20% EtOAc/hexanes): R_f = 0.42, visualized by UV absorbance. ^{1}H NMR ($CDCl_3$, 600 MHz): δ 8.10 (d, *J* = 7.8 Hz, 2H), 7.59 (t, *J* = 7.2 Hz, 1H), 7.46 (t, *J* = 7.8 Hz, 2H), 1.55–1.51 (m, 1H), 1.06–1.00 (m, 2H). This spectrum is in agreement with previously reported spectral data.[4]

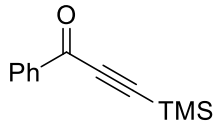

SI-5.2d

1-phenyl-3-trimethylsilyl-prop-2-yn-1-one (SI-5.2d) was obtained as yellow oil (0.638 g, 63% isolated yield). DI water was used to quench the reaction mixture rather than saturated ammonium chloride. TLC (10% EtOAc/hexanes): R_f = 0.67, visualized by UV absorbance. ^{1}H NMR ($CDCl_3$, 500 MHz): δ 8.3 (d, *J* = 7.5 Hz, 2H), 7.61 (t, *J* = 7.5 Hz, 1H), 7.49 (t, *J* = 7.5 Hz, 2H), 0.32 (s, 3H). This spectrum is in agreement with previously reported spectral data.[5]

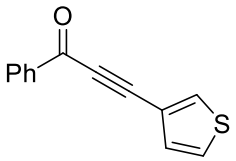

SI-5.2e

1-phenyl-3-(thiophen-3-yl)prop-2-yn-1-one (SI-5.2e) was obtained as orange oil (0.793 g, 75% isolated yield). TLC (20% EtOAc/hexanes): R_f = 0.38, visualized by UV absorbance. ^{1}H NMR ($CDCl_3$, 500 MHz): δ 8.22–8.20 (m, 2H), 7.86–7.85 (m, 1H), 7.65–7.62 (m, 1H), 7.54–7.51 (m, 2H), 7.39–7.37 (m, 1H), 7.34–7.33 (m, 1H). This spectrum is in agreement with previously reported spectral data.[6]

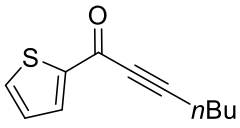

SI-5.2f

1-(thiophen-2-yl)hept-2-yn-1-one (SI-5.2f) was obtained as orange oil (0.854 g, 89% isolated yield). TLC (20% EtOAc/hexanes): R_f = 0.58, visualized by UV absorbance. ^{1}H NMR ($CDCl_3$, 500 MHz): δ 7.89–7.88 (m, 1H), 7.68–7.67 (m, 1H), 7.15–7.13 (m, 1H), 2.48 (t, *J* = 7.2 Hz, 2H),

1.65 (t, *J* = 7.2 Hz, 2H), 1.50 (sextet, *J* = 7.2 Hz, 2H), 0.96 (t, J = 7.2 Hz, 3H). This spectrum is in agreement with previously reported spectral data.[6]

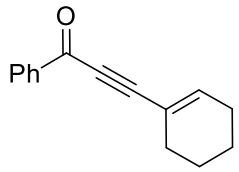

SI-5.2g

3-(cyclohex-1-en-1-yl)-1-phenylprop-2-yn-1-one (SI-5.2g) was obtained as yellow oil (0.828 g, 79% isolated yield). TLC (10% EtOAc/hexanes): R_f = 0.48, visualized by UV absorbance. ^{1}H NMR ($CDCl_3$, 600 MHz): δ 8.15–8.13 (m, 2H), 8.15–8.13 (m, 2H), 7.61–7.58 (m, 1H), 7.49–7.47 (m, 2H), 6.58 (septet, *J* = 1.8 Hz, 1H), 2.30–2.27 (m, 2H), 2.23–2.19 (m, 2H), 1.73–1.69 (m, 2H), 1.67–1.63 (m, 2H). This spectrum is in agreement with previously reported spectral data.[7]

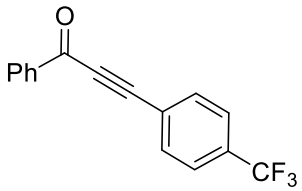

SI-5.2h

1-phenyl-3-(4-(trifluoromethyl)phenyl)prop-2-yn-1-one (SI-5.2h) was obtained as pale yellow solid (0.972 g, 71% isolated yield). TLC (20% EtOAc/hexanes): R_f = 0.39, visualized by UV absorbance. ^{1}H NMR ($CDCl_3$, 600 MHz): δ 8.21 (d, *J* = 7.8 Hz, 2H), 7.80 (d, *J* = 7.8 Hz, 2H), 7.70 (d, *J* = 7.8 Hz, 2H), 7.66 (m, 1H), 7.54 (t, *J* = 7.2 Hz, 2H). This spectrum is in agreement with previously reported spectral data.[8]

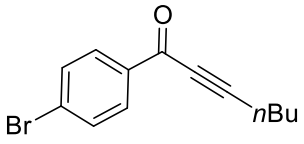

SI-5.2i

1-(4-bromophenyl)hept-2-yn-1-one (SI-5.2i) was obtained as a clear brown solid on a 10.0 mmol scale of starting material (2.295 g, 87% isolated yield). TLC (20% EtOAc/hexanes): R_f = 0.55, visualized by UV absorbance. ^{1}H NMR ($CDCl_3$, 500 MHz): δ 7.98 (d, *J* = 8.5 Hz, 2H), 7.62 (d, *J* = 8.0 Hz, 2H), 2.50 (t, *J* = 7.0 Hz, 2H), 1.66 (quintet, *J* = 7.5 Hz, 2H), 1.50 (sextet, *J* = 7.5 Hz, 2H), 0.96 (t, *J* = 7.5 Hz, 3H). This spectrum is in agreement with previously reported spectral data.[9]

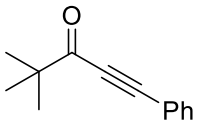

SI-5.2j

4,4-dimethyl-1-phenylpent-1-yn-3-one (SI-5.2j) was obtained as orange oil (0.623 g, 67% isolated yield). TLC (20% EtOAc/hexanes): R_f = 0.50, visualized by UV absorbance. ^{1}H NMR ($CDCl_3$, 500 MHz): δ 7.59–7.57 (m, 2H), 7.47–7.43 (m, 1H), 7.38 (t, *J* = 7.5Hz, 2H), 1.28 (s, 9H). This spectrum is in agreement with previously reported spectral data.[10]

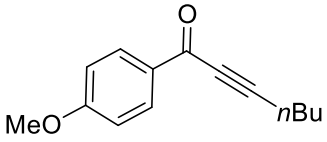

SI-5.2k

1-(4-methoxyphenyl)hept-2-yn-1-one (SI-5.2k) was obtained as yellow oil (0.948 g, 88% isolated yield). TLC (20% EtOAc/hexanes): R_f = 0.36, visualized by UV absorbance. ^{1}H NMR ($CDCl_3$, 500 MHz): δ 8.12–8.09 (m, 2H), 6.96–6.95 (m, 2H), 3.88 (s, 3H), 2.49 (t, *J* = 7.5 Hz, 2H),

1.65 (t, *J* = 7.5 Hz, 2H), 1.50 (sextet, *J* = 7.5 Hz, 2H), 0.96 (t, *J* = 7.5 Hz, 3H). This spectrum is in agreement with previously reported spectral data.[11]

Preparation of alkynyl hydrazone 5.1a–5.1k was performed by undergraduate student Scott Kim.

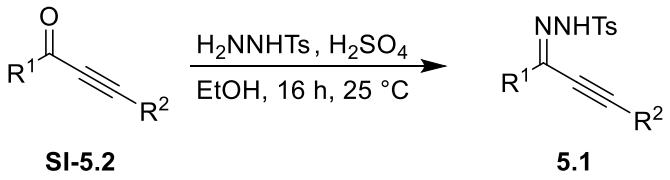

SI-5.2 **5.1**

General Procedure A: Alkynyl hydrazones were prepared according to a literature procedure.[11] Open to air, a 25 mL round bottom flask was charged with **SI-5.2** (1 mmol, 1.0 equiv), hydrazine (1.1, mmol, 1.1 equiv), EtOH (5 mL) and a stir bar. The flask was capped with a septum and sulfuric acid (1.1 mmol, 1.1 equiv) was added dropwise to the solution over 1 min via syringe. The reaction was allowed to stir for 18 h. A precipitate was present, which was then filtered using a cellulose filter paper and the solid was collected from the filter paper, dissolved in 20 mL of DCM. The organic layer was washed with saturated $NaHCO_3$ (20 mL), brine (20 mL), dried over Na_2SO_4 and concentrated in vacuo. The crude solid was triturated using cold EtOH or recrystallized in hot (60 °C) EtOH (solid was collected after ~ 30min), or purified through silica gel flash chromatography to afford hydrazone **5.1**.

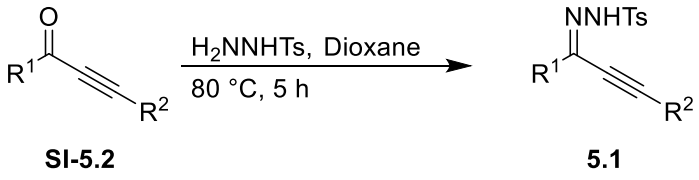

SI-5.2 **5.1**

General Procedure B: Alkynyl hydrazones were prepared according to a literature procedure.[12] Open to air, a 25 mL round bottom flask was charged with **SI-5.2** (1 mmol, 1.0 equiv), *p*-

toluenesulfonyl hydrazide (1.1, mmol, 1.1 equiv) and dioxane (5 mL). The flask was capped with a septum and the mixture was heated at 80 °C. The reaction mixture was stirred for 5–18 h at 80 °C, after which the mixture was cooled and then concentrated in vacuo. Crude solids were triturated using EtOH (~ 5 mL) to afford hydrazone **5.1**. Crude oils were purified by flash chromatography using elution gradients from 100% hexanes to 40% EtOAc in hexanes to afford hydrazone **5.1**.

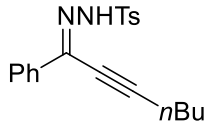

5.1a

4-methyl-N'-(1-phenylhept-2-yn-1-ylidene)benzenesulfonohydrazide (5.1a) was obtained as white solid (0.273 g, 77% isolated yield) using general procedure A after 17 h, and the crude was triturated using cold EtOH (~ 5 mL). TLC (20% EtOAc/hexanes): R_f = 0.27, visualized by UV absorbance. ^{1}H NMR δ 8.50 (s, 1H), 7.89 (d, *J* = 8.5 Hz, 2H), 7.82–7.80 (m, 2H), 7.36–7.33 (m, 3H), 7.31 *J* = 8.5 Hz, 2H), 2.57 (t, *J* = 7.0 Hz, 2H), 2.40 (s, 3H), 1.67 (quintet, *J* = 7.5 Hz, 2H), 1.50 (sextet, *J* =7.5 Hz, 2H), 0.98 (t, *J* = 7.5 Hz, 3H). This spectrum is in agreement with previously reported spectral data.[13]

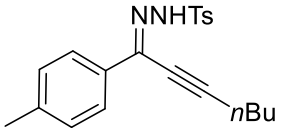

5.1b

4-methyl-N'-(1-(p-tolyl)hept-2-yn-1-ylidene)benzenesulfonohydrazide (5.1b) was obtained as white solid (0.141 g, 38% isolated yield) using general procedure A after 17 h, and the crude was triturated using cold EtOH (~ 5 mL). TLC (20% EtOAc/hexanes): R_f = 0.33, visualized by UV

absorbance. ^{1}H NMR ($CDCl_3$, 600 MHz): δ 8.43 (s, 1H), 7.88 (d, *J* = 8.4 Hz, 2H), 7.70 (d, *J* = 8.4 Hz, 2H), 2.56 (t, *J* = 7.2, 2H), 2.40 (s, 3H), 2.34 (s, 3H), 1.66 (quintet, *J* = 7.2, 2H), 2.56 (sextet, *J* = 7.2, 2H), 1.50 (t, *J* = 7.2, 2H), 0.97 (t, *J* = 7.2, 3H). ^{13}C NMR ($CDCl_3$, 125 MHz): δ 144.3, 140.4, 136.7, 135.4, 133.6, 135.8, 131.7, 129.8, 129.2, 128.0, 126.7, 107.5, 70.2, 30.4, 22.2, 21.7, 21.5, 19.5, 13.7. HRMS (ESI+) *m / z* calcd for $C_{21}H_{24}N_2O_2SNa$ ($[M+Na]^+$) 391.1456, found 391.1452.

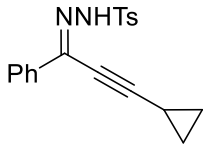

5.1c

N'-(3-cyclopropyl-1-phenylprop-2-yn-1-ylidene)-4-methylbenzenesulfonohydra-zide (5.1c) was obtained as white solid (0.081 g, 12% isolated yield) using general procedure B on a 2 mmol scale of starting material. The crude product was purified by silica gel chromatography using an elution gradient from 100% hexanes to 20% EtOAc. R_f = 0.19, visualized by UV absorbance. ^{1}H NMR ($CDCl_3$, 500 MHz): δ 8.46 (s, 1H), 7.88 (d, *J* = 8.5 Hz, 2H), 7.78–7.76 (m, 2H), 7.35–7.30 (m, 5H), 2.40 (s, 3H), 1.62–1.54 (m, 1H), 1.08–1.04 (m, 2H), 0.96–0.93 (m, 2H). ^{13}C NMR ($CDCl_3$, 125 MHz): δ 144.3, 136.3, 135.7, 134.4, 130.1, 129.8, 128.4, 128.0, 126.7, 111.0, 65.2, 21.7, 10.0, 0.5. HRMS (ESI+) *m / z* calcd for $C_{19}H_{18}N_2O_2SNa$ ($[M+Na]^+$) 361.0987, found 361.0985.

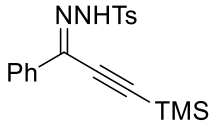

5.1d

4-Methyl-N´-(1-phenyl-3-(trimethylsilyl)prop-2-yn-1-ylidene)benzenesulfonohydra-zide (5.1d) was obtained as white solid (0.231 g, 62% isolated yield) using general procedure B (25 °C,

and 17 h). The crude was triturated using cold EtOH (~ 5 mL). TLC (20% EtOAc/hexanes): R_f = 0.38, visualized by UV absorbance. ^{1}H NMR (CDCl3, 500 MHz): δ 8.53 (s, 1H), 7.90–7.88 (d, *J* = 8.3 Hz, 2H), 7.81–7.79 (m, 2H), 7.36–7.34 (m, 3H), 7.33–7.31 (d, *J* = 8.3 Hz, 2H), 2.41 (s, 3H), 0.32 (s, 3H). This spectrum is in agreement with previously reported spectral data.[14]

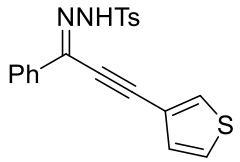

5.1e

4-methyl-N'-(1-phenyl-3-(thiophen-3-yl)prop-2-yn-1-ylidene)benzenesulfonohydra-zide (5.1e) was obtained as white solid (0.145 g, 19% isolated yield) using general procedure B on a 2 mmol scale of starting material. The crude was triturated using cold EtOH (~ 5 mL). TLC (20% EtOAc/hexanes): R_f = 0.35, visualized by UV absorbance. ^{1}H NMR ($CDCl_3$, 500 MHz): δ 8.55 (s, 1H), 7.91 (d, *J* = 8.0 Hz, 2H), 7.88–7.86 (m, 2H), 7.74 (m, 1H), 7.41–7.38 (m, 4H), 7.32 (d, *J* = 8.0 Hz, 2H), 7.27–7.26 (m, 1H), 2.41 (s, 3H). This spectrum is in agreement with previously reported spectral data.[13]

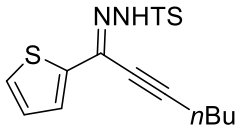

5.1f

(E)-4-methyl-N'-(1-(thiophen-2-yl)hept-2-yn-1-ylidene)benzenesulfonohydrazide (5.1f) was obtained as white solid (0.937 g, 67% isolated yield) using general procedure A on a 4 mmol scale of starting material. The crude product was recrystallized using hot EtOH (60 °C) for 30 min. TLC (20% EtOAc/hexanes): R_f = 0.31, visualized by UV absorbance. ^{1}H NMR ($CDCl_3$, 600 MHz): δ 8.28 (s, 1H), 7.87 (d, *J* = 8.4 Hz, 2H), 7.35– 7.34 (m, 1H), 7.31–7.30 (m, 3H), 6.98–6.97 (m, 1H),

2.54 (t, *J* = 7.2 Hz, 2H), 2.41 (s, 3H), 1.64 (quintet, *J* = 7.2 Hz, 2H), 1.48 (sextet, *J* = 7.2 Hz, 2H), 0.97 (t, *J* = 7.2 Hz, 2H). ^{13}C NMR ($CDCl_3$, 125 MHz): δ 144.4, 140.0, 135.5, 132.3, 129.8, 128.6, 128.2, 128.1, 127.3, 106.3, 69.5, 30.2, 22.2, 21.8, 19.4, 13.6. HRMS (ESI+) *m / z* calcd for $C_{18}H_{20}N_2O_2S_2Na$ ($[M+Na]^+$) 383.0864, found 383.0850.

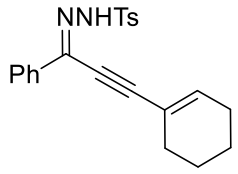

5.1g

N'-(3-(cyclohex-1-en-1-yl)-1-phenylprop-2-yn-1-ylidene)-4-methylbenzenesulfono-hydrazide (5.1g) was obtained as white solid (0.081 g, 21% isolated yield) using general procedure B (25 °C and 17 h). The crude product was triturated using cold EtOH (~ 5 mL). TLC (20% EtOAc/hexanes): R_f = 0.38, visualized by UV absorbance. ^{1}H NMR ($CDCl_3$, 600 MHz): δ 8.43 (s, 1H), 7.89 (d, *J* = 8.4 Hz, 2H), 7.82–7.81 (m, 2H), 7.36–7.34 (m, 3H), 7.31 (d, *J* = 8.4 Hz, 2H), 6.44 (septet, *J* = 1.8 Hz, 1H), 2.41 (s, 3H), 2.27–2.25 (m, 2H), 2.23–2.19 (m, 2H). 1.74–1.70 (m, 2H), 1.68–1.64 (m, 2H). ^{13}C NMR ($CDCl_3$, 125 MHz): δ 144.4, 140.7, 136.4, 135.7, 134.3, 130.1, 129.8, 128.5, 128.1, 126.7, 119.2, 107.1, 75.2, 28.9, 26.1, 22.1, 21.8, 21.3. HRMS (ESI+) *m / z* calcd for $C_{22}H_{22}N_2O_2SNa$ ($[M+Na]^+$) 401.1300, found 401.1299.

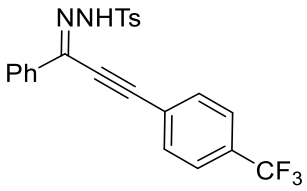

5.1h

4-methyl-N'-(1-phenyl-3-(4-(trifluoromethyl)phenyl)prop-2-yn-1-ylidene)benzene-sulfonohydrazide (5.1h) was obtained as white solid (0.378 g, 85% isolated yield) using general

procedure A for 17 h, and the crude product was triturated using cold EtOH (~ 5 mL). TLC (20% EtOAc/hexanes): R_f = 0.33, visualized by UV absorbance. ^{1}H NMR (CDCl3, 500 MHz): δ 8.58 (s, 1H), 7.92 (d, *J* = 8.0 Hz, 2H), 7.88–7.86 (m, 2H), 7.74–7.69 (m, 4H), 7.33 (d, *J* = 8.5 Hz, 2H), 2.42 (s, 3H). This spectrum is in agreement with previously reported spectral data.[13]

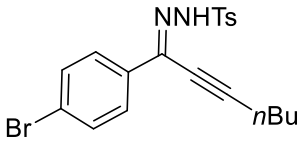

5.1i

N'-(1-(4-bromophenyl)hept-2-yn-1-ylidene)-4-methylbenzenesulfonohydrazide (5.1i) was obtained as yellow solid (0.813 g, 51% isolated yield) using general procedure A. The crude product was purified by silica gel chromatography using an elution gradient from 100% hexanes to 20% EtOAc. TLC (20% EtOAc/hexanes): R_f = 0.28, visualized by UV absorbance. ^{1}H NMR ($CDCl_3$, 600 MHz): δ 8.48 (s, 1H), 7.87 (d, *J* = 8.5 Hz, 2H), 7.66 (d, *J* = 9.0 Hz, 2H), 7.47 (d, *J* = 9.0 Hz, 2H), 7.31 (d, *J* = 8.0 Hz, 2H), 2.57 (t, *J* = 7.0 Hz, 2H), 2.41 (s, 2H), 1.66 (quintet, *J* = 7.0 Hz, 2H), 1.49 (sextet, *J* = 7.5 Hz, 2H), 0.98 (t, *J* = 7.5 Hz, 3H). ^{13}C NMR ($CDCl_3$, 125 MHz): δ 144.5, 135.6, 135.3, 133.3, 131.6, 129.87, 128.2, 128.0, 124.5, 108.3, 67.8, 30.3, 22.2, 21.8, 19.5, 13.6. HRMS (ESI+) *m / z* calcd for $C_{20}H_{22}BrN_2O_2S$ ($[M+H]^+$) 433.0585, found 433.0571.

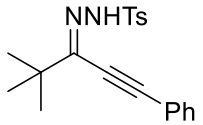

5.1j

N'-(4,4-dimethyl-1-phenylpent-1-yn-3-ylidene)-4-methylbenzenesulfonohydrazide (5.1j) was obtained as white solid (0.455 g, 64% isolated yield) using general procedure A and a 2 mmol scale of starting material. The crude product was purified by silica gel chromatography using an

elution gradient from 100% hexanes to 20% EtOAc. TLC (20% EtOAc/hexanes): R_f = 0.30 visualized by UV absorbance. ^{1}H NMR ($CDCl_3$, 500 MHz): δ 8.16 (s, 1H), 7.84 (d, *J* = 8.0 Hz, 2H), 7.52–7.50 (m, 2H), 7.46–7.37 (m, 3H), 7.31 (d, *J* = 8.0 Hz, 2H), 2.43 (s, 3H), 1.17 (s, 9H). This spectrum is in agreement with previously reported spectral data.[13]

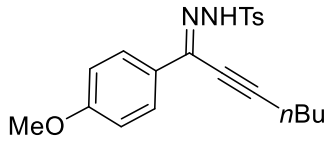

5.1k

N'-(1-(4-methoxyphenyl)hept-2-yn-1-ylidene)-4-methylbenzenesulfonohydrazide (5.1k) was obtained as white solid (0.183 g, 48% isolated yield) using general procedure A. The crude product was purified by silica gel chromatography using an elution gradient from 100% hexanes to 20% EtOAc. TLC (20% EtOAc/hexanes): R_f = 0.22 visualized by UV absorbance. ^{1}H NMR ($CDCl_3$, 500 MHz): δ 8.38 (s, 1H), 7.87 (d, *J* = 8.5 Hz, 2H), 7.74 (m, 2H), 7.30 (d, *J* = 8.0 Hz, 2H), 6.86 (m, 2H), 3.82 (s, 3H), 2.56 (t, *J* = 7.2, 2H), 2.40 (s, 3H), 2.40 (s, 3H), 1.66 (quintet, *J* = 7.2, 2H), 1.49 (sextet, *J* = 7.2, 2H), 0.97 (t, *J* = 7.5, 3H). ^{13}C NMR ($CDCl_3$, 125 MHz): δ 144.3, 140.4, 136.7, 135.4, 133.6, 135.8, 131.7, 129.8, 129.2, 128.0, 126.7, 107.5, 70.2, 30.4, 22.2, 21.7, 21.5, 19.5, 13.7. HRMS (ESI+) *m / z* calcd for $C_{21}H_{24}N_2O_3S$ ($[M+Na]^+$) 407.1405, found 407.1405.

Optimization of B–N σ bond formation in 5.2a.

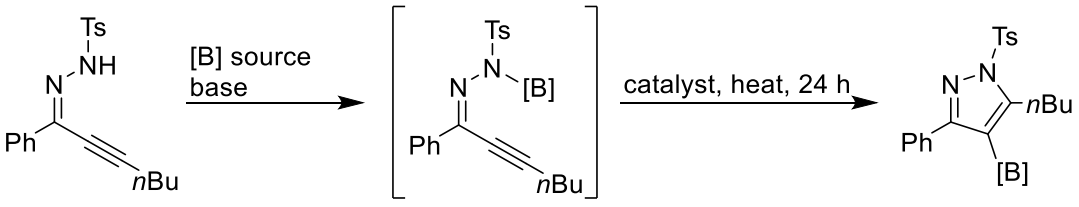

5.1a **5.2a** **5.3a**

Amino boric ester 5.2a. The reaction was performed inside N_2-filled glovebox. A 1-dram vial was charged with **5.1a** (35.4 mg, 0.100 mmol, 1.00 equiv). To this vial was added a base (0.100 mmol, 1 equiv) in d_8-toluene (0.20 mL) at 25 °C, then a boron source (0.100 mmol, 1.00 equiv) in d_8-toluene (0.10 mL) at 25 °C. Formation of **5.2a** was monitored by ^{1}H and ^{11}B NMR spectroscopy and the results were reported in Table 5.1.

Optimization of aminoboration reaction conditions

Amino boric ester 5.2a. The reaction was performed inside N_2-filled glovebox. A 1-dram vial was charged with **5.1a** (35.4 mg, 0.100 mmol, 1.00 equiv). To this vial was added a solution of *B*-chlorocatecholborane (15.4 mg, 0.100 mmol, 1.00 equiv) in d_8-toluene (0.20 mL) via pipet at 25 °C. The reaction mixture was stirred for 20 min at 25 °C, then Et_3N (14 μL, 0.10 mmol, 1.0 equiv) was added via gas-tight syringe to the reaction mixture, during which precipitation of triethylammonium chloride was observed with concurrent generation of **5.2a**. The precipitate was removed using a 0.2-μm Target® PTFE syringe filter, and the filtrate was used directly in the screen of reaction conditions without further purification. The results were summarized in Table 5.2.

General procedure NMR conversions

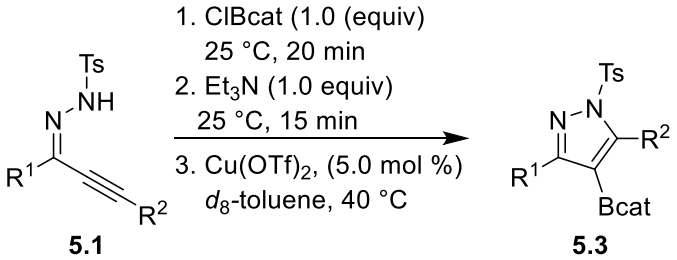

5.1 **5.3**

In a N_2-filled glovebox, to a 1-dram vial containing alkynyl hydrazone **5.1** (0.10 mmol, 1.0 equiv) was added a solution of *B*-chlorocatecholborane (0.10 mmol, 1.0 equiv) in 0.2 mL d_8-toluene via pipet. The reaction mixture was allowed to stirred at 25 °C for 20 min, producing a suspension. The base Et_3N (0.10 mmol, 1.0 equiv) was then added to the resulting suspension via gas-tight syringe. The resulting suspension was allowed to stir at room temperature for 15 min. The precipitate was removed using a 0.2-μm Target® PTFE syringe filter, and the filtrate was dispensed into a vial containing the catalyst $Cu(OTf)_2$ (0.0050 mmol, 5.0 mol %) and a stir bar. The vial was rinsed twice with d_8-toluene (2 x 0.15 mL) and the rinses were transferred via syringe to the solution above. The vial was capped and the mixture was heated at 40 °C inside the glovebox for 24 h. The ^{1}H NMR yield of **5.3** was measured using single scan ^{1}H NMR spectroscopy (600 MHz, d_8-toluene) using the internal phenanthrene standard. The table below shows the NMR spectroscopy yield calculated using this method.

Table S5.1: ^{1}H NMR spectroscopy yield of borylated pyrazole **5.3**

	R^1	R^2	NMR yield (%)	Time (h)	Temperature (°C)
5.3a	Ph	Bu	77%	24 h	40 °C
5.3b	4-MePh	Bu	66%	24 h	40 °C
5.3c	Ph	Cpr	54%	24 h	40 °C
5.3e	Ph	3-thiophene	73%	24 h	40 °C
5.3f	2-thiophene	Bu	80%	24 h	40 °C
5.3g	Ph	cyclohexenyl	56%	24 h	40 °C
5.3h	Ph	4-CF_3Ph	75%	24 h	40 °C
5.3i	4-BrPh	Bu	78%	24 h	40 °C
5.3k	4-MeOPh	Bu	74%	24 h	40 °C

Synthesis of pinacol boronates 5.4: General procedure.

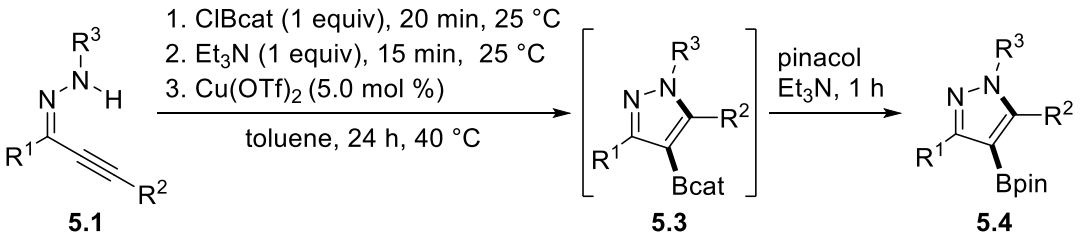

In a N_2-filled glovebox, to a 1-dram vial containing alkynyl hydrazone **5.1** (0.10 mmol, 1.0 equiv) was added a solution of *B*-chlorocatecholborane (0.10 mmol, 1.0 equiv) in 0.2 mL d_8-toluene via pipet. The reaction mixture was stirred at 25 °C for 20 min, producing a suspension. The compound Et_3N (0.10 mmol, 1.0 equiv) was then added to the resulting suspension via gas-tight syringe. The resulting suspension was allowed to stir at room temperature for 15 min. The precipitate was removed using a 0.2-µm Target® PTFE syringe filter, and the filtrate was dispensed into a vial containing the catalyst $Cu(OTf)_2$ (0.0050 mmol, 5.0 mol %) and a stir bar. The vial was rinsed twice with d_8-toluene (2 x 0.15 mL) and the rinses were transferred via syringe to the solution above. The vial was capped and the mixture was stirred at 40 °C inside the glovebox for 24 h.

Pinacol (23.6 mg, 0.200 mmol, 2.00 equiv) was dissolved in anhydrous Et_3N (0.70 mL, 0.50 mmol, 5.0 equiv). The resulting solution was added to the reaction mixture, and the resulting suspension was stirred at 25 °C for 1 h. The reaction mixture was then removed from the glovebox. Volatiles were removed in vacuo. The resulting dark brown oil was purified by silica gel chromatography using an elution gradient from 100% hexanes to 100% CH_2Cl_2. Solvents were removed in vacuo to afford the desired pinacol boronate **5.4**. All of the pinacol boronates **5.4a**–**5.4k** are missing one carbon signal in the ^{13}C NMR spectroscopy data. This carbon atom is assigned to the carbon in the newly formed C–B σ bond. This is expected due to the quadrupolar relaxation of B.[15]

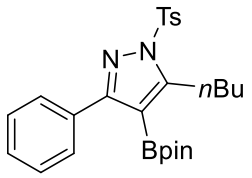

5.4a

Pinacol boronate (5.4a) was obtained as a clear oil (38.3 mg, 74% isolated yield). TLC (40% CH_2Cl_2/hexanes): R_f = 0.08, visualized by UV absorbance. ^{1}H NMR ($CDCl_3$, 600 MHz): δ 7.91 (d, *J* = 8.4 Hz, 2H), 7.71–7.69 (m, 2H), 7.34–7.28 (m, 5H), 3.17 (t, *J* = 8.4 Hz, 2H), 2.40 (s, 3H), 2.36 (s, 3H), 1.67 (quintet, *J* = 7.2 Hz, 2H), 1.45 (sextet, *J* = 7.2 Hz, 2H), 1.27 (s, 12H), 0.96 (t, *J* = 7.2 Hz, 3H). ^{13}C NMR ($CDCl_3$, 150 MHz): δ 159.6, 157.4, 145.4, 135.6, 133.1, 129.9, 129.1, 128.7, 128.2, 127.8, 83.8, 33.8, 26.8, 24.9, 23.0, 21.8, 13.9. ^{11}B NMR ($CDCl_3$, 192 MHz): δ 29.9 (s). HRMS (ESI+) *m / z* calcd for $C_{26}H_{33}BN_2O_4SNa$ ($[M+Na]^+$) 503.2157, found 503.2155.

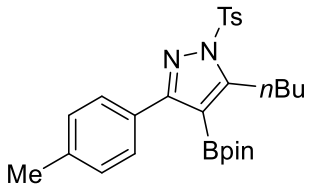

5.4b

Pinacol boronate (5.4b) was obtained as a clear oil (31.0 mg, 63% isolated yield). TLC (40% CH_2Cl_2/hexanes): R_f = 0.09, visualized by UV absorbance. ^{1}H NMR ($CDCl_3$, 500 MHz): δ 7.90 (d, *J* = 8.5 Hz, 2H), 7.61 (d, *J* = 8.0 Hz, 2H), 7.28 (d, *J* = 8.0 Hz, 2H), 7.14 (d, *J* = 8.0 Hz, 2H), 3.16 (t, *J* = 8.0 Hz, 2H), 2.40 (s, 3H), 2.36 (s, 3H), 1.67 (quintet, *J* = 7.5 Hz, 2H), 1.45 (sextet, *J* = 7.5 Hz, 2H), 1.28 (s, 12H), 0.96 (t, *J* = 7.0 Hz, 3H). ^{13}C NMR ($CDCl_3$, 125 MHz): δ 159.6, 157.3, 145.3, 138.5, 135.6, 130.2, 129.9, 128.9, 128.6, 128.2, 83.7, 33.8, 26.8, 24.9, 23.0, 21.8, 21.5, 13.9.

^{11}B NMR ($CDCl_3$, 192 MHz): δ 30.1 (s). HRMS (ESI+) *m / z* calcd for $C_{27}H_{36}BN_2O_4S$ ($[M+H]^+$) 495.2494, found 495.2486.

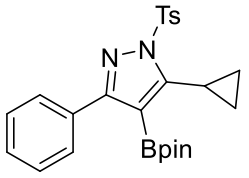

5.4c

Pinacol boronate (5.4c) was obtained as a light yellow oil (21.0 mg, 44% isolated yield). TLC (40% CH_2Cl_2/hexanes): R_f = 0.06, visualized by UV absorbance. ^{1}H NMR ($CDCl_3$, 600 MHz): δ 7.93 (d, *J* = 8.4 Hz, 2H), 7.65–7.63 (m, 2H), 7.34–7.33 (m, 3H), 7.30 (d, *J* = 8.4 Hz, 2H), 2.41 (s, 3H), 2.33–2.28 (m, 1H), 1.28 (s, 12H), 1.06–1.02 (m, 2H), 0.81–0.78 (m, 2H). ^{13}C NMR ($CDCl_3$, 150 MHz): δ 158.5, 154.7, 145.4, 135.6, 133.3, 129.9, 128.8, 128.6, 128.3, 128.1, 84.4, 29.8, 25.1, 21.8, 8.6, 8.5. ^{11}B NMR ($CDCl_3$, 192 MHz): δ 30.2 (s). HRMS (ESI+) *m / z* calcd for $C_{25}H_{30}BN_2O_4S$ ($[M+H]^+$) 465.2024, found 465.2076.

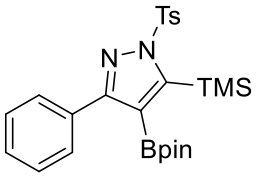

5.4d

Pinacol boronate (5.4d) was obtained as a yellow oil (31.8 mg, 64% isolated yield). TLC (40% CH_2Cl_2/hexanes): R_f = 0.30, visualized by UV absorbance. ^{1}H NMR ($CDCl_3$, 500 MHz): δ 7.89 (d, *J* = 8.5 Hz, 2H), 7.59–7.57 (m, 2H), 7.34–7.33 (m, 3H), 7.28 (d, *J* = 8.5 Hz, 2H), 2.41 (s, 3H), 1.23 (s, 12H), 0.51 (s, 9H).^{13}C NMR ($CDCl_3$, 150 MHz): δ 160.0, 152.0, 145.3, 135.4, 133.5, 129.7, 129.0, 128.8, 128.5, 128.0, 84.7, 25.7, 21.8, 1.2. ^{11}B NMR ($CDCl_3$, 192 MHz): δ 30.5 (s). HRMS (ESI+) *m / z* calcd for $C_{25}H_{33}BN_2O_4SSiNa$ ($[M+Na]^+$) 519.1926, found 519.1768.

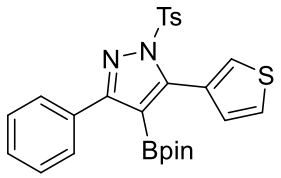

5.4e

Pinacol boronate (5.4e) was obtained as a white solid (30.2 mg, 60% isolated yield). TLC (40% CH_2Cl_2/hexanes): R_f = 0.11, visualized by UV absorbance. ^{1}H NMR ($CDCl_3$, 600 MHz): δ 7.80–7.78 (m, 2H), 7.62 (d, *J* = 8.4 Hz, 2H), 7.38–7.33 (m, 5H), 7.22–7.20 (m, 3H), 2.39 (s, 3H), 1.11 (s, 12H). ^{13}C NMR ($CDCl_3$, 125 MHz): δ 158.5, 148.1, 145.5, 135.1, 132.8, 130.4, 129.8, 129.5, 129.0, 128.4, 128.24, 128.21, 127.4, 124.3, 84.2, 24.6, 21.8. ^{11}B NMR ($CDCl_3$, 192 MHz): δ 30.0 (s). HRMS (ESI+) *m / z* calcd for $C_{26}H_{27}BN_2O_4S_2Na$ ($[M+H]^+$) 529.1408, found 529.1426.

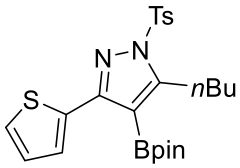

5.4f

Pinacol boronate (5.4f) was obtained as a clear oil on a 0.20 mmol scale of starting material (73.1 mg, 74% isolated yield). TLC (50% CH_2Cl_2/hexanes): R_f = 0.18, visualized by UV absorbance. ^{1}H NMR ($CDCl_3$, 600 MHz): δ 7.91 (d, *J* = 8.4 Hz, 2H), 7.84–7.83 (m, 1H), 7.30–7.26 (m, 3H), 7.01–7.00 (m, 1H), 3.18 (t, *J* = 7.8 Hz, 2H), 2.40 (s, 3H), 1.69–1.62 (m, 2H), 1.45 (sextet, *J* = 7.2 Hz, 2H), 1.32 (s, 12H), 0.96 (t, *J* = 7.2 Hz, 3H). ^{13}C NMR ($CDCl_3$, 150 MHz): δ 158.2, 153.6, 145.5, 135.9, 135.4, 129.9, 128.3, 128.2, 127.2, 126.5, 83.8, 33.8, 26.5, 25.0, 22.9, 21.8, 13.9. ^{11}B NMR ($CDCl_3$, 192 MHz): δ 29.8 (s). HRMS (ESI+) *m / z* calcd for $C_{24}H_{32}BN_2O_4S_2$ ($[M+H]^+$) 487.1901, found 487.1926.

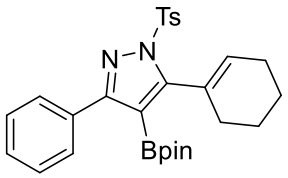

5.4g

Pinacol boronate (5.4g) was obtained as a light yellow solid (21.1 mg, 42% isolated yield). TLC (40% CH_2Cl_2/hexanes): R_f = 0.08, visualized by UV absorbance. ^{1}H NMR ($CDCl_3$, 600 MHz): δ 7.83 (d, *J* = 8.4 Hz, 2H), 7.77–7.75 (m, 2H), 7.34–7.33 (m, 3H), 7.26–7.25 (m, 1H), 5.50 (m, 1H), 2.42–2.39 (m, 5H), 2.16–2.15 (m, 2H), 1.84–1.80 (m, 2H), 1.74–1.71 (m, 2H), 1.25 (s, 12H). ^{13}C NMR ($CDCl_3$, 150 MHz): δ 156.4, 145.3, 136.6, 135.5, 132.9, 130.34, 130.31, 129.7, 128.8, 128.5, 128.2, 128.1, 84.0, 30.6, 25.7, 24.8, 22.7, 21.82, 21.80. ^{11}B NMR ($CDCl_3$, 192 MHz): δ 30.5 (s). HRMS (ESI+) *m / z* calcd for $C_{28}H_{34}BN_2O_4S$ ($[M+H]^+$) 505.2338, found 505.2362.

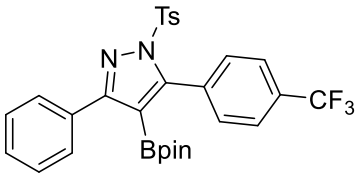

5.4h

Pinacol boronate (5.4h) was obtained as a light brown solid (41.3 mg, 73% isolated yield). TLC (40% CH_2Cl_2/hexanes): R_f = 0.10, visualized by UV absorbance. ^{1}H NMR ($CDCl_3$, 600 MHz): δ 7.80–7.79 (m, 2H), 7.68–7.65 (m, 4H), 7.50 (d, *J* = 7.8 Hz, 2H), 7.38–7.37 (m, 3H), 7.26–7.24 (m, 2H), 2.40 (s, 3H), 1.05 (s, 12H). ^{13}C NMR ($CDCl_3$, 150 MHz): δ 158.9, 151.8, 145.8, 134.9, 134.1, 132.4, 131.5, 131.3, 131.2, 129.9, 129.2, 128.6, 128.3, 124.3, 124.3. ^{11}B NMR ($CDCl_3$, 192 MHz): δ 29.9 (s). ^{19}F NMR ($CDCl_3$, 564 MHz): δ -62.7 (s).HRMS (ESI+) *m / z* calcd for $C_{29}H_{28}BF_3N_2O_4SNa$ ($[M+Na]^+$) 591.1718, found 591.1669.

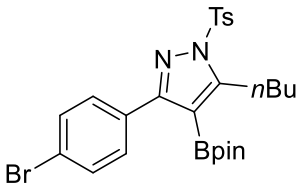

5.4i

Pinacol boronate (5.4i) was obtained as a clear oil on a 0.20 mmol scale of starting material (76.1 mg, 68% isolated yield). TLC (40% CH_2Cl_2/hexanes): R_f = 0.09, visualized by UV absorbance. ^{1}H NMR ($CDCl_3$, 600 MHz): δ 7.90 (d, *J* = 7.6 Hz, 2H), 7.60 (d, *J* = 7.5 Hz, 2H), 7.46 (d, *J* = 7.5 Hz, 2H), 7.30 (d, *J* = 7.5 Hz, 2H), 3.18 (t, *J* = 7.5 Hz, 2H), 2.41 (s, 3H), 1.66 (quintet, *J* = 7.2 Hz, 2H), 1.45 (sextet, *J* = 7.2 Hz, 2H), 1.27 (s, 12H), 0.96 (t, *J* = 7.2 Hz, 3H). ^{13}C NMR ($CDCl_3$, 150 MHz): δ 158.5, 157.8, 145.6, 142.8, 135.4, 132.0, 131.0, 130.7, 130.0, 128.2, 123.0, 83.8, 33.8, 26.7, 24.9, 23.0, 21.8, 13.9. ^{11}B NMR ($CDCl_3$, 192 MHz): δ 29.9 (s). HRMS (ESI+) *m / z* calcd for $C_{26}H_{32}BBrN_2O_4SNa$ ($[M+Na]^+$) 581.1262, found 581.1269.

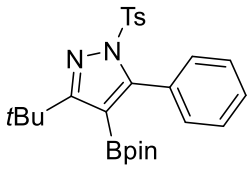

5.4j

Pinacol boronate (5.4j) was obtained as a clear oil on a 0.20 mmol scale of starting material (71.0 mg, 74% isolated yield). TLC (50% CH_2Cl_2/hexanes): R_f = 0.12, visualized by UV absorbance. ^{1}H NMR ($CDCl_3$, 600 MHz): δ 7.58 (d, *J* = 8.4 Hz, 2H), 7.41 (t, *J* = 7.2 Hz, 1H), 7.35 (t, *J* = 7.8 Hz, 2H), 7.30 (d, *J* = 7.2 Hz, 2H), 7.20 (d, *J* = 8.4 Hz, 2H), 2.39 (s, 3H), 1.33 (s, 9H), 1.04 (s, 12H). ^{13}C NMR ($CDCl_3$, 150 MHz): δ 168.4, 153.2, 145.0, 135.4, 130.7, 130.6, 129.4, 129.1, 128.1, 127.3, 84.0, 33.9, 30.0, 24.6, 21.8. ^{11}B NMR ($CDCl_3$, 192 MHz): δ 30.3 (s). HRMS (ESI+) *m / z* calcd for $C_{26}H_{33}BN_2O_4SNa$ ($[M+Na]^+$) 503.2157, found 503.2159.

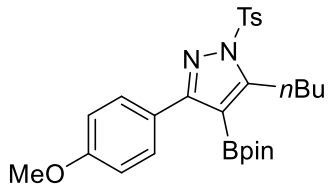

5.4k

Pinacol boronate (5.4k) was obtained as a clear oil on a 0.20 mmol scale of starting material (70.4 mg, 69% isolated yield). TLC (40% CH_2Cl_2/hexanes): R_f = 0.09, visualized by UV absorbance. ^{1}H NMR ($CDCl_3$, 600 MHz): δ 7.90 (d, *J* = 8.4 Hz, 2H), 7.66 (d, *J* = 9.0 Hz, 2H), 7.28 (d, *J* = 8.4 Hz, 2H), 6.86 (d, *J* = 9.0 Hz, 2H), 3.83 (s, 3H), 3.16 (t, *J* = 7.8 Hz, 2H), 2.40 (s, 3H), 1.66 (quintet, *J* = 7.2 Hz, 2H), 1.45 (sextet, *J* = 7.2 Hz, 2H), 1.28 (s, 12H), 0.96 (t, *J* = 7.2 Hz, 3H). ^{13}C NMR ($CDCl_3$, 150 MHz): δ 160.1, 159.3, 157.4, 145.3, 135.6, 130.3, 129.9, 128.1, 125.7, 113.2, 83.7, 55.4, 33.8, 26.7, 24.9, 23.0, 21.8, 13.9. ^{11}B NMR ($CDCl_3$, 192 MHz): δ 30.0 (s). HRMS (ESI+) *m / z* calcd for $C_{27}H_{35}BN_2O_5SNa$ ($[M+Na]^+$) 533.2263, found 533.2255.

Gram-scale preparation of 5.4f

The gram-scale aminoboration reaction was conducted in a N_2-filled glovebox. To a 20-dram vial was added hydrazone **5.1f** (1.08 g, 3.00 mmol, 1.00 equiv). The compound *B*-chlorocatecholborane (462 mg, 3.00 mmol, 1.00 equiv) was dissolved in anhydrous toluene (4.0 mL) and transferred to the 20-dram vial via pipet. The mixture was allowed to react at 25 °C for 30 min, after which time a suspension had formed. To the resulting suspension was added Et_3N (0.42 mL, 3.0 mmol, 1.0 equiv) via syringe, and this mixture was allowed to sit at 25 °C for 90 min. The resulting precipitate was removed using two 0.2-μm Target® PTFE syringe filters due to the large amount of precipitate formed, and the filtrate was then dispensed into a 20-dram vial containing the catalyst $Cu(OTf)_2$ (54.0 mg, 0.150 mmol, 5.00 mol %) and a stir bar. The vial was capped and the reaction mixture was stirred for 24 h at 40 °C inside the glovebox.

Pinacol (708 mg, 6.00 mmol, 2.00 equiv) was dissolved in anhydrous Et_3N (2.1 mL, 15 mmol, 5.0 equiv). The resulting solution was added to the reaction mixture, and the resulting suspension was stirred at 25 °C for 1 h. The reaction mixture was then removed from the glovebox. Volatiles were removed in vacuo. The resulting dark brown oil was purified by silica gel chromatography using an elution gradient from 100% hexanes to 100% CH_2Cl_2. Solvents were removed in vacuo to afford the desired pinacol boronate **5.4f** as a clear oil (816 mg, 56% isolated yield). Spectral data were identical to those previously obtained for this compound on a smaller scale.

References for Experimental Section

(1) Karpov, A. S.; Müller, T. J. J. *Org. Lett.* **2003**, *5*, 3451–3454.
(2) Trost, B. M.; Schmidt, T. *J. Am. Chem. Soc.* **1988**, *110*, 2301–2303.
(3) Huang, B.; Yin, L.; Cai, M. *New J. Chem.* **2013**, *37*, 3137–3144.
(4) Yuan, H.; Shen, Y.; Yu, S.; Shan, L.; Sun, Q.; Zhang, W. *Synth. Commun.* **2013**, *43*, 2817–2823.
(5) Arnold, D. M.; LaPorte, M. G.; Anderson, S. M.; Wipf, P. *Tetrahedron* **2013**, *69*, 7719–7731.
(6) Wang, Q.; He, L.; Li, K. K.; Tsui, G. C. *Org. Lett.* **2017**, *19*, 658–661.
(7) Waldo, J. P.; Larock, R. C. *Org. Lett.* **2005**, *7*, 5203–5205.
(8) Kawaguchi, S.; Minamida, Y.; Okuda, T.; Sato, Y.; Saeki, T.; Yoshimura, A.; Nomoto, A.; Ogawa, A. *Adv. Synth. Catal.* **2015**, *357*, 2509–2519.
(9) Natte, K.; Chen, J.; Neumann, H.; Beller, M.; Wu, X.-F. *Org. Biomol. Chem.* **2014**, *12*, 5590–5593.
(10) Alonso, D. A.; Nájera, C.; Pacheco, M. C. *J. Org. Chem.* **2004**, *69*, 1615–1619.
(11) Liang, B.; Huang, M.; You, Z.; Xiong, Z.; Lu, K.; Fathi, R.; Chen, J.; Yang, Z. *J. Org. Chem.* **2005**, *70*, 6097–6100.
(12) Zora, M.; Kivrak, A.; Yazici, C. *J. Org. Chem.* **2011**, *76*, 6726–6742.
(13) Wang, Q.; He, L.; Li, K. K.; Tsui, G. C. *Org. Lett.* **2017**, *19*, 658–661.
(14) Li, N.; Li, B.; Chen, S. *Synlett* **2016**, *27*, 1597–1601.
(15) Akitt, J. W. *J. Magn. Reson.* **1970**, *3*, 411–414.

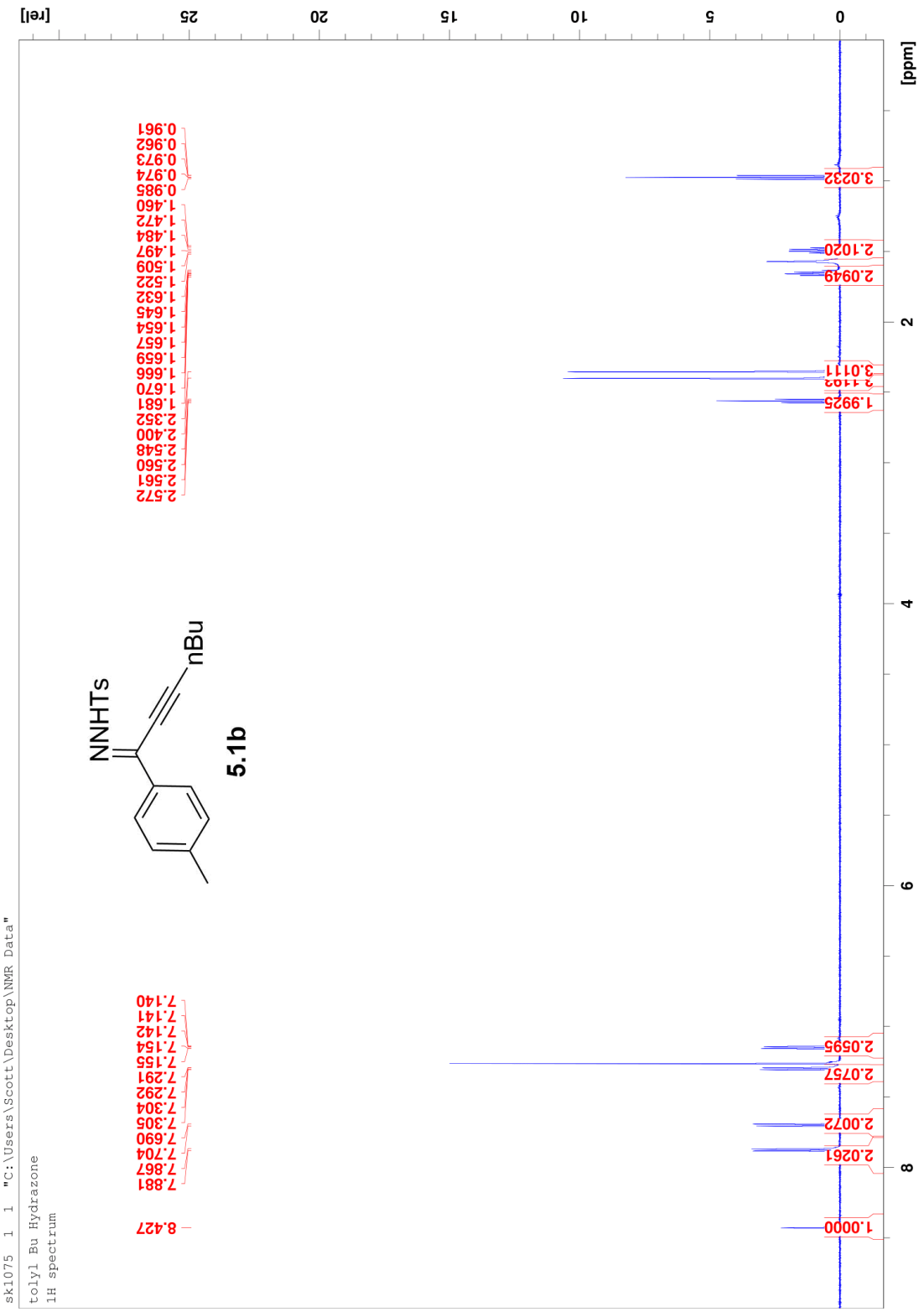
sk1075 1 1 "C:\Users\Scott\Desktop\NMR Data"
tolyl Bu Hydrazone
1H spectrum
NNHTs
nBu
5.1b
[rel]
[ppm]
1.0000
2.0261
2.0072
2.0757
2.0595
3.0111
2.1102
1.9925
3.0232
2.1020
2.0949
8.427
7.881
7.867
7.704
7.690
7.305
7.304
7.292
7.291
7.155
7.154
7.142
7.141
7.140
2.572
2.561
2.560
2.548
2.400
2.352
1.681
1.670
1.666
1.659
1.657
1.654
1.645
1.632
1.522
1.509
1.497
1.484
1.472
1.460
0.985
0.974
0.973
0.962
0.961

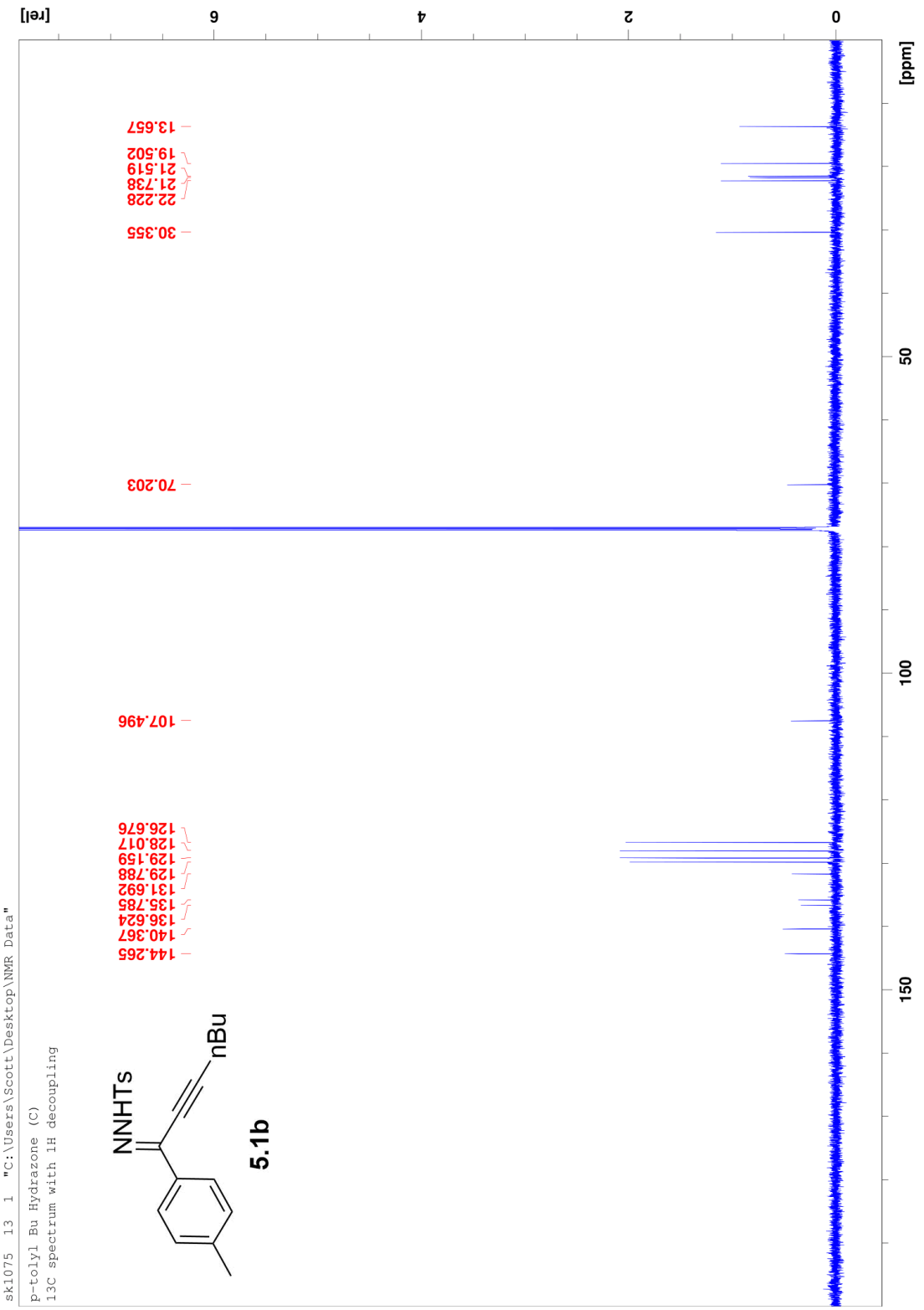
sk1075 13 1 "C:\Users\Scott\Desktop\NMR Data"
p-tolyl Bu Hydrazone (C)
13C spectrum with 1H decoupling
NNHTs
nBu
5.1b
144.265
140.367
136.624
135.785
131.692
129.788
129.159
128.017
126.676
107.496
70.203
30.355
22.228
21.738
21.519
19.502
13.657
[rel]
[ppm]

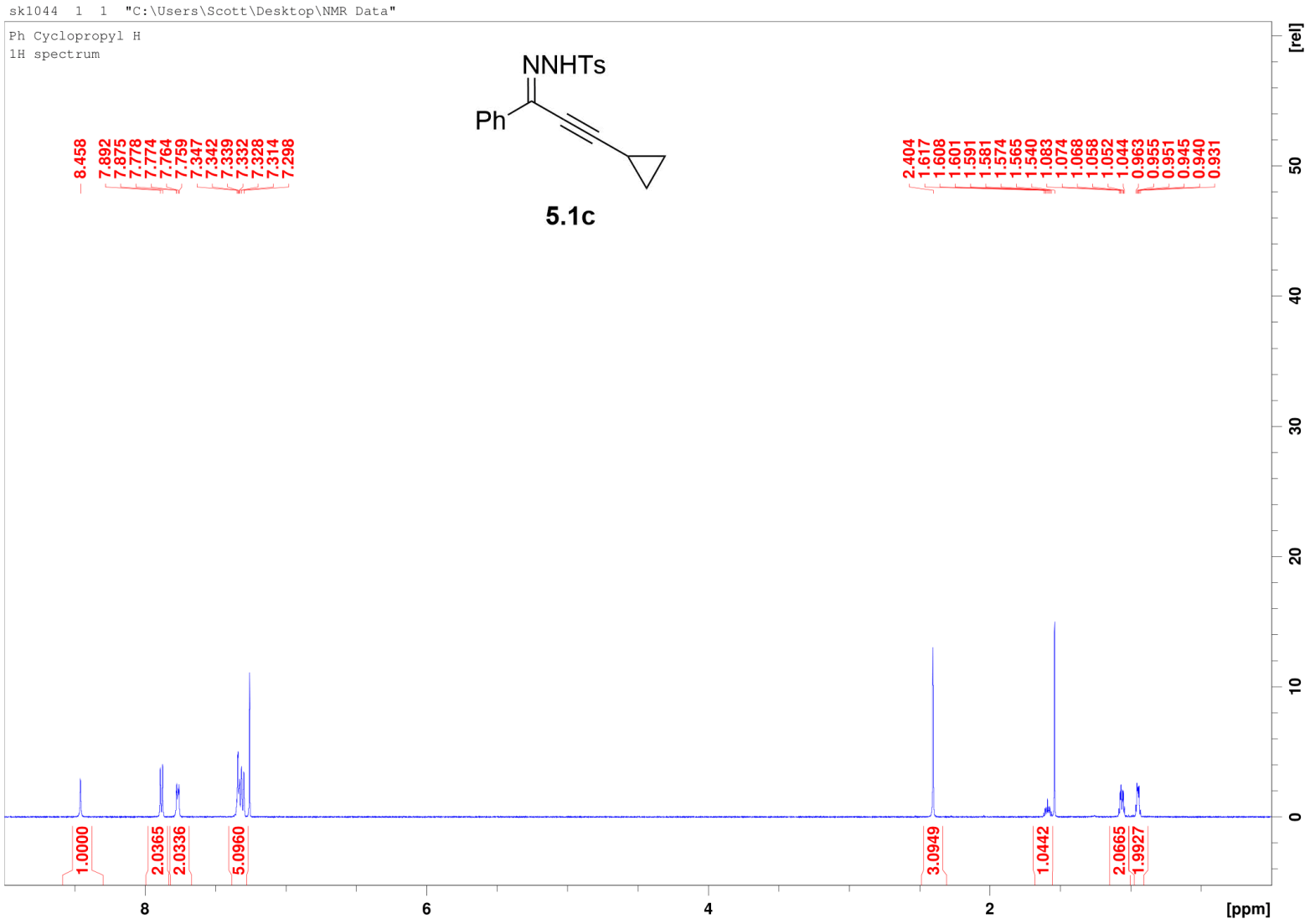
sk1044 1 1 "C:\Users\Scott\Desktop\NMR Data"
Ph Cyclopropyl H
1H spectrum
NNHTs
Ph
5.1c
8.458
7.892
7.875
7.778
7.774
7.764
7.759
7.347
7.342
7.339
7.332
7.328
7.314
7.298
2.404
1.617
1.608
1.601
1.591
1.581
1.574
1.565
1.540
1.083
1.074
1.068
1.058
1.052
1.044
0.963
0.955
0.951
0.945
0.940
0.931
1.0000
2.0365
2.0336
5.0960
3.0949
1.0442
2.0665
1.9927
8
6
4
2
[ppm]
[rel]
0
10
20
30
40
50

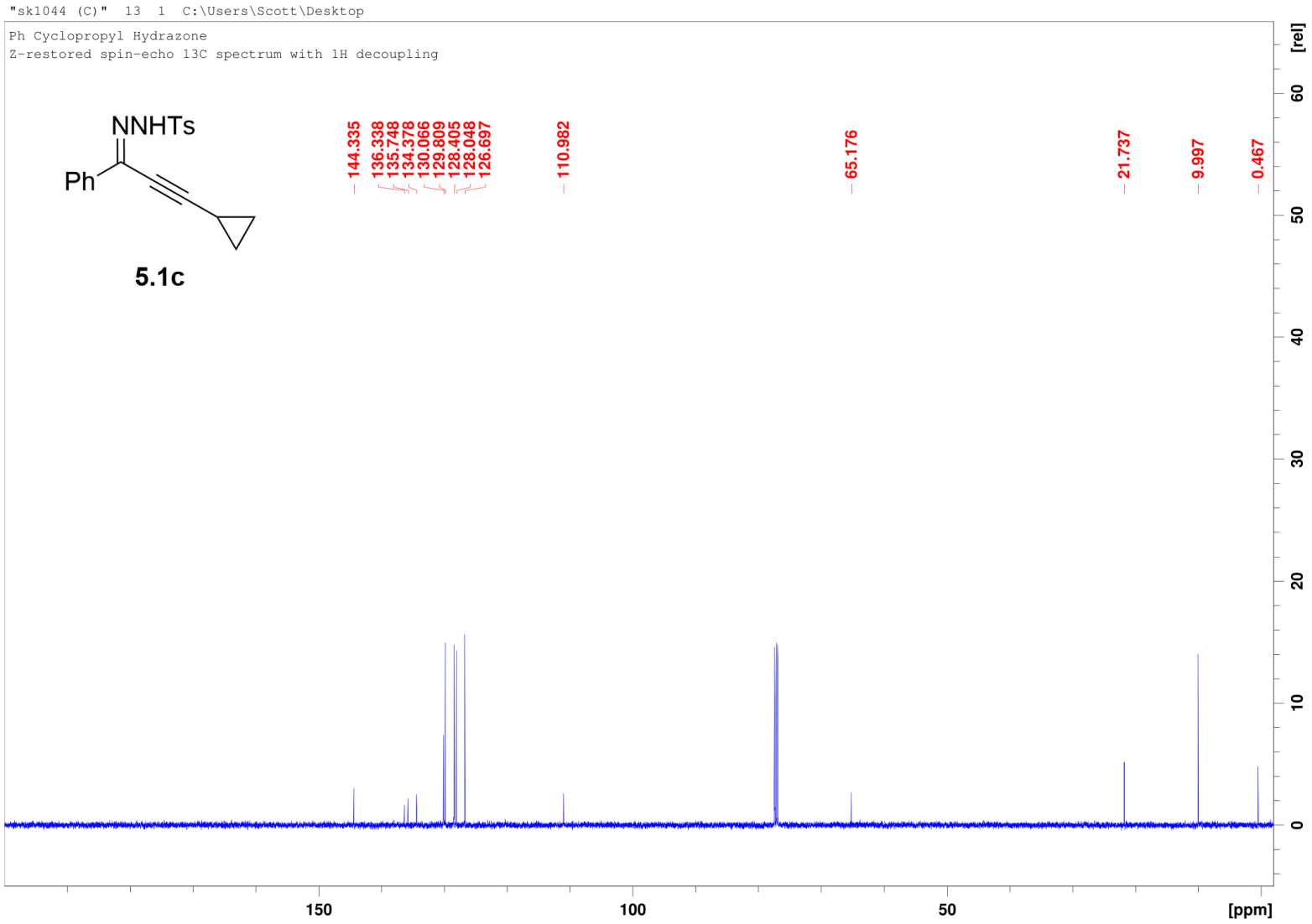
"sk1044 (C)" 13 1 C:\Users\Scott\Desktop
Ph Cyclopropyl Hydrazone
Z-restored spin-echo 13C spectrum with 1H decoupling
NNHTs
Ph
5.1c
144.335
136.338
135.748
134.378
130.066
129.809
128.405
128.048
126.697
110.982
65.176
21.737
9.997
0.467
[rel]
60
50
40
30
20
10
0
150
100
50
[ppm]

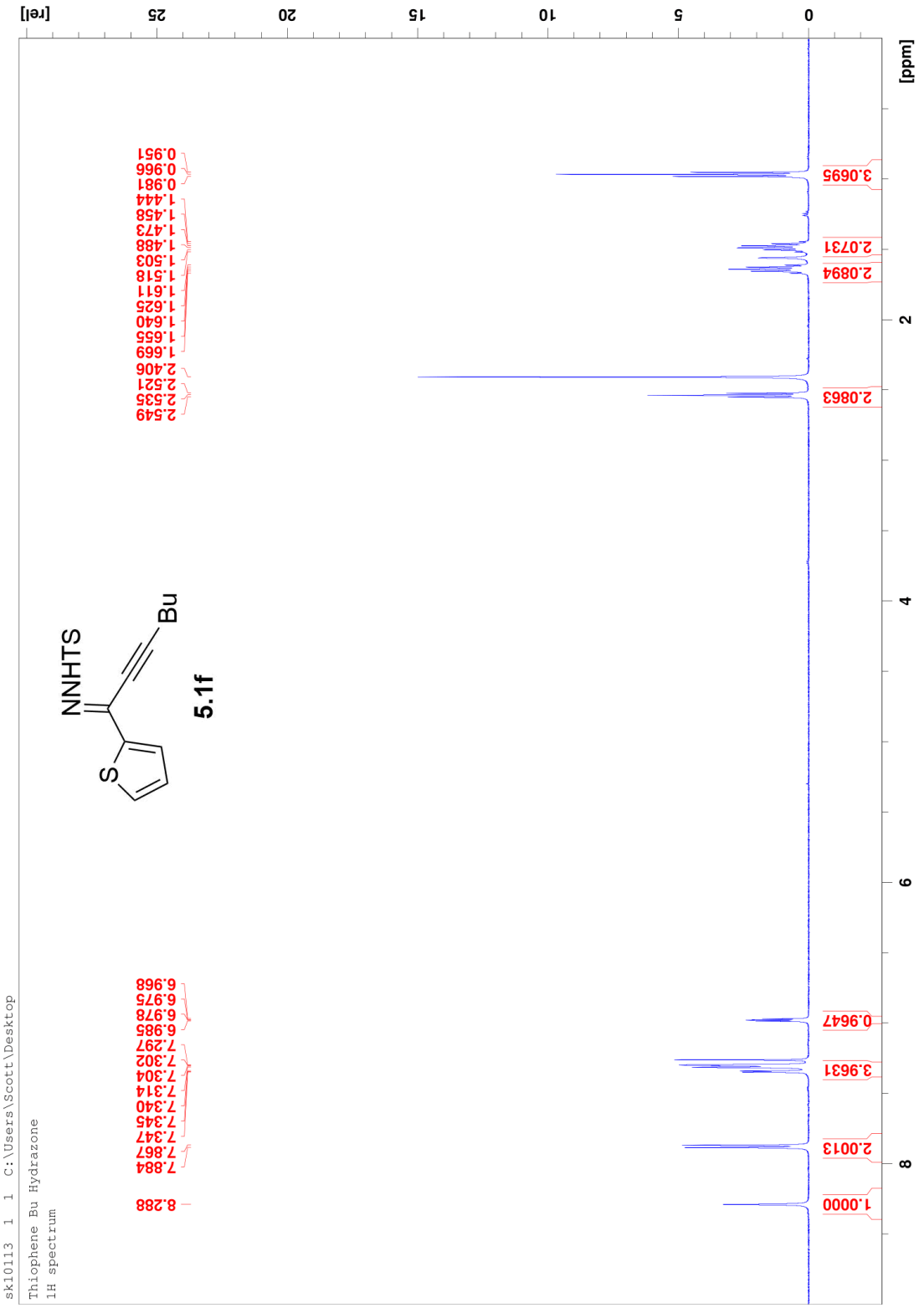
sk10113 1 1 C:\Users\Scott\Desktop
Thiophene Bu Hydrazone
1H spectrum
NNHTS
Bu
S
5.1f
[rel]
25
20
15
10
5
0
[ppm]
8
6
4
2
1.0000
2.0013
3.9631
0.9647
2.0863
2.0894
2.0731
3.0695
8.288
7.884
7.867
7.347
7.345
7.340
7.314
7.304
7.302
7.297
6.985
6.978
6.975
6.968
2.549
2.535
2.521
2.406
1.669
1.655
1.640
1.625
1.611
1.518
1.503
1.488
1.473
1.458
1.444
0.981
0.966
0.951

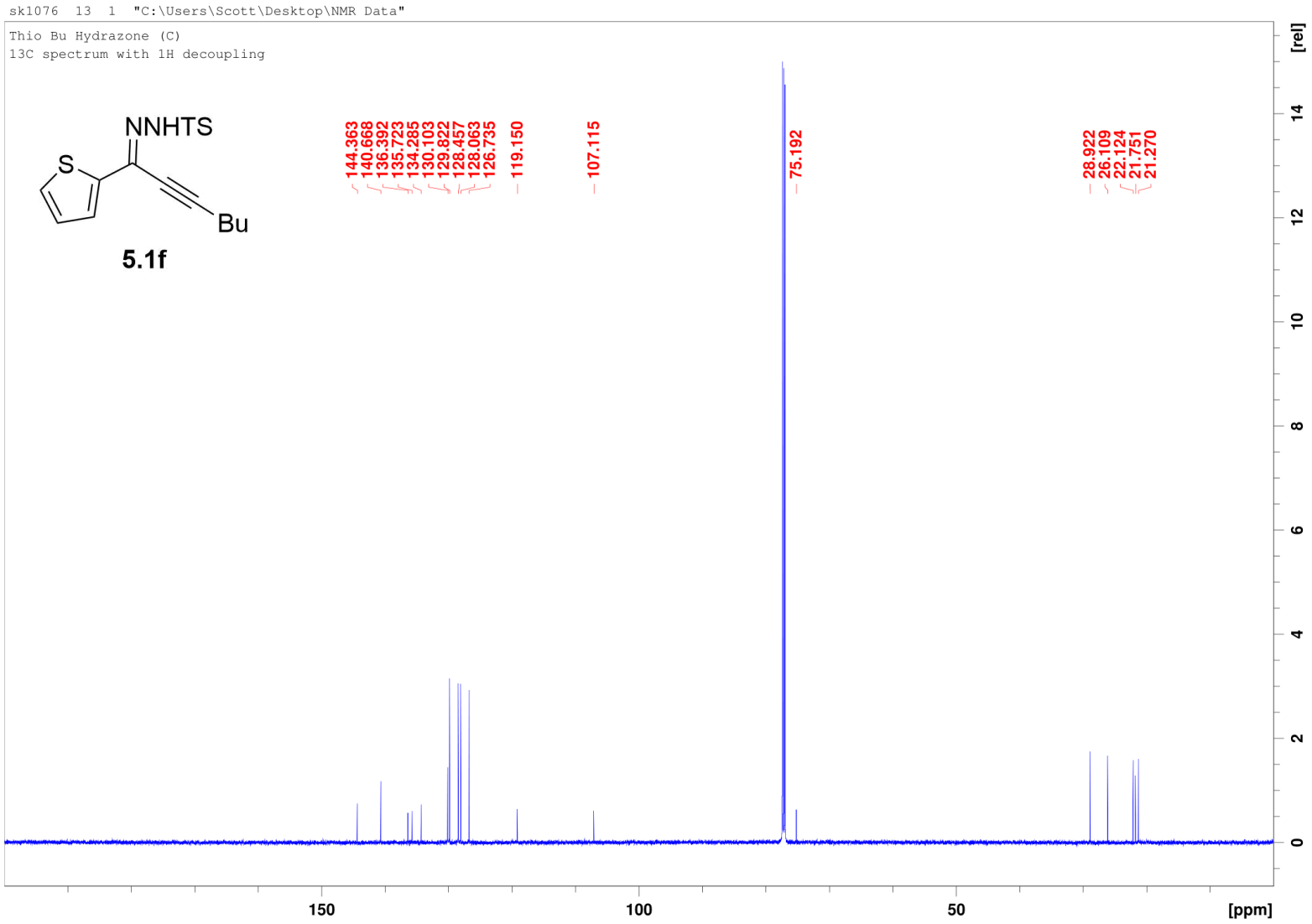
sk1076 13 1 "C:\Users\Scott\Desktop\NMR Data"
Thio Bu Hydrazone (C)
13C spectrum with 1H decoupling
NNHTS
S
Bu
5.1f
144.363
140.668
136.392
135.723
134.285
130.103
129.822
128.457
128.063
126.735
119.150
107.115
75.192
28.922
26.109
22.124
21.751
21.270
[rel]
14
12
10
8
6
4
2
0
150
100
50
[ppm]

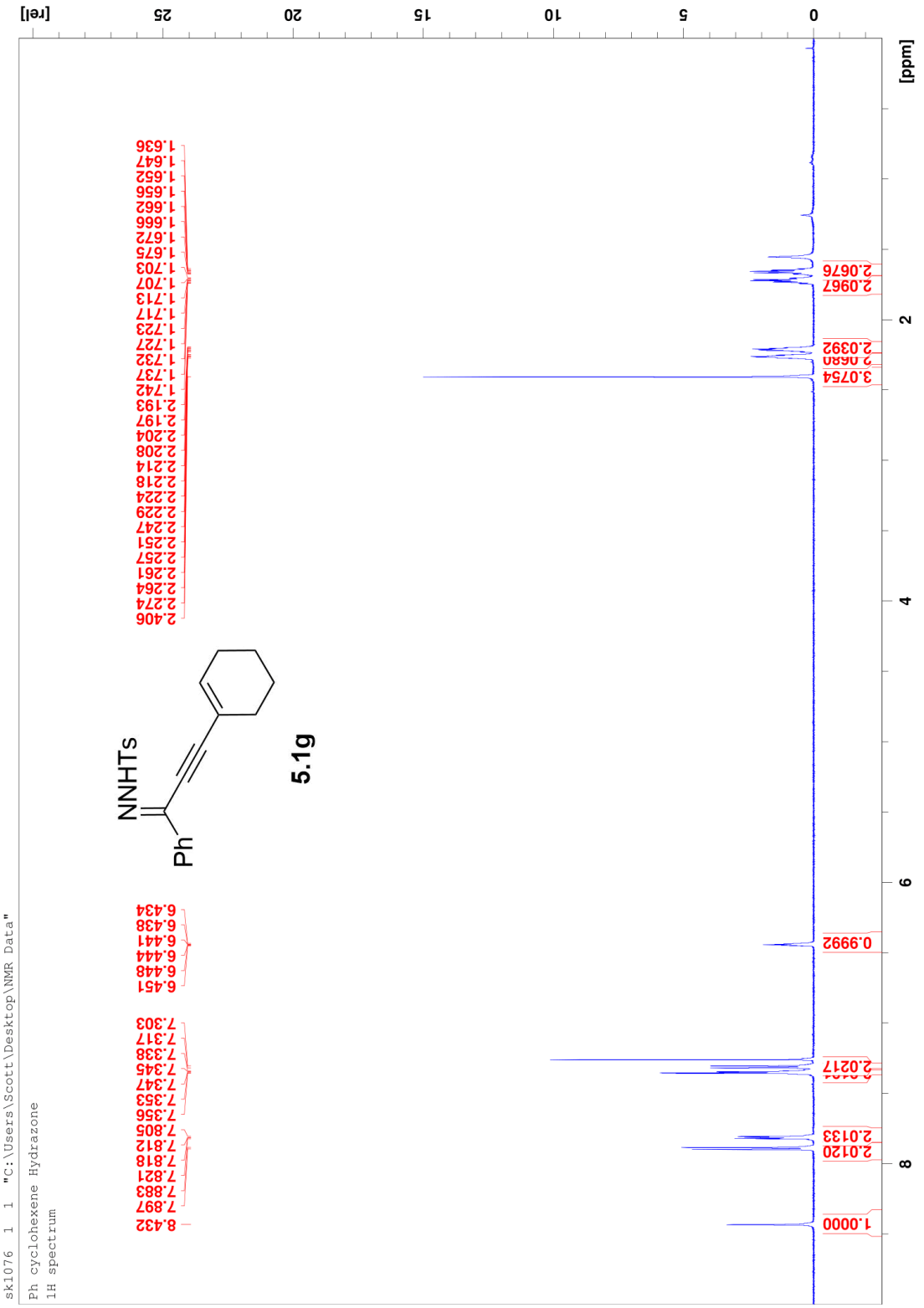
sk1076 1 1 "C:\Users\Scott\Desktop\NMR Data"
Ph cyclohexene Hydrazone
1H spectrum
NNHTs
Ph
5.1g
[rel]
[ppm]
1.0000
2.0120
2.0133
2.0217
0.9992
3.0754
2.0392
2.0967
2.0676

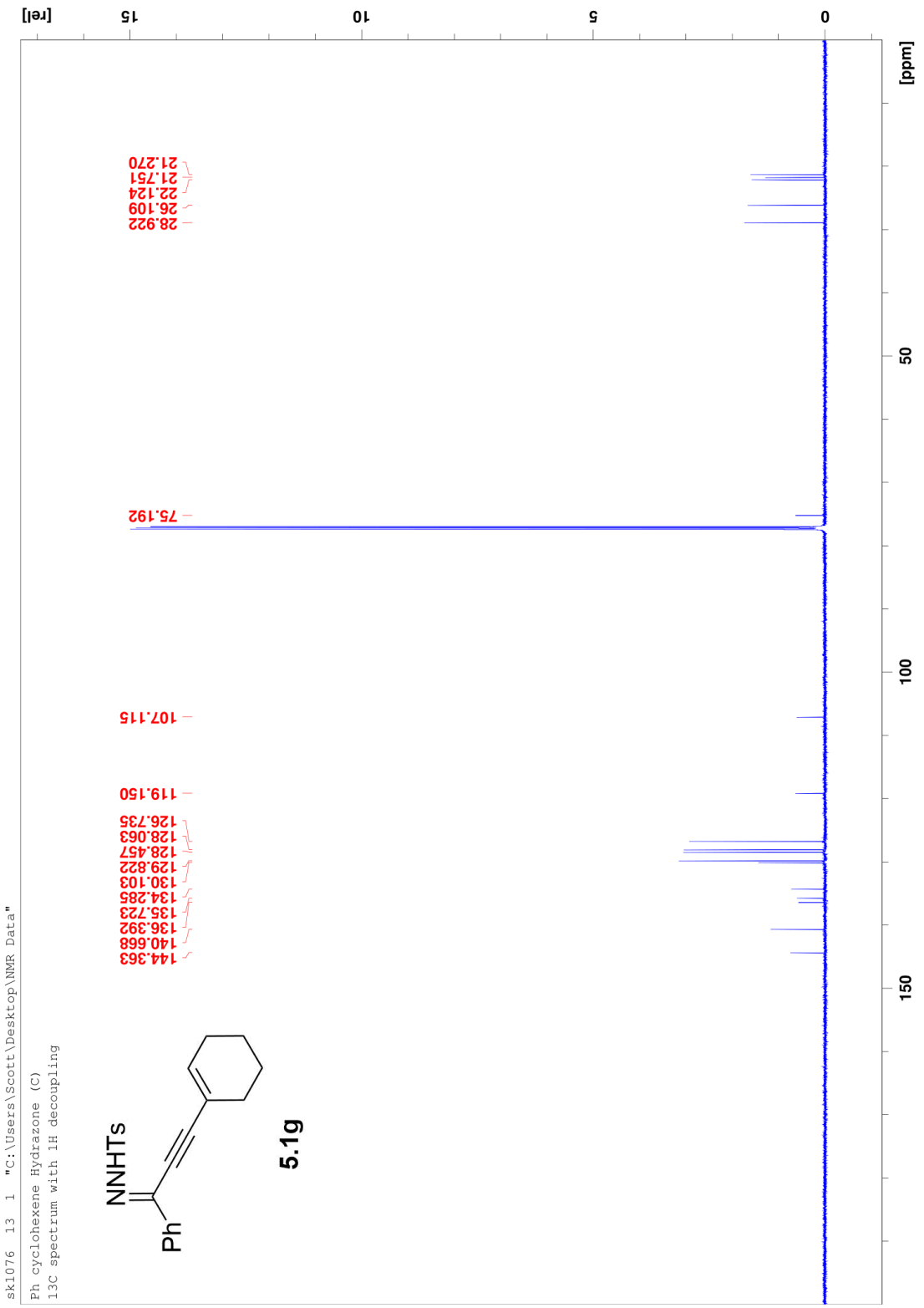
sk1076 13 1 "C:\Users\Scott\Desktop\NMR Data"
Ph cyclohexene Hydrazone (C)
13C spectrum with 1H decoupling
NNHTs
Ph
5.1g
144.363
140.668
136.392
135.723
134.285
130.103
129.822
128.457
128.063
126.735
119.150
107.115
75.192
28.922
26.109
22.124
21.751
21.270
[rel]
15
10
5
0
[ppm]
50
100
150

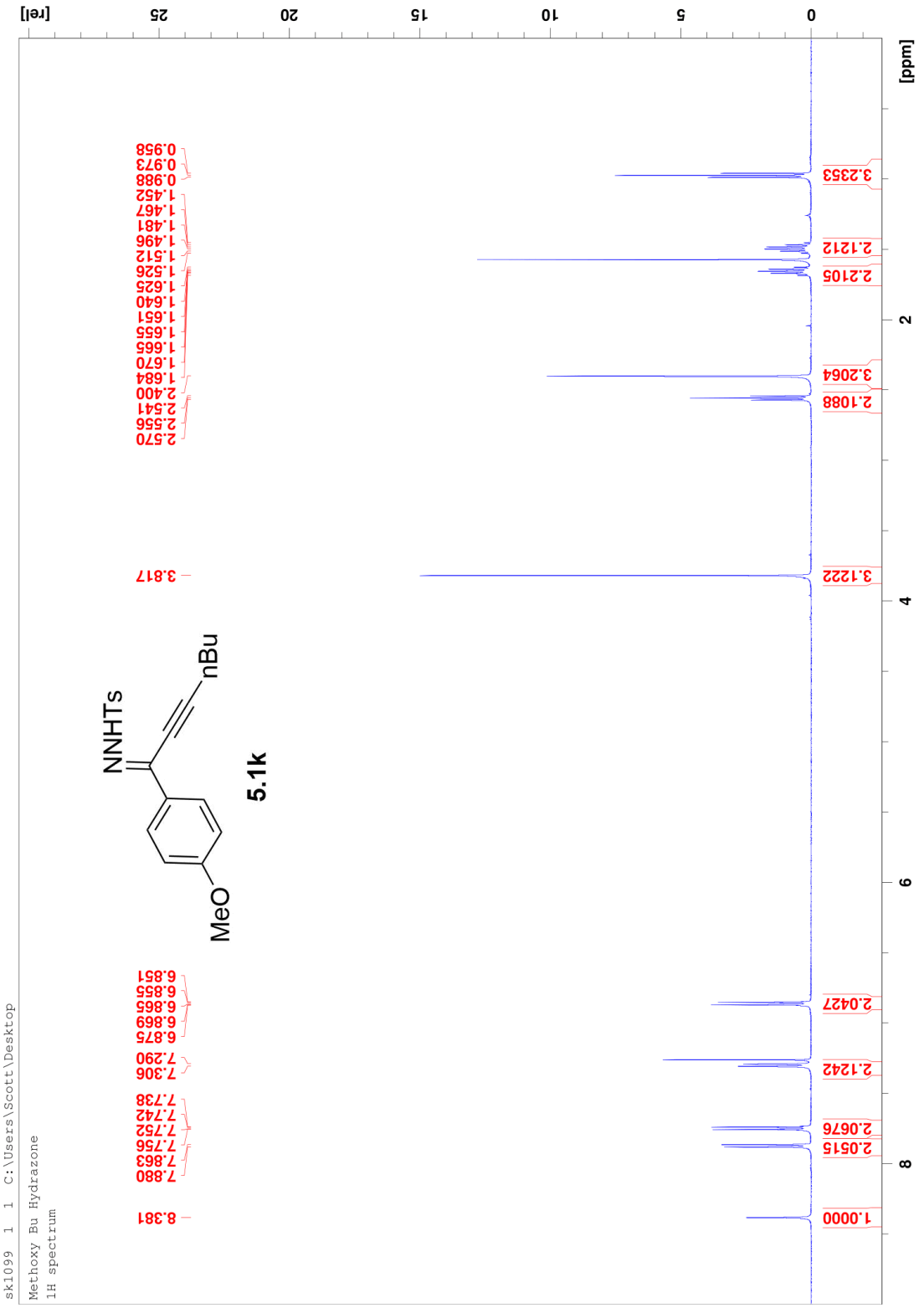
sk1099 1 1 C:\Users\Scott\Desktop
Methoxy Bu Hydrazone
1H spectrum
[rel]
25
20
15
10
5
0
[ppm]
2
4
6
8
0.958
0.973
0.988
1.452
1.467
1.481
1.496
1.512
1.526
1.625
1.640
1.651
1.655
1.665
1.670
1.684
2.400
2.541
2.556
2.570
3.817
6.851
6.855
6.865
6.869
6.875
7.290
7.306
7.738
7.742
7.752
7.756
7.863
7.880
8.381
1.0000
2.0515
2.0676
2.1242
2.0427
3.1222
2.1088
3.2064
2.2105
2.1212
3.2353
NNHTs
nBu
MeO
5.1k

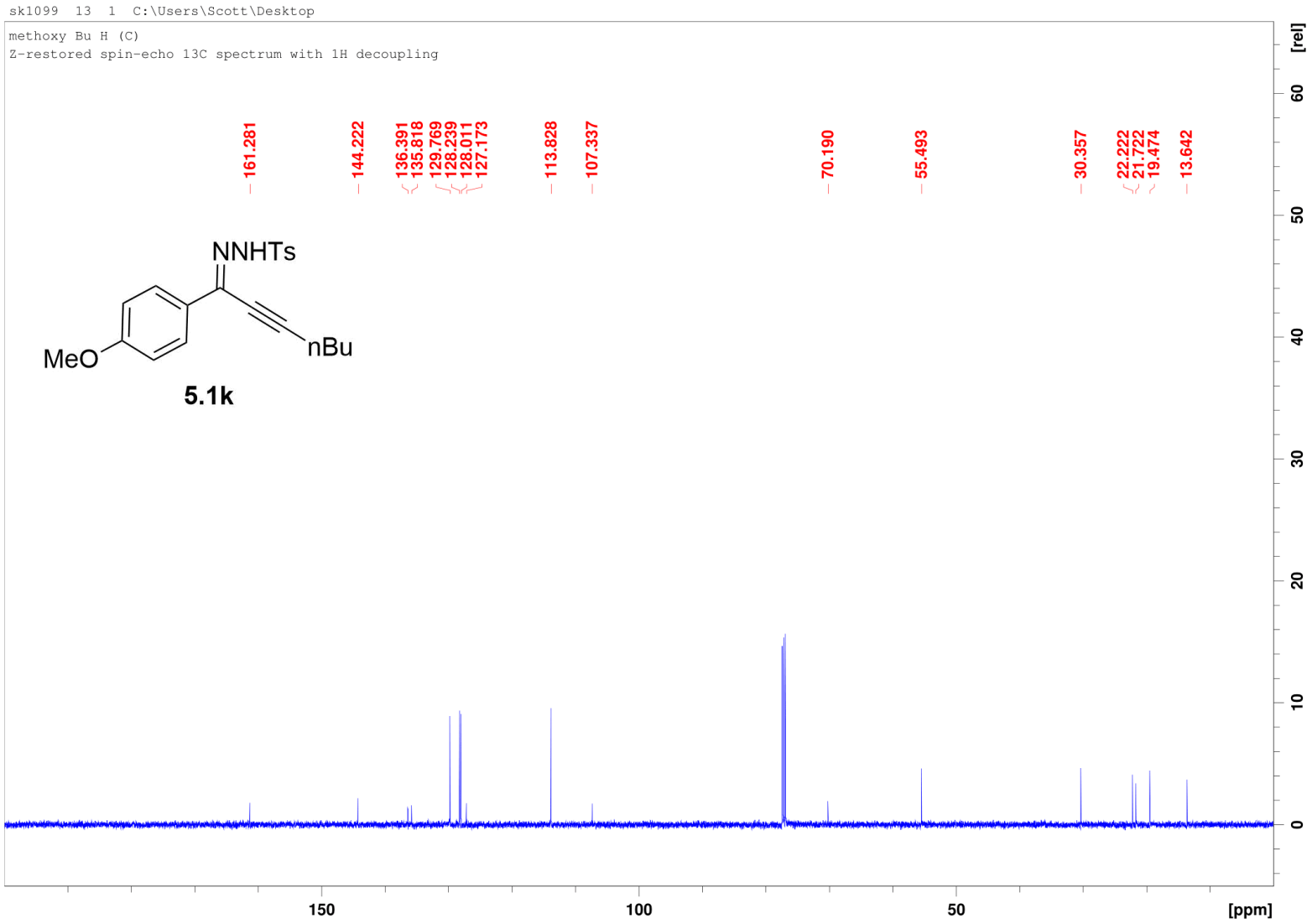
sk1099 13 1 C:\Users\Scott\Desktop
methoxy Bu H (C)
Z-restored spin-echo 13C spectrum with 1H decoupling
161.281
144.222
136.391
135.818
129.769
128.239
128.011
127.173
113.828
107.337
70.190
55.493
30.357
22.222
21.722
19.474
13.642
NNHTs
MeO
nBu
5.1k
[rel]
60
50
40
30
20
10
0
150
100
50
[ppm]

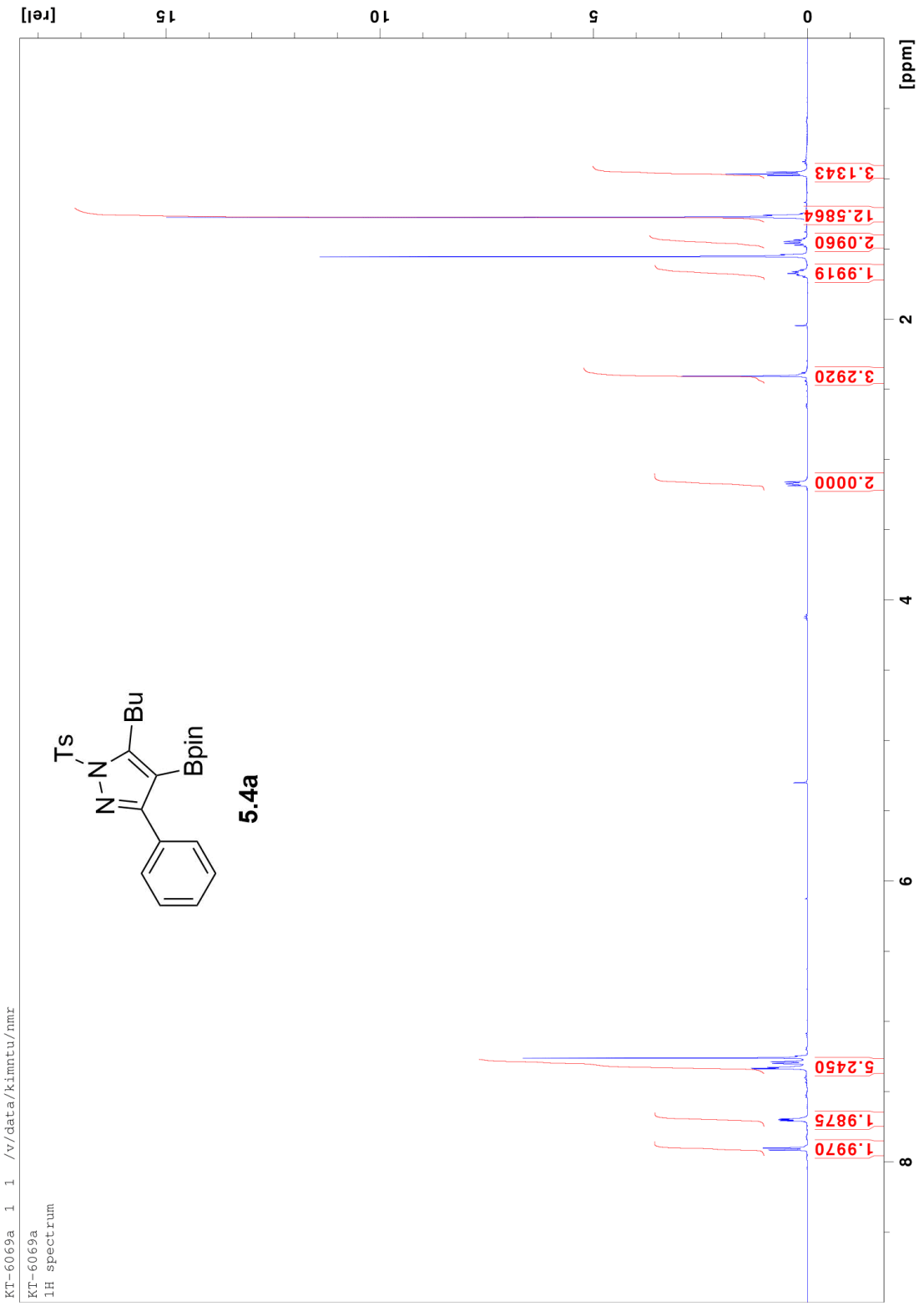
KT-6069a 1 1 /v/data/kimntu/nmr
KT-6069a
1H spectrum
[rel]
15
10
5
0
[ppm]
8
6
4
2
1.9970
1.9875
5.2450
2.0000
3.2920
1.9919
2.0960
12.5864
3.1343
Ts
N
N
Bu
Bpin
5.4a

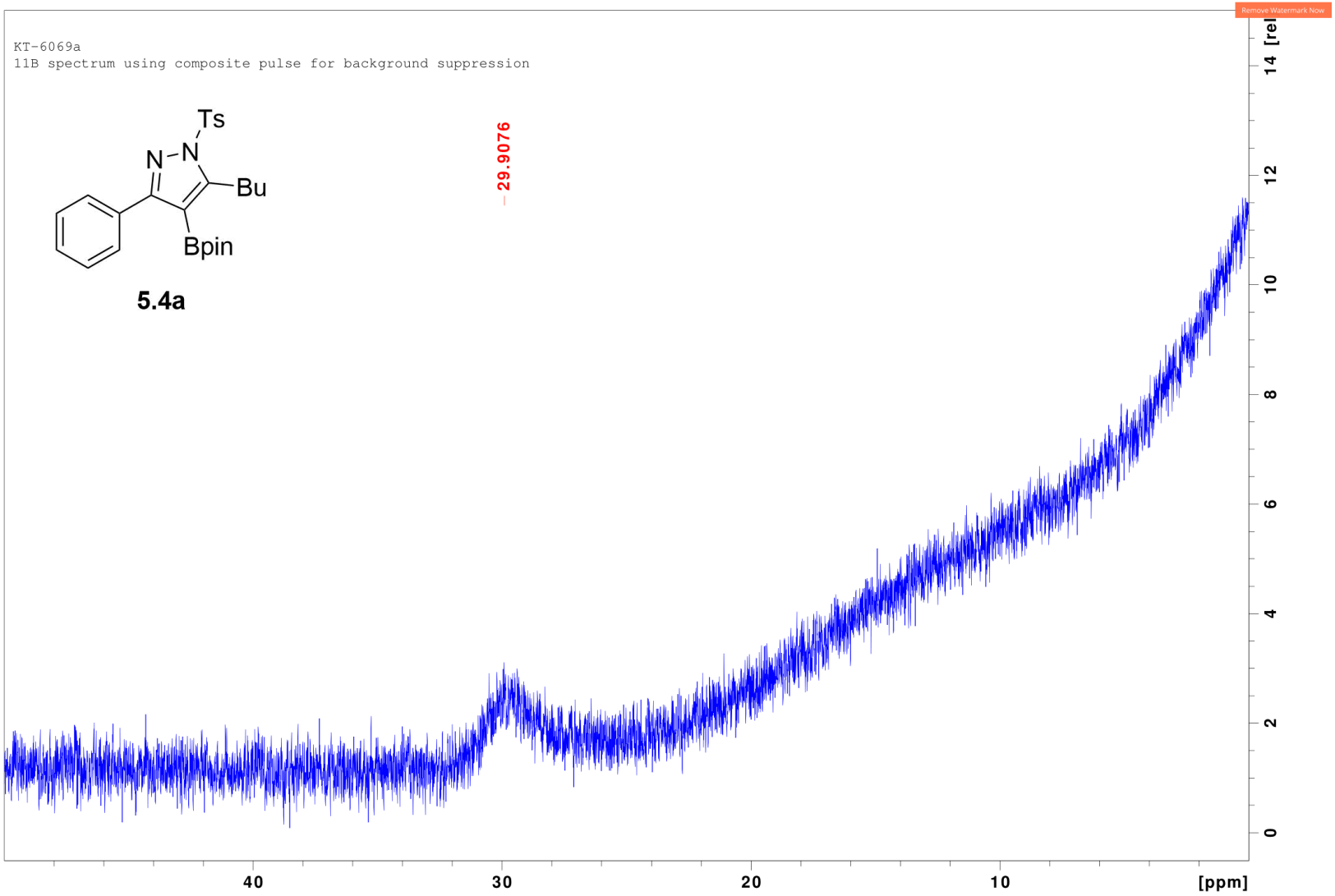
KT-6069a
11B spectrum using composite pulse for background suppression
Ts
N
N
Bu
Bpin
5.4a
29.9076
14
12
10
8
6
4
2
0
[rel
40
30
20
10
[ppm]

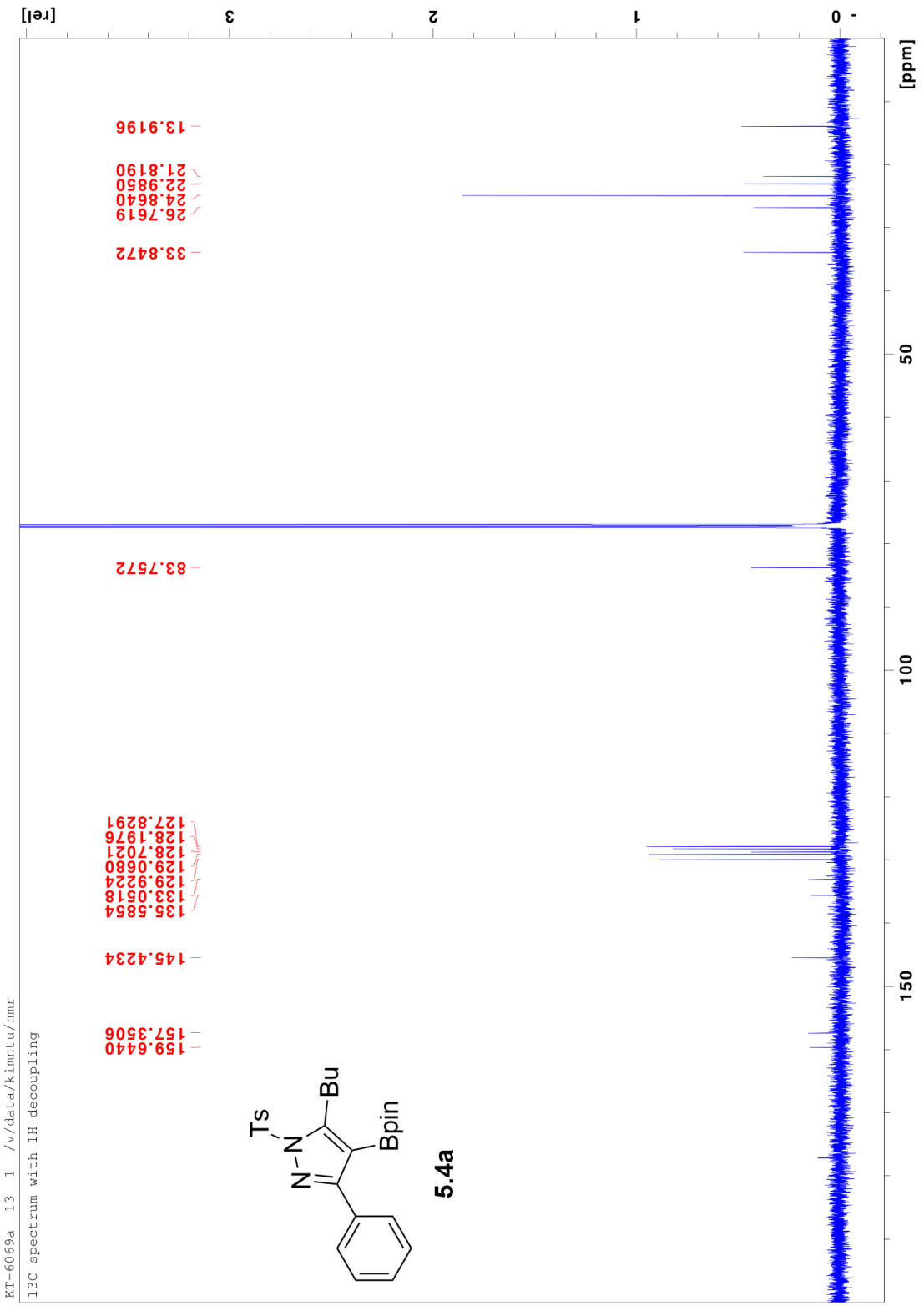
KT-6069a 13 1 /v/data/kimntu/nmr
13C spectrum with 1H decoupling
[rel]
3
2
1
0
[ppm]
150
100
50
159.6440
157.3506
145.4234
135.5854
133.0518
129.9224
129.0680
128.7021
128.1976
127.8291
83.7572
33.8472
26.7619
24.8640
22.9850
21.8190
13.9196
Ts
N
N
Bu
Bpin
5.4a

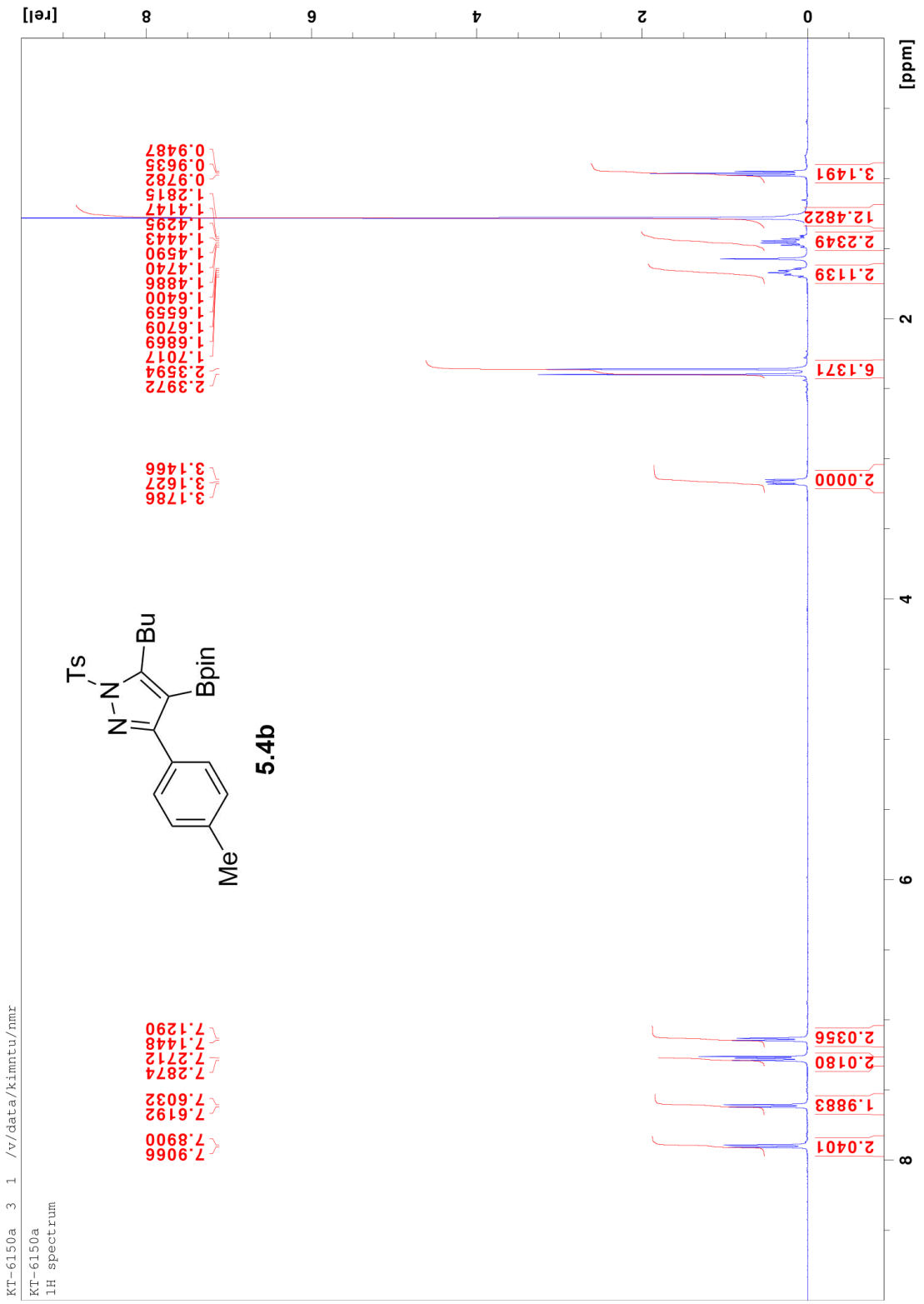
KT-6150a 3 1 /v/data/kimntu/nmr
KT-6150a
1H spectrum
[rel]
[ppm]
Ts
N
N
Bu
Bpin
Me
5.4b
7.9066
7.8900
7.6192
7.6032
7.2874
7.2712
7.1448
7.1290
3.1786
3.1627
3.1466
2.3972
2.3594
1.7017
1.6869
1.6709
1.6559
1.6400
1.4886
1.4740
1.4590
1.4443
1.4295
1.4147
1.2815
0.9782
0.9635
0.9487
2.0401
1.9883
2.0180
2.0356
2.0000
6.1371
2.1139
2.2349
12.4822
3.1491

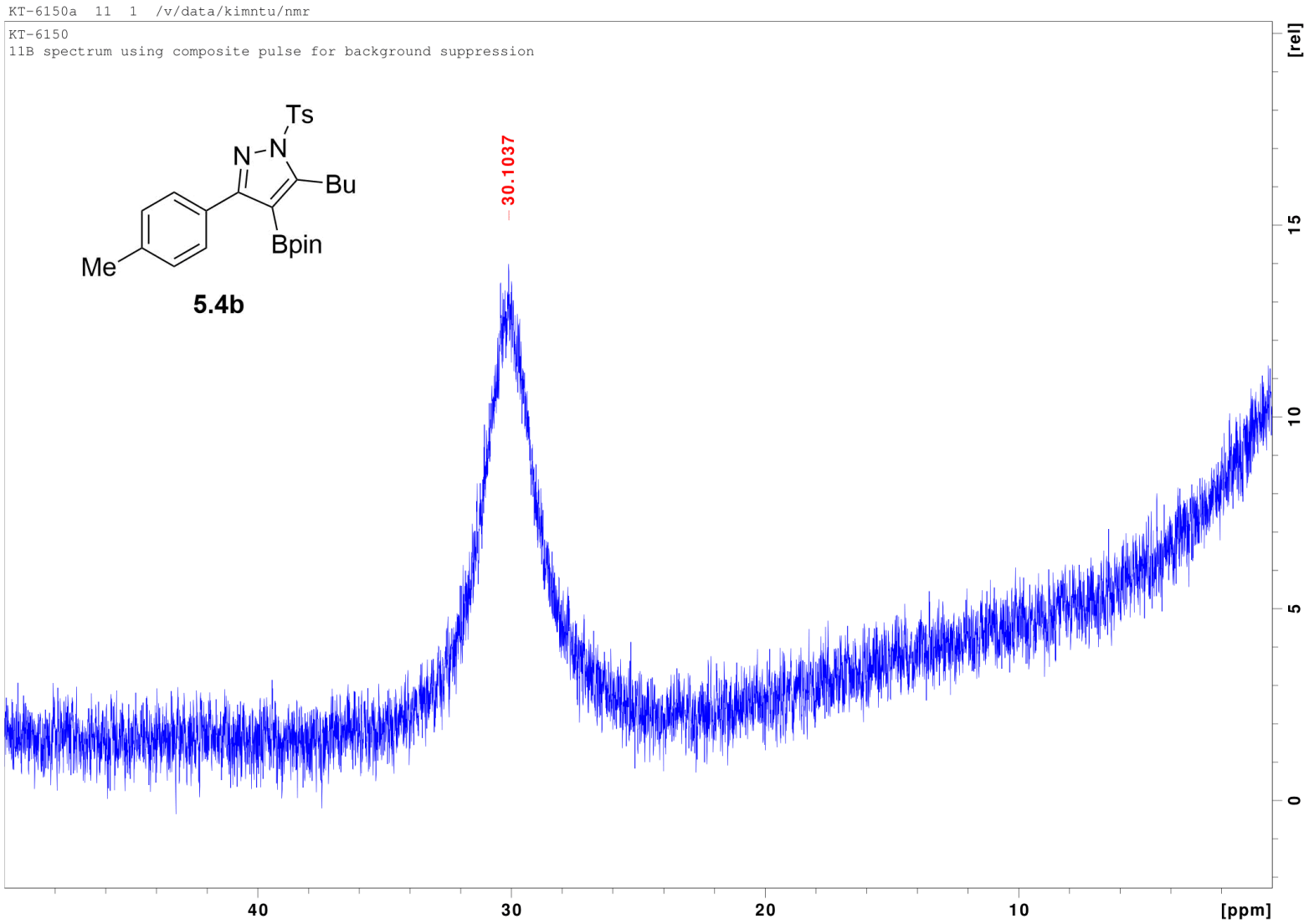
KT-6150a 11 1 /v/data/kimntu/nmr
KT-6150
11B spectrum using composite pulse for background suppression
Ts
N
N
Bu
Bpin
Me
5.4b
30.1037
[rel]
0
5
10
15
40
30
20
10
[ppm]

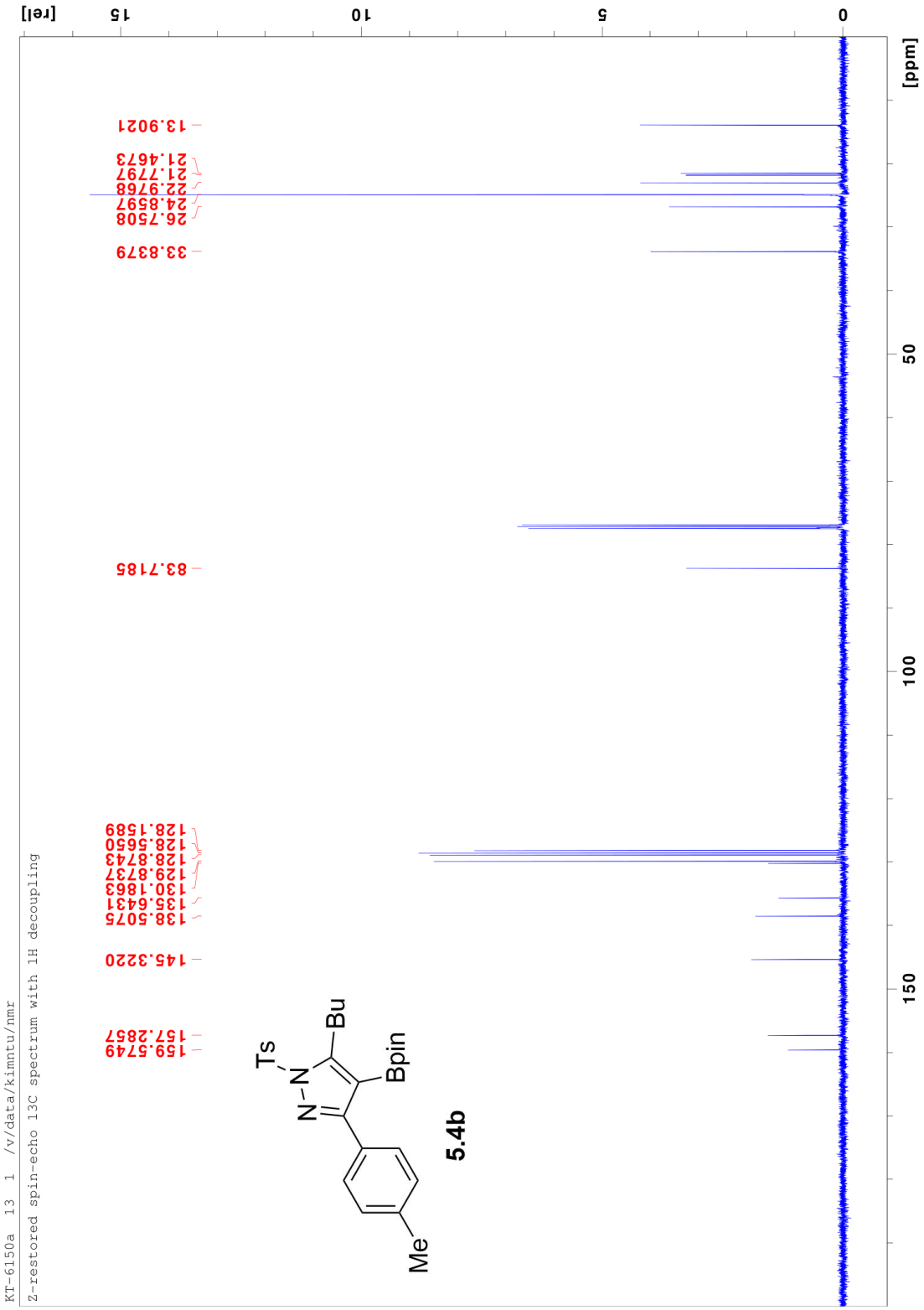
KT-6150a 13 1 /v/data/kimntu/nmr
Z-restored spin-echo 13C spectrum with 1H decoupling
[rel]
15
10
5
0
[ppm]
50
100
150
13.9021
21.4673
21.7797
22.9768
24.8597
26.7508
33.8379
83.7185
128.1589
128.5650
128.8743
129.8737
130.1863
135.6431
138.5075
145.3220
157.2857
159.5749
Ts
N
N
Bu
Bpin
Me
5.4b

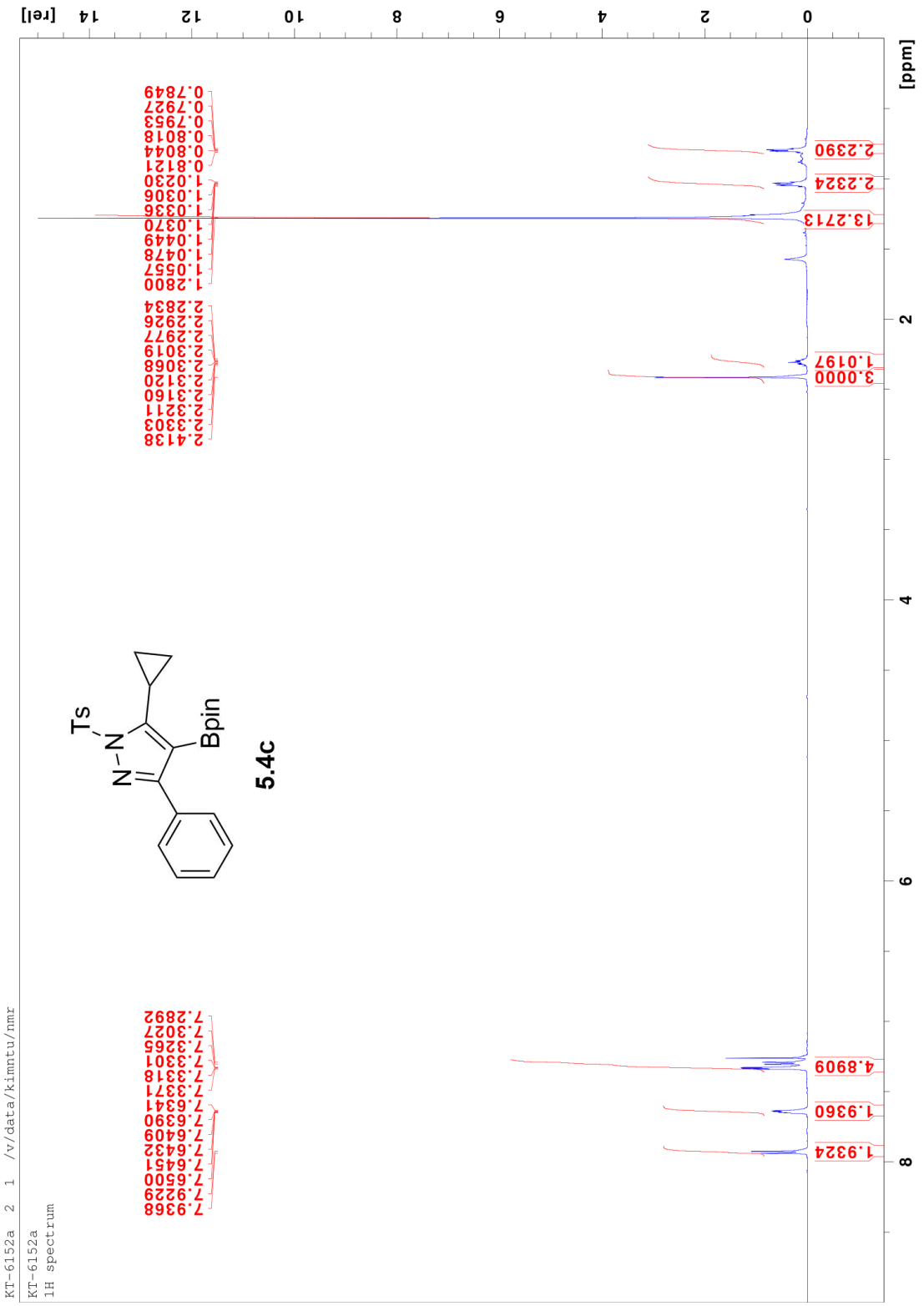
KT-6152a 2 1 /v/data/kimntu/nmr
KT-6152a
1H spectrum
[rel]
[ppm]
Ts
N
N
Bpin
5.4c

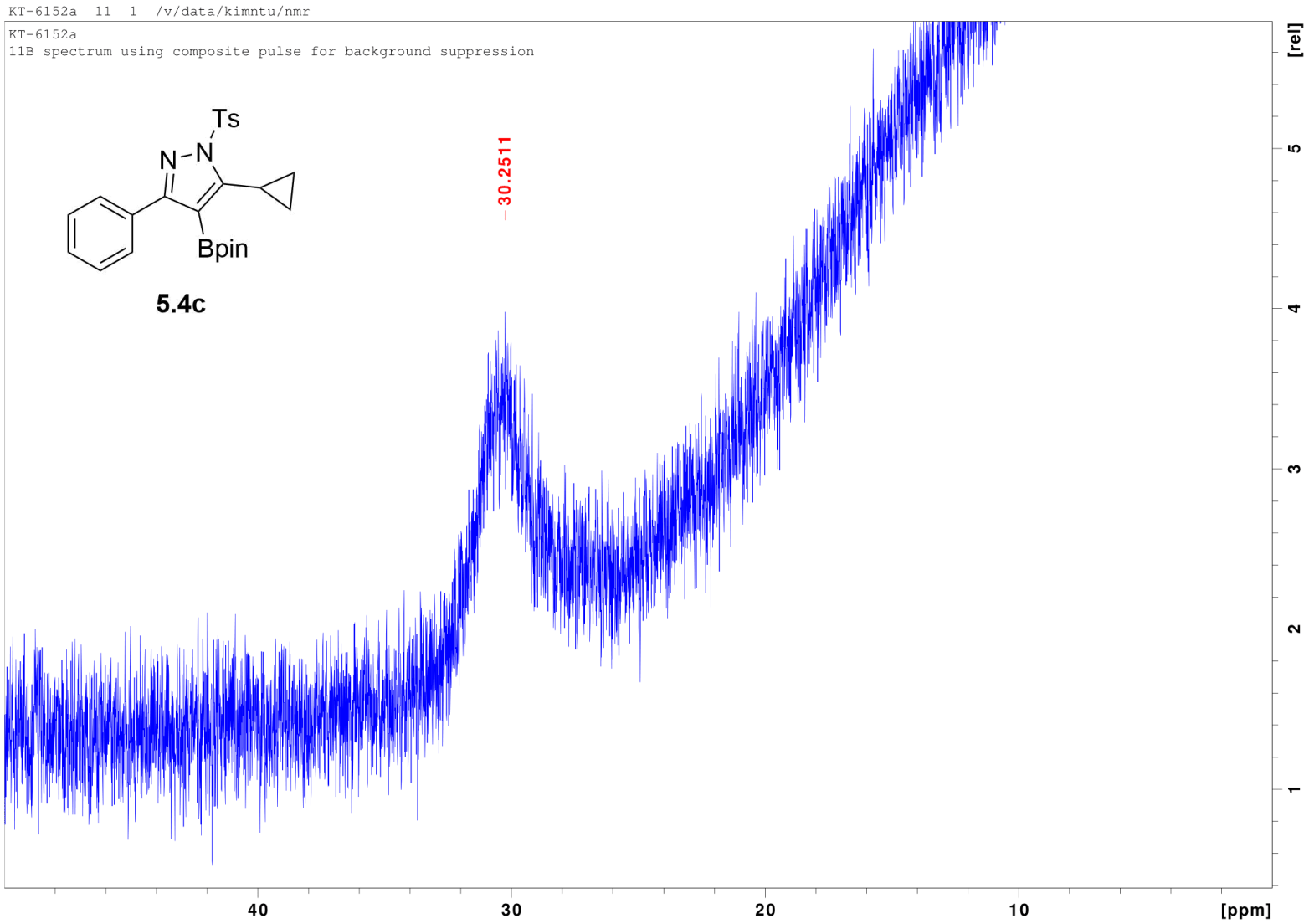
KT-6152a 11 1 /v/data/kimntu/nmr
KT-6152a
11B spectrum using composite pulse for background suppression
Ts
N
N
Bpin
5.4c
30.2511
[rel]
5
4
3
2
1
40
30
20
10
[ppm]

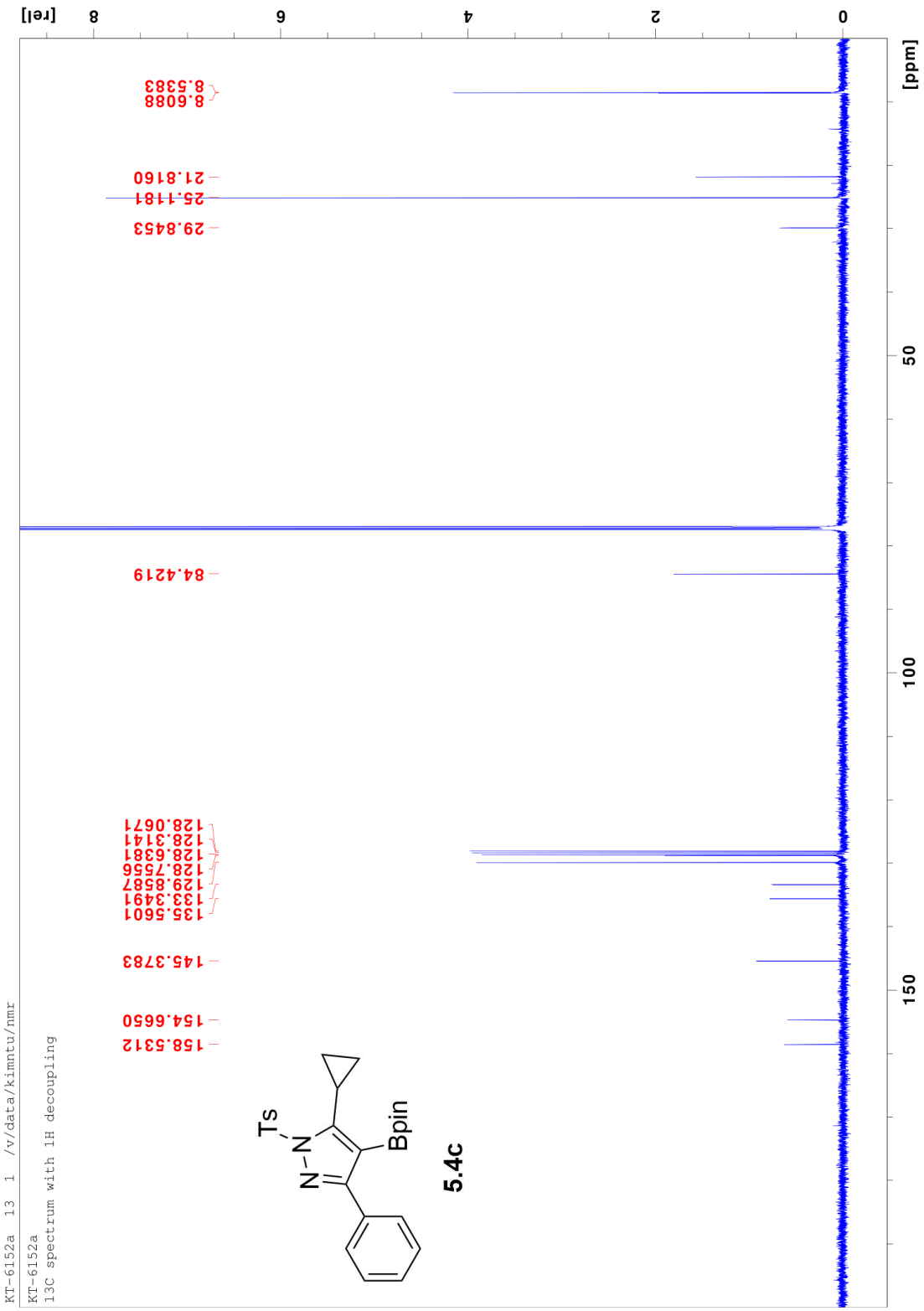
KT-6152a 13 1 /v/data/kimntu/nmr
KT-6152a
13C spectrum with 1H decoupling
158.5312
154.6650
145.3783
135.5601
133.3491
129.8587
128.7556
128.6381
128.3141
128.0671
84.4219
29.8453
25.1181
21.8160
8.6088
8.5383
Ts
N
N
Bpin
5.4c
[rel]
8
6
4
2
0
[ppm]
50
100
150

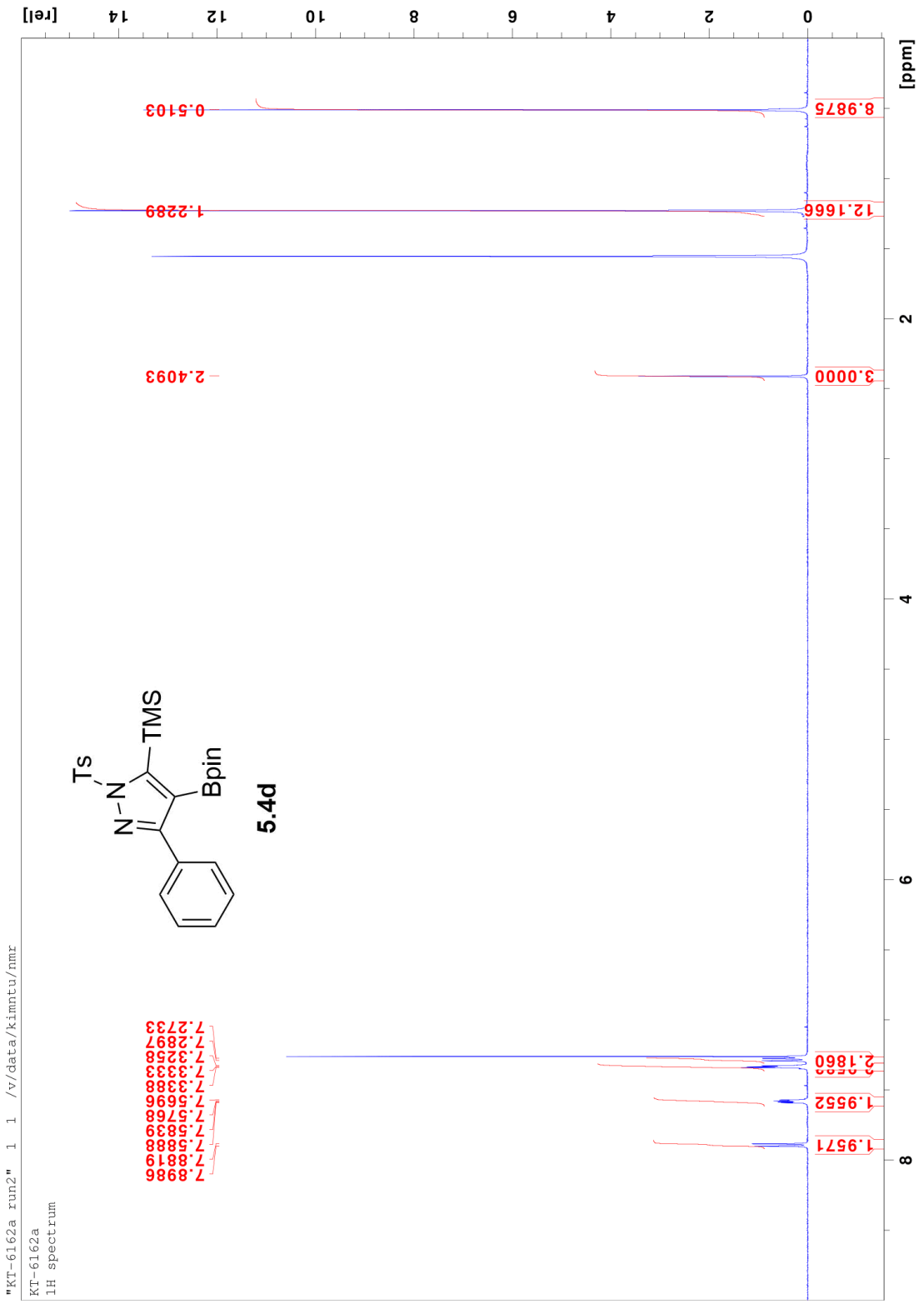
"KT-6162a run2" 1 1 /v/data/kimntu/nmr
KT-6162a
1H spectrum
[rel]
[ppm]
0
2
4
6
8
10
12
14
8.9875
12.1666
3.0000
2.1860
1.9571
1.9552
0.5103
1.2289
2.4093
7.8986
7.8819
7.5888
7.5839
7.5768
7.5696
7.3388
7.3333
7.3258
7.2897
7.2733
TMS
Ts
N
N
Bpin
5.4d

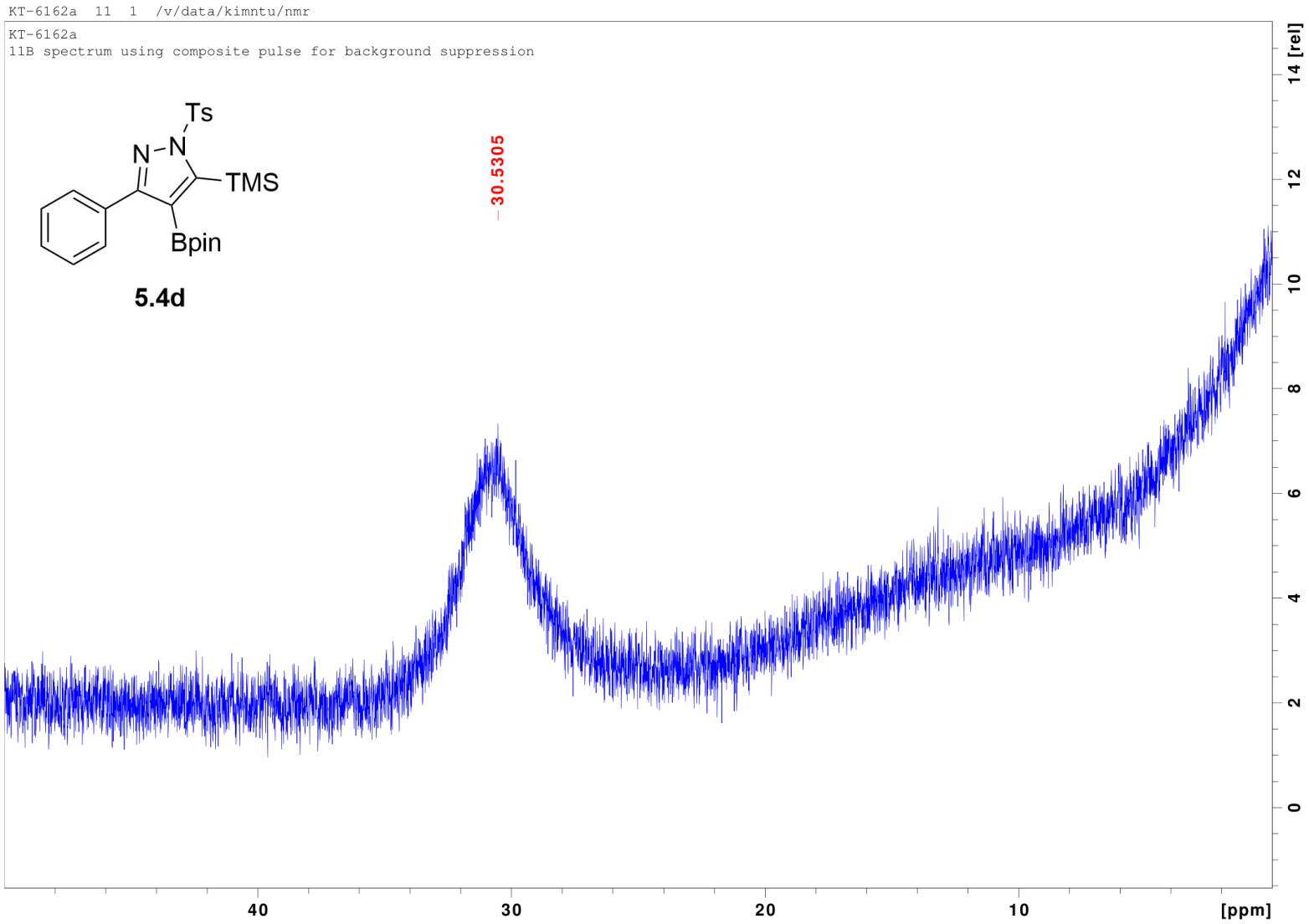
KT-6162a 11 1 /v/data/kimntu/nmr
KT-6162a
11B spectrum using composite pulse for background suppression
Ts
N
N
TMS
Bpin
5.4d
30.5305
14 [rel]
12
10
8
6
4
2
0
40
30
20
10
[ppm]

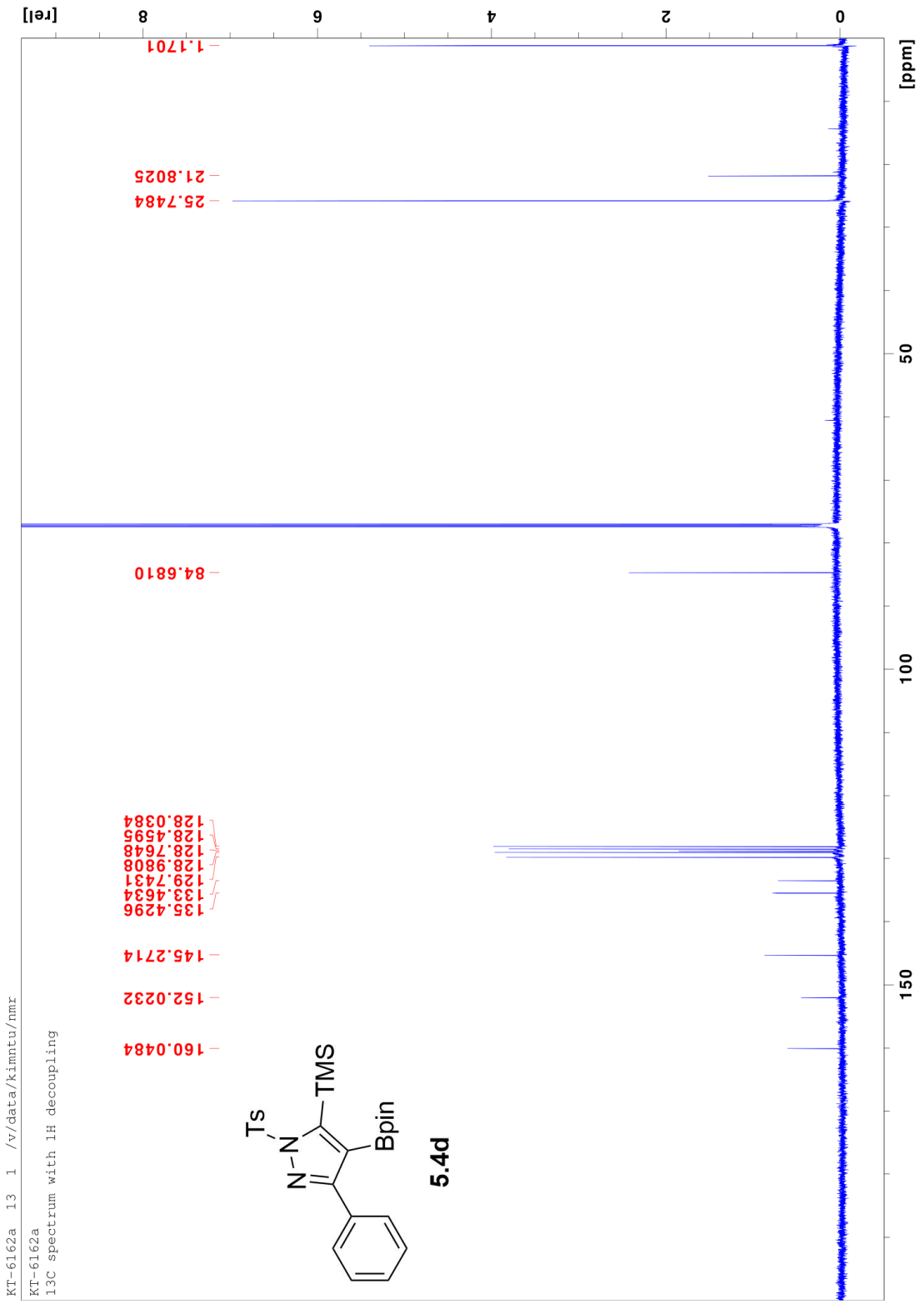
KT-6162a 13 1 /v/data/kimntu/nmr
KT-6162a
13C spectrum with 1H decoupling
160.0484
152.0232
145.2714
135.4296
133.4634
129.7431
128.9808
128.7648
128.4595
128.0384
84.6810
25.7484
21.8025
1.1701
TMS
Ts
N
N
Bpin
5.4d
[rel]
8
6
4
2
0
[ppm]
150
100
50

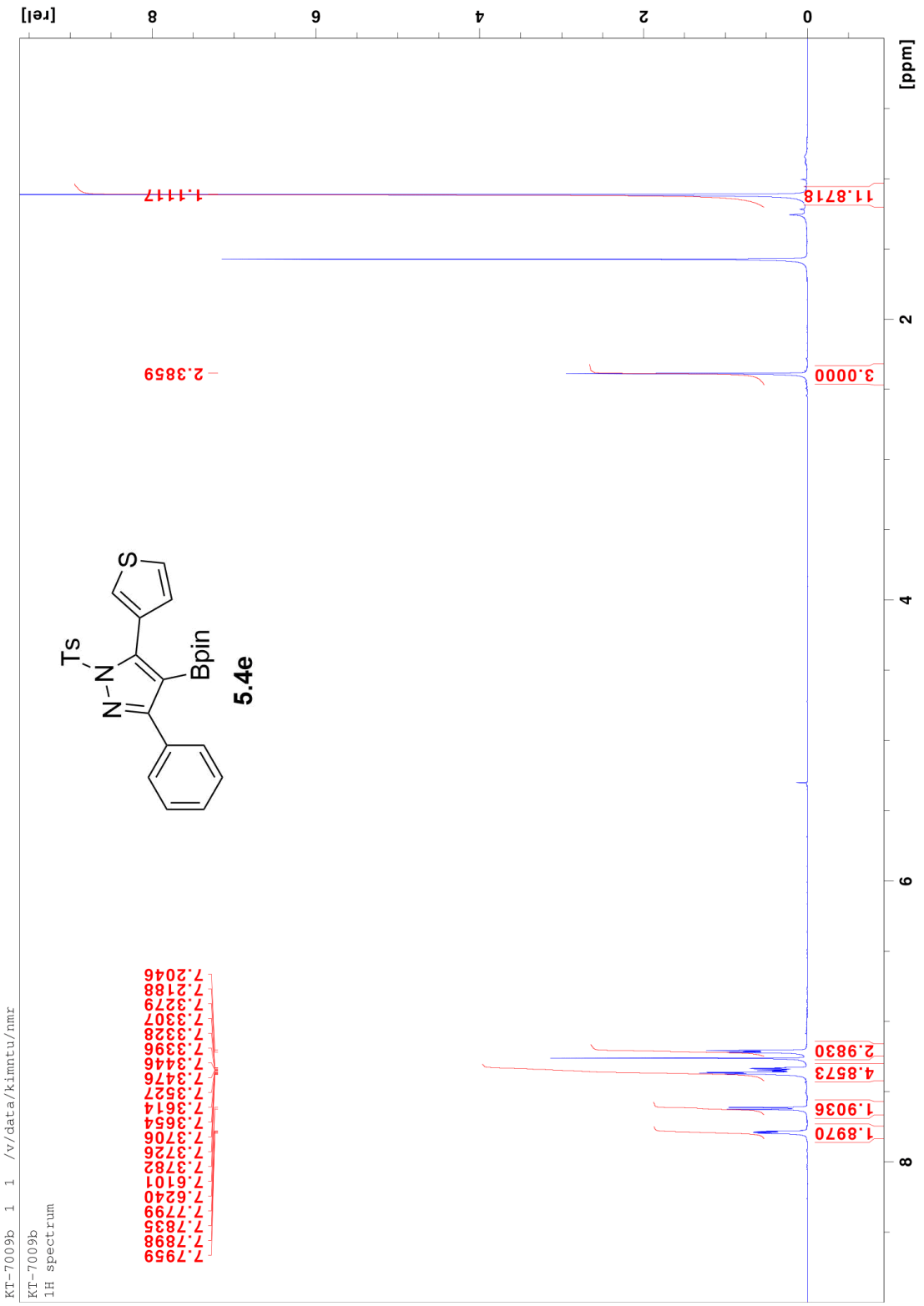
KT-7009b 1 1 /v/data/kimntu/nmr
KT-7009b
1H spectrum
[rel]
[ppm]
11.8718
3.0000
2.9830
4.8573
1.9036
1.8970
1.1117
2.3859
7.2046
7.2188
7.3279
7.3307
7.3328
7.3396
7.3446
7.3476
7.3527
7.3614
7.3654
7.3706
7.3726
7.3782
7.6101
7.6240
7.7799
7.7835
7.7898
7.7959
Ts
Bpin
5.4e

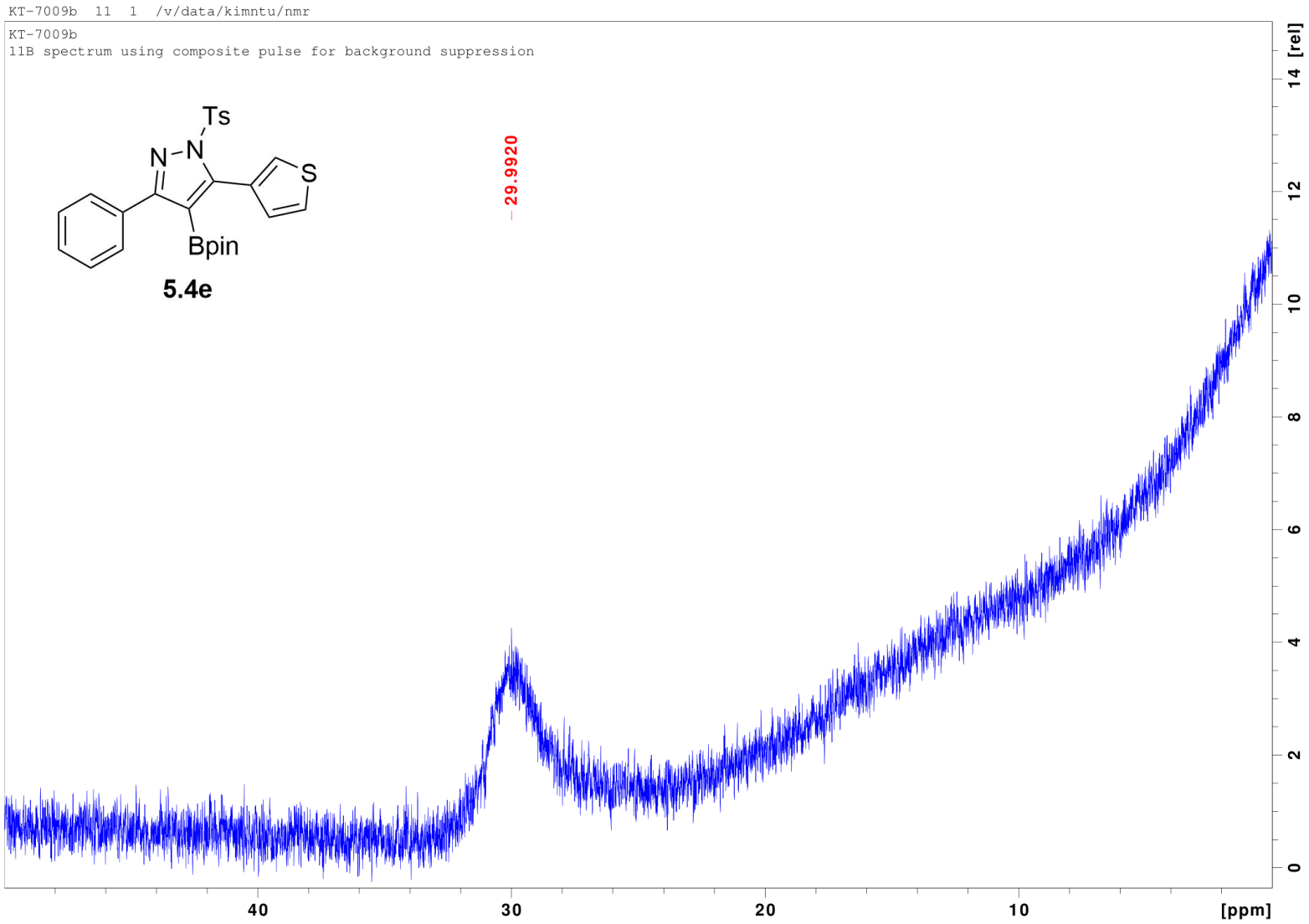
KT-7009b 11 1 /v/data/kimntu/nmr
KT-7009b
11B spectrum using composite pulse for background suppression
Ts
N
N
S
Bpin
5.4e
29.9920
14 [rel]
12
10
8
6
4
2
0
40
30
20
10
[ppm]

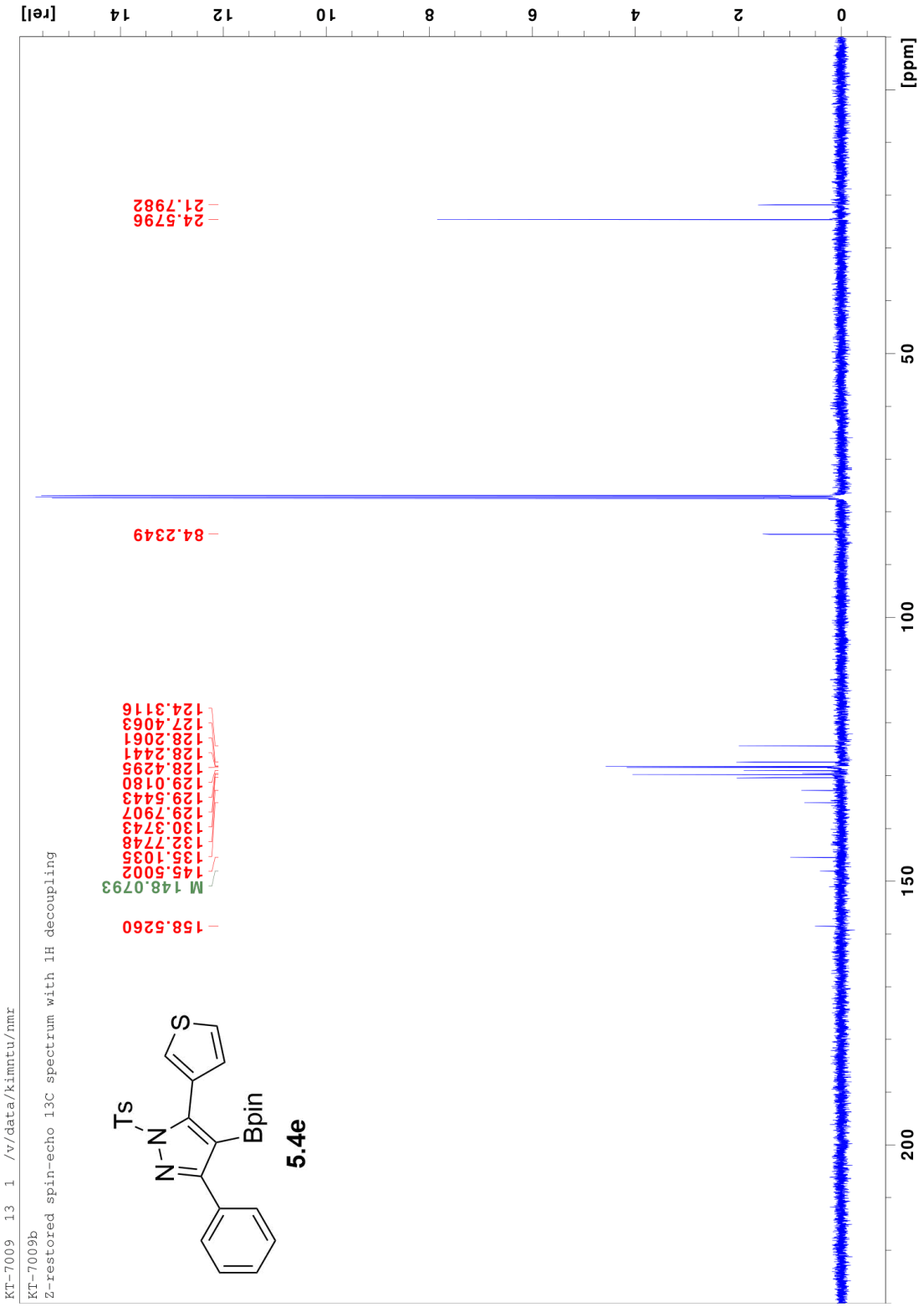
KT-7009 13 1 /v/data/kimntu/nmr
KT-7009b
Z-restored spin-echo 13C spectrum with 1H decoupling
158.5260
M 148.0793
145.5002
135.1035
132.7748
130.3743
129.7907
129.5443
129.0180
128.4295
128.2441
128.2061
127.4063
124.3116
84.2349
24.5796
21.7982
Ts
Bpin
5.4e
[rel]
[ppm]

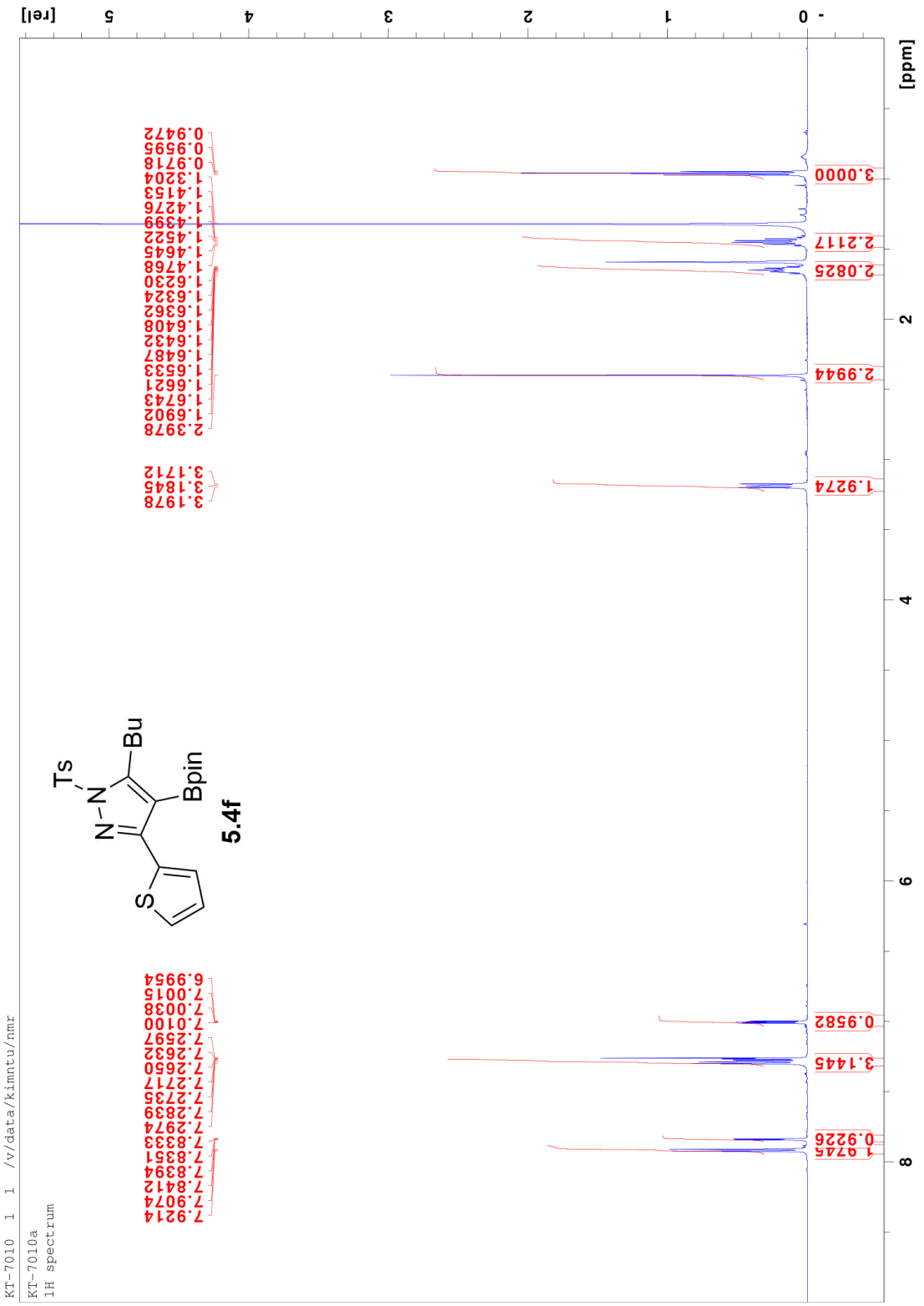
KT-7010 1 1 /v/data/kimntu/nmr
KT-7010a
1H spectrum
[rel]
[ppm]
Ts
N
N
Bu
Bpin
S
5.4f
7.9214
7.9074
7.8412
7.8394
7.8351
7.8333
7.2974
7.2839
7.2735
7.2717
7.2650
7.2632
7.2597
7.0100
7.0038
7.0015
6.9954
3.1978
3.1845
3.1712
2.3978
1.6902
1.6743
1.6621
1.6533
1.6487
1.6432
1.6408
1.6362
1.6324
1.6230
1.4768
1.4645
1.4522
1.4399
1.4276
1.4153
1.3204
0.9718
0.9595
0.9472
1.0745
0.9226
3.1445
0.9582
1.9274
2.9944
2.0825
2.2117
3.0000

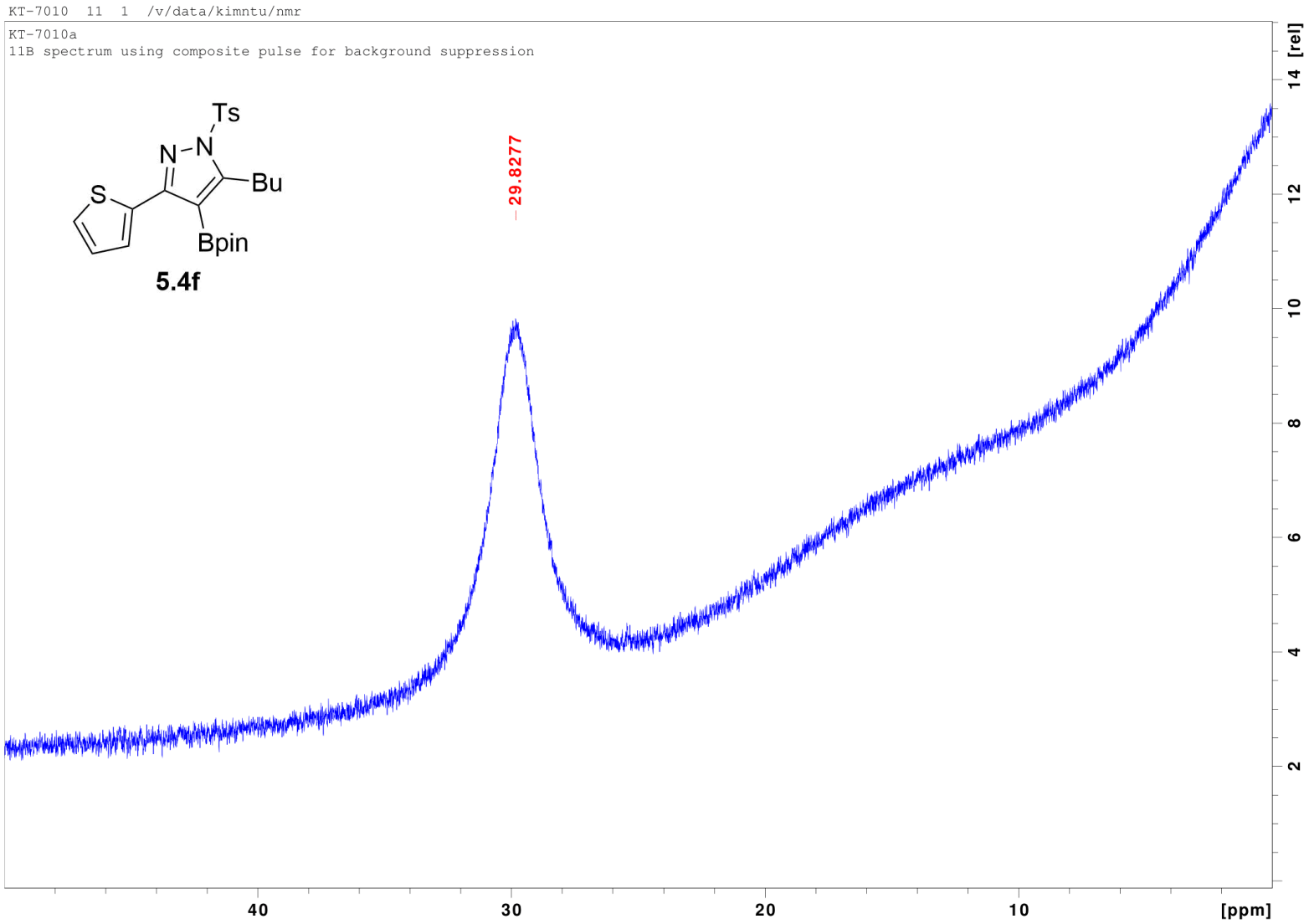
KT-7010 11 1 /v/data/kimntu/nmr
KT-7010a
11B spectrum using composite pulse for background suppression
Ts
N
N
S
Bu
Bpin
5.4f
29.8277
14 [rel]
12
10
8
6
4
2
40
30
20
10
[ppm]

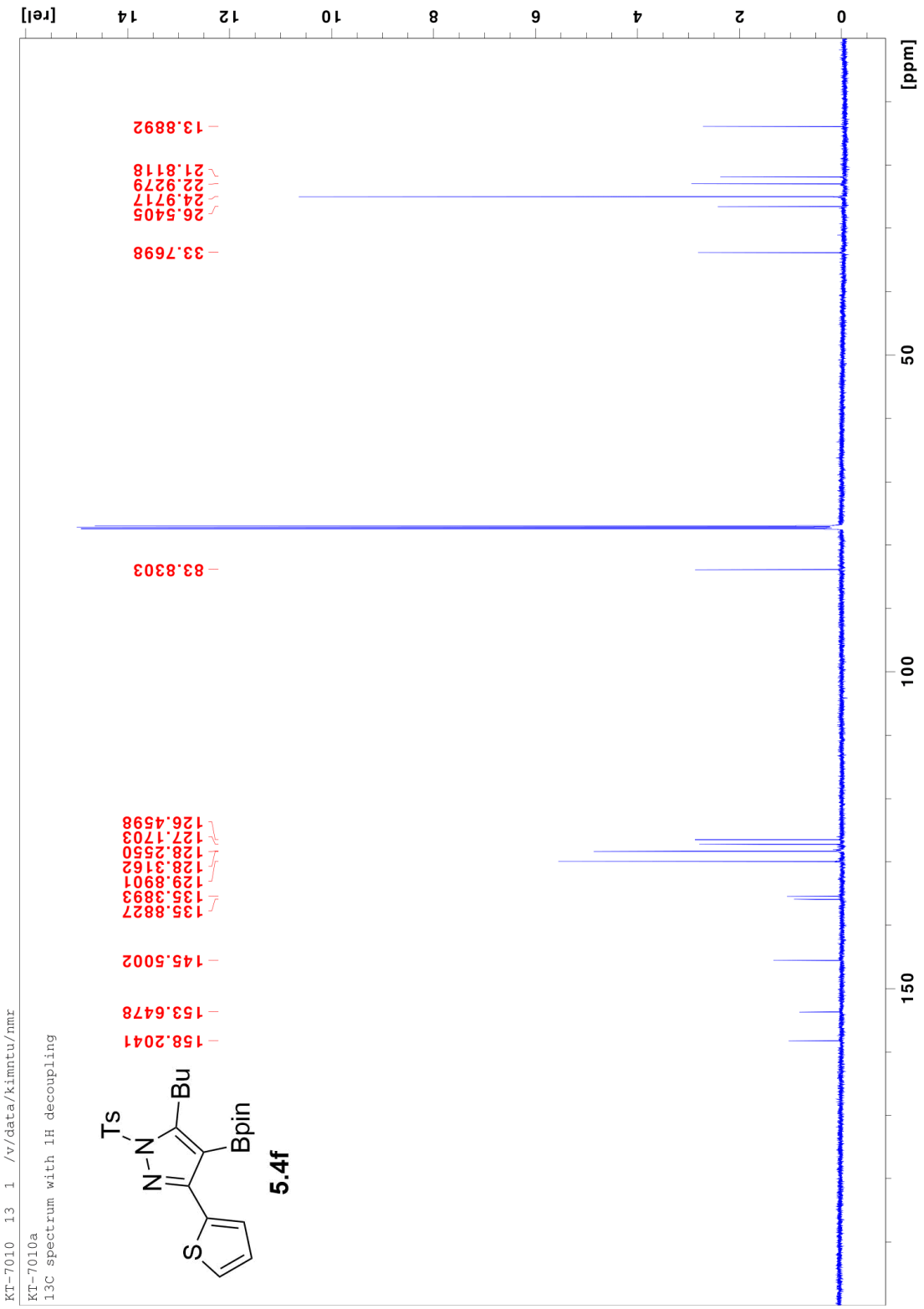
KT-7010 13 1 /v/data/kimntu/nmr
KT-7010a
13C spectrum with 1H decoupling
158.2041
153.6478
145.5002
135.8827
135.3893
129.8901
128.3162
128.2550
127.1703
126.4598
83.8303
33.7698
26.5405
24.9717
22.9279
21.8118
13.8892
Ts
N
N
Bu
Bpin
S
5.4f
[rel]
14
12
10
8
6
4
2
0
[ppm]
150
100
50

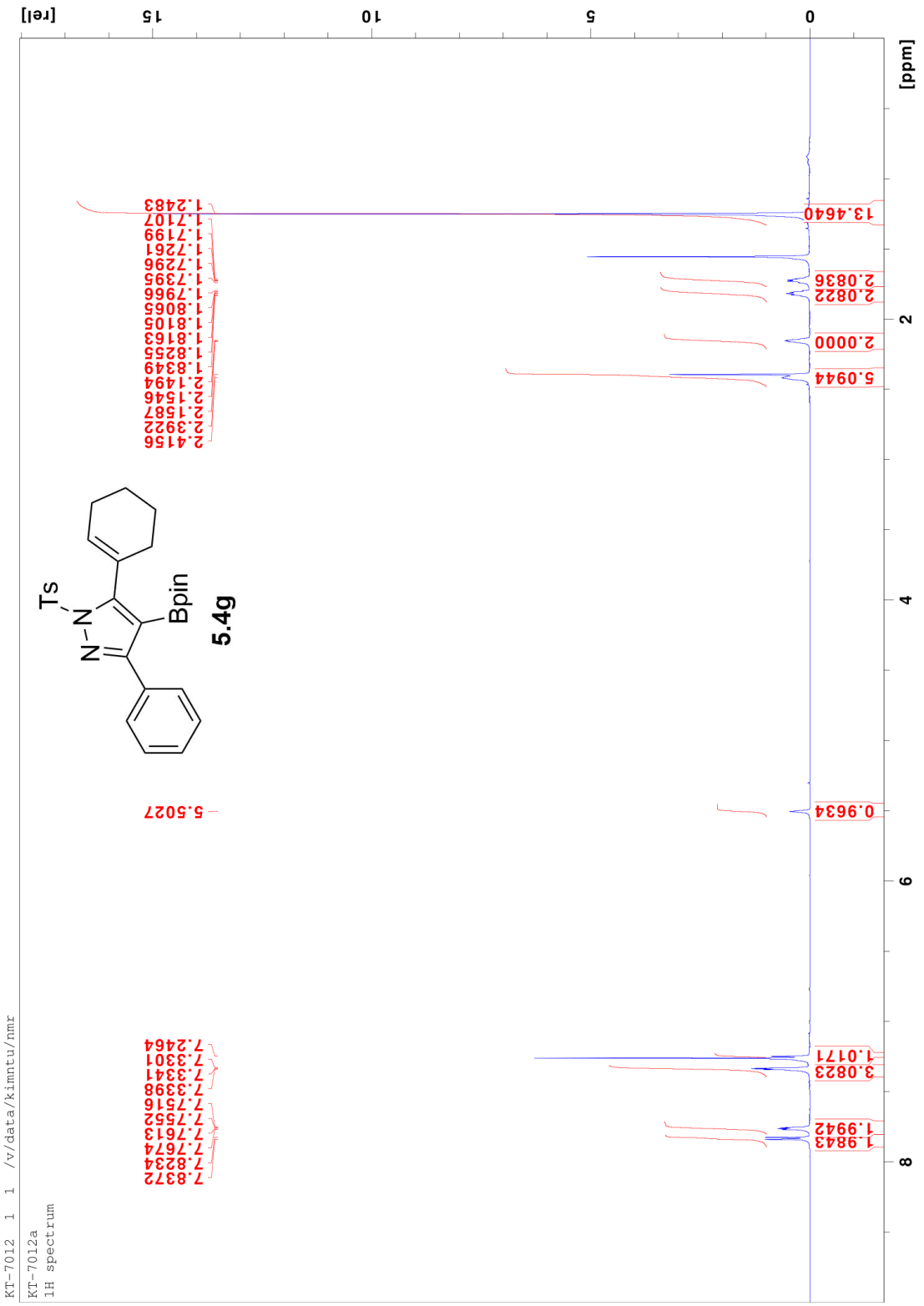
KT-7012 1 1 /v/data/kimntu/nmr
KT-7012a
1H spectrum
[rel]
15
10
5
0
[ppm]
2
4
6
8
13.4640
2.0836
2.0822
2.0000
5.0944
0.9634
1.0171
3.0823
1.9843
1.9942
2.4156
2.3922
2.1587
2.1546
2.1494
1.8349
1.8255
1.8163
1.8105
1.8065
1.7966
1.7395
1.7296
1.7261
1.7199
1.7107
1.2483
5.5027
7.8372
7.8234
7.7674
7.7613
7.7552
7.7516
7.3398
7.3341
7.3301
7.2464
Ts
N
N
Bpin
5.4g

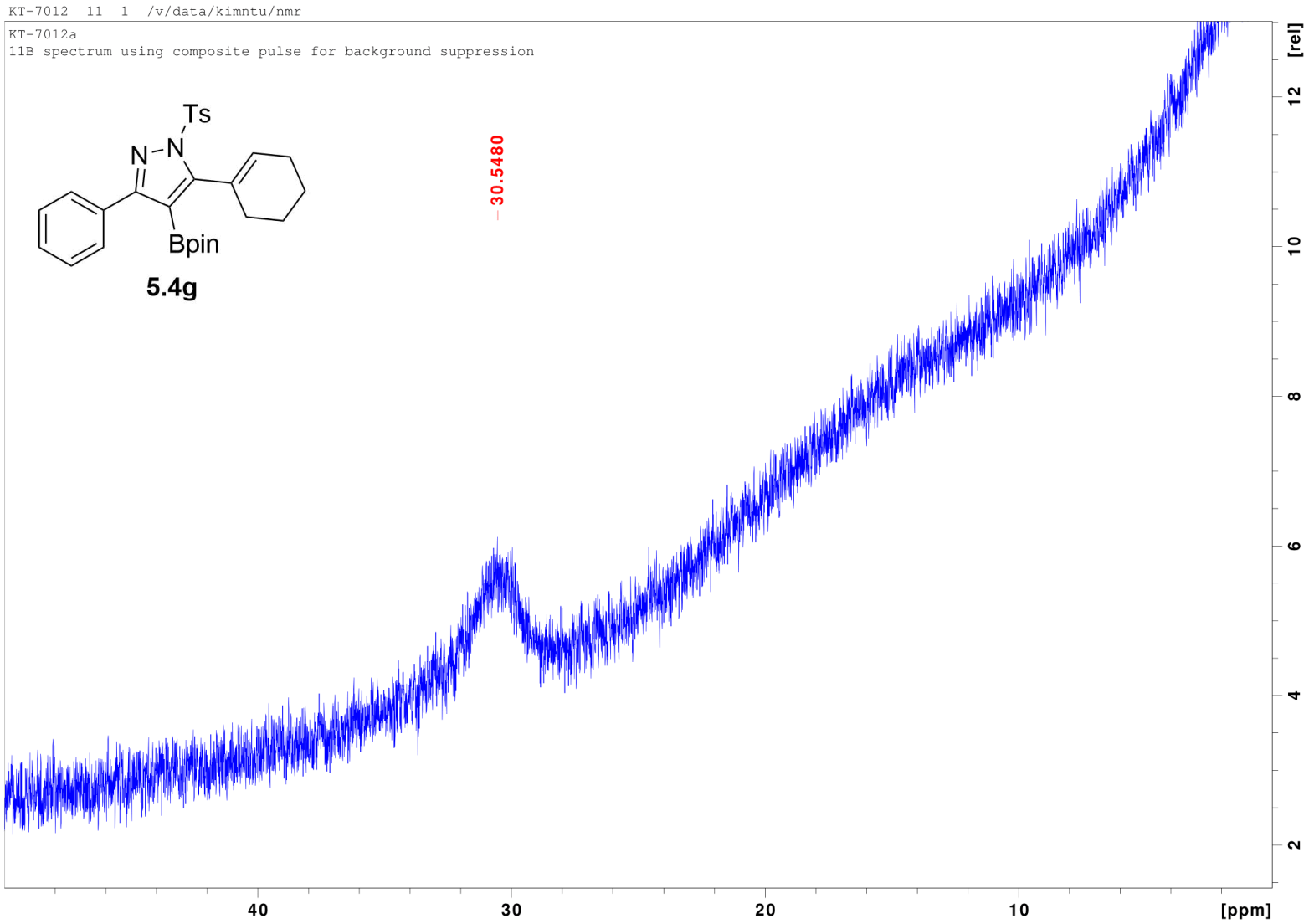
KT-7012 11 1 /v/data/kimntu/nmr
KT-7012a
11B spectrum using composite pulse for background suppression
Ts
N
N
Bpin
5.4g
30.5480
[rel]
12
10
8
6
4
2
40
30
20
10
[ppm]

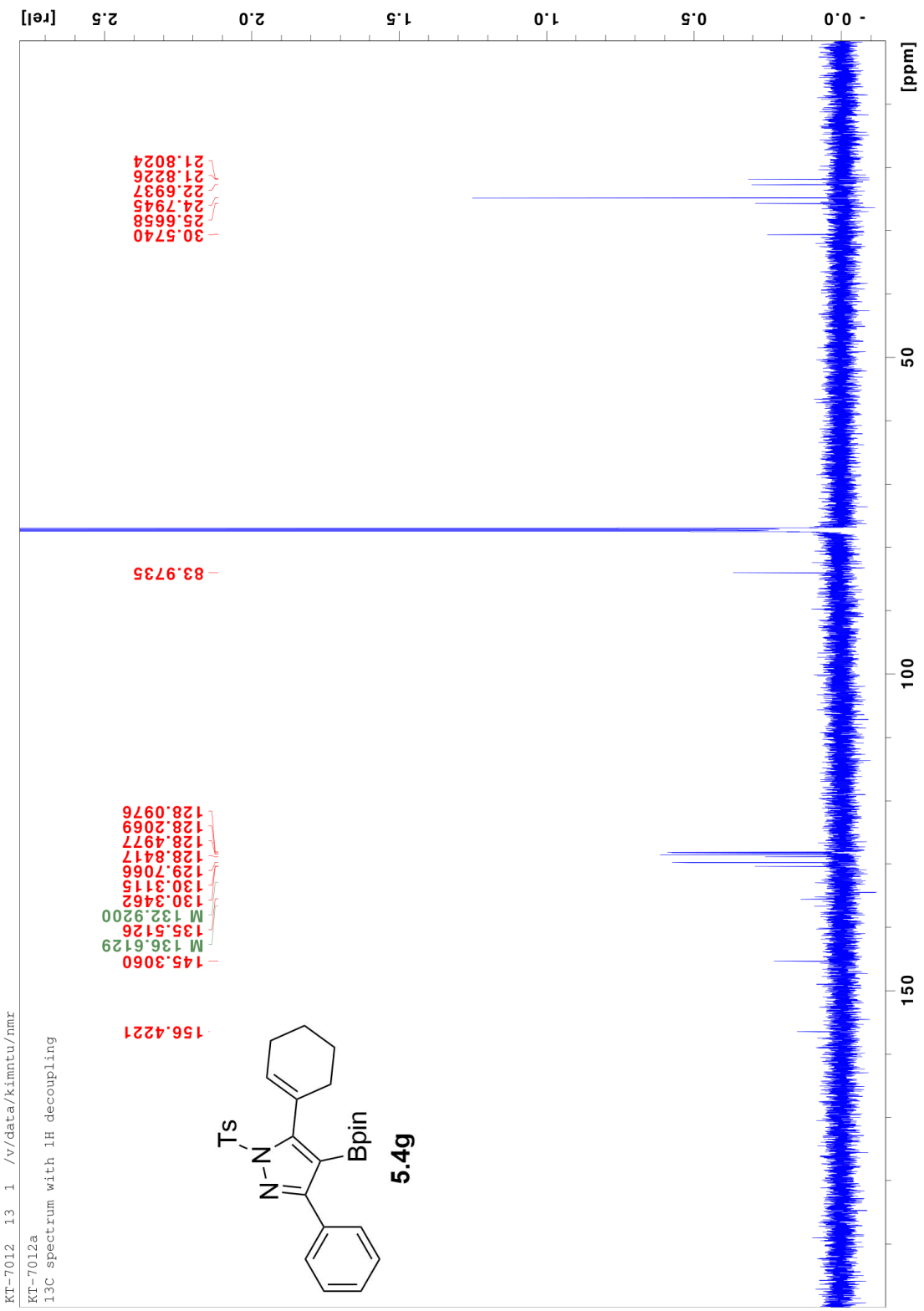
KT-7012 13 1 /v/data/kimntu/nmr
KT-7012a
13C spectrum with 1H decoupling
156.4221
145.3060
M 136.6129
135.5126
M 132.9200
130.3462
130.3115
129.7066
128.8417
128.4977
128.2069
128.0976
83.9735
30.5740
25.6658
24.7945
22.6937
21.8226
21.8024
Ts
N
N
Bpin
5.4g
[rel]
2.5
2.0
1.5
1.0
0.5
0.0
[ppm]
150
100
50

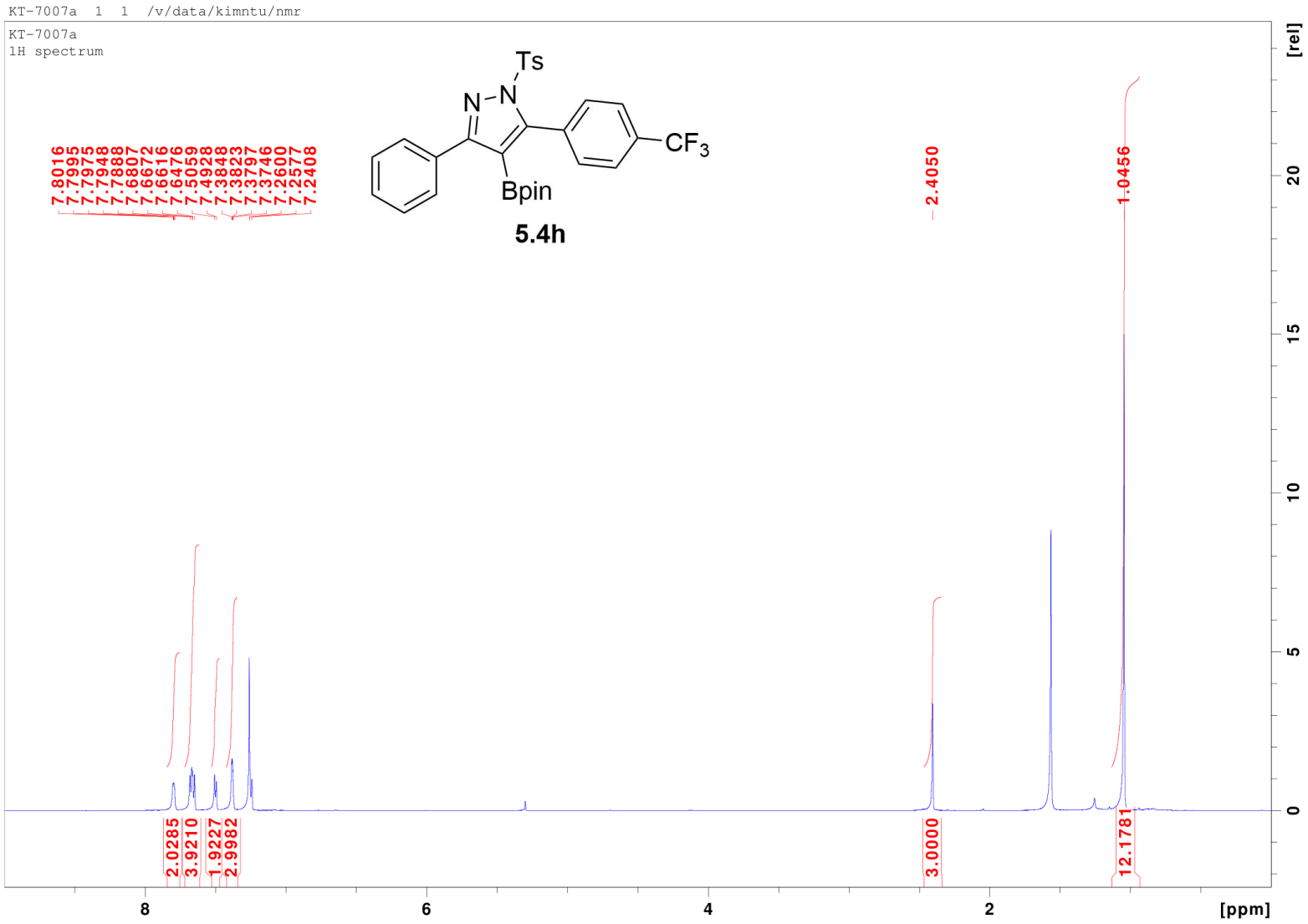
KT-7007a 1 1 /v/data/kimntu/nmr
KT-7007a
1H spectrum
7.8016
7.7995
7.7975
7.7948
7.7888
7.6807
7.6672
7.6616
7.6476
7.5059
7.4928
7.3848
7.3823
7.3797
7.3746
7.2600
7.2577
7.2408
Ts
N
N
CF3
Bpin
5.4h
2.4050
1.0456
2.0285
3.9210
1.9227
2.9982
3.0000
12.1781
8
6
4
2
[ppm]
0
5
10
15
20
[rel]

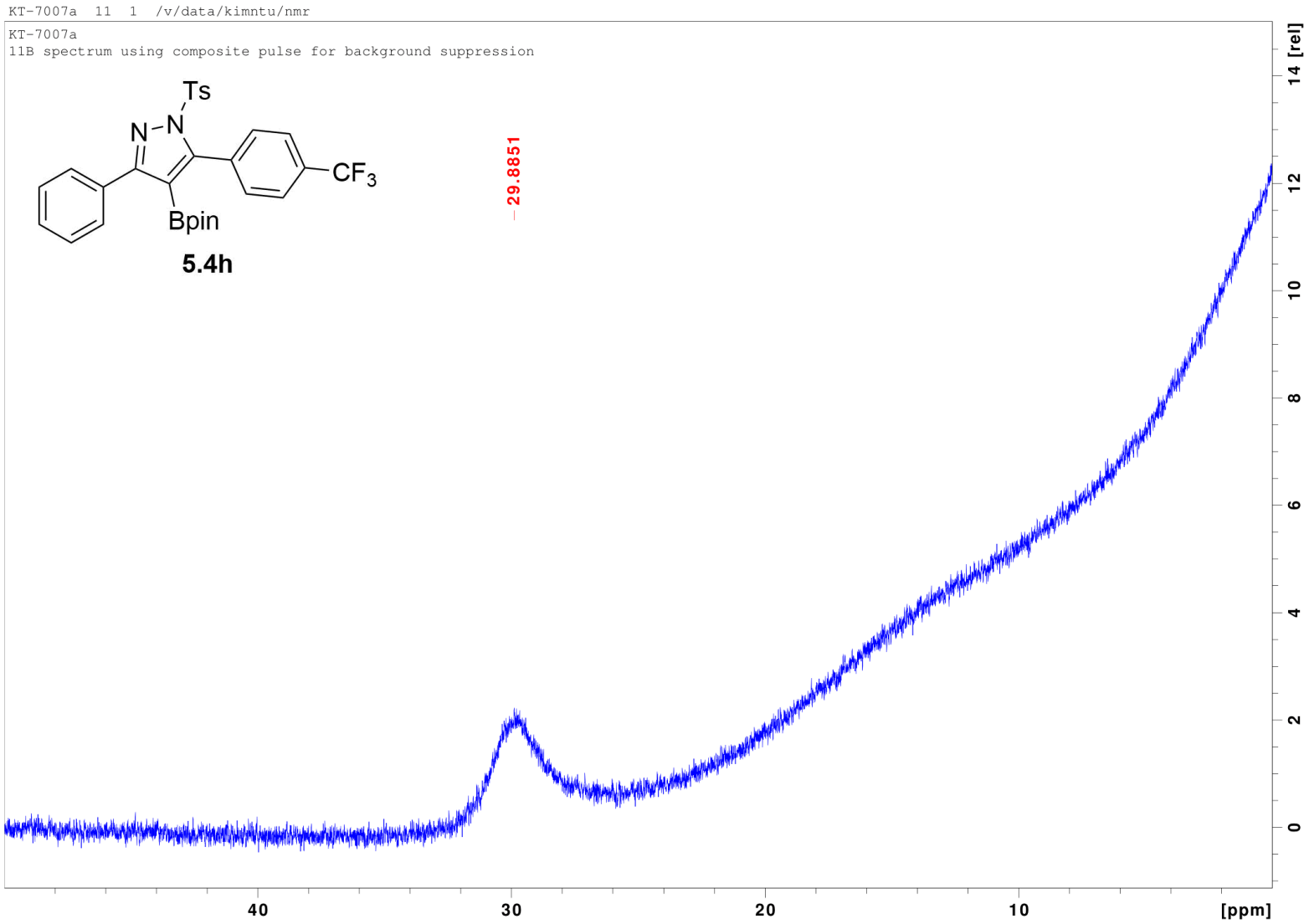
KT-7007a 11 1 /v/data/kimntu/nmr
KT-7007a
11B spectrum using composite pulse for background suppression
Ts
N
N
CF3
Bpin
5.4h
29.8851
14 [rel]
12
10
8
6
4
2
0
40
30
20
10
[ppm]

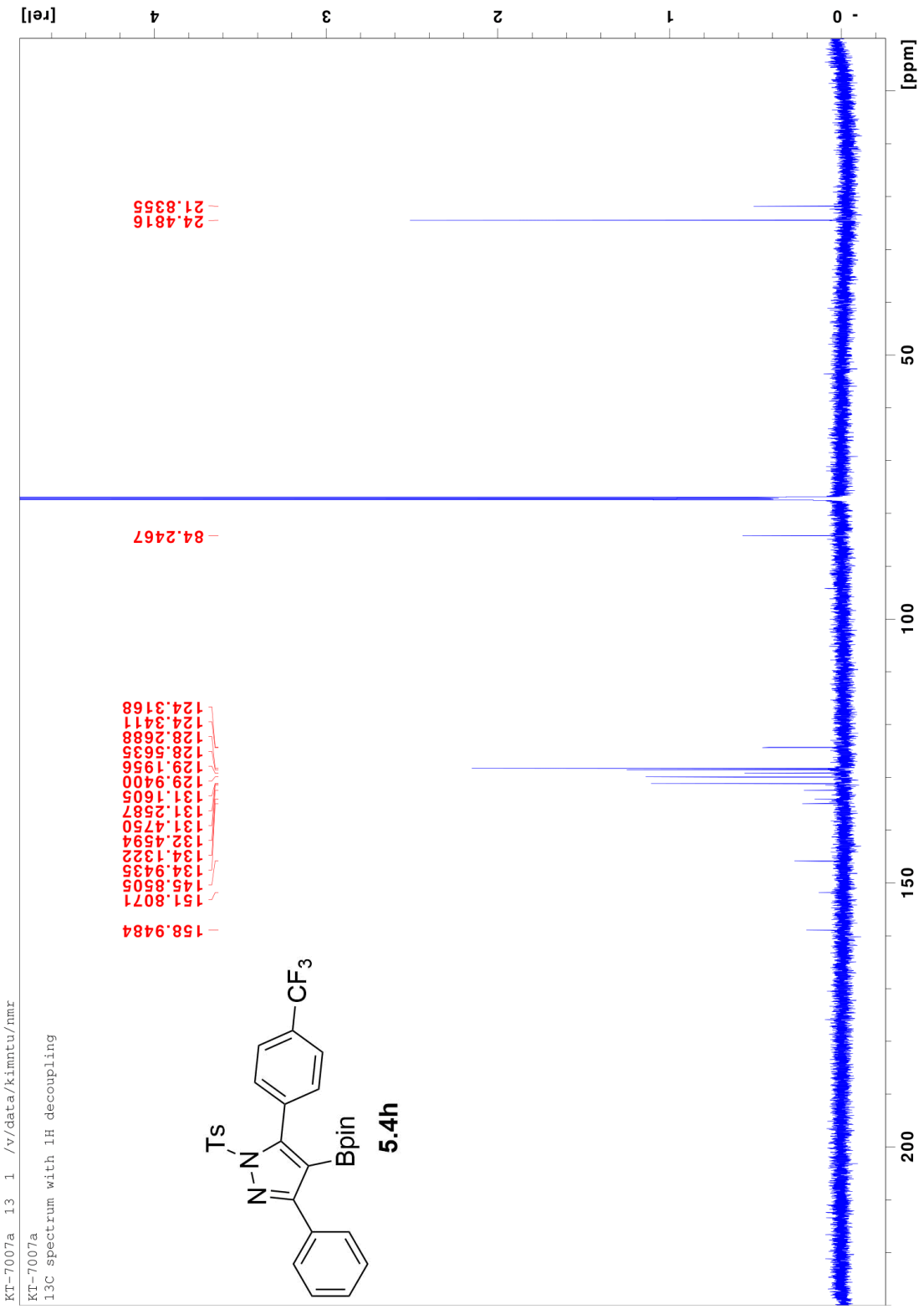
KT-7007a 13 1 /v/data/kimntu/nmr
KT-7007a
13C spectrum with 1H decoupling
[rel]
4
3
2
1
0
[ppm]
50
100
150
200
21.8355
24.4816
84.2467
124.3168
124.3411
128.2688
128.5635
129.1956
129.9400
131.1605
131.2587
131.4750
132.4594
134.1322
134.9435
145.8505
151.8071
158.9484
CF3
Ts
N
N
Bpin
5.4h

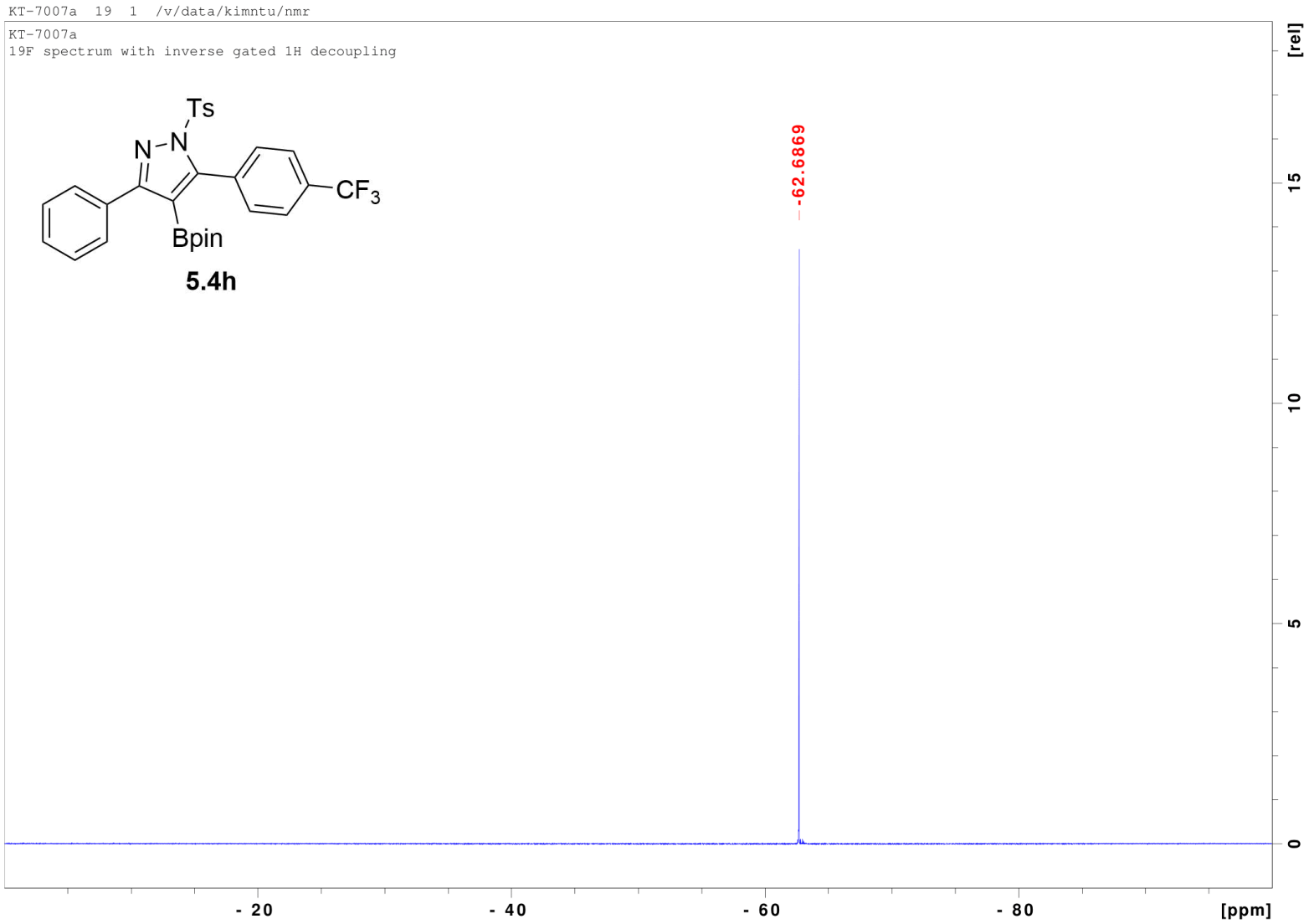
KT-7007a 19 1 /v/data/kimntu/nmr
KT-7007a
19F spectrum with inverse gated 1H decoupling
Ts
N
N
CF3
Bpin
5.4h
-62.6869
[rel]
15
10
5
0
- 20
- 40
- 60
- 80
[ppm]

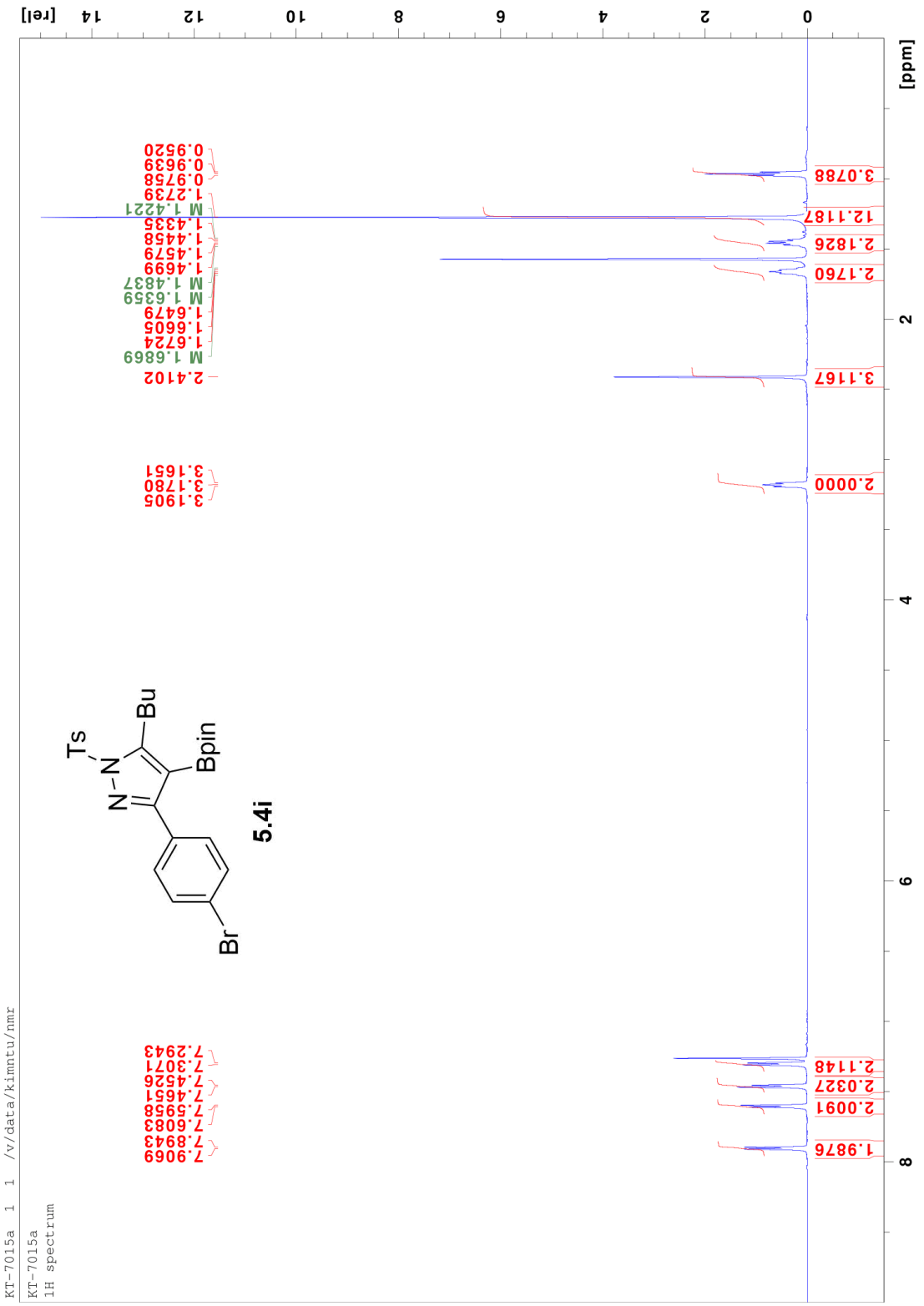
KT-7015a 1 1 /v/data/kimntu/nmr
KT-7015a
1H spectrum
[rel]
[ppm]
Ts
N
N
Bu
Bpin
Br
5.4i
7.9069
7.8943
7.6083
7.5958
7.4651
7.4526
7.3071
7.2943
3.1905
3.1780
3.1651
2.4102
M 1.6869
1.6724
1.6605
1.6479
M 1.6359
M 1.4837
1.4699
1.4579
1.4458
1.4335
M 1.4221
1.2739
0.9758
0.9639
0.9520
1.9876
2.0091
2.0327
2.1148
2.0000
3.1167
2.1760
2.1826
12.1187
3.0788

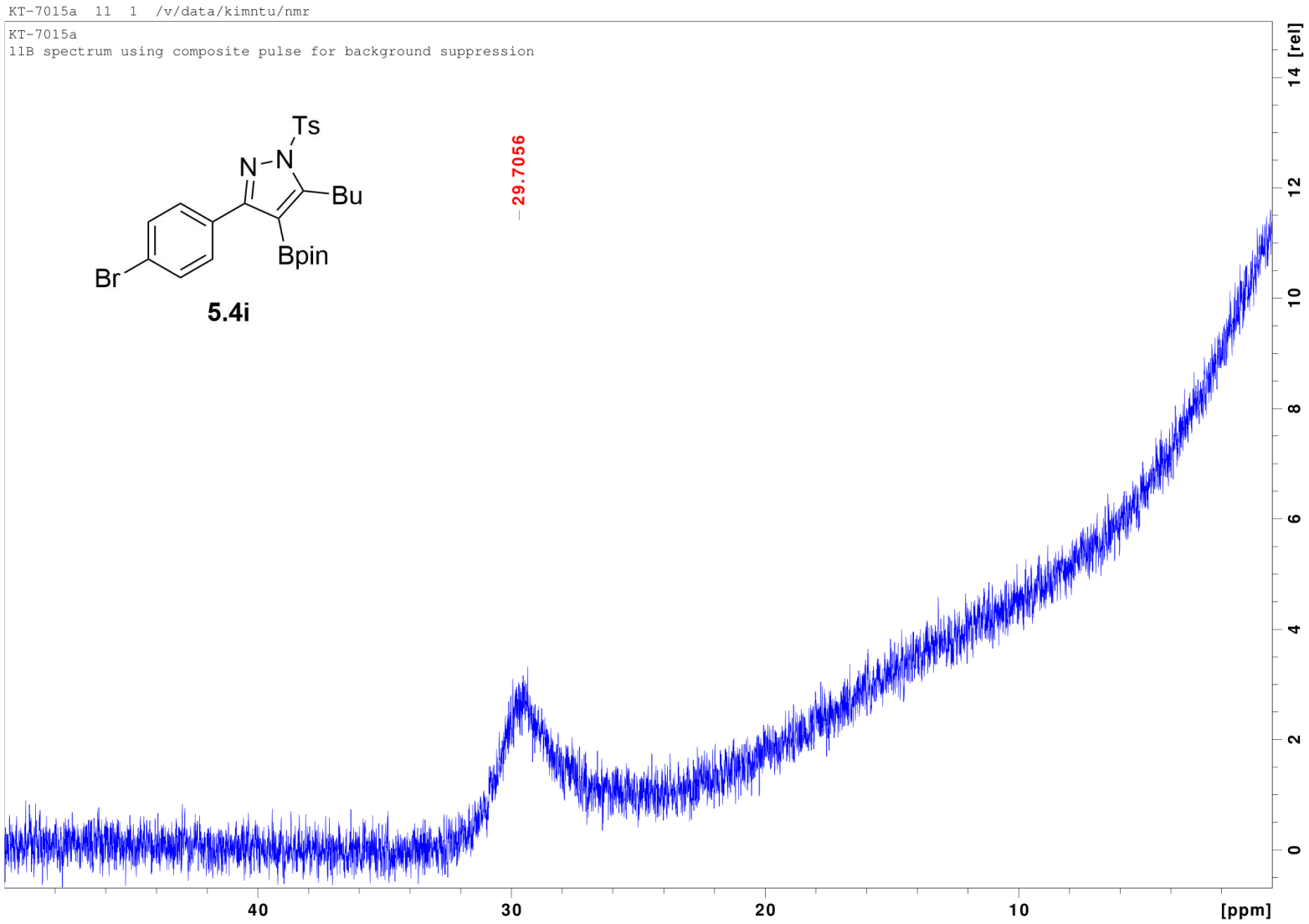
KT-7015a 11 1 /v/data/kimntu/nmr
KT-7015a
11B spectrum using composite pulse for background suppression
Ts
N
N
Bu
Bpin
Br
5.4i
29.7056
14 [rel]
12
10
8
6
4
2
0
40
30
20
10
[ppm]

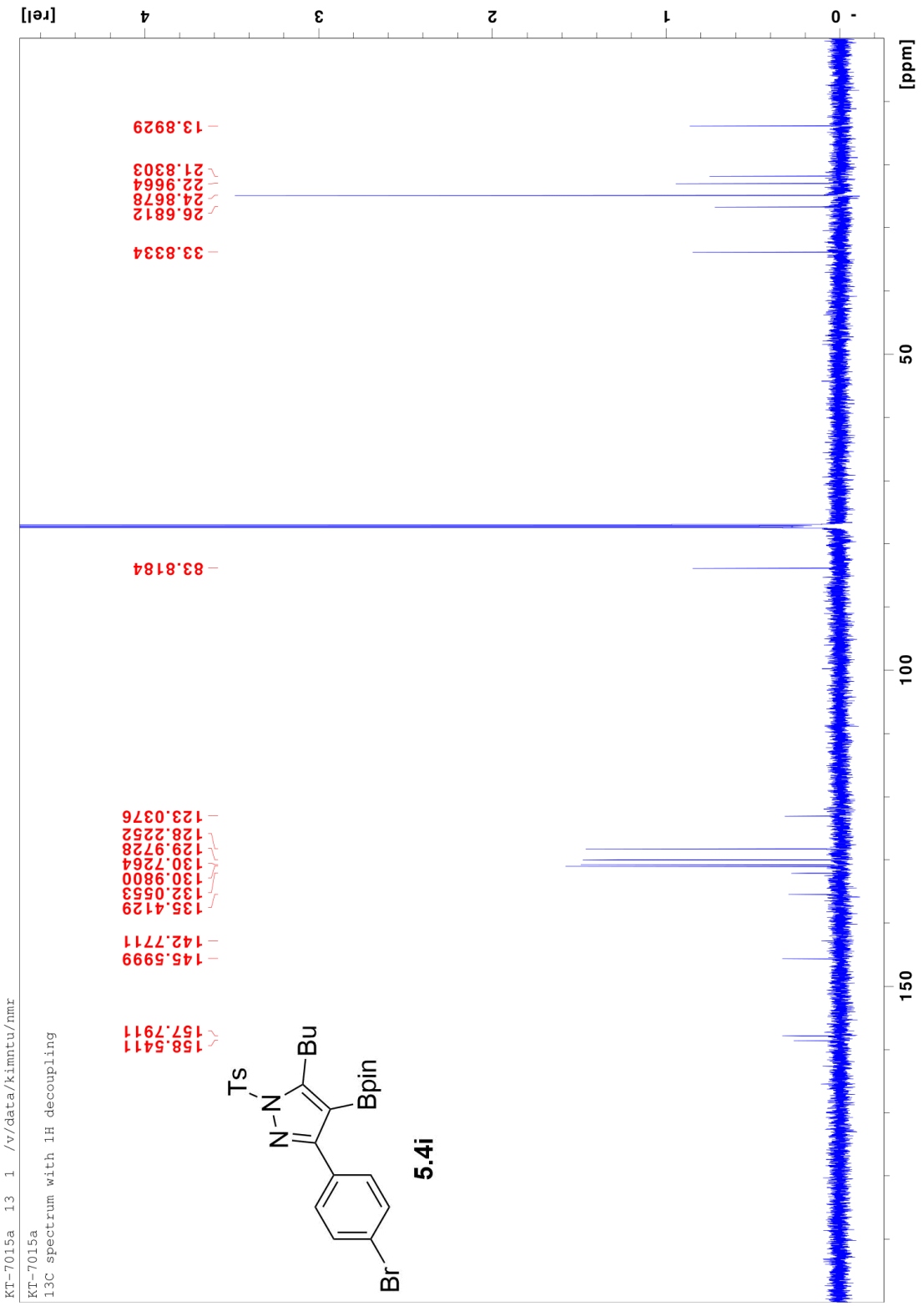
KT-7015a 13 1 /v/data/kimntu/nmr
KT-7015a
13C spectrum with 1H decoupling
[rel]
4
3
2
1
0
[ppm]
50
100
150
13.8929
21.8303
22.9664
24.8678
26.6812
33.8334
83.8184
123.0376
128.2252
129.9728
130.7264
130.9800
132.0553
135.4129
142.7711
145.5999
157.7911
158.5411
Ts
N
N
Bu
Bpin
Br
5.4i

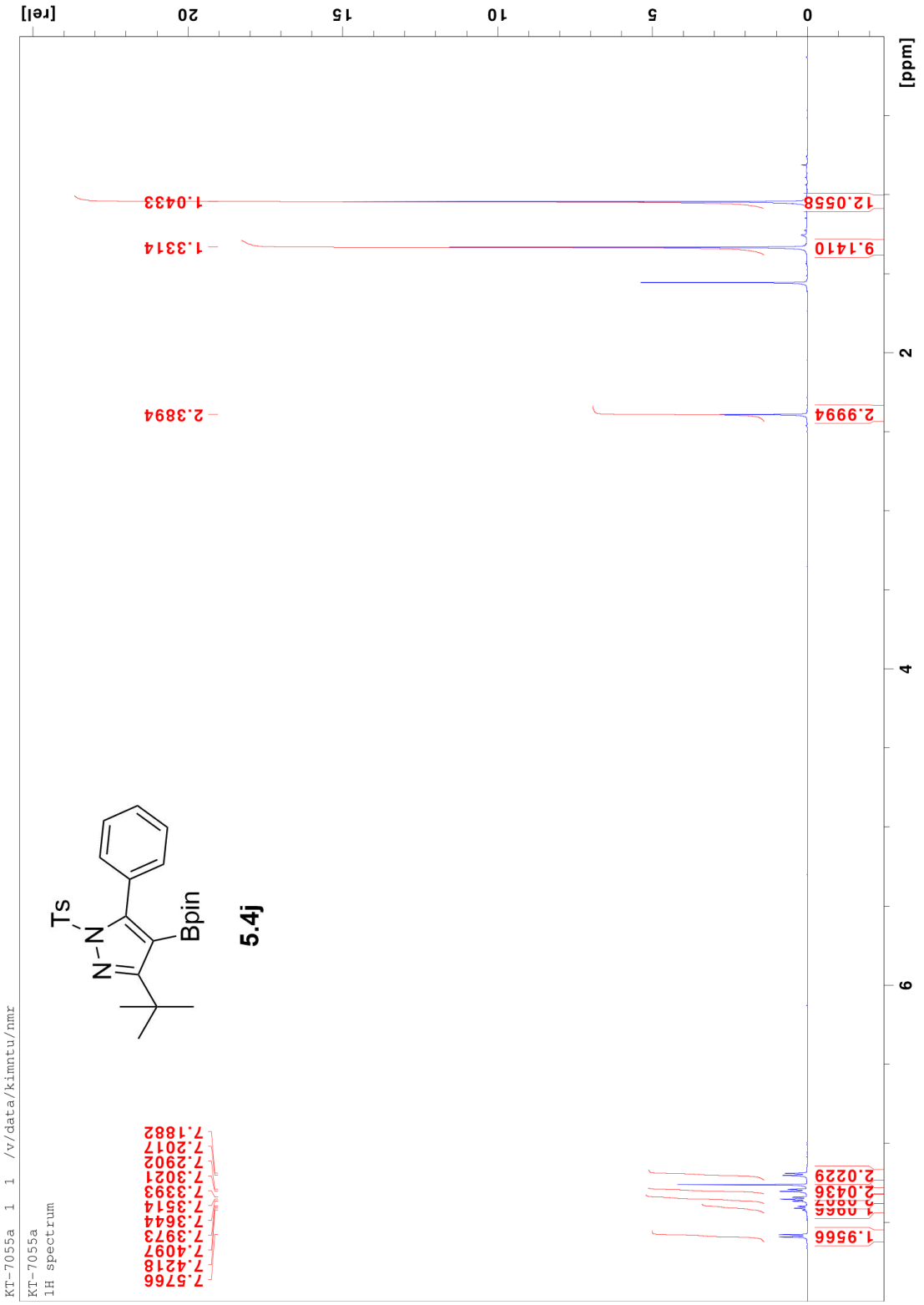
KT-7055a 1 1 /v/data/kimntu/nmr
KT-7055a
1H spectrum
7.5766
7.4218
7.4097
7.3973
7.3644
7.3514
7.3393
7.3021
7.2902
7.2017
7.1882
2.3894
1.3314
1.0433
2.0229
2.0436
1.9566
2.9994
9.1410
12.0558
Ts
N
N
Bpin
5.4j
[rel]
20
15
10
5
0
[ppm]
6
4
2

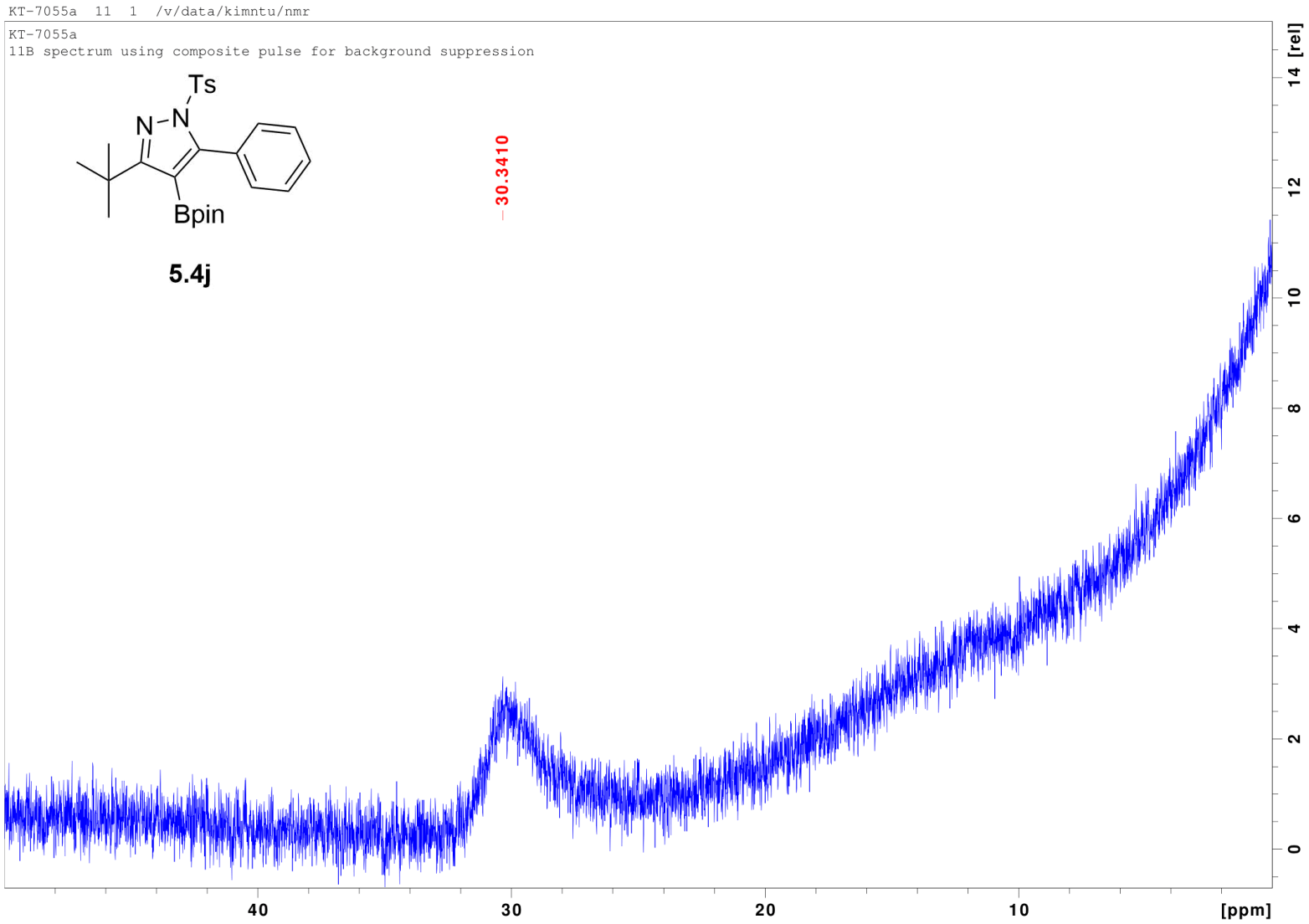
KT-7055a 11 1 /v/data/kimntu/nmr
KT-7055a
11B spectrum using composite pulse for background suppression
Ts
N
N
Bpin
5.4j
30.3410
14 [rel]
12
10
8
6
4
2
0
40
30
20
10
[ppm]

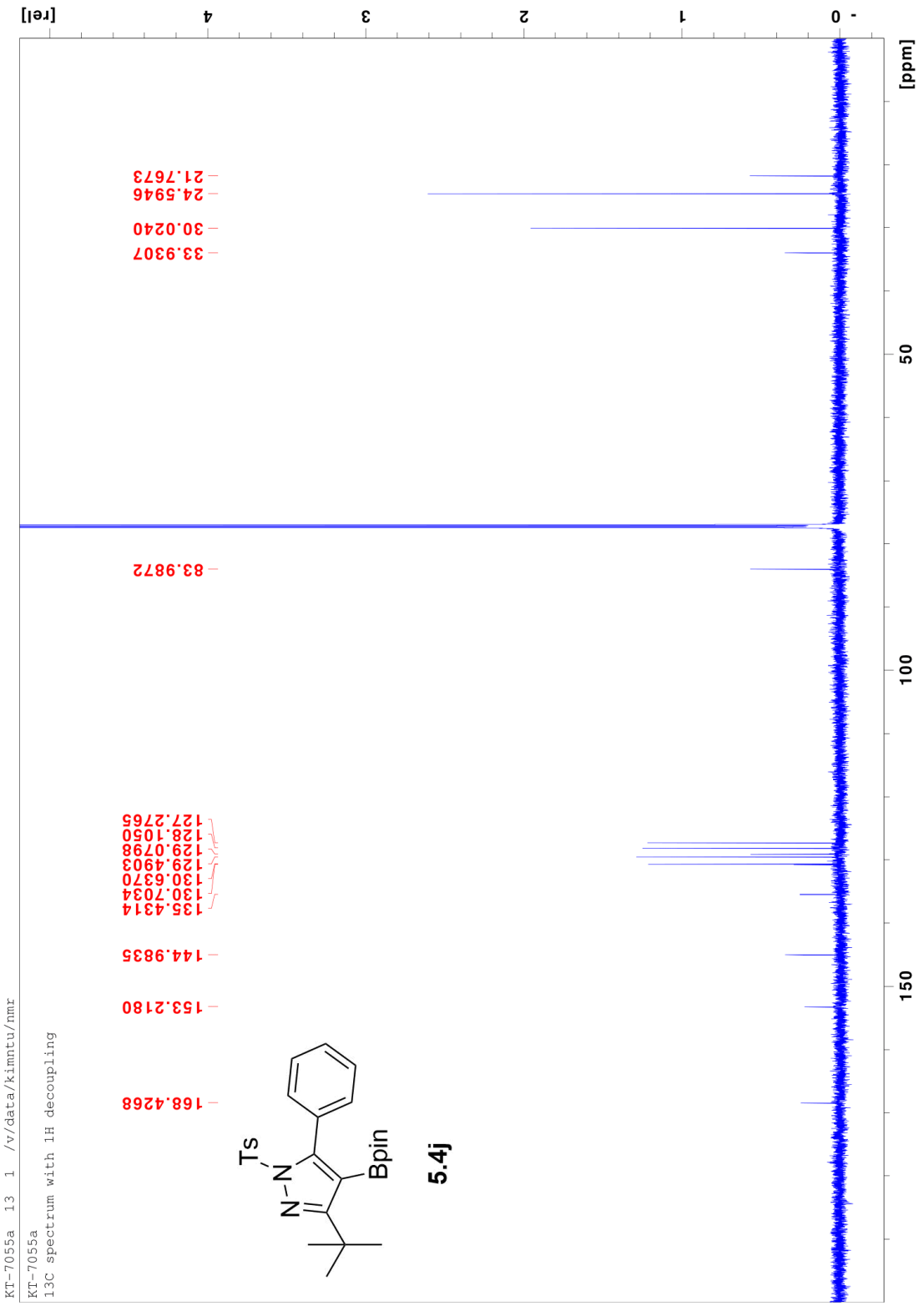
KT-7055a 13 1 /v/data/kimntu/nmr
KT-7055a
13C spectrum with 1H decoupling
[rel]
[ppm]
168.4268
153.2180
144.9835
135.4314
130.7034
130.6370
129.4903
129.0798
128.1050
127.2765
83.9872
33.9307
30.0240
24.5946
21.7673
Ts
Bpin
5.4j

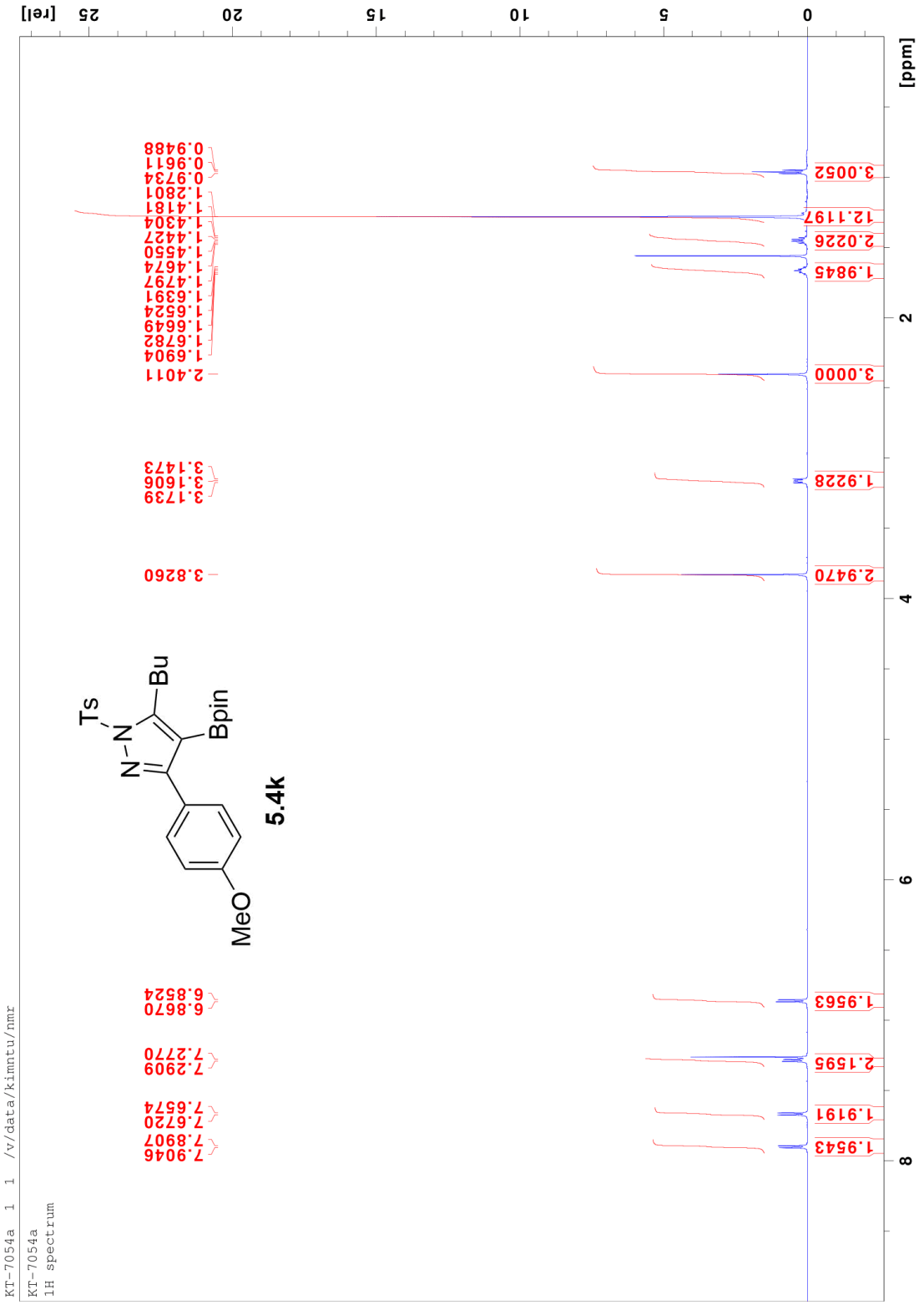
KT-7054a 1 1 /v/data/kimntu/nmr
KT-7054a
1H spectrum
[ppm]
[rel]
0
5
10
15
20
25
2
4
6
8
3.0052
12.1197
2.0226
1.9845
3.0000
1.9228
2.9470
1.9563
2.1595
1.9191
1.9543
7.9046
7.8907
7.6720
7.6574
7.2909
7.2770
6.8670
6.8524
3.8260
3.1739
3.1606
3.1473
2.4011
1.6904
1.6782
1.6649
1.6524
1.6391
1.4797
1.4674
1.4550
1.4427
1.4304
1.4181
1.2801
0.9734
0.9611
0.9488
Ts
N
N
Bu
Bpin
MeO
5.4k

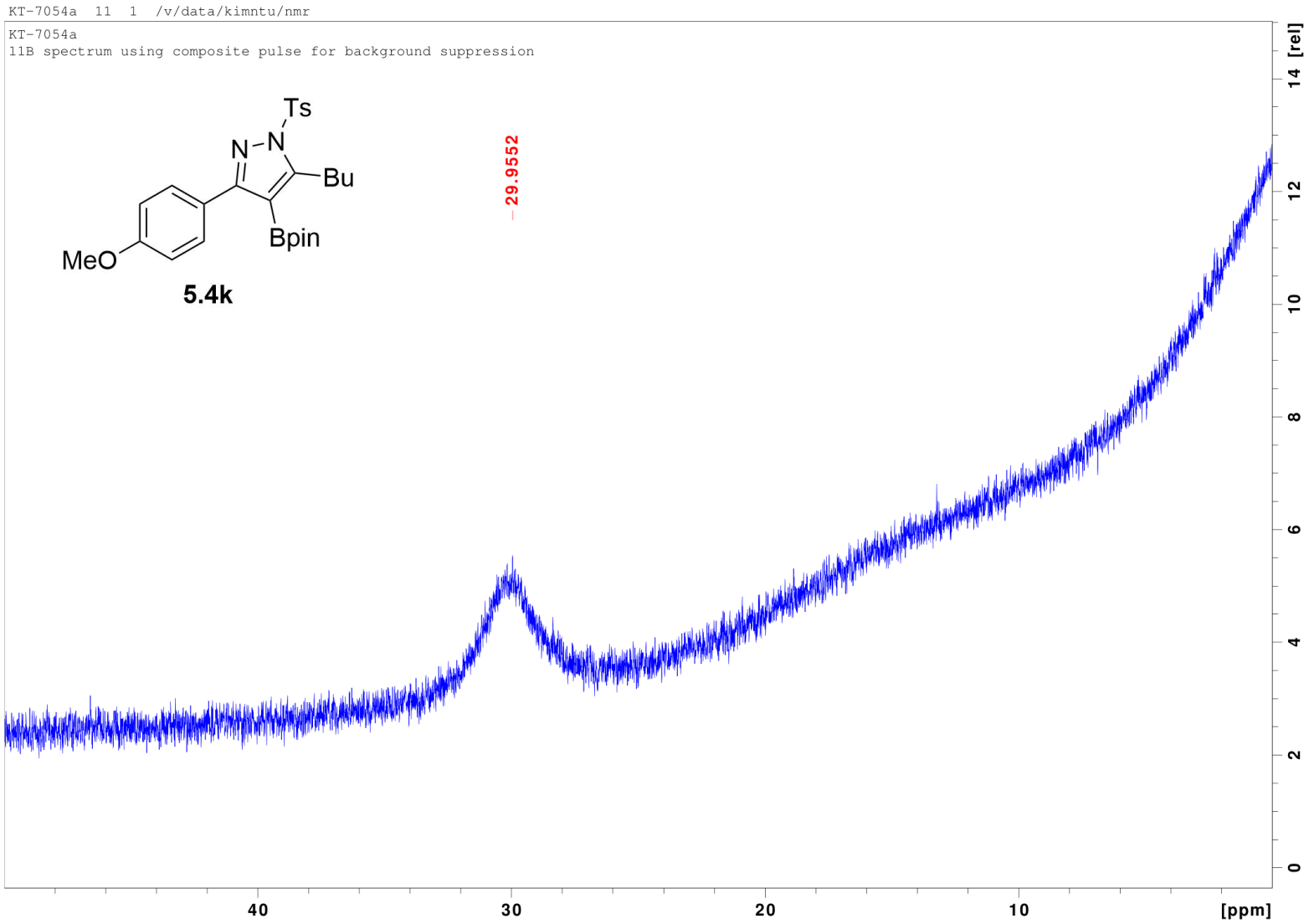
KT-7054a 11 1 /v/data/kimntu/nmr
KT-7054a
11B spectrum using composite pulse for background suppression
Ts
N
N
Bu
Bpin
MeO
5.4k
29.9552
14 [rel]
12
10
8
6
4
2
0
40
30
20
10
[ppm]

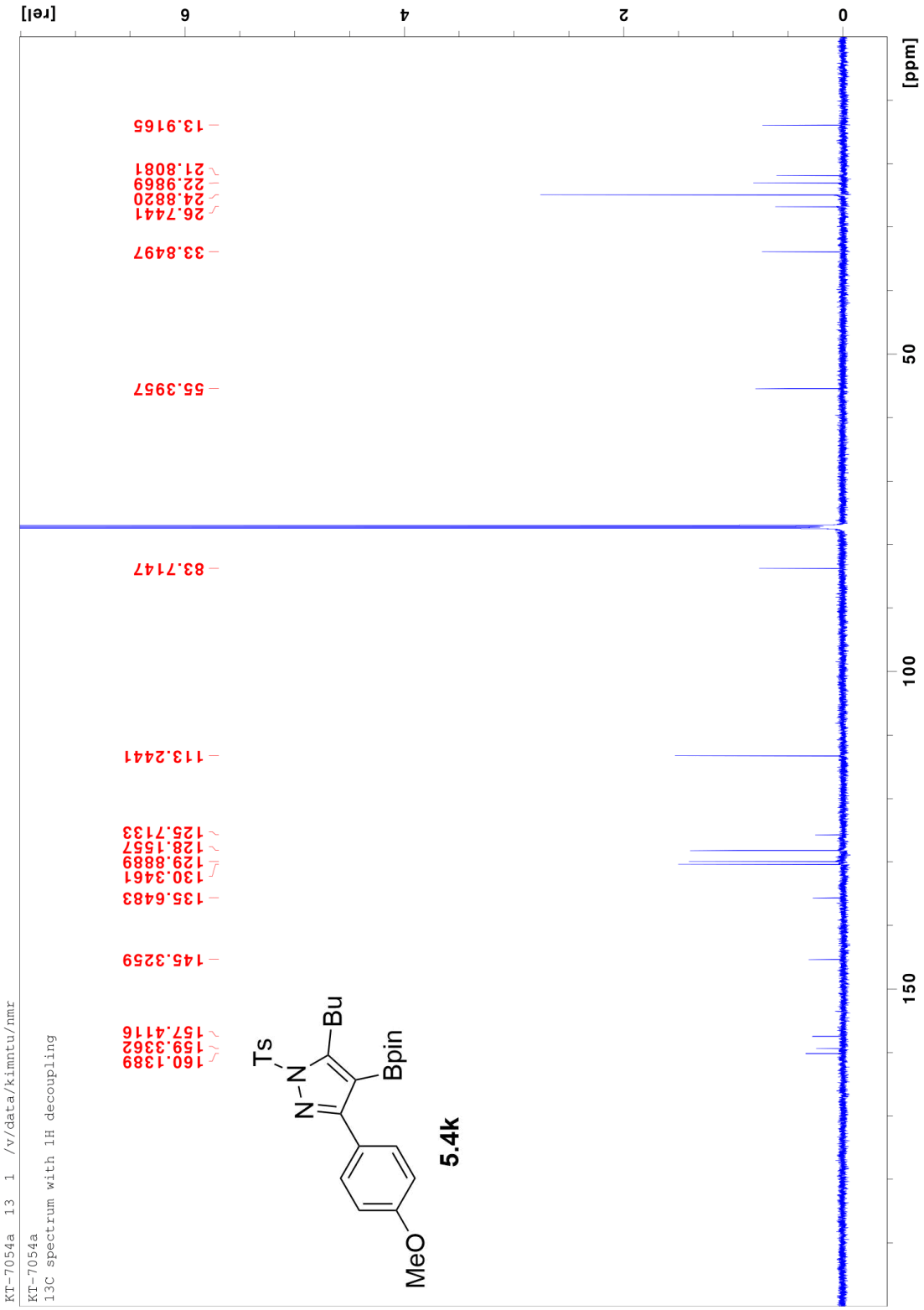
KT-7054a 13 1 /v/data/kimntu/nmr
KT-7054a
13C spectrum with 1H decoupling
160.1389
159.3362
157.4116
145.3259
135.6483
130.3461
129.8889
128.1557
125.7133
113.2441
83.7147
55.3957
33.8497
26.7441
24.8820
22.9869
21.8081
13.9165
Ts
N
N
Bu
Bpin
MeO
5.4k
[rel]
6
4
2
0
[ppm]
50
100
150